Alma Mater Studiorum – Università di Bologna

DOTTORATO DI RICERCA IN

Ingegneria Energetica, Nucleare e del Controllo Ambientale

Ciclo XXIX

Settore Concorsuale di afferenza: 09/C2

Settore Scientifico disciplinare: ING-IND/10

Dynamic modeling and seasonal performance evaluation of air-to-water heat pump systems

Candidato: **Matteo Dongellini**

Coordinatore Dottorato: **Prof. Nicolò Cavina**

Relatore: **Prof. Gian Luca Morini**

Esame finale anno 2017

PhD Thesis – Bologna. 2017

Dynamic modeling and seasonal performance evaluation of air-to-water heat pump systems
Modellazione dinamica e valutazione delle prestazioni energetiche stagionali di sistemi basati su pompe di calore aria-acqua

Università di Bologna
Dottorato di ricerca in Ingegneria Energetica, Nucleare e del Controllo Ambientale (XXIX ciclo)

E-mail: matteo.dongellini@unibo.it

It is impossible for a self-acting machine, unaided by any external agency, to convey heat from one body to another at a higher temperature

--William Thomson (Lord Kelvin)

Here is the essence of this thesis: for the last three years I have been dealing with the second Law of Thermodynamics and I hope to go on for a while more

Acknowledgments

The research activity conducted during last three years would not have been possible without the support and the help received from many people: I am grateful to them all for their contribution.

First and foremost, I would express my gratitude to my supervisor, Prof. Gian Luca Morini, for his guidance, suggestions and valuable revision during these years. Prof. Morini supervised my work during my entire academic career: Bachelor Degree, Master Degree and PhD studies; he inspired in me and highlighted the passion for research and outlined the academic path that I am still walking: for these reasons, I am forever grateful.

This work was supported by the heat pump manufacturer Galletti Spa. I owe for the exchange of experience, the suggestion of practical ideas to solve unexpected problems and, last but not least, the provision of detailed technical and experimental data about heat pumps. None of the obtained results would have been possible without the support of Galletti Spa. In particular, the help of Dr. Alessandro Casolari, Dr. Antonio Loreto and Dr. Francesco Caselli needs to be acknowledged:

I am also very thankful to everyone in the Thermodynamics Laboratory of the University of Bologna, my current work place, for their help, technical support, friendship and for making every day here very enjoyable. A special mention goes to Dr. Stefania Falcioni, the first person to ask in the Lab when a doubt or a problem occurs.

I am deeply grateful with my colleagues Dr. Giacomo Puccetti and Dr. Claudia Naldi. We spent the major part of our academic studies together and they represent a milestone for my research activity, as well as precious friends.

Finally, my thoughts go to my family, for their encouragement, help, patience and support, to my friends and every person who spent a small part of its time with me during these last three years: there is a small share of all of them within this Thesis.

Abstract

In this Thesis a series of numerical models for the evaluation of heat pump systems seasonal performance are presented. More in detail, the work has been addressed to the analysis of the behavior of reversible air-to-water heat pumps coupled to residential and non-residential buildings.

During last decades, several studies demonstrated that heat pumps are a suitable solution to achieve the targets imposed by the European Union in terms of energy saving and use of renewable sources since these devices are able to provide building space heating, space cooling and domestic hot water production with a single device using significant renewable energy contributions. Nevertheless, the exploitation of the full energy saving potential linked to the adoption of heat pumps in heating and cooling systems is a hard task for designers due to the influence on their energy performance of several factors, like the external climate variability, the heat pump modulation capacity, the system control strategy and the hydronic loop configuration. The aim of this Thesis is to study in detail all these aspects. It is important to stress that all the models presented in this work have been carried out with the cooperation of a heat pump manufacturer: this relationship has been important to obtain detailed data useful for the tuning of the developed models.

In the first part of this Thesis, a series of models which use a temperature class approach for the prediction of the seasonal performance of HVAC systems based on air source heat pumps are shown. An innovative methodology for the calculation of the seasonal performance of an air-to-water heat pump system operating in heating and cooling mode has been proposed as an extension of the procedure reported by the European Standard EN 14825. This methodology can be applied for the analysis of different kinds of air-to-water heat pumps, such as single-stage units (On-off HPs), multi-stage units (MSHPs) and inverter-driven units (IDHPs). By applying this method, the seasonal performance of the heat pump system is assessed as a function of the site in which the system is located, the building thermal loads, the size of the unit and the heat pump modulation capacity. If one considers heating operating mode, results point out that the optimal size of the heat pump strongly depends on its modulation capacity: for a fixed thermal load, a slight oversizing of multi-stage and variable-speed heat pumps leads to an increase of their seasonal efficiency, while the best seasonal

performance of a single-stage unit is achieved selecting the bivalent temperature larger than the design temperature. Furthermore, if the annual performance of a reversible heat pump is considered, the obtained results suggest to develop a building design able to achieve balanced heating and cooling loads during the year, in order to reduce the use of back-up systems or the adoption of a significant number of on-off cycles to match the required load.

In the second part of this Thesis, dynamic simulations have been described with the aim to optimize the control systems of the heat pump and of the HVAC plant. A series of dynamic models, developed by means of TRNSYS, are presented in order to study the behavior of On-off HPs, MSHPs and IDHPs for building space heating and/or cooling. The main goal of the dynamic simulations presented in this work is to show the influence of the control logics linked to the heat pump and to the hydronic loop used in order to couple the heat pump to the emitters on the seasonal performance of the system and the indoor thermal comfort conditions guaranteed in a building. A particular focus is given to the implementation of innovative control strategies for the optimization of the heat pump energy consumption and to the modeling of the energy losses linked to on-off cycling.

It has been demonstrated that the adoption of optimized control logics can enhance the energy performance of the heat pump system because:

i. the hourly number of on-off cycles can be significally reduced (Sections 4.5.2 and 4.5.3);
ii. the heat pump can use on-off cycles only for a limited number of hours during the winter (Section 3.7.1;
iii. the optimization of the hydronic loop configuration allows to stabilize the temperature of the water supplied to the emitters, improving the indoor thermal comfort conditions.

Sommario

Questa Tesi presenta una serie di modelli numerici sviluppati per la valutazione delle prestazioni stagionali di sistemi a pompa di calore. In particolare, il lavoro svolto durante questo periodo ha riguardato lo studio delle prestazioni energetiche di pompe di calore reversibili del tipo aria-acqua e accoppiate ad edifici residenziali e non residenziali.

Nel corso degli ultimi decenni, numerosi studi hanno dimostrato che le pompe di calore sono una soluzione promettente per raggiungere gli obiettivi imposti dall'Unione Europea in merito al risparmio energetico ed all'utilizzo di fonti energetiche rinnovabili, dal momento che questi sistemi sono in grado di soddisfare i fabbisogni energetici per il riscaldamento, il condizionamento e la produzione di acqua calda sanitaria per mezzo di un unico dispositivo e per giunta utilizzano quote significative di energia rinnovabile. Tuttavia, il pieno sfruttamento del potenziale risparmio energetico legato all'adozione di sistemi di riscaldamento/condizionamento a pompa di calore è un compito di difficile realizzazione da parte dei progettisti, in quanto diversi fattori come la variabilità delle condizioni climatiche esterne, la capacità delle pompe di calore di modulare la potenza termica/frigorifera erogata, la logica di controllo del sistema e la configurazione impiantistica utilizzata influiscono sulle prestazioni energetiche ottenibili. Lo scopo di questa Tesi è quello di studiare in dettaglio tutti questi aspetti. Si sottolinea come lo sviluppo di tutti modelli di simulazione presentati in questa Tesi sia stato effettuato in cooperazione con un produttore di pompe di calore. Tale collaborazione è stata determinante per ottenere dati tecnici dettagliati per la calibrazione dei modelli sviluppati.

Nella prima parte di questo lavoro, viene presentata una serie di modelli basati su un approccio di tipo "temperature class" per la previsione delle prestazioni stagionali di sistemi HVAC basati su una pompa di calore. Viene proposta una innovativa procedura di calcolo per la determinazione dell'efficienza stagionale di un impianto a pompa di calore ad aria operante in regime di riscaldamento e/o raffrescamento, costruita come una estensione della metodologia riportata dalla norma europea EN 14825. Tale procedura può essere estesa per lo studio di diverse tipologie di pompa di calore aria-acqua, quali pompe di calore monocompressore (On-off HPs), pompe di calore multi-compressore (MSHPs) e pompe di calore a velocità variabile (IDHPs). Impiegando la

metodologia di calcolo riportata in questo lavoro, l'efficienza stagionale del sistema viene valutata in funzione della località in cui si trova l'impianto, del carico termico richiesto dell'edificio, della taglia della pompa di calore e del sistema di controllo del dispositivo. Se si considera un sistema che opera nel solo regime di riscaldamento, i risultati indicano che la taglia ottimale della pompa di calore dipende fortemente dalla capacità di modulazione della potenza termica/frigorifera erogata dalla pompa di calore: una volta fissato il carico termico richiesto dall'edificio, un leggero sovradimensionamento della taglia di pompe di calore modulanti comporta un aumento dell'efficienza stagionale del sistema, mentre per quanto riguarda pompe di calore mono-compressore, la migliore performance stagionale si ottiene fissando una temperatura bivalente superiore alla temperatura di progetto. Inoltre, se si valutano le performance annuali di un sistema basato su una pompa di calore reversibile, i risultati ottenuti indicano che per ricavare la massima efficienza annuale sarebbe necessario progettare un edificio caratterizzato da carichi di progetto di riscaldamento e raffrescamento simili, al fine di ridurre l'utilizzo di sistemi di back-up o l'adozione di un numero significativo di cicli di on-off per adeguare la potenza termica/frigorifera erogata dalla pompa di calore al carico richiesto dall'edifiicio.

Nella seconda parte di questa Tesi sono descritti modelli di simulazione dinamica costruiti con lo scopo di ottimizzare il sistema di regolazione di un impianto di riscaldamento. I modelli dinamici sono stati realizzati per mezzo di TRNSYS e permettono di valutare il comportamento in regime dinamico delle tipologie di pompe di calore precedentemente indicate (On-off HPs, MSHPs e IDHPs). Lo scopo principale dei modelli di simulazione dinamica presentati all'interno di questa tesi è quello di evidenziare l'influenza dei sistemi di regolazione della pompa di calore e del circuito idronico utilizzato per accoppiare il generatore di calore ai terminali di emissione sulle prestazioni stagionali dell'impianto e sulle condizioni di comfort garantite dall'impianto stesso. Particolare attenzione è stata rivolta all'implementazione di strategie di regolazione innovative ed alla modellazione delle perdite energetiche legate ai cicli di on-off della pompa di calore. E' stato dimostrato che l'adozione di logiche di controllo ottimizzate può migliorare le prestazioni energetiche degli impianti basati su una pompa di calore per differenti motivi:

i. il numero di cicli di on-off effettuati dalla pompa di calore può essere notevolmente ridotto (Paragrafi 4.5.2 e 4.5.3);

ii. la pompa di calore è in grado di effettuare cicli di on-off per una parte limitata della stagione;
iii. l'ottimizzazione della configurazione idraulica dell'impianto permette di stabilizzare la temperatura di mandata dell'acqua, migliorando le condizioni di comfort termico che si realizzano all'interno dell'edificio.

Contents

List of figures

List of Tables

Nomenclature

Roman letters

A	Area
APF	Annual Performance Factor
C_c	Degradation coefficient for on-off cycling penalization
CF	Corrective Factor during heat pump start-up
COP	Coefficient Of Performance
COP_C	Carnot Coefficient Of Performance
c_p	Specific heat capacity at constant pressure
CR	Capacity Ratio
CS	Cooling control Signal
d	Disturb variable of a generic control system
DB	Dead Band
DD	Degree Days
DT	Temperature Difference
e	Error signal of a generic control system
EER	Energy Efficiency Ratio
EER_C	Carnot Energy Efficiency Ratio
EP	Energy Performance indicator
f_{corr}	Corrective factor for on-off cycling penalization (bin method)
f_p	Primary energy conversion coefficient for electrical energy
H	Number of hours
HS	Heating control Signal
i	i-th bin or hour
j	j-th inverter frequency
K	Number of tank nodes
k	Thermal conductivity
K_d	Derivative gain of a PID controller
K_i	Integral gain of a PID controller
K_p	Proportional gain of a PID controller
L	Distance
lDB	Lower Dead Band

m	Mass flow rate
n	Number of active compressors of a multi-stage heat pump
N	Compressor number of a multi-stage heat pump
OP	Oversizing Parameter
p	Pressure
P	Power
PLF	Part Load Factor
PMV	Predicted Mean Vote
P_{th}	Thermal power delivered by the heat pump
Q	Thermal power
Q_h	Thermal power rejected to the hot heat source
Q_l	Thermal power absorbed from the cold heat source
RH	Relative Humidity
S	Slope of the building energy signature
$SCOP$	Seasonal Coefficient Of Performance
$SEER$	Seasonal Energy Efficiency Ratio
T	Temperature
t	Time
T_d	Characteristic derivative time of a PID controller
T_h	Hot heat source temperature
T_i	Characteristic integral time of a PID controller
T_l	Cold heat source temperature
T_{op}	Operative Temperature
u	Input signal of a generic control system
U	Thermal transmittance
uDB	Upper Dead Band
UI	Unbalance Indicator
V	Volume
W_{el}	Compressor electrical work
X	Output variable of a generic control system

Greek letters

$\Delta\tau$	Timestep duration
Φ	Frequency
ρ	Density

η	Efficiency

Subscripts/superscripts

abs	Absorbed
air	Air
aux	Auxiliary
avg	Average
b	Building
base	Base value
bin	Bin
biv	Bivalent
bottom	Bottom part of the tank
BU	Back-up
c	Cooling
ck	Crankcase Heater
cnd	Conduction
compr	Compressor
cond	Condenser
cyc	Cycling
DC	Defrosting Cycle
des	Design
dspr	Desuperheater
edge	Edge part of the tank
eff	Effective
el	Electric
env	Environment
eva	Evaporator
ext	External
FC	Fan-coil
FL	Full Load
flow	Flow of a fluid stream
h	Heating
in	Inlet
lim	Limit
loss	Energy losses

max	Maximum
min	Minimum
mix	Mixing
net	Of the heat pump
off	Off
on	Of the heat pump and the back-up system
opt	Optimal
out	Outlet
pen	Penalization
r	Return
ref	Reference
sb	Stand-by
SP	Set-Point
SU	Start-up
tank	Storage tank
to	Thermostat-off
top	Top part of the tank
tot	Total
w	Water

Acronyms

AAHP	Air-to-Air Heat Pump
AHP	Absorption Heat Pump
ASHP	Air Source Heat Pump
Av	Average reference climate
AWHP	Air-to-Water Heat Pump
BES	Building Energy Signature
BHE	Borehole Heat Exchanger
CLET	Cooling Heating Limit Temperature
Co	Colder reference climate
DHL	Direct Hydraulic Loop
DHW	Domestic Hot Water
EEV	Electronic Expansion Valve
EHP	Electric Heat Pump
EHPA	European Heat Pump Association

EU	European Union
GCHP	Ground Coupled Heat Pump
GHG	Green House Gas
GHP	Gas-engine Heat Pump
GSHP	Ground Source Heat Pump
GWHP	Ground Water Heat Pump
HiL	Hardware-in-the-Loop
HLET	Heating Limit External Temperature
HP	Heat Pump
HVAC	Heating, Ventilating and Air Conditioning
IDHP	Inverter-Driven Heat Pump
IDL	Indirect Hydraulic Loop
MSHP	Multi-Stage Heat Pump
NZEB	Nearly Zero Energy Building
On-off HP	Single-stage On-off Heat Pump
PID	Proportional-Integrative-Derivative
RES	Renewable Energy Source
Sep	Hydraulic Separator
SPF	Seasonal Performance Factor
SWHP	Surface Water Heat Pump
TEV	Thermostatic Expansion Valve
TOL	Temperature Outlet Limit
TS	Thermal Storage
TRY	Test Reference Year
Wa	Warmer reference climate

Chapter 1

Introduction

1.1. Overview of energy use in the European Union

The economic growth achieved during the previous century has been based on a progressive increase of energy consumptions. During the last decade, this trend undergoned a change, with an unexpected decrease of the energy demand due to the financial crisis occurred in 2009 and, of course, the increase of energy efficiency. In Figure 1.1, the European annual use of gross energy from 1990 to 2015, according to Eurostat data [1], is reported, subdivided for energy source.

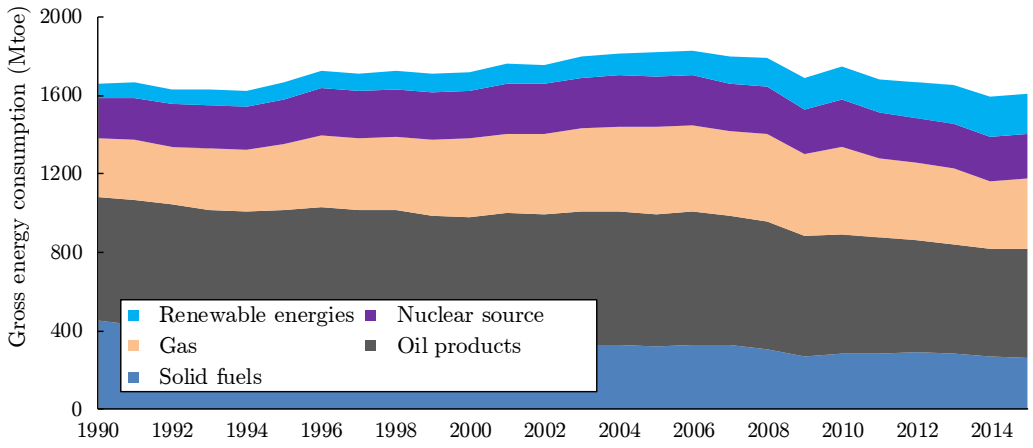

Figure 1.1. Annual gross energy consumption by energy source in Europe, from 1990 to 2015, (from [1]).

As pointed out by Figure 1.1, the contribution of fossil fuel energy sources (i.e. carbon, oil and gas) on the European gross energy consumption is predominant. Nevertheless a slow but continous decreasing trend, the share of fossil-fuel-based energy sources accounted in 2015 for about the 73% of the overall gross energy consumption. The exploitation of fossil fuels causes a series of environmental problems as the emission of carbon dioxide and other pollution; for this reason, the European Union (EU) is struggling to decrease the overall energy

consumption by means of the improvement of energy efficiency and to spread the use of Renewable Energy Sources (RES).

The negative environmental effects of fossil fuel combustion has been an increasing concern for the European Union during the last decades. Several targets have been defined in order to achieve a significant reduction of Greenhouse Gas (GHG) emissions, both on supply and demand side, with the aim to significantly increase the share of Renewable Energy Sources (RES) among the global energy consumptions. In addition to the European targets imposed for 2020, known as the 20-20-20 targets and reported by the Directive 2209/29/EC [2], the EU has established more restrictive targets to be achieved by 2030 [3], namely: the reduction of 40% of GHG emissions, compared to 1990 level, a RES share of 27% in the final energy consumption and the increase of energy efficiency at least of 27%.

Figure 1.2 illustrates the European final energy demand by sector from 1990 to 2015 (data are extracted from Ref. [1]). It is evident from Figure 1.2 that the share of energy use in the residential and service sectors is relevant: the mentioned sectors accounted for about the 39% of the overall European final energy consumption in 2015, corresponding to about 420 MToe. The energy consumption of the residential and the service sectors are mainly due to building operation energy demand.

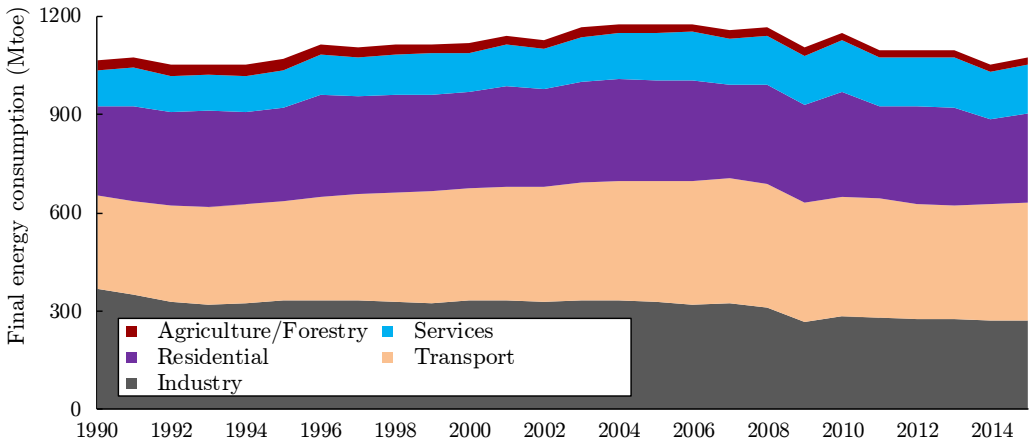

Figure 1.2. Annual final energy consumption by sector in Europe, from 1990 to 2015, (from [1]).

The fractions of energy sources used in residential sector during 2015 are better highlighted by Figure 1.3, from which it is evident that almost the half of final

energy consumption linked to residential building operation is provided by fossil fuels (i.e. petroleum products and natural gas).

As a consequence, EU made a strong effort to achieve a significant decrease of both new and refurbished building energy consumptions through a reduction of the use of fossil fuels, the enhancement of buildings energy efficiency and a wider diffusion of RES systems. During last ten years, a series of European Directives, aimed to promote the use of renewable sources and improve the energy efficiency in buildings, have been published. In particular, the Energy Performance of Building Directive, known as the EPBD Directive [4], promotes in the EU Member States the transition to Nearly Zero Energy Buildings (NZEB, namely buildings with very low energy needs) within 2020 and defines the minimum energy performance requirements for the building envelope and the heating, cooling and air-conditioning (HVAC) systems for new and old buildings.

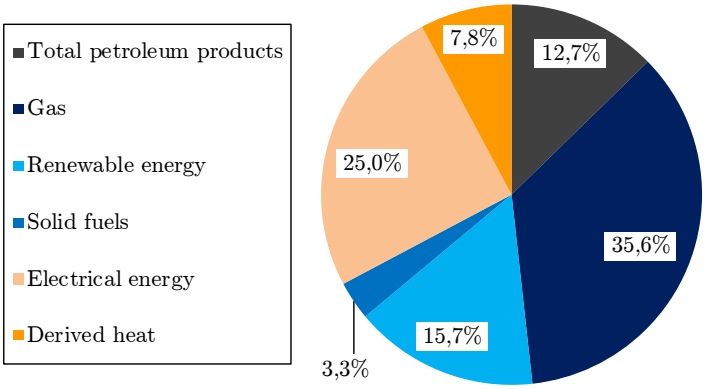

Figure 1.3. Fraction of energy sources in the residential sector in Europe in 2015, (from [1]).

In 2012, another important Directive was adopted: the Energy Efficiency Directive (EED) [5]. According to the EED, the Member States have to indicate several targets of primary energy savings for 2020: more in detail, concerning buildings, the EED imposes that European countries must renovate a share of 3% of buildings owned or occupied by the Public Administration, each year.

Furthermore, in 2009 the Directive 2009/28/EC ([6]) has officially recognized the Heat Pumps (HPs) as systems which use renewable energy sources. For this reason, heat pumps are a suitable solution for the replacement of boilers in new and retrofitted buildings and this kind of systems can contribute to achieve the targets reported by the mentioned European Directives, since aero-thermal,

geothermal and hydrothermal sources have been recognized as renewable energy sources

1.2. Heat pumps market survey

Heat pumps are typically grouped into three main categories: ground source heat pumps (GSHPs), which use as external thermal reservoir the ground, hydrothermal heat pumps, whose external heat source is water (from ground, rivers or lakes), and air source heat pumps (ASHPs), which extract thermal energy from air (outdoor, exhaust or indoor air). In order to carry out a survey on the last developments of the heat pump market within the European Union, we have merged the ground source and hydrothermal heat pumps statistics for sake of convenience.

Climate strongly influences the use of heat pump systems. In the coldest part of Europe, heat pumps are basically employed for heating purposes. In hotter areas as the Western and Southern Europe regions (Italy, Spain and France), the market of reversible heat pumps is bigger, because the cooling demand increases significantly and in some countries becomes predominant.

1.2.1. EurObserv' ER statistic data

If one considers the European market as a whole, 2015 was a positive year for the heat pump sector. According to EurObserv' ER 2015 data, reported in [7], over 2 600 000 heat pump units were sold in 2015, taking all above-mentioned technologies into account, corresponding to 20% growth with respect to 2014. Within the European market, up to 88% of sales are related to air-to-air heat pumps (AAHPs), corresponding to about 2 300 000 units. Low investment costs and easy installation make this kind of systems more suitable for the renovation market sector and constitute the basis for their very significant market share. Nowadays most of the air-to-air units sold in Europe are reversible and cooling needs have a strong influence on their high demand: market sales were in fact boosted by high summer temperatures in the Southern countries. Among ASHPs sales, the impact of units which extract heat from exhaust air is negligible, since only 28 000 units were sold in Europe in 2015.

The heat pump market for hydronic systems (i.e. GSHPs and air-to-water heat pumps, AWHPs) has sharply increased, too. This market gained 10% in

2015, with almost 300 000 units sold in the whole Europe. The air-to-water heat pump market segment is characterized by the biggest share, with about 220 000 units sold in 2015, corresponding to 14.5% growth on the year before. The ground-source heat pump market appears to be stable after many years of declining sales: about 82 500 units were sold in 2015, compared to about 82 750 units sold in 2014 (-0.3%).

In Figure 1.4 and Figure 1.5 the distribution of the air-to-air and hydronic heat pump units sold in 2015 is spreaded among the main European countries, respectively. As pointed out by Figure 1.4, the annual sales of air-to-air units in the larger Southern European markets (i.e. Italy, Spain and France) are strongly higher than other European countries. However, data from these markets are not directly comparable to the others, since the sales of heat pumps characterized by cooling as principal function are included. On the contrary, in Northern European countries they is a high demand of heat pumps in heating operating mode, since cooling needs are negligible.

It is evident from Figure 1.5 that in Europe the sales of hydronic heat pump systems are about one order of magnitude lower with respect to air-to-air units sales. Within this category, the air-to-water heat pumps (AWHPs) represent around 73% of the market in 2015, against the 27% share of ground source heat pumps [7]. This is due to the higher complexity and the higher installation costs of the GSHP systems, mainly associated to the boreholes drilling expenses, which delay the economic savings of ground source heat pumps. Improved and innovative methods for the boreholes drilling are needed to reduce the installation costs and the impact on the surroundings of this kind of systems, in order to achieve a higher ground source heat pumps penetration in the market.

Among the main European markets for hydronic systems, one can note important differences. The major number of ground source heat pumps are located in Northern and Central Europe; the highest percentage of GSHPs sales (with respect to the total of sold hydronic systems) can be found in Sweden and Finland, in which about 77% of this market sector is related to ground source units. Furthermore, the countries located in the European Central region present a market share of GSHPs higher than the average: in Denmark, Germany and Austria this sector covers a percentage of 37%, 34% and 30% on the total of hydronic systems sales, respectively. Finally, GSHPs are also used in Southern Europe, but at a very small scale: the sales of this kind of systems are completely negligible if compared to air-to-air systems market (as highlighted by Figure 1.4 and Figure 1.5).

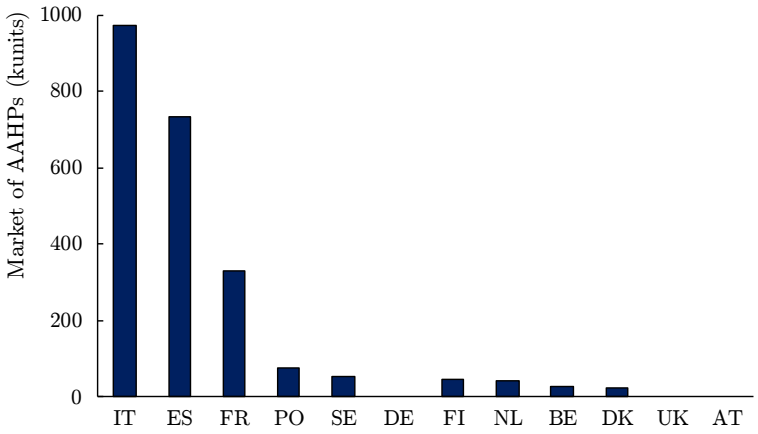

Figure 1.4. Air-to-air heat pumps sold in the main European markets in 2015 (from [7]).

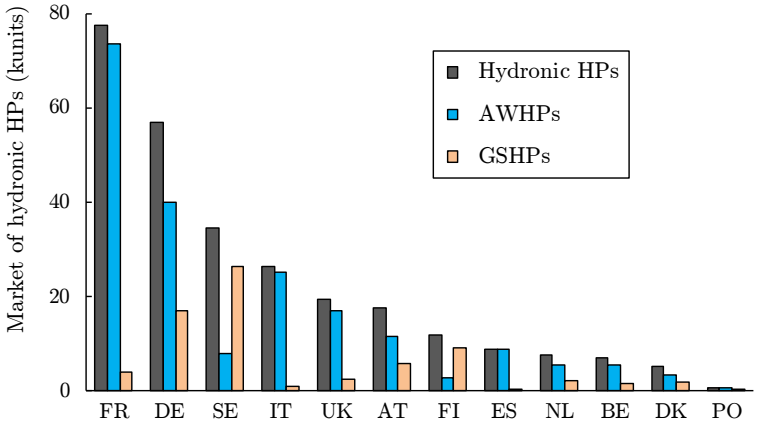

Figure 1.5. Hydronic heat pumps sold in the main European markets in 2015 (from [7]).

From another point of view, it is hard to estimate the total number of the installed heat pumps from the data supplied by industry associations and by European Member States. According to [7], the heat pumps installed in the European Union approaches 29.5 million units at the end of 2015. Table 1.1 reports the number of operating heat pumps for each Member State, subdivided among air source and ground source systems.

Concerning the installed thermal capacity and renewable energy outputs of this kind of systems, EurObserv' ER indicates a total capacity of 206.7 GW installed at the end of 2015, including 188.2 GW of air source heat pumps thermal capacity and 44.2 GW of thermal capacity linked to hydronic systems (25.7 GW of air-to water units; 18.5 GW of geothermal and hydrothermal units).

Table 1.1. Heat pumps stock in Europe in 2015 (from [7]).

Country	Air source heat pumps (Air-to-air, air-to-water, exhaust air)	Ground source heat pumps (Ground coupled, ground water, surface water)	Total (k-units)
Italy	18 430	16	18 446
France	4 638	149	4 787
Spain	1 497	1	1 498
Sweden	988	498	1 486
Germany	567	330	897
Finland	578	95	673
Denmark	245	56	301
Netherlands	248	47	295
Poland	255	0.8	256
Austria	67	96	163
United Kingdom	115	27	142
Belgium	84	8	92
Others	431	81	512
European total (k-units)	28 143	1 405	29 548

Heat pump technology is a widespread solution in the new buildings sector because it is particularly suitable for well-insulated constructions. Heating and cooling systems for these kinds of buildings are characterized by low temperature terminal units and are characterized by low specific energy consumptions. The mentioned characteristics can be coupled very well with the features of the heat pumps, which are the main candidate for the heating and cooling supply in low energy buildings (i.e. NZEB). On the other hand, until now a challenge for the heat pump industry is to make inroads into the renovation building market (primarily for the replacing of gas-fired boilers), which dominates HVAC system sales.

This trend is nowadays emerging in mature markets like France and North Europe. It means that these innovative devices can meet the needs of renovation operations and can also gain market shares in countries where heating systems based on heat pumps are less widespread. Finally, another reason for this positive

trend in the renovation market comes from the new expectations of building dwellers for comfort, especially being able to cool their homes during summer.

According to this trend, new products that are dedicated to the renovation market have been recently launched on the heat pump market. One of the widespread solutions includes a hybrid system composed by a condensing boiler and a heat pump within the same device. This system offers the advantage of enabling old housing renovation without the replacement of their original high-temperature radiators. The use of an auxiliary system (i.e. the boiler) implies that the heat pump does not need to be oversized and that the system efficiency is increased when the external temperature is very low. The energy manager of the system calculates the most efficient operating mode (boiler only, hybrid or heat pump only), according to the values of internal and external parameters, such as gas and electricity prices, external temperature and thermal capacity required. It is worth noting that hybrid heat pump systems were originally developed by heating market generalists that are not only boiler but also heat pump experts. Nowadays, this market is also targeted by the most important air-conditioning players.

Recently, modulation heat pumps have been launched and this product segment represents the most promising technology. These units use an inverter to continuously modulate the compressor rotating speed to match the requested thermal load. Electricity consumption can be optimized, maximum energy performance can be obtained and noise can be minimized by managing the compressor frequency. While conventional single-stage heat pumps operate at full load until the set-point temperature is reached and then are switched off, inverter-driven units operate continuously to provide a more efficient control of the system. These variable-speed compressor heat pumps have been successfully used since many years in air-conditioning technology and they were initially engineered by the major Asian players.

The proliferation of new technological solutions offered by heat pump manufacturers is an indication of the growth potential of this market. Therefore, the promulgation of a series of European Directives ([4]-[6]), aimed to improve the energy efficiency of buildings and HVAC systems by means of a series of targets imposed to Member States, leads to a continuous increase of industry financial profit.

1.2.2. EHPA statistic data

An interesting source of data for the analysis of the heat pump market is the European Heat Pump Association (EHPA); EHPA publishes each year the European Heat Pump Market and Statistics Report, in which it incorporates only the fraction linked to the heating mode of the reversible air-to-air heat pump sales in the countries where they are installed. This choice is justified by its objective to monitor the market of heat pump systems primarily used for heating and for this reason it distinguishes them from the market of systems mainly used for cooling. More in detail, EHPA considers that reversible air-to-air heat pumps are principally used for heating in countries characterized by cold climates (North and East Europe). Moreover, the Association avoids to incorporate air-to-air heat pump sales within the sales statistics of countries located in temperate zones (i.e. Middle Europe). Finally, with regard to countries located in the Southern part of Europe and characterized by hot climates, EHPA takes into account only a small fraction of air-to-air heat pump sales (actually about 10%), which represents the percentage of heat pumps used for heating needs only.

In Figure 1.6 the European heat pump market of the last ten years is represented, according to EHPA statistic data [8] and definitions (i.e. only the sales of reversible air-to-air heat pump mainly used for heating are considered). As pointed out by Figure 1.6, the heat pump market has been characterized by different trends within the last ten years. Between 2005 and 2008 a significant increasing tendency of sales can be observed, while from 2009 to 2012 the market dropped down due to the financial crisis occurred in 2009 and, although it has partially recovered during 2010 and 2011, the heat pump sales dropped again in 2012 to values below the sales of four years before. This last drop can be explained by the crisis of the construction sector occurred in some countries and by the increase of the electricity prices, among others. Since 2013, the tendency reversed again: heat pump sales increased year by year and in 2015 they reached the record year sales of about 880 000 units.

Figure 1.6 also splits heat pump sales within three main categories: air-to-air units (AAHPs), air-to-water units (AWHPs) and ground source units (GSHPs, which include heat pumps that extract heat from ground or water). The reported data highlight that air source units have been the most widespread solution in the heat pump market: only a share that ranges between 10% and 20% of yearly heat pump sales covered by ground source devices. Moreover, compared with a

slightly decrease of ground source heat pumps market during last years, air-to-water units sales have significantly increased.

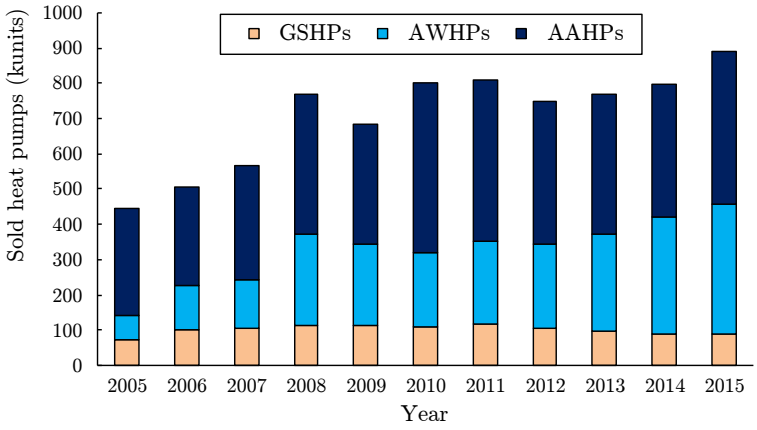

Figure 1.6. Heat pump sales in the European Union market (from [8]).

In addition, the EHPA Statistic Report [8] highlights how the heat pump European market continues to be characterized by three main trends:

- air is the most employed energy source for heat pumps;
- domestic hot water (DHW) heat pump systems are the most promising market segment within Europe. Domestic hot water systems combine a heat pump and a hot water thermal storage and they may be sold as stand-alone units, with the heat pump and the tank combined in the same device, or as separate systems. In 2015 about 118 000 domestic hot water heat pumps were sold in Europe, corresponding to an increase of about 4% over 2014 sales and as much as 84% over 2012 sales;
- large heat pumps for industrial, tertiary and district heating applications are widespread solutions. They often employ geothermal or hydrothermal energy sources, but also for this kind of systems air is an attractive thermal source.

In [8] EHPA puts in evidence that the installed electric heat pump units delivered in 2015 about 148 TWh (12.7 Mtoe) of thermal energy, including 95 TWh counted as renewable energy. The difference between the total thermal energy and renewable energy is linked to the electrical energy consumption of the heat pumps. In this sense, the use of heat pumps allowed to save about 121 TWh

of final primary energy in 2015 and this kind of systems contributed to about 24 Mt of CO_2 emission savings.

Finally, EHPA reports that the revenue generated by heat pump sales was about 5.7 billion euro in 2015 (including VAT), corresponding to an increase of +10% compared to the result of 2014 [8]. Air-to-water units account for about 37% of this total (31% non-reversible and 6% reversible devices, respectively), while reversible air-to-air heat pumps mainly used for heating account for about 31% of the total revenue. Geothermal and hydrothermal systems (merged within the ground-source category) dedicated to heating purposes account for 25% of this turnover. EHPA also highlights that the European heat pump industry directly employs 48 073 workers in Europe, 36% involved in unit manufacturing, 18% involved in component manufacturing, 16% dedicated to service and maintenance activities and 30% in installation.

1.3. Motivation and main goals of the Thesis

As pointed out in Section 1.1, the EU Member States have to deal with the challenges associated to climate changes.

The buildings sector, which includes both residential and services sectors, represents about 39% of the final energy consumption in EU [1] during 2015. Besides its significant energy consumption, the buildings market is considered one of the most suitable sectors to reach the EU energy targets. due to its high savings potential. Within the whole EU residential buildings energy demand, the consumption for space heating and hot water production account for about 79% of total final energy use (192.5 Mtoe) [1]. Cooling is at the moment a small share of entire final energy use, but the cooling energy demand from households has strongly increased during last years.

Besides the focus to significantly improve the energy efficiency of the building envelope (both for new and refurbished buildings), it is also needed to increase the diffusion of renewable energy appliances. With the electricity generation becoming a competitive and cleaner solution by means of photovoltaic panels, this period is a profitable occasion to decrease the consumption of fossil fuels and to promote the adoption of high efficient devices, which employs renewable energy sources, for space conditioning. For these reasons, electric heat pumps are one of the most suitable solutions for energy efficiency improvement in buildings.

Several studies have demonstrated that heat pumps are a very promising technology to enhance the building sector decarbonization and to decrease the primary energy consumption in the EU countries ([9], [10]). Nevertheless, the accurate evaluation of the energy savings achievable by using electric heat pumps is generally a difficult task for the designers of HVAC systems due to the dependence of the achievable energy savings by several factors which are in many cases difficult to evaluate by designers.

More in detail, the run-time performance of these devices (thus, their energy consumption) depends by many parameters like the climate, the building thermal loads, the heat pump capacity modulation, the hydronic loop adopted to couple the heat pump and the emitters and its thermal inertia, the heat pump size and, last but not least, the interactions among the multiple control logics adopted for each component of the HVAC system (i.e. terminal units, heat pump, circulating pumps).

According to the above-mentioned reasons, the optimal desing and the correct evaluation of the seasonal performance of electric heat pump systems is still an open problem for designers. This last aspect becomes crucial because heat pumps work at full load only for a limited period of the heating/cooling season and for this reason in the calculation of the seasonal efficiency the behavior of heat pumps at partial loads must be carefully evaluated. As recalled, the energy performance of heat pumps are strongly influenced by the capacity of the unit to maintain high values of efficiency at partial loads. For a designer this kind of detailed analysis can be complicated for the lacking of available accurate data about the performance of heat pumps far from the rated conditions: large part of the heat pump manufacturers still avoid to give detailed information about this point on their technical data sheets.

Furthermore, the analysis of the literature points out that the evaluation of the seasonal performance and the energy saving potentiality of systems based on different kinds of electric heat pumps (i.e. single-stage, multi-stage, inverter-driven), with respect to traditional heating and cooling systems, is still missing. Moreover, this topic has not yet been completely clarified also in current technical standards

This Thesis is aimed to present a series of models developed in order to evaluate the seasonal efficiency of different typologies of reversible air-source heat pump systems. The developed models have been used to assess and optimize the seasonal performance of these components, taking into account the influence of the main parameters recalled before. In addition, in this Thesis the analysis and

the optimization of different control strategies applied to the heat pump system has been performed in order to show their effects on the energy performance of these systems.

The main contributions of this work are the assessment of a series of optimal sizing rules for air-to-water heat pump systems with the aim to obtain the best exploitable performance of the system as a function of climate, building thermal load and heat pump characteristics. The relationship between external conditions, heating and cooling required load, the control logic and the overall system efficiency is highlighted in order to provide a complete set of technical information to HVAC designers.

1.4. Thesis outline

This dissertation presents a series of models based on the bin method and the dynamic simulation having the goal to help manufacturers and designers with the optimization of thermal plants based on an air-to-water heat pump.

First of all, in order to introduce the subject of this Thesis, a classification of the most common heat pump systems available in the market is shown, as well as a review of different control strategies typically employed with this kind of systems, is presented in Chapter 2.

Chapter 3 summarizes the methodology proposed by actual standards to calculate the seasonal performance of heat pump systems. This calculation procedure, based on the bin method, is deeply described and its critical points are discussed. In the second part of Chapter 3 a new mathematical method for the simulation of air-to-water heat pump systems, still based on the bin method, is presented. Through the proposed method it is possible to calculate the seasonal efficiency of different typologies of heat pumps which are not taken into account by the standards like multi-stage heat pumps (MSHPs) and inverter-driven heat pumps (IDHPs). In the final part of Chapter 3 a series of applications of the described model is presented and the influence of climate, modulation capacity, as well as heat pump sizing, on the seasonal performance of the system is investigated.

In Chapter 4, new models for the dynamic simulation of air-to-water heat pump systems are presented and discussed. The dynamic models have been developed by means of the software TRNSYS and allow to simulate the behavior of the above-mentioned heat pump typologies (i.e. On-off HPs, MSHPs and

IDHPs) and of the other components of the HVAC system to which they are coupled, such as the hydronic loop and the terminal units. The developed models are used to analyze and optimize the seasonal performance of heat pump systems as a function of the hydraulic loop configuration, the thermal inertia of the distribution system and the heat pump control strategy. A series of case studies, aimed to highlight the potential of the developed dynamic models, is presented.

Finally, Chapter 5 summarizes the main achievements of this work and reports some suggestions and opportunities for future research work.

Chapter 2

State of the art on heat pump applications and their control systems

In this chapter, some introductory concepts and definitions related to the Thesis content are shown. A review of the state of the art of heat pump systems coupled to residential buildings and the main algorithms used by the control system to match the heat pump capacity with the effective load required by the building are introduced and explained.

An overview about the typical methods for the characterization of heat pump systems and the evaluation of their seasonal performance, is presented.

The main control algorithms applied to these systems are discussed, in order to highlight the main advantages and disadvantages of the proposed control strategies.

2.1. Heat Pump systems: basic concepts

A heat pump is a device which transfers heat from a low temperature source to a higher temperature source. Since in nature spontaneous heat flow only occurs from a high temperature media [11] to a low temperature one, a heat pump needs external energy, in form of work or heat, to move thermal energy in the opposite direction of free heat transfer.

One can note that the term " heat pump" could be referred to all devices of a refrigeration system. Anyway, it is a common practice of engineering terminology to relate the term heat pump only to units with predominant heating purpose, in which the useful effect is linked to the high temperature source. On the other hand, the term chiller is referred to devices characterized by prevailing refrigeration aims. Finally, a reversible appliance is a unit which is able to provide both heating and cooling useful effects, alternatively.

Historically, Carnot and Kelvin contrived the first concept of a heat pump already during the 19th century, but the first patent related to a practical heat

pump unit belongs to T.G.N Haldane (1930, [12]). The first heat pump system was installed in Oregon in 1948, but this technology is worldwide available in the market only since the 1970s [13].

As mentioned above, a certain amount of external energy is needed to transfer thermal energy from the cold source to the hot one: a first classification of heat pump systems is proposed according to the characteristics of the cooling cycle. If the cooling cycle is based on an absorption cycle, the device is identified as an Absorption Heat Pump (AHP) while in case of a cooling cycle based on a vapor-compression cycle, the device is a vapor-compression heat pump. Within this category, a further classification can be performed according to the energy source which provides mechanical work: i.e. electricity of fuel. In the first case, we relate to Electrical Heat Pump systems (EHP), while in the second case we relate to Gas Driven Heat Pumps (GHP).

The most diffuse configuration for a refrigeration system is the vapor-compression cycle, coupled to an electrical engine; the logical layout of this kind of system is reported in Figure 2.1.

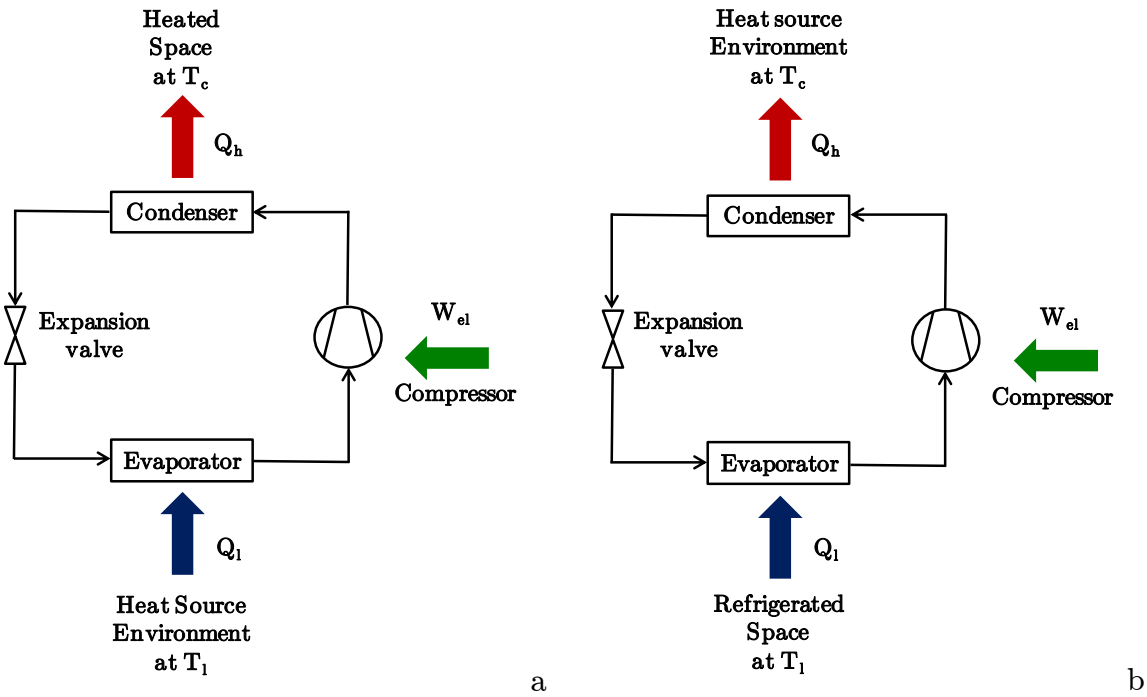

Figure 2.1. Logical scheme of a vapor-compression reversible heat pump: heating mode (a) and cooling mode (b).

In this refrigeration cycle, four main components are involved: a compressor, a condenser, an expansion device and an evaporator. The refrigerant fluid enters in the compressor as a gas, characterized by low pressure and temperature, then it is compressed to the condenser pressure and heated. Then, the overheated gas cools down in the condenser, by means of desuperheating and condensation processes, rejecting heat to the hot heat source. The liquid refrigerant enters into an expansion device (i.e. a capillary tube or an expansion valve) where its temperature and pressure drastically drop. Finally, the low-temperature and low-pressure refrigerant enters in the evaporator, where it absorbs heat from the cold heat source and evaporates. The refrigerant gas leaves the evaporator, re-enters in the compressor and the cycle is repeated.

The energy performance of an EHP system working in heating mode is typically expressed in terms of Coefficient of Performance (*COP*), which is defined as the ratio between the thermal energy rejected to the hot heat source at temperature T_h (i.e. the useful thermal effect) and the total energy input (i.e. the compressor and the auxiliaries electrical power). Similarly, during the cooling mode the performance of the system is evaluated by means of the Energy Efficiency Ratio (*EER*), which is still defined as the ratio between the useful thermal effect (in this case the thermal energy absorbed from the cold heat source at temperature T_l) and the total energy input. The two coefficients can be obtained by the following Equations:

$$COP = \frac{Q_h}{W_{el}} = \frac{Q_h}{Q_h - Q_l} = \frac{1}{1 - \frac{Q_l}{Q_h}} \tag{2.1}$$

$$EER = \frac{Q_l}{W_{el}} = \frac{Q_l}{Q_h - Q_l} = \frac{1}{\frac{Q_h}{Q_l} - 1} \tag{2.2}$$

in which Q_h and Q_l are the heat rejected at the condenser and absorbed at the evaporator, respectively, and W_{el} is the total electrical input of the system.

According to the thermodynamic basic principles, the most efficient cycle is the one that consists of reversible processes (reversible cycle), that is to say a process which can be entirely reversed without any effect on the surroundings. Unfortunately, reversible cycles cannot be performed in practice because of the

unavoidable irreversibilities linked to each process, but they represent the upper limit of the performance of real systems. An ideal heat pump (or a refrigerator) that operates on a reversible cycle is called Carnot heat pump (or Carnot refrigerator); by following the second law of thermodynamics, it is possible for a reversible heat pump (or refrigerator) to replace the heat transfer ratios shown in Eq. (2.1) (or in Eq. (2.2)) with the corresponding heat sources absolute temperature ratios. The maximum efficiency achievable by an ideal vapor-compression cycle (COP_C and EER_C for a heat pump and a refrigerator, respectively) can be calculated as:

$$COP_C = \frac{1}{1 - \frac{T_l}{T_h}} \tag{2.3}$$

$$EER_C = \frac{1}{\frac{T_h}{T_l} - 1} \tag{2.4}$$

These are the maximum theoretical efficiencies of a heat pump or a refrigerating system which operates between the heat sources temperatures T_h and T_l. Real systems cannot reach those values but it is possible to approach them by improving the system design [11].

It is clear from Eqs. (2.3) and (2.4) that the energy performance of an EHP system increases when the difference between heat sources temperatures decreases; for that reason, heat pump designers pursue the highest value of cold source temperature and the lowest value of hot source temperature. As an example, a measure such as the improvement of insulation level in a building would decrease the supply temperature which the heating system has to provide, improving the energy performance of a heat pump.

In addition to thermodynamic constraints, the effective evaporating/condensing temperatures are necessarily lower/higher than the ones of the corresponding cold/hot heat sources. The real performance of this kind of systems is strongly affected by the temperature difference between the refrigerant fluid and the heat sources: higher energy efficiency can be achieved improving the heat transfer coefficients and/or by means of larger heat exchangers. In

conclusion, the design of the heat pump components strongly influences the overall performance of the system.

2.2. Classification of electrical heat pump

Heat pump systems classification can be performed according to different criteria, as the heat sources medium, the fluid used for energy distribution, the thermodynamic cycle (i.e. vapor-compression or absorption cycle, as presented below) and the capacity modulation capability.

According to ASHRAE Handbook [14], in this Thesis heat pumps are classified referring to the external heat source (i.e. low temperature medium in heating mode and high temperature medium in cooling mode). More in detail, we refer to:

- Air Source Heat Pumps (ASHP), when the external heat source is air;
- Ground Source Heat Pumps (GSHP), when the external heat source is ground or water.

Within the last category, many different technologies and systems may be considered: Surface Water Heat Pumps (SWHPs), when they use water from lakes, ponds, etc.., Ground Water Heat Pumps (GWHPs), when they extract water from the soil by means of wells and Ground Coupled Heat Pumps (GCHPs), when the heat is extracted or rejected to the ground through a heat transfer liquid (brine, a solution of water and glycol).

2.2.1. Surface Water Heat Pumps

Surface water can be a very suitable heat source or sink. Thermodynamic properties of water, as the maximum density occurring at 4°C and not at the freezing point, leads to significant heat pump operation advantages: in case of building located in proximity of relevant water bodies, SWHP systems represent the most effective solution ([16]-[19]) for heating and cooling plants. Several water circulation configurations are possible and the more common are classified between open-loop systems and closed-loop systems.

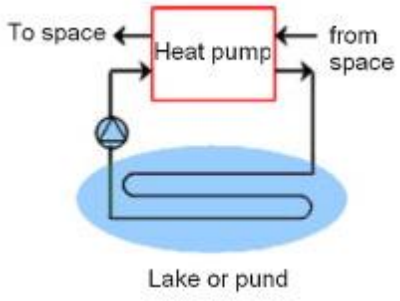

Figure 2.2. Logical layout of a SWHP system (from [15]).

A closed-loop system is characterized by a coil submerged in the water body (see Figure 2.2 from [15]). Heat is exchanged to or from the heat source by means of the heat transfer liquid, which circulates along the coil. In a open-loop system the water is drawn from the surface aquifer, it crosses an heat exchanger and it returns to the water body in point different to the one in which it was extracted. For heat pumps operating in heating mode, this configuration is limited to warmer climates, because the intake water temperature must remain above 5-6°C to avoid freezing.

2.2.2. Ground Water Heat Pumps

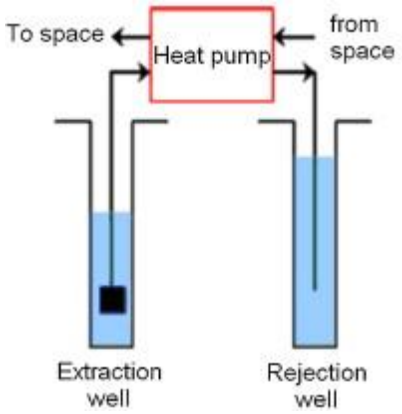

Figure 2.3. Logical layout of a GWHP system (from [15]).

A ground water heat pump system extracts water from the soil trough a well and delivers it to the heat pump or to an intermediate heat exchanger [15]. The former solution, which defines the so-called direct systems, is recommended only on very small applications; on the other hand, the latter solution, typical of the

open-loop configuration, employs a heat exchanger between the refrigerant fluid and the ground water, which is subject to fouling and corrosion issues. In both configurations, the water must be re-injected into the soil by a separate well.

The use of water, either surface or ground water, as heat source involves interesting energy performance (see for instance [15], [20]-[23]), but external factors like public regulations or water quality can restrict the application range of this kind of systems.

2.2.3. Ground Coupled Heat Pumps

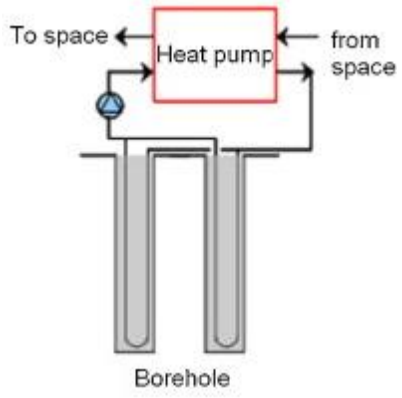

Figure 2.4. Logical layout of a GCHP system (from [15]).

Ground coupled heat pump systems are the last subset of ground source systems; this apparatus is a closed-loop heat pump and consists of a coupled to heat exchangers directly buried in the ground. The use of soil as a heat source is attractive in a heat pump system because the temperature profile of the ground is nearly constant during the year and generally similar to the zone conditions that the system has to guarantee both for heating and cooling modes.

GCHPs are further subdivided according to ground heat exchangers configurations: vertical and horizontal. Horizontal heat exchangers consist of a series of parallel pipes laid out in trenches located at short depth with respect to the ground surface (typically 1-2 m). Different kinds of heat exchangers can be considered, according to the typology and the disposition of pipes [24]: in Figure 2.5a the most common layouts of horizontal heat exchangers are represented. Due to their proximity to the ground surface, the heat source temperature and consequently the heat pump performance is affected by ambient air fluctuation;

furthermore, the laying of horizontal pipes needs more ground area than vertical GCHP systems ([25]-[27]).

For those reasons, the use of vertical ground heat exchangers, typically referred as Borehole Heat Exchangers (BHEs), is the most widespread configuration within GCHP systems (Figure 2.5b). This configuration may include one or several boreholes, each one containing a single or a double U-tube, or a coaxial tube; a typical U-tube is made of polyethylene and has a nominal diameter within the range 20-40 mm, while the borehole is characterized by a diameter ranging from 100 mm to 200 mm and a depth between 20 and 150 m [15]. The borehole is finally filled with a conductive medium (i.e. grout) that prevents the contamination of ground water and ensures a high heat transfer coefficient between the ground and the pipe. Vertical GCHP systems have the significant advantages to require small ground area if compared to horizontal systems and the stability of ground in terms of temperature determines highest heat pump energy performance; on the other hand, these systems present large investment costs, because of the cost linked to drilling ([29]-[31]).

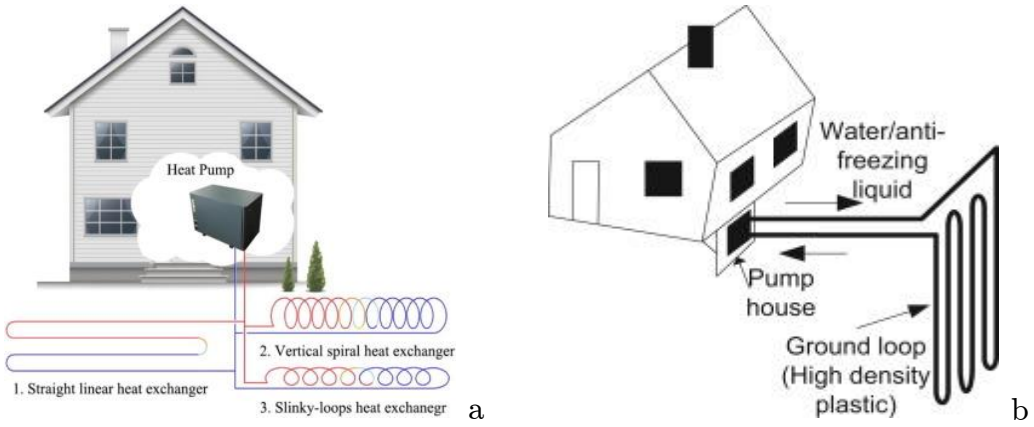

Figure 2.5. Typical layout of a horizontal heat exchanger configuration (a, from [24]) and a vertical heat exchanger configuration (b, from [28]).

2.2.1. Air Source Heat Pumps

Air source heat pumps use air as external heat source from which thermal energy is extracted (in heating mode) or rejected (in cooling mode); outdoor air is the most common heat source employed in this kind of systems, while the use

of exhaust air is restricted to buildings characterized by a mechanical ventilation system [32].

Exhaust air offers advantageous working conditions for the heat pump, if compared to the ambient temperature ones: the temperature of the exhaust air is approximately 20 °C during winter and 26 °C during summer. One drawback of exhaust air heat pumps is an upper limit on the output thermal/cooling capacity, caused by the nominal airflow of the mechanical ventilation system.

An ASHP may be designed for direct conditioning of indoor air or for the connection to a hydronic distribution loop: in the first case we refer to Air-to-Air heat pump systems (AAHPs), while in the former one we refer to Air-to-Water heat pumps (AWHPs). Furthermore, AAHPs may be connected to a ducted air distribution system or they may be designed to exchange heat directly in a room. The ducted air system solution is widespread in the United States market while is uncommon in Europe: especially in the Southern part of Europe, in which cooling loads are predominant and buildings are often characterized by no hydronic distribution system for cooling needs, air-to-air heat pump systems are the most suitable solution.

Air-to-air heat pumps may be designed as a split-unit [33]. A split device is a heat pump configuration in which the components are divided between the indoor and the outdoor space. The outdoor part contains the compressor and the outdoor coil, a finned tube heat exchanger working alternately as an evaporator and a condenser, while the indoor part is composed by the indoor coil, another finned tube heat exchanger that works as a condenser or an evaporator. Air-to-water heat pumps may be designed both as a split unit and as a compact unit [34]. A compact heat pump contains all the subsystems (i.e. compressor, condenser, expansion valve and evaporator) in a unique appliance, which can be installed inside or outside the building. An installation inside the building requires a duct system for ambient air distribution towards the heat pump while an outside installation leads to a reduction of indoor space requirement and noise level.

2.2.2. Developments in air source heat pumps design

As reported by Figure 2.1 the basic hydraulic configuration of an air source heat pump is a single circuit refrigerant loop: the unit is characterized by a fixed speed compressor and the refrigerant flow rate is constant while the heat pump is active, nevertheless the effective values of heat source temperatures and thermal load required by the indoor environment. This kind of systems works at

full load since it is not able to vary the compressor rotating speed and consequently its thermal capacity: this device is called single-stage unit. According to their basic configuration and the relative low installation costs, single-stage heat pumps are the most widespread solution for small size applications, as the conditioning of single-family residential buildings.

Several studies reported that the compressor subsystem is the main source of exergy losses within the heat pump system and it is suitable for energy performance improvements [35]. An improvement of manufacturing tolerances led to the replacement of reciprocating piston compressors with scroll compressors, characterized by approximately 10% additional energy efficiency. Moreover, the separation of suction and discharge processes and the cooling of compressor and electric motor assembly allow to reduce the compressor electrical power up to 16% [36].

In order to improve the efficiency of air source heat pumps, multi-stage compressors can be employed to optimize the energy performance of the system. A multi-compressor heat pump allows to reduce the mass flow rate of refrigerant when the required thermal load decreases: when the temperature difference between outdoor and indoor heat sources decreases (i.e. during the milder part of the heating season), it is possible to switch off one or more compressor stages and reduce the pressure difference between the condenser and the evaporator. For that reason, multi-stage heat pumps are able to modulate their thermal capacity simply by varying the number of active compressor stages; when all stages are active the refrigerant flow rate is equal to the nominal value and the heat pump behavior is equivalent to that of a single-stage unit, while when the thermal load decreases, the stages are switched off and the refrigerant flow rate decreases.

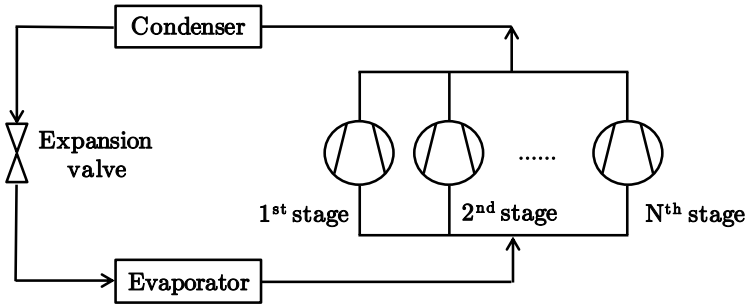

Figure 2.6. Logical layout of a multi-stage heat pump characterized by N-stage compressor linked in parallel.

A logical scheme of a multi-stage heat pump composed by an N-stage compressor is shown in Figure 2.6: all compressor stages are connected in parallel within a single refrigerant circuit. It is important to take into account that at partial loads the heat exchanger surfaces become oversized with respect to the full load operating mode: this effect generally improves the performance of multi-stage heat pumps at partial loads. By observing Figure 2.6 it is evident that all stages of the compressor assembly are coupled to fixed area heat exchangers (i.e. condenser and evaporator); the heat surface of these exchangers has been sized according to the design value of refrigerant flowrate. When one or more stages are switched off the refrigerant flow rate circulating in the unit decreases and the heat transfer coefficient within heat exchangers increases.

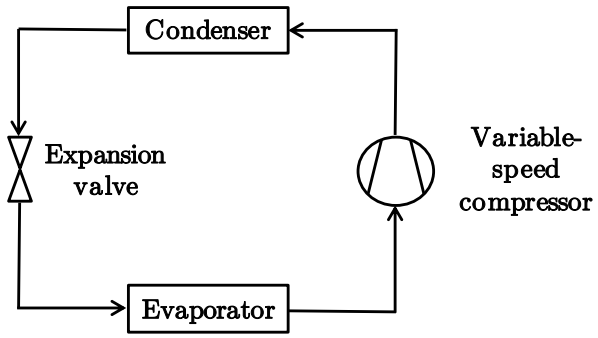

Figure 2.7. Logical layout of an inverter-driven heat pump.

Heat pump units provided with an inverter-driven motor are nowadays the most widespread solution to obtain higher energy efficiency. In units with a variable-speed compressor the refrigerant cycle may operate at different speeds, depending on temperature and heating loads. By adjusting the inverter frequency, thus the compressor rotating speed, it is possible to modulate continously the delivered thermal capacity, avoiding the energy losses caused by on-off cycling within the inverter modulation range. In some heat pump models, the inverter technology may also reduce operating noise and extend the life of the compressor, according to the reduction of mechanical stress linked to on-off cycles.

A logical scheme of an inverter-driven heat pump is shown in Figure 2.7.

2.2.3. Frosting and defrosting cycles

Although ASHPs are the most widespread systems in mild climates, they have some limitations since, as the outdoor air temperature decreases, their efficiency decreases, as indicated by Eq. (2.3) for an ideal heat pump. Moreover, when outdoor air temperature drops below a threshold value, depending on several parameters as air humidity ratio, outdoor heat exchanger geometry and heat pump control logic, the evaporator freezes and the system efficiency is reduced. This is one of the main reasons why ASHPs are not commonly installed in cold and humid climates.

As mentioned before, at low ambient temperature frost can be accumulated on the external surface of the outside heat exchanger of an ASHP. This phenomenon worsens the heat transfer from the outside air to the refrigerant fluid because of the additional thermal resistance given by the frost layer; in order to recover the proper efficiency of the system the ice must be removed by using a defrost cycle.

The physical phenomena underlying the frost formation on the outdoor coil is well known. During the heat pump working mode, the outdoor heat exchanger works as the evaporator and extracts heat form the outdoor air. If the wall temperature of the outdoor coil is lower than the air dew point temperature, condensation occurs on the heat exchanger surface; furthermore, if the wall temperature is also below the freezing point of water (i.e. 0 °C), the condensed water freezes and a frost layer grows up.

Several authors have focused their research on experimental and theoretical studies of frosting characteristics ([37]-[39]). According to [37] the presence of a frost layer can reduce the heat flux from the ambient air to the refrigerant by about 40%, while the experimental results reported by [38] and [39] put in evidence that the heating capacity of an air source heat pump is decreased up to 35% when the outdoor heat exchanger is covered by frost.

For above-mentioned reasons, periodic defrosting cycles are needed to restore the original capacity of the evaporator and thus improve the energy efficiency of the unit, although defrosting itself consumes energy and can generate an undesired fluctuation of the indoor air temperature. Several defrosting methods have been developed in order to remove the frost layer [40]: natural defrosting, refrigerant reverse-cycle, hot gas bypass, sensible heat defrosting method, dielectric barrier discharge, ultrasonic wave method; although all the referenced

methods are energy efficient procedures, the real defrosting efficiency depends on the accuracy and precision of defrost control strategy.

Various defrosting control methods have been developed and described in literature [41], such as fan power sensing, temperature difference control, air pressure difference, refrigerant superheating degree, fan power, frost thickness, artificial neural network, photoelectric technology. Nevertheless, temperature-time control strategy is the most widespread used defrosting method [42]. As reflected by its name, temperature-time control logic is based on temperature and time and is adopted in most ASHP units due to its simplicity. The outdoor heat exchanger (evaporator) surface temperature is monitored: when this temperature drops below a threshold value, for example 3°C, the controller starts to measure the heating operation time. Then, when the wall temperature decreases below a second threshold value (i.e. -3°C), and the operation time is higher than a standard defrosting period (as an example 45 minutes), a defrost cycle will be performed by the heat pump. However, the reliability of this method can be considered questionable; in fact, this procedure avoids to take into account the role played by one of the main parameters which affects the ice formation: air humidity

For the above-mentioned reasons, in practical applications defrosting cycles are sometimes carried out improperly, when a "critical" amount of frost has been accumulated or when no frost was developed on the outdoor coil surface.

2.3. Control systems: basic concepts

The control of a generic physical system means to impose a desired mode of operation on all the components of the system. This is typically expressed by the request to maintain an output variable $X(t)$, said controlled output, as close as possible to its set point value $X_{SP}(t)$, which specifies the desired time trend. This aim is achieved by acting on the system by means of an input signal $u(t)$, indicated as control input (or control signal) [43]. The component of the heat pump system which determines, time by time, the control signal in order to guarantee a proper monitoring of the reference signal is the controller.

The evaluation of the optimal value of the control signal is not generally a simple issue because the time behavior of the control variable depends not only from the control signal, but also by other variables ($d(t)$) not directly controllable

(disturb). In Figure 2.8 the logical scheme of a generic controlled scheme is reported.

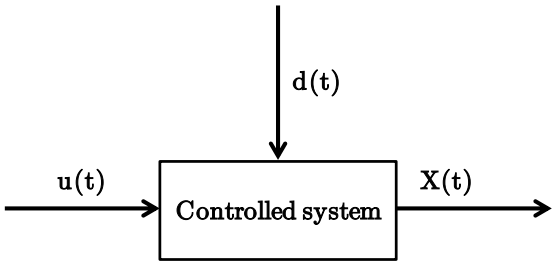

Figure 2.8. Logical scheme of a generic controlled system.

For the calculation of the control signal *u(t)* at a generic instant *t*, the controller may use several information: the most valuable information needed by the controller is the set-point signal $X_{SP}(t)$, while other data may relate to the value of the disturb *d(t)* and the controlled output value *X(t)*.

It is possible to identify various control schemes, which differ one another according to the type of information used by the controller for the calculation of the control signal. The most widespread scheme is the closed-loop (or feedback) control scheme: in Figure 2.9 an overview of a feedback control of a generic system is shown.

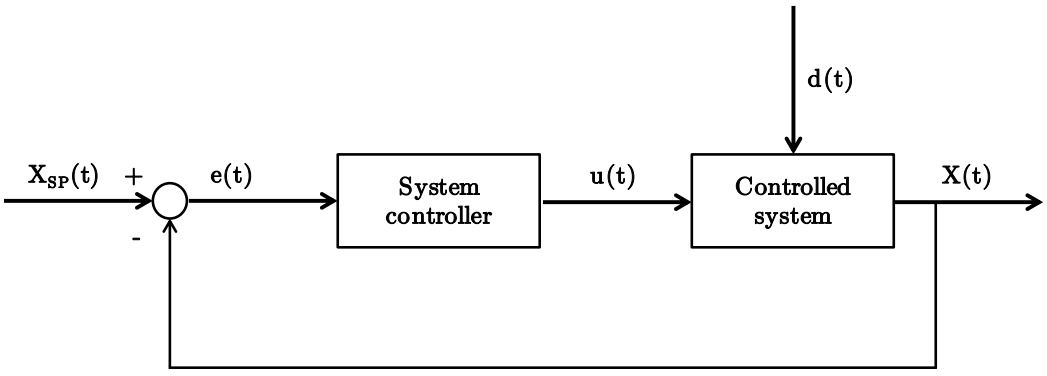

Figure 2.9. Logical scheme of a closed-loop control system.

To be noted that the controller, after receiving a signal relating to the controlled variable *X(t)* and after comparing this value with that of the reference variable $X_{SP}(t)$, calculates the error *e(t)* (i.e. the difference between the two variables) and uses this value to evaluate the control action *u(t)*.

As mentioned above, an automatic controller compares the actual value of controlled variable with the reference signal value, evaluates the in-time deviation from the set-point and calculates the value of control signal that brings the error within the prefixed range.

The most common controllers are classified into two categories based on their control action:

- On-off controllers, also indicated as two state controls;
- Proportional-Integral-Derivatives controllers, also known as PID controllers.

2.3.1. On-off controllers

The on-off controllers have only two operating conditions that, in the case of the control of thermal or cooling capacity of a heat pump system, correspond to the following states: "compressor on" or "compressor off". Referring to nomenclature reported in Figure 2.9, the behavior of an on-off controller can be summarized as follows:

$$u(t) = \begin{cases} u_1 \ \ if \ \ e(t) > 0 \\ u_2 \ \ if \ \ e(t) < 0 \end{cases} \tag{2.5}$$

where u_1 and u_2 are the maximum and the minimum value of the control signal, respectively. These two values of the control signal may correspond to "on" and "off" states, which are imposed by the controller depending on whether the error is negative or positive.

The schematization reported by Eq. (2.5) represents the ideal behavior of an on-off controller; however, this operation mode has a problematic drawback: when the output variable $X(t)$ reaches the set-point value $X_{SP}(t)$, the controller tends to switch the system from one state to another with an excessive frequency, trying to eliminate the error. An excessive switching frequency involves a series of problems, which will be further discussed. To overcome this problem, real systems involve the use of on-off controllers with a hysteresis cycle, whose characteristics are highlighted in Figure 2.10.

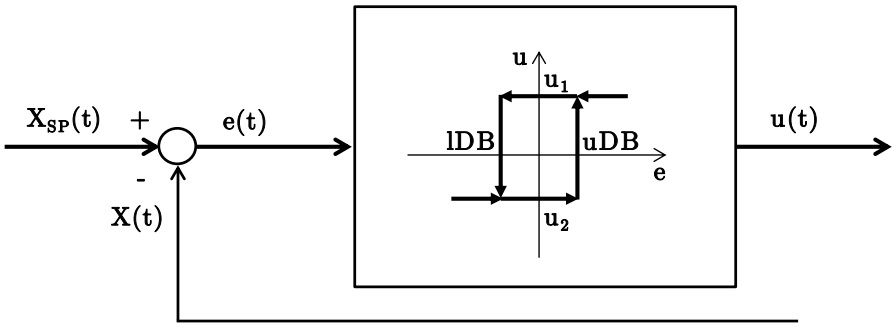

Figure 2.10. Highlight on the hysteresis cycle of an on-off controller.

In these controllers, the switch from u_1 to u_2 occurs not when the error $e(t)$ is larger than zero, but when it exceeds a threshold value, the upper Dead Band (uDB). In a similar way, the switch from u_1 to u_2 occurs when the error falls below another threshold value, the lower Dead Band (lDB). The values of lower and upper dead bands are also called differential thresholds. According to this control algorithm it is possible to obtain a finite switching frequency from one state to another and, by adjusting the threshold values, to impose an acceptable switching frequency. This reduction of the switching frequency is not completely free: the error is not strictly zero during the normal operating mode, but it will fluctuate within the range [$-lDB$; $+uDB$]. The algorithm imposed by an on-off controller with hysteresis cycle is described by the following Equations:

$$\text{if } u(t-1)=u_2 \begin{cases} u(t)=u_2 \text{ if } e(t) < lDB \\ u(t)=u_1 \text{ if } e(t) > uDB \end{cases} \tag{2.6}$$

$$\text{if } u(t-1)=u_1 \begin{cases} u(t)=u_2 \text{ if } e(t) < -lDB \\ u(t)=u_1 \text{ if } e(t) > -lDB \end{cases} \tag{2.7}$$

2.3.2. PID controllers

PID controllers are control devices in which the control signal $u(t)$ is generated by the sum of three contributions, respectively proportional action, integral action and derivative action. First, they are considered separately and then the contributions will be evaluated in an integrated way.

In a PID controller with proportional action only (Figure 2.11) the control signal *u(t)* is proportional to the error signal *e(t)*. The input-output relationship, shown in Figure 2.11, can then be expressed as follows:

$$u(t) = K_p e(t) \tag{2.8}$$

where K_p is the action proportional coefficient or proportional gain.

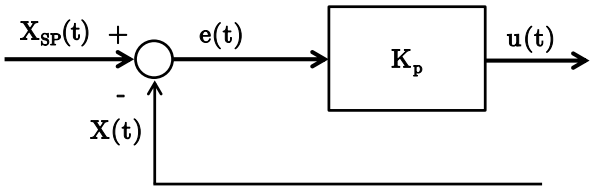

Figure 2.11. Logical scheme of pure proportional (P) controller.

In a PID controller with the only integral action (Figure 2.12), on the other hand, the control signal *u(t)* is proportional to the integral of the error signal *e(t)*. The input-output relationship is then evaluated as:

$$u(t) = K_i \int_0^t e(\tau) d\tau \tag{2.9}$$

where K_i is called integral action coefficient or integral gain.

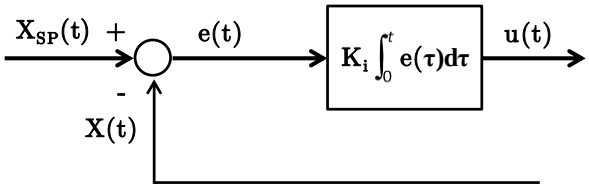

Figure 2.12. Logical scheme of pure integral (I) controller.

Finally, in a controller characterized by a single derivative action (Figure 2.13) the control signal *u(t)* is proportional to the derivative of the error signal *e(t)*. The relationship between the control signal and the error is shown in Fig. 3.8 and in Eq. (2.10):

$$u(t) = K_d \frac{de(t)}{dt} \tag{2.10}$$

where K_d is the coefficient of the derivative action or derivative gain.

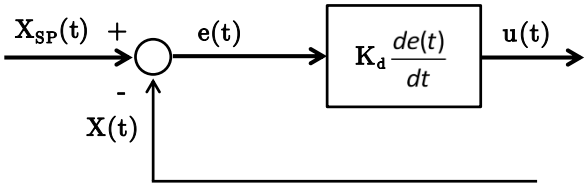

Figure 2.13. Logical scheme of pure derivative (D) controller.

More generally, a PID controller calculates the value of the control variable *u(t)* as the sum of the proportional, integral and derivative contributions, following the relationship:

$$u(t) = K_p e(t) + K_i \int_0^t e(\tau) d\tau + K_d \frac{de(t)}{dt} \tag{2.11}$$

It is common practice to write Eq. (2.11) as follows:

$$u(t) = K_p \left[e(t) + \frac{1}{T_i} \int_0^t e(\tau) d\tau + T_d \frac{de(t)}{dt} \right] \tag{2.12}$$

in which T_i and T_d are the characteristic integral and derivative time, respectively.

2.3.3. A typical control algorithm of a heat pump system

In this Section, the basic principles of control theory reported in previous section are applied to a real system. Typically, in an air-to-water heat pump system the controlled output *X(t)* is the temperature of the return water $T_r(t)$ (condenser inlet in heating mode); this temperature must be as close as possible to the reference signal $X_{SP}(t)$, i.e. the temperature set-point evaluated by the designer during the system design phase and imposed by the controller.

The compressor controller receives information on the return water temperature at the heat pump inlet, compares this value with the set-point by calculating an error and, according to the magnitude of the error, sends a control signal to the compressor.

The logical scheme of this control loop is represented in Figure 2.14, where $T_{r,SP}(t)$ is the temperature set-point of the heat transfer fluid (water in this case) ingoing to the unit, $P_{th}(t)$ is the thermal power delivered by the compressor and $T_r(t)$ is the effective temperature of the water at the unit inlet. The heat pump system is coupled to a variable load, which represents the disturb $d(t)$ introduced in Figure 2.8. Depending on the controller typology, the value of the output control variable influences the compressor state.

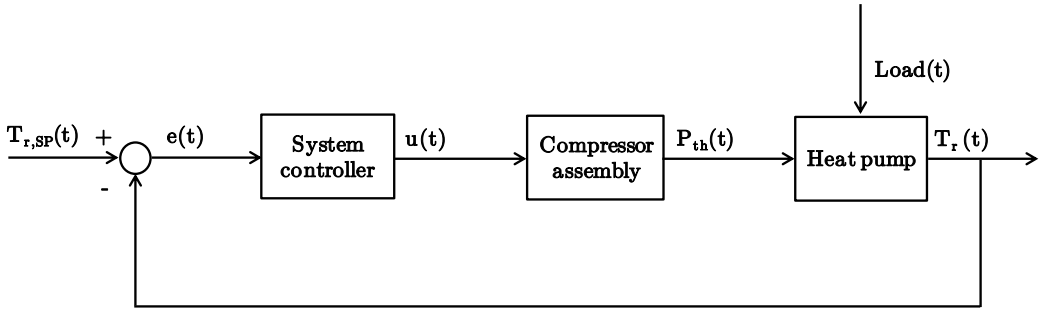

Figure 2.14. Logical scheme of the control loop of a heat pump system.

In case of an on-off controller the control variable $u(t)$ can assume only two possible values, u_1 and u_2, which corresponds to the "on" and "off" states of the compressor, respectively. As an example, we consider the heating operating mode; when the return temperature of the heat transfer fluid $T_r(t)$ exceeds the set-point temperature $T_{r,SP}(t)$ plus the upper dead band uDB, the compressor control variable takes the value "on" and the compressor delivers a certain thermal power $P_{th}(t)$ to the terminal units. On the contrary, if $T_r(t)$ is lower than $(T_{r,SP}(t) - lDB)$, the compressor control variable assumes the "off" value and the heat pump is switched off.

A PID control algorithm is typically employed by the controller of an inverter-driven heat pump in order to modulate the thermal or cooling capacity supplied to the system. As in the case of the on-off control system, the control variable and the reference variable are respectively the temperature of the return water T_r and its set-point temperature $T_{r,SP}$. However, while for the on-off controller the control signal $u(t)$ can assume only two values, in the case of PID controller the

control variable represents the rotational frequency of the inverter (thus, the compressor rotational speed) and may assume, ideally, an infinite number of values. In a real heat pump system, a lower and an upper limit on inverter frequency are imposed, which correspond respectively to the minimum and the maximum rotational speed suggested by the compressor manufacturer.

2.4. Influence of the control system on the energy performance of a heat pump system

All air conditioning and refrigeration systems, whether they are functional to the heat or cold production, operate for most of the operational time at partial load.

Historically, the most common mode for the modulation of thermal or cooling capacity is represented by intermittent operation of the generating unit. According to its simple operating principle, the on-off control strategy is even today the most widespread adopted solution, especially for small size systems [44].

Unfortunately, the on-off control logic is characterized by a series of problems, both of technical and energetic nature. The first problem, well-known to designers, is the need to limit the maximum number of unit startups per hour [45]. An excessive frequency of on-off cycles would drastically reduce the operative life of the compressor: in fact, it requires for each startup of the unit a surge current needed to reestablish the pressure ratio between high and low pressure sides; this surge current is higher than the steady state absorbed electrical power and causes an increase in temperature of the electric coils of the motor. For that reason, compressor manufacturers report in their technical datasheets the maximum allowed frequency of startups to avoid mechanical stress: a typical value of the maximum on-off frequency is 6 on-off cycles/hour [46]. The number of on-off cycles performed by a heat pump is still an open problem for designers and it will be further discussed in this thesis.

During on-off energy cycling losses are present; these losses are due to the increasing electrical energy absorbed by a unit operating with intermittent regime, if compared to the electrical energy absorbed by the unit working in steady state, under the same operating state (i.e. with the same evaporation and condensation temperature). Several authors ([47]-[51]) investigated in the past the phenomenon of cycling losses, realizing the strong influence of this kind of energy losses on the performance of the system, especially in presence of an on-off control strategy. It was found that, depending on the unit and the considered

working conditions, a continuously operating system can lead to an increase, in terms of energy efficiency, between 5% and 25% compared to the same unit operating cyclically.

It was shown that the main reason of these energy losses is the migration of refrigerant fluid from the high-pressure side to the low pressure side of the unit during the off phase, which is coupled to the equalization of the evaporation and condensation pressures. For that reason, at each start-up of the unit, the performance of the heat pump is reduced during the whole duration of the start-up period: the compressor must restore the pressure difference between condenser and evaporator and the thermal (or cooling) capacity of the unit gradually increase up to its steady state value.

A suitable solution to mitigate the above-mentioned problems may be the adoption of multi-stage and variable-speed compressors, able to modulate the thermal capacity supplied to the load. The evaluation of the number of stages switched on is performed by means of a multi-level on-off controller, where each level follows an on-off algorithm, as explained in Section 2.3.1. On the other hand, in an inverter-driven heat pump the adjustment of the rotation frequency of the compressor is typically carried out by a PID control in which the controlled variable is the supply or the return temperature of the thermo-vector fluid (i.e. water in an AWHP) as explained in Section 2.3.2.

It is important to highlight that although the modulation capacity of variable-speed volumetric compressors is not infinite, since the compressor is designed to work until minimum frequencies between 15 Hz and 30 Hz, depending on the operating conditions, the adjustment of inverter frequency allows to reduce the number of startups of the unit, if compared to the classic on-off control logic. For this reason, the issues related to cycling losses and compressor mechanical stress play a less critical role in presence of variable-speed compressors.

Finally, a further advantage of the thermal (or cooling) capacity modulation performed by multi-stage or variable-speed compressors is the reduction of the pressures ratio at partial loads with respect to those of equivalent units controlled by the traditional on-off control logic. It must be considered that a modulating heat pump delivers to the system the same output energy of a single stage unit but in a longer time scale. It follows that, with a modulating system, it is possible to work with an average temperature of supply water significantly lower than that supplied by the same unit operating intermittently [52]. A lower average temperature of the supply water during the on-period allows to operate with a

lower average condensation temperature, if compared to an on-off unit, obtaining a higher average *COP* (see Eq. (2.1)).

Until now we have listed the main energy benefits of thermal capacity modulation through multi-stage or variable speed compressors (compared to the fixed speed compressor units). Several authors have, however, pointed out how the use of modulating units is not devoid of disadvantages.

A first disadvantage, which directly influences the performance of a heat pump (or refrigerating) modulating unit, is related to the phenomenon of reduction of the isentropic compression efficiency by varying the compressor rotation frequency with respect to the rated frequency [53].

For high rotation frequencies, the decrease of the isentropic efficiency is due to the increase of the pressure drop losses of the refrigerant in the suction and discharge chambers of the compressor; on the other hand, the drastic reduction of the isentropic efficiency at low rotational frequencies is due to the decreasing oil seal between high and low pressure compressor rooms ([53], [54]).

The above-mentioned energy losses, linked to reduced isentropic efficiency obtainable in particular operating conditions, are typical of variable-speed compressors, since fixed speed compressors (thus controlled according to an on-off logic) are designed to have a maximum isentropic efficiency in correspondence to their only working rotation frequency.

A further disadvantage of variable-speed compressors is the need of an inverter, generally characterized by electrical efficiencies that range between 95% and 98%, depending on the rotation frequency considered [53].

The main drawback of a multi-stage heat pump is related to a particular working condition: when the unit operates outside its modulation range (i.e. the unit is working with only the first stage active and it is not possible to further modulate the delivered thermal capacity), it performs a higher number of on-off cycles with respect to an equivalent single stage heat pump [55]. As will be further investigated in this thesis, the typical control algorithm of a multi-compressor heat pump may be improved in order to increase the energy performance of the system.

Finally, if we consider the use of the auxiliary components of the heating system, as circulating pumps and fans, which are not generally modulating, their energy consumption will be higher in a multi-stage or inverter-driven heat pump system because, with the same thermal energy delivered to the load, they must work for more time with respect to the case of a single-stage unit.

Chapter 3

Air-to-water heat pumps modeling and seasonal performance evaluation through the bin-method

In this chapter, a review of the methods for the modeling of heat pump systems is firstly presented. More in detail, the procedure reported by the current European standard EN 14825 [56] and Italian standard UNI/TS 11300-4 [57] is described and compared to other simulation models presented in literature.

An extension of the bin-method procedure reported by the above-mentioned standards is described, highlighting the possibility of the seasonal performance evaluation of modulating heat pumps, which is not contemplated by the above-mentioned standards.

Results obtained by applying the proposed mathematical procedure to several case studies are presented: the system optimal sizing rules are pointed out, in relation to the location, the characteristic of the thermal load and the heat pump control logic.

3.1. Heat pump performance modeling

Various approaches for the modeling of heat pump performance are available in literature. Several models, with the aim to improve the heat pump performance from a thermodynamic point of view, analyze each single component of the heat pump system, such as the evaporator, the compressor, the condenser and the expansion valve, and investigate the performance of the individual element of the unit. These models are generally based both on the resolution of physical equations and on numerical correlations derived from experimental results ([58]-[62]); a fewer number of models ([63]-[65]) is instead based on CFD simulations of the single devices (i.e. evaporator, condenser, etc...). A common aspect of these kinds of models is their very high computational time required to simulate the behavior of a heat pump and evaluate its energy performance.

Kinab et al. [59] developed a simulation model able to assess the heat pump performance by means of detailed sub-models for each component of the unit. The heat pump model evaluates the values of *COP*/*EER* for different part load conditions and external temperatures; on the other hand, the model of the building to which the heat pump is coupled provides a series of weighting coefficients to calculate the seasonal performance of the system.

Tangwe et al. [60] developed a mathematical model of a small size air-source water heater heat pump, based on multiple linear regression, by means of the simulation environment MATLAB/Simulink. The model was calibrated according to an experimental monitoring campaign on the real device: a data acquisition system was employed to assess the predictors of the electric power input and the delivered thermal capacity of the heat pump. Moreover, an optimization of the regression coefficients used in the mathematical model was performed by using the linear least squares method, in order to minimize the influence of measurement errors.

Ibrahim et al. [61] presented a dynamic model of an air-source heat pump water heater employing the moving boundary approach for both heat exchangers of the heat pump (i.e. condenser and evaporator). Furthermore, in this work the influence of the use of mini-tubes condensers on the energy performance of the unit was assessed, by considering a condenser immersed in a water storage tank. The developed mathematical model considers static approaches to simulate the behavior of compressor and expansion valve, since their dynamics are much faster than those of heat exchangers. On the contrary, the moving boundary approach allows to handle transient load changes, to simulate the complex behavior of heat exchangers and to maintain low computational time, preserving the simplicity of lumped parameters approach.

Finally, Aprile et al. [62] implemented a mathematical model of a gas-driven absorption heat pump by means of the FORTRAN code. The authors started from modular simulation models specifically developed for absorption cycles and added new components. The numerical model was validated according to the experimental analysis of the heat pump performance, evaluated at full load and at partial load, as a function of the part load factor and the hot water temperature.

If we consider simulation models based on the CFD approach, for example, Huisseuine et al. [63] studied the effect of punching delta winglet vortex generators placed on the louvered fin surface of the outdoor heat exchanger of a heat pump. Their work pointed out that the delta wings allow to reduce the size

of heat exchanger tubes enhancing the heat transfer and obtaining a more compact device.

Congedo et al. [64] developed a CFD model of a horizontal air-ground heat exchanger system coupled to a heat pump system. In their work the energy performance of the system was evaluated as a function of different environmental conditions, representative of winter and summer Mediterranean climate.

Kong et al. [65] investigated on the thermal performance of borehole heat exchangers coupled to a ground source heat pump, considering a set of different U-tubes profiles (i.e. smooth or with different petals). The analysis was carried out by means of experimental measurements and CFD simulation models (validated through the experimental values); results pointed out that the heat transfer coefficient between U-tubes and ground increases if the inlet velocity increases. Furthermore, the turbulent diffusion effect is increased by adopting U-tubes with different petals but in this case the flow resistance is also increased.

Another simulation approach is based on the analysis of the whole device, avoiding to distinguish among the specific component of the heat pump. According to this approach, the heat pump is considered as a ' black box' , able to deliver thermal or cooling energy to the load; the internal dynamic of the heat pump is neglected (i.e. heat exchangers thermal inertia, compressor efficiency) and the energy performance of the unit depends only on the temperature of the heat sources. By considering the black box approach, the level of detail of models is lower, if compared to individual component simulations, but the computational time required to perform them is strongly reduced. The aim of this category of heat pump simulation models is the maximization of the seasonal performance of the whole system, by the improvement of the system control logic or carrying out a series of optimal sizing rules.

Within the black box simulation models, temperature class methods [66], as the bin-method, where representative operating conditions are weighted with specific multipliers based on time and energy, are one of the most widely used solution. As an example, current standards propose temperature class methods in order to compare different models of commercial heat pumps. These calculation methods are based on the use of simplified maps, in which heat pump performance are reported as a function of several factors, as the temperature values of the heat sources.

The analysis of literature puts in evidence that several researchers employed temperature class methods to evaluate the energy performance of heat pump

systems. As an example, Sarbu et al. [67] developed a computational model for the evaluation of the annual energy consumption of an air-to-water heat pump coupled to a residential building to provide space heating and domestic hot water production. This model is based on the degree-day method and the bin-method defined in the current European standard EN 14825 [56], which evaluates the heat pump performance according to technical performance data given by the manufacturer. The authors presented the assessment of the economic, energetic and environmental criteria which influence the feasibility of a heating system based on an air-to-water heat pump, by considering different system configurations.

Hucthemann et al. [68] implemented a numerical model which considers a black box approach to evaluate the heat pump energy performance. According to the developed model, the heat pump consists of four sub-models (i.e. heat exchangers, expansion valve and compressor), connected one another, which calculate heat flows and the electrical power input by using look-up tables based on manufacturer datasheets. In this case, the heat pump model was parametrized by means of static measurements, evaluated for standard working points. The authors pointed out the influence of the supply water temperature on the seasonal efficiency of an air-to-water heat pump coupled to a single-family house, by varying the system heating curve accorrding to an adaptive control algorithm.

Klein et al. [69] followed the same approach to simulate a hybrid system composed by an air-to-water heat pump and a gas boiler coupled to a 1970s single family home. The heat pump model developed by the authors is table-based, which means that the thermodynamic cycle is not physically modeled; furthermore, the performance of the unit are evaluated by a two-dimensional map, which returns the thermal capacity and the electrical power input of the heat pump as a function of the source (external air) and sink (water) temperatures. Similarly, the boiler efficiency calculation is table-based, using experimental data depending on the return water temperature and the boiler part load factor. Several simulations were carried out to study the influence of the heat pump size as well as the volume of the thermal storage on the energy performance of the system.

Shen et al. [70] proposed an active building envelope, characterized by pipes embedded in the structure, to reduce the thermal losses through the envelope during winter. To reduce the heating system energy consumption, an air-source heat pump was proposed by the authors to provide low-temperature hot water for the pipe-embedded envelope; a numerical model of the whole system was

developed and the hourly values of the heat pump *COP* was evaluated as a function of the condensing temperature, equal to the supply hot water temperature, the evaporating temperature, equal to the external air temperature, the efficiency of electromotor, compressor, heat exchangers and control system of the unit, which are given by the heat pump manufacturer.

Busato et al. [71] assessed the seasonal energetic and economic performance of a heating system based on an air-to-water heat pump, characterized by a fixed-speed compressor operated through on-off cycles. The seasonal efficiency of electric driven heat pumps and gas-engine heat pumps was compared. In order to calculate the heat pumps performance, the manufacturer thermal capacity and *COP* data was employed by the authors: these data were given for a range of temperatures of the heat sources and the unit performance was calculated for a generic operating condition by means of a double linear interpolation of the data.

Naldi et al. [72] developed a hourly computational model able to evaluate the seasonal performance of both single-stage and inverter-driven air-to-water heat pumps through MATLAB environment. If one considers a single-stage unit, the thermal capacity delivered by the heat pump and its *COP* are expressed in the model as second order polynomial functions of the external temperature and the supply hot water, calculated through linear interpolations of manufacturer data. On the contrary, if one considers an inverter-driven heat pump, the same methodology is employed: the polynomial functions are evaluated by considering different values of the inverter frequency. The authors applied this model to to assess the influence of the chosen bivalent temperature (depending on the heat pump size) and of the thermal storage volume on the seasonal performance of a heat pump system coupled to a residential building located in Bologna (Italy).

In conclusion, these methods based on a temperature class approach present several drawbacks, because their application guarantees reliable results only if applied to known components in known configuration systems and they are not suitable to test new unit configurations.

As reported before, the performance maps employed by several models to evaluate the energy performance of heat pump systems, refer to the thermal/cooling capacity and *COP*/*EER* data given by the manufacturers. Heat pump performance are measured in correspondence to standardized values of heat source temperature, according to the method reported by European standards EN 14511-2 [73] and EN 14511-3 [74]. Testing procedures are conducted at defined operating conditions, including ambient air and outlet temperatures, as defined by tables provided by EN 14511-2: an extract of testing conditions for AWHPs

reported by the standard is shown in Table 3.1 and Table 3.2 for heating operating mode and in Table 3.3 for cooling operating mode. In order to analyze the behavior of the heat pump coupled with different terminal units, testing conditions for the indoor heat exchanger are differentiated between low, medium, high and very high temperature applications for heating mode, which correspond respectively to radiant floor, fan-coils, low-temperature and high-temperature radiators, and low and medium temperature applications for cooling mode, corresponding to radiant floor and fan-coils, respectively.

For each application, the standard energy performance (i.e. thermal capacity and *COP* for heating operating mode) of the heat pump is conventionally determined: as an example, if one considers a heat pump coupled to radiant floor (low temperature application), the standard heating capacity and *COP* of the unit are calculated with a dry-bulb air temperature of 7 °C (wet-bulb temperature equal to 6 °C) and rejecting heat to water with a supply temperature of 35 °C and a return temperature of 30 °C. Additional tests are performed with the same water flow rate of the standard test (i.e. the ambient air and the indoor heat exchanger outlet temperatures are defined and the water inlet temperature varies accordingly) for different values of the external air temperature.

Table 3.1. Test conditions for air-to-water heat pumps in heating mode according to EN 14511-2 [73] (Low temperatures).

	Outdoor heat exchanger		Indoor heat exchanger - Low temperature applications	
	Inlet dry bulb temperature (°C)	Inlet wet bulb temperature (°C)	Inlet temperature (°C)	Outlet temperature (°C)
Standard rating conditions	7	6	30	35
Application rating conditions	-15	-	a	35
	-7	-8	a	35
	2	1	a	35
	12	11	a	35

a The test is performed at the flow rate obtained during the test at the standard rating conditions

Table 3.2. Test conditions for air-to-water heat pumps in heating mode according to EN 14511-2 [73] (High temperatures).

	Outdoor heat exchanger		Indoor heat exchanger - High temperature applications	
	Inlet dry bulb temperature (°C)	Inlet wet bulb temperature (°C)	Inlet temperature (°C)	Outlet temperature (°C)
Standard rating conditions	7	6	47	55
Application rating conditions	-15	-	a	55
	-7	-8	a	55
	2	1	a	55
	12	11	a	55

a The test is performed at the flow rate obtained during the test at the standard rating conditions

Table 3.3. Test conditions for air-to-water heat pumps in cooling mode according to EN 14511-2 [73] (Low temperatures).

	Outdoor heat exchanger		Indoor heat exchanger - Low temperature applications	
	Inlet dry bulb temperature (°C)	Inlet wet bulb temperature (°C)	Inlet temperature (°C)	Outlet temperature (°C)
Standard rating conditions	35	-	12	7
Application rating conditions	20	-	a	7
	25	-	a	7
	30	-	a	7

a The test is performed at the flow rate obtained during the test at the standard rating conditions

3.2. Heat pump seasonal performance evaluation according to the European Standard EN 14825

According to the testing procedure reported in the standard EN 14511 and described in the previous Section, only a comparison between single operating

conditions can be performed, but no evaluation of the seasonal performance of the whole heat pump system can be carried out. Recently, many researchers ([58]-[60], [66]-[72]) have proposed several approaches for the rigorous evaluation of heat pump seasonal efficiency, corresponding to the system efficiency during a complete heating/cooling season; the Seasonal Performance Factor (*SPF*) is calculated as the ratio between the total thermal/cooling energy supplied to the load and the total electric energy absorbed by the system (including auxiliary devices) during the season.

The proper evaluation of the seasonal performance of a heat pump system is very problematic for designers, since the efficiency of AWHPs is strongly variable during the season, depending on several parameters. During the heating or cooling season the energy consumption of the heat pump is strongly affected by a series of external factors, like the heat pump operation mode, the working schedule, the variability of building thermal loads, the heating distribution system, the outdoor temperature, which changes continuously in time, and the control system of the heat pump. As we shall discuss later, the last aspect becomes crucial because heat pumps operate at rated conditions only for a small part of the season and for this reason the behavior of the heat pump at partial load strongly influences the overall seasonal performance factor.

The calculation of the heat pump seasonal efficiency is usually performed by a quasi steady-state approach, in which the interval calculation time is fixed equal to one month for heat pumps linked to stable heat sources (i.e. GCHPs); on the contrary, for an air-to-water heat pump, in order to take into account the high variability of the external temperature, the bin-method is typically employed for the evaluation of the seasonal heat pump performance.

The European standard EN 14825 [56] and the Italian standard UNI/TS 11300-4 [57] report the methodology which allows to evaluate the heat pump seasonal performance factors for heating (Seasonal Coefficient Of Performance, *SCOP*) and cooling (Seasonal Energy Efficiency Ratio, *SEER*) modes. The above-mentioned standards reproduce the outdoor climate through the bin-method. A bin represents the number of hours in which the outdoor air has a value of temperature within a fixed 1 K wide interval, centered on an integer value of temperature. As an example, a bin duration of 100 hours in correspondence of an outdoor temperature equal to 10°C means that for 100 hours during the season the external air temperature has a value between 9.5 °C and 10.5 °C.

The standard EN 14825 splits Europe in three winter reference climates (Colder, Average and Warmer) and directly reports the bin profiles for the

heating season of each climate. Bin trend calculation has been performed on the basis of historical weather data series collected over the 1982-1999 period for the locations of Helsinki, Strasbourg and Athens, representative of the Colder (Co), Average (Av) and Warmer (Wa) reference climate, respectively. Regarding the evaluation of the heat pump seasonal performance during the cooling season, the standard [56] indicates a single bin profile for Europe, derived from the weather data series of Strasbourg. The following figures report the bin distribution for the reference climates proposed by standard EN 14825: in Figure 3.1 the bin profiles of the standard heating seasons (Colder, Average and Warmer) are shown, while Figure 3.2 depicts the bin trend of the single standard cooling season.

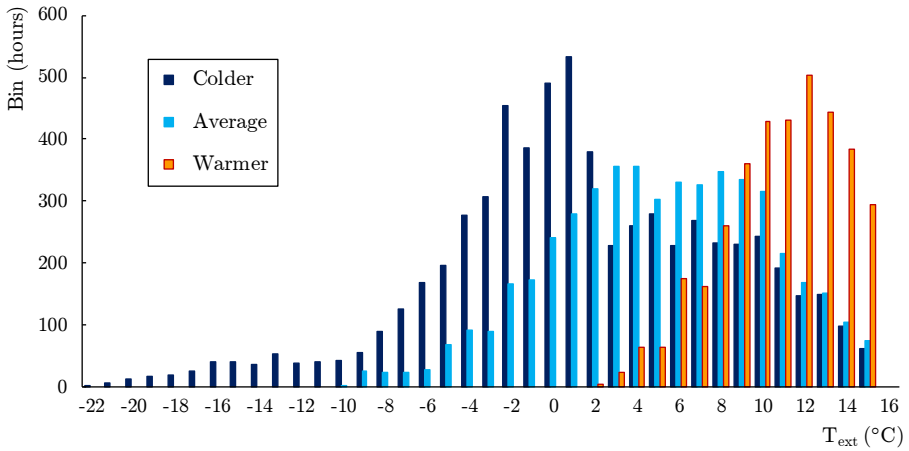

Figure 3.1. Bin distribution of the Colder, Average and Warmer reference heating seasons provided by EN 14825 ([56]).

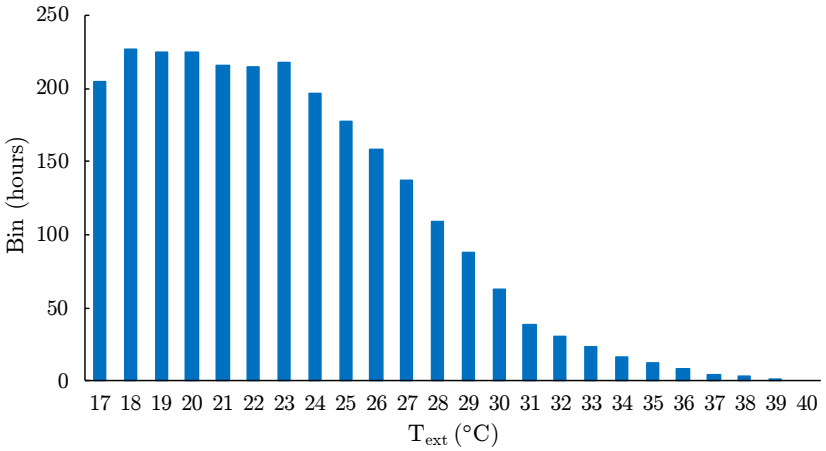

Figure 3.2. Bin distribution of the reference cooling season provided by EN 14825 ([56]).

3.2.1. The Building Energy Signature method

The aim of the standard EN 14825 is to define a procedure which allows to compare the seasonal performance factor of different heat pumps; for this reason, the heat pump is considered coupled to an ideal building, whose heating and cooling loads are evaluated as a linear function of the outdoor air temperature. This procedure to express the building thermal load as a function of the only external air temperature is based on the Building Energy Signature (BES) firstly introduced by Fels in 1986 [76].

As mentioned before, BES method considers the outdoor temperature as the main parameter which influences the building energy consumption; in addition, it is assumed that the internal temperature is constant along the selected period. In order to apply this method, the knowledge of energy consumption data and outside air temperature values at regular time intervals are needed: these data may be evaluated from a simulation model or collected from energy bills or directly on site, by means of gas flow meter lectures. If one considers the last case one-hour sample interval can be considered sufficient, while in the case of manually data collection it is appropriate to use a longer time interval between two measurements, (i.e one week). Finally, the values of external temperature can be obtained from the meteorological data available from the weather station nearest to the location where the considered building is situated.

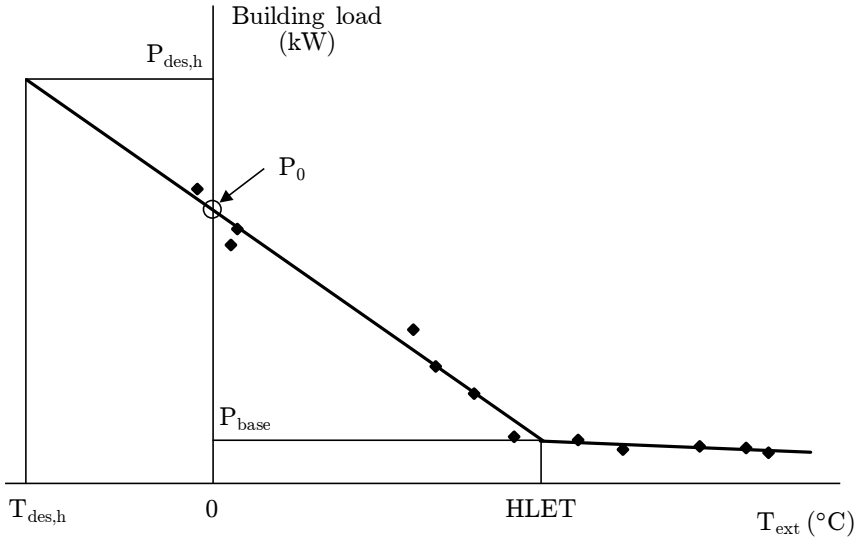

Figure 3.3. Representation of a Building Energy Signature for the heating energy demand.

Figure 3.3 shows a typical example of Building Energy Signature obtained from on site lectures of the building gas flow meter; the measuring campaign covered the whole year and each point reported in Figure 3.3 refers to a monthly lecture.

In this case, BES represents the average building thermal load during the considered time interval (evaluated as the ratio between the building energy consumption and the length of the period) as a function of the average external temperature.

The remarkable points reported in Figure 3.3 are the building design peak load $P_{des,h}$, which is the heating load required by the building in correspondence of the external design temperature $T_{des,h}$, the heating limit external temperature, HLET, namely the external temperature in correspondence of which the building thermal load vanishes, the base load P_{base} and the thermal load required by the building in correspondence of 0 °C, P_0.

The diagonal solid line represents the linear regression of required building load during the period in which the heating system is active (winter months) while the horizontal regression line represents the base load, namely the minimum power required by the building, which is independent from the outside temperature. Typically, in a residential application, the base load accounts for the energy consumption due to the domestic hot water production and food cooking.

During the heating season (i.e. for the oblique part of the BES), the relationship between the required building thermal load P_b and the external temperature T_{ext} can be expressed by means of the following Equation:

$$P_b = P_0 - ST_{ext} \tag{3.1}$$

where the slope of the BES S is evaluated as:

$$S = \frac{P_0 - P_{base}}{HLET} \tag{3.2}$$

and represents the sensitivity of the required building load with respect to the external temperature.

It is possible to conclude that the energy signature method is a useful qualitative analysis tool for the evaluation of the building energy performance: in

fact, through this method the main informations about the building thermal behavior can be obtained. As an example, the slope of the BES, S can be linked to the overall heat transfer coefficient of the building, Moreover, the base load value can give useful informations about the heat generator behavior: if it provides space heating only, the base load represents the system energy losses occurring during the heating system inactivity period. On the contrary, for the most common case of combined heat production for space heating and DHW production, the base load takes just into account the energy demand for DHW production.

Furthermore, the value of the design load required by the building at the external design temperature can be easily assessed from BES; this value allows to evaluate the heat generator sizing. For example, if the installed generator is characterized by a thermal power much larger than the building design load (i.e. it is largely oversized with respect to the required needs), it will always operate at partial load, thus introducing energy losses.

Currently, BES method is described within the European standard EN 15603 [77] and it is employed by the standard EN 14825 [56] to define the thermal load required the building coupled to a heat pump system. EN 14825 considers a building thermal load that vanishes in correspondence to an air external temperature equal to 16 °C, for both heating and cooling reference seasons; for this reason, the bin trends reported in Figure 3.1 and Figure 3.2 are set to zero when the outdoor air temperature is equal to 16 °C for all climates in heating and cooling standard seasons.

If one considers the heating mode, for each reference climate the standard EN 14825 sets the corresponding external design temperature, $T_{des,h}$, equal to -22 °C for the Colder climate, -10 °C and 2 °C for the Average and Warmer climate, respectively. On the contrary, the design outdoor temperature for the reference cooling season, $T_{des,c}$ is equal to 35 °C. It is evident from Figure 3.1 and Figure 3.2 that for the heating climates the design temperature coincides with the minimum outdoor temperature reported in the bin trends, while for the cooling climate the bin trend is characterized by values of the external air temperature greater than the reference design temperature.

3.2.2. Assessment of heat pump performance according to EN 14825

The standard EN 14825 describes the methodology to calculate the seasonal performance factor of a heat pump system for both heating and cooling mode.

The standard puts in evidence the part load conditions at which the heat pump performance data must be given by the manufacturers: these data are used as input values in the calculation method.

Part load performance data must be evaluated according to the procedures and testing conditions reported by standards [73] and [74]; as described in these standards, testing conditions are differentiated depending on the heat pump typology (i.e. air-to-water, water-to-water,…) and on the indoor heat exchanger temperature, thus the indoor emitter typology. For each part load condition, the standard EN 14825 differentiates the heat pump system between fixed and variable outlet systems: in the first case, the indoor heat exchanger outlet temperature is constant for each part load condition along the season, while in the second case a climatic compensation logic, which allows the variation of the outlet temperature as a function of the external air temperature, is introduced.

As an example, in Table 3.4 the part load testing conditions indicated in [56] for an air-to-water heat pump coupled to a low temperature application for the heating mode are reported. For each part load condition from A to G, the standard gives the Part Load Ratio (PLR), defined as the ratio between the thermal load required by the building in correspondence of a specific condition and the building design load $P_{des,h}$. Condition E refers to the Temperature Operative Limit (TOL), i.e. the minimum value of external air temperature at which the heat pump is able to operate; the TOL value is given by the unit manufacturer. It is highlighted that if the TOL declared by the manufacturer is lower than the outdoor design temperature of the considered climate, it may be considered equal to $T_{des,h}$. Furthermore, the part load condition F refers to the bivalent temperature ($T_{biv,h}$), which is defined as the outdoor air temperature in correspondence of which the thermal capacity of the heat pump is equal to the building load. As we will see later within this Thesis, the choice of the bivalent temperature strongly affects the seasonal performance of the system and it is a crucial point for the system design. The standard EN 14825, however, suggests to use a value of $T_{biv,h}$ lower than or equal to -7 °C for the Colder climate, lower than or equal to 2°C for the Average climate and lower than or equal to 7°C for the Warmer climate.

Finally, one can note that the part load condition G, referred to a value of air temperature equal to -15°C, it is not applicable to reference climates Average and Warmer, characterized by a $T_{des,h}$ equal to -10°C and 2°C, respectively. For the same reason, the part load condition A does not apply to the Warmer standard climate.

The part load conditions at which an AWHP coupled to medium, high and very high temperature applications must be tested in order to calculate the seasonal performance factor during heating mode are shown in the standard EN 14825, but these data are not reported in this Thesis for sake of brevity.

Table 3.4. Part load conditions of AWHPs in low temperature applications for the reference heating seasons.

Condition	Part Load Ratio (%)				Outdoor heat exchanger	Indoor heat exchanger			
					Inlet dry (wet) bulb temperature (°C)	Fixed outlet (°C)	Variable outlet (°C)		
	Formula	Av	Wa	Co		All climates	Av	Wa	Co
A	$\frac{(-7-16)}{(T_{des,h}-16)}$	84	n/a	61	-7 (-8)	[a] / 35	[a] / 34	n/a	[a] / 30
B	$\frac{(+2-16)}{(T_{des,h}-16)}$	54	100	37	+2 (+1)	[a] / 35	[a] / 30	[a] / 35	[a] / 27
C	$\frac{(+7-16)}{(T_{des,h}-16)}$	35	64	24	+7 (+6)	[a] / 35	[a] / 27	[a] / 31	[a] / 25
D	$\frac{(+12-16)}{(T_{des,h}-16)}$	15	29	11	+12 (+11)	[a] / 35	[a] / 24	[a] / 26	[a] / 24
E	$\frac{(TOL-16)}{(T_{des,h}-16)}$				TOL	[a] / 35	[a] / [b]	[a] / [b]	[a] / [b]
F	$\frac{(T_{biv}-16)}{(T_{des,h}-16)}$				$T_{biv,h}$	[a] / 35	[a] / [c]	[a] / [c]	[a] / [c]
G	$\frac{(-15-16)}{(T_{des,h}-16)}$	n/a	n/a	82	-15	[a] / 35	n/a	n/a	[a] / 32

[a] With the water flow rate as determined at the standard rating conditions given in EN 14511-2 at 30/35 conditions

[b] Variable outlet shall be calculated by interpolation from $T_{des,h}$ and the temperature which is closest to the TOL

[c] Variable outlet shall be calculated by interpolation between the upper and the lower temperatures which are closest to the bivalent temperature

Table 3.5 reports the part load conditions that must be considered in order to evaluate the *SEER* of air-to-water heat pump systems. Unlike the methodology applied for the heating season performance calculation, only four part load conditions (A-D) are given by the standard [56]. In cooling operating mode, the bivalent temperature is equal to 35 °C, as shown by the PLR related to the condition A, which is 100%.

Table 3.5. Part load conditions of AWHPs for the reference cooling season.

Condition	Part Load Ratio (%)		Outdoor heat exchanger	Indoor heat exchanger		
			Air dry bulb temperature (°C)	Fan coil application Inlet/outlet water temperatures		Cooling floor application Inlet/outlet water temperatures (°C)
	Formula			Fixed outlet (°C)	Variable outlet (°C)	
A	$\frac{(35-16)}{(T_{des,c}-16)}$	100	35	12 / 7	12 / 7	23 / 18
B	$\frac{(30-16)}{(T_{des,c}-16)}$	74	30	[a] / 7	[a] / 8.5	[a] / 18
C	$\frac{(25-16)}{(T_{des,c}-16)}$	47	25	[a] / 7	[a] / 10	[a] / 18
D	$\frac{(20-16)}{(T_{des,c}-16)}$	21	20	[a] / 7	[a] / 11.5	[a] / 18

[a] With the water flow rate as determined during " A" test conditions given in the standard EN 14511-2

In order to calculate the seasonal efficiency of a heat pump system, the standard EN 14825 requires the evaluation of heat pump thermal capacity and *COP*/*EER* for each bin of the considered heating/cooling season.

The methodology is the following: in the first step, the heat pump performance at full load must be determined in correspondence of the operating conditions reported in the standard (see Table 3.4 and Table 3.5) and compared to the required load. If the heat pump thermal/cooling capacity is lower than the building load, the corresponding full load performance must be considered in the calculation. On the contrary, if the heat pump capacity overcomes the required

thermal load, the unit performance at partial load must be calculated. In the second step, the heat pump performance in each bin is evaluated through a linear interpolation between the values of thermal capacity and *COP*/*EER* of the two closest part load testing conditions. Finally, if one considers the heating mode, the heat pump performance in correspondence to values of external air temperature higher than the part load condition D are extrapolated from the values evaluated at the part load conditions C and D; on the other hand, regarding cooling operating mode, for values of air temperature below the testing condition D or above the testing condition A, the same performance of the unit evaluated for the conditions D and A must be used, respectively.

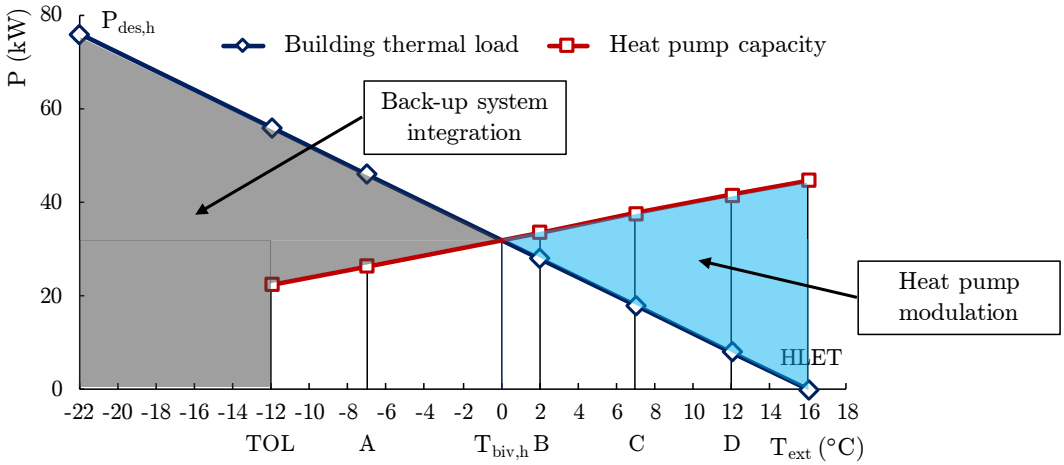

Figure 3.4. Example of BES and characteristic curve of a single-stage air-to-water heat pump in heating mode (Colder reference climate).

In Figure 3.4 an example of a linear building energy signature and the characteristic curve of a single-stage AWHP for the Colder reference heating season are reported. If one considers the BES (blue line), it is evident from Figure 3.4 that the design peak load $P_{des,h}$ is the thermal load required by the building in correspondence of the outdoor design temperature, $T_{des,h}$, which is equal to -22°C for the considered reference season. The characteristic curve of the single-stage unit (red line) has been obtained by interpolating the values of the heat pump thermal capacity at the part load conditions A-F. The selected heat pump is not able to deliver thermal capacity for values of the air temperature below -12°C, which corresponds to the Temperature Operative Limit (TOL) of the system.

The BES crosses the heat pump characteristic curve in a single point, called balance point; the outdoor air temperature which corresponds to the balance point is the bivalent temperature $T_{biv,h}$. For values of the external temperature below $T_{biv,h}$ (in the reported sample equal to 0°C, blue area of the plot), the heat pump capacity is lower than the building load; for that reason the unit works at full load and an additional heat generator is needed to fulfill the whole heating energy demand. In practice, the choice of the back-up system is influenced by several factors, as regulatory constraints, fuel prices and technical limits, but the standard EN 14825 considers only electric heaters as back-up system. For values of air temperature lower than the TOL, the heat pump is switched off and the back-up system must provide the whole thermal need. As pointed out by Figure 3.4, for values of external air temperature higher than $T_{biv,h}$ (corresponding to the blue sector), the heat pump thermal capacity overcomes the building thermal load and the unit must operate at partial load. As will be further investigated in this Thesis, the heat pump performance at partial load depend on the unit modulation capability and strongly influence the seasonal performance of the whole system.

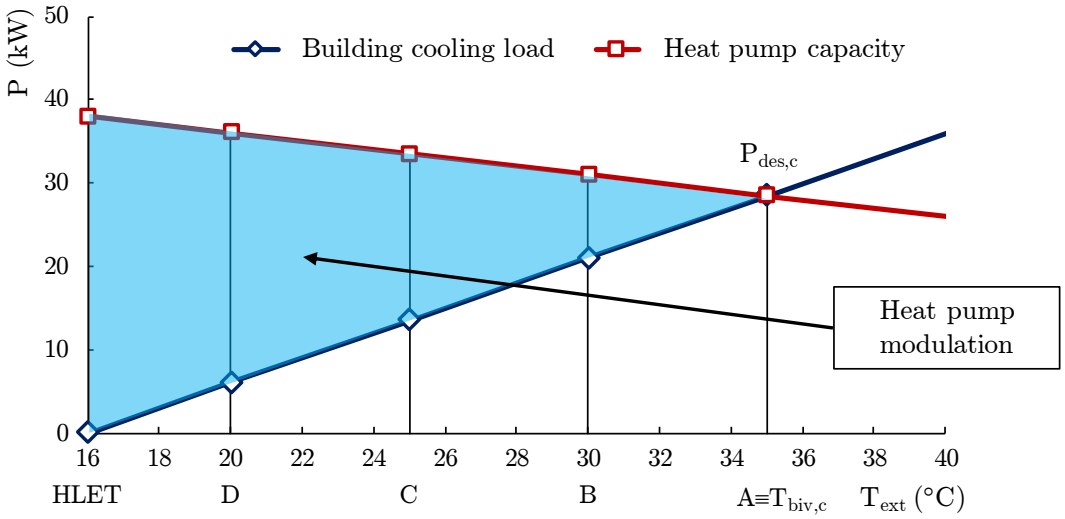

Figure 3.5. Example of BES and characteristic curve of a single-stage air-to-water heat pump in cooling mode (cooling reference climate).

If one considers the cooling season, the heat pump cooling capacity is always higher than the building load for values of the external air temperature lower than $T_{biv,c}$, which is imposed equal to 35°C by the standard EN 14825 (see Table 3.3). In Figure 3.5 an example of a cooling season BES coupled to a characteristic

curve of an AWHP is shown; it can be noted that for outdoor temperatures above the balance point (i.e. part load condition A), the building cooling load cannot be satisfied by the heat pump, but in this case no back-up systems are taken into account for the cooling season.

3.3. The mathematical model for the heating operating mode

In this section the mathematical model for the evaluation of the seasonal performance factor during winter of different kinds of heat pump systems is presented. The developed model is based on the bin methodology reported by the European standard EN 14825 [56] and described in the previous section; the model presented in this Thesis allows to evaluate the seasonal performance of the above-mentioned typologies of air-to-water heat pumps (i.e. single-stage, multi-stage and inverter-driven units), while the procedure described in [56] considers only mono-compressor devices.

3.3.1. Proposed methodology for heating operating mode

The developed mathematical model for the evaluation of the seasonal coefficient of performance (*SCOP*) of an electric air-to-water heat pump is still based on the bin-method. Since the standard EN 14825 allows to calculate the seasonal efficiency of a heat pump system only considering a reference climate described within the standard (i.e. Colder, Average and Warmer), the proposed method is applicable to a heat pump located in a generic location: the only required data are the bin distribution of the specific climate and the extension of the heating season.

3.3.2. Bin profile and building energy signature

In order to evaluate the bin profile of a specific climate, the Italian standard UNI/TS 11300-4 [57] suggests for the heating season a calculation method based on a normal distribution of the outdoor temperature, obtained starting from the local data of monthly average outdoor temperature, outdoor design temperature and monthly average daily solar radiation on a horizontal plane. These data may be available from standards (as an example, weather data for Italy are reported in standards UNI 10349-1 [78] and UNI EN 12831 [79]) or from climatic databases,

as Meteonorm [80]. On the other hand, it is possible to derive the local bin distribution by using the hourly external temperature values quoted by the Test Reference Year (TRY) for the specific location.

As an example, in Figure 3.6 the bin profiles of the city of Bologna (North Italy; 44.29 °N, 11.20 °E) evaluated by means of the method reported in [57] and by the Meteonorm TRY are reported. The conventional heating season, which starts on October 15th and ends on April 15th, has been considered. By comparing the reported trends, it is possible to note that the bin distributions are similar: the bin profile obtained by hourly values of outdoor temperature (red series) can be approximated with a normal distribution. By observing Figure 3.6, it is possible to note that the minimum external temperature which occurs in Bologna (according to TRY data) is equal to -5°C, but this value occurs for only 3 hours during the heating season. On the other hand, according to Ref. [57] method the lowest temperature is equal to -4°C and the mode of the bin distribution is equal to 6°C.

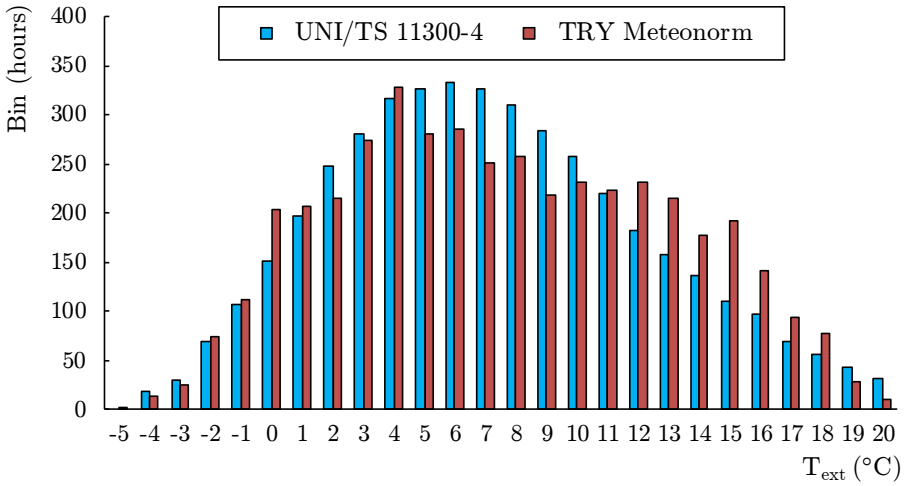

Figure 3.6. Bin distribution during the heating season in Bologna (Italy) according to standard UNI/TS 11300-4 and the TRY of the location.

For the analysis of the energy interaction between the heat pump and the coupled building, it is convenient to introduce the Building Energy Signature (BES), previously described in Section 3.2, which is defined as the thermal load required by the building at the outlet of the generation subsystem as a function of the external air temperature T_{ext} (see Figure 3.4). When the thermal load can be modeled by means of a linear BES, in order to characterize the curve only two parameters are needed: it is sufficient to know the values of *HLET* (heating limit

external temperature, i.e. the external temperature in correspondence of which the building heating demand vanishes) and of the design peak load, $P_{des,h}$, defined as the thermal load required by the building in correspondence of the outdoor design temperature, $T_{des,h}$.

Thus, for each bin the heating load required by the building ($P_{b,h}$) can be evaluated as a function of the outdoor temperature according to the following Equation:

$$P_{b,h}(i) = P_{des,h} \frac{(HLET - T_{ext}(i)}{(HLET - T_{des,h})} \tag{3.3}$$

where $P_{b,h}(i)$ is the thermal load required by the building in the i-th bin.

The corresponding thermal energy demand can be expressed as:

$$E_{b,h}(i) = P_{b,h}(i)\ t_{bin}(i) \tag{3.4}$$

in which $E_{b,h}(i)$ represents the building heating energy demand evaluated for the i-th bin and $t_{bin}(i)$ is the duration of the i-th bin.

3.3.3. Development of heat pump characteristic curve

Once characterized the thermal load and the energy demand required by the building during the whole heating season, a mathematical model able to calculate the heat pump performance (i.e. thermal capacity and *COP*) is needed. According to the procedure reported by [56] and presented in Section 3.2, it is possible to obtain the characteristic curve of an air source heat pump by the technical data sheets given by the heat pump manufacturer (see Figure 3.4). Nevertheless, a detailed and standard methodology is foreseen in the current national standards for air-to-water heat pumps. However, this procedure for the estimation of the characteristic curves of Multi-Stage heat pumps (MSHPs) and Inverter-Driven heat pumps (IDHPs) is still missing in technical standards and is proposed in this Thesis.

In fact, if one considers a mono-compressor heat pump (On-off HP), the thermal capacity delivered by the unit is a function of the temperature of the two sources (i.e. air and water) between which the heat pump operates. On the other hand, for MSHPs characterized by N compressors, the thermal capacity of the

heat pump depends also on the number of compressors switched on (n). Finally, for IDHPs the delivered capacity is a function of the inverter frequency (Φ), as well as the values of air and water temperatures. The thermal capacity ($P_{HP,h}$) of the considered kinds of air-to-water heat pumps can be expressed as:

$$\begin{cases} P_{HP,h} = f(T_{ext},\ T_{w,h}) & \text{for On-off HPs} \\ P_{HP,h} = f(T_{ext},\ T_{w,h}, n) & \text{for MSHPs} \\ P_{HP,h} = f(T_{ext},\ T_{w,h}, \phi) & \text{for IDHPs} \end{cases} \tag{3.5}$$

where $T_{w,h}$ is the temperature of the hot water supplied by the heat pump.

The model presented in this Thesis considers a fixed value of $T_{w,h}$ for the evaluation of the seasonal performance of the system: this situation is met in practice when the heat pump is coupled to a radiant floor heating loop working with a constant inlet water temperature during the heating season (typically 35-40°C). This means that On-off HPs are represented by a single curve in the chart $(T_{ext},\ P)$, since the delivered thermal capacity is a function of the external temperature only. On the contrary, MSHPs are represented by N curves (N is the number of the heat pump compressors), while IDHPs may be ideally characterized by a family of infinite curves, obtained by varying the inverter frequency between the maximum (Φ_{max}) and minimum (Φ_{min}) allowed frequency.

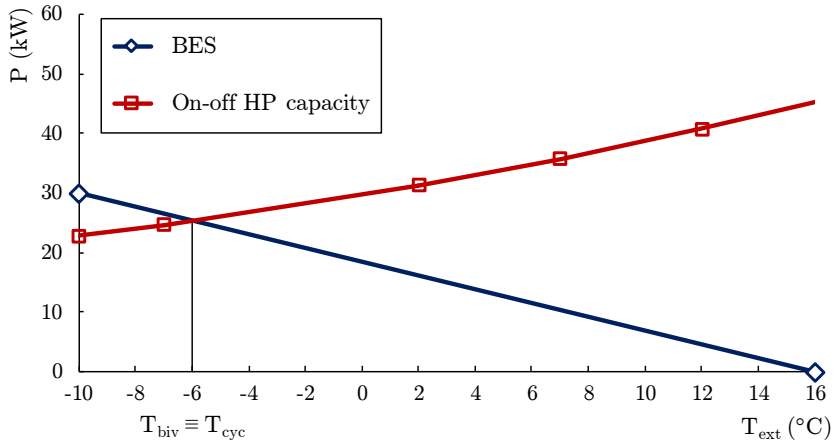

Figure 3.7. Winter BES and characteristic curve of a single-stage On-off HP.

In Figure 3.7 the characteristic curve of a mono-compressor On-off heat pump coupled to a winter BES is reported. In this case the balance point, i.e. the

intersection point between the BES and the characteristic curve of the heat pump, corresponds to a bivalent temperature of -6°C. As mentioned in the previous Section, when the external temperature is lower than $T_{biv,h}$ a back-up system (i.e. electrical resistances or gas boiler) must be activated since the heat pump thermal capacity is lower than the building thermal load. On the contrary, when the outdoor air temperature is higher than $T_{biv,h}$, the heat pump thermal capacity exceeds the required load and a capacity control strategy is needed. According to the lack of any form of heating capacity modulation the only way of a single stage On-off HP to match the building load is to operate with on-off cycles (see Section 2.3.3). For this kind of heat pump, the external temperature in correspondence of which the on-off cycling starts ($T_{cyc,h}$) is necessarily equal to the bivalent temperature.

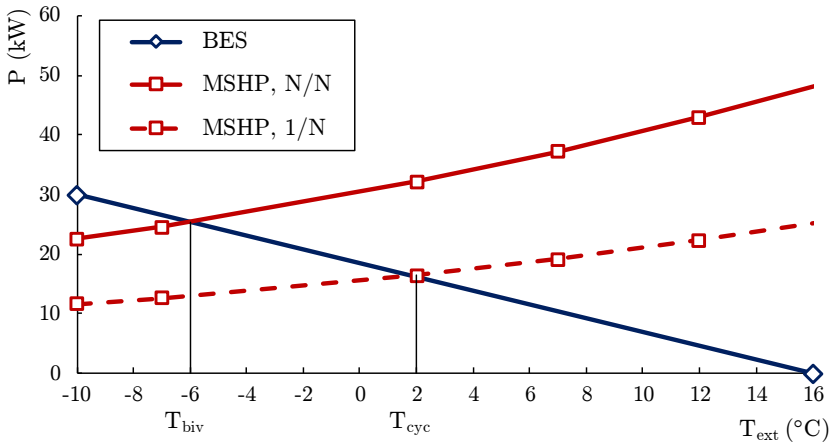

Figure 3.8. Winter BES and characteristic curves of a MSHP composed by 2 compressors.

In Figure 3.8 the same graph is shown for a multi-stage heat pump, coupled to the same BES reported in the previous Figure 3.7. In this case two characteristic curves are drawn: the continue line corresponds to the maximum thermal capacity deliverable by the unit, when the maximum number of compressors is operating (N/N), while the dashed line corresponds to the minimum thermal capacity (i.e. only one compressor is switched on (1/N)). This kind of heat pump is able to modulate the delivered thermal capacity for values of external temperature above the bivalent temperature by switching off the compressors when the thermal load is reduced. When the minimum thermal capacity is attained, i.e. when only one compressor is working, no further modulation is possible: the intersection between the characteristic curve

corresponding to 1/N compressors switched on and the BES fixes the temperature above which the multi-stage heat pump performs on-off cycles ($T_{cyc,h}$). In the case reported in Figure 3.8 $T_{cyc,h}$ is equal to 2°C and the MSHP avoids cycling for external temperatures between -10°C and 2°C.

Finally, in Figure 3.9 the characteristic curves of an IDHP are shown, coupled to the same winter BES of previous units. In this case five characteristic curves are reported: the thermal capacity delivered by the heat pump in correspondence of maximum, minimum and three intermediate frequencies are drawn. The selected IDHP is able to reduce its heating capacity up to 80% of the full load thermal power; for this reason, the variable-speed unit performs on-off cycles only for outdoor air temperature larger than 10°C ($T_{cyc,h}$), i.e. the external temperature that corresponds to the intersection between the BES and the curve evaluated for the minimum inverter frequency. It is evident that an IDHP is able to match exactly the building load for large part of the winter season.

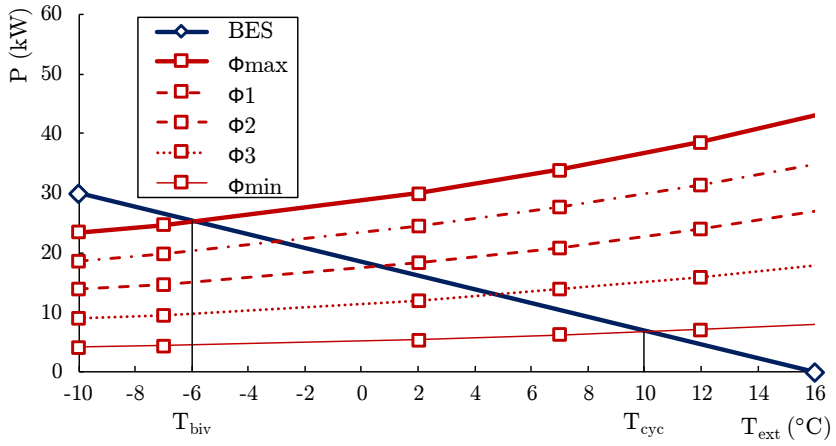

Figure 3.9. Winter BES and characteristic curves of an IDHP evaluated for maximum, minimum and three intermediate frequencies.

In addition to the knowledge of the heat pump characteristic curves, for a complete characterization of an electric air-to-water heat pump it is mandatory to evaluate the heat pump *COP* in correspondence of given values of the outdoor air temperature T_{ext} and of the supplied hot water temperature $T_{w,h}$. In a similar way to the heat pump thermal capacity curves, *COP* curves are obtained.

The model presented in this Thesis requires as input data for the complete characterization of a heat pump different values depending on the heat pump typology. For a single-stage On-off HP values (given by the manufacturer) of the heat pump thermal capacity and *COP* for different values of T_{ext} and for a fixed

value of $T_{w,h}$ are needed. On the other hand, for a MSHP and an IDHP, the same values evaluated in correspondence of the activation of each compressor or in correspondence of the maximum, minimum and at least an intermediate inverter frequency, are mandatory.

The developed model derives the heat pump thermal capacity and *COP* curves by interpolating the input data as functions of the external temperature, using second-order polynomial functions.

For a single-stage on-off heat pump one can write:

$$\begin{cases} P_{HP,h}(i) = a_1\left(T_{w,h}\right){T_{ext}}^2(i) + b_1\left(T_{w,h}\right)T_{ext}(i) + c_1\left(T_{w,h}\right) \\ COP(i) = a_2\left(T_{w,h}\right){T_{ext}}^2(i) + b_2\left(T_{w,h}\right)T_{ext}(i) + c_2\left(T_{w,h}\right) \end{cases} \tag{3.6}$$

In this way, the thermal capacity $P_{HP,h}$ and the *COP* become functions of the *i*-th bin considered. The six coefficients a_1, a_2, b_1, b_2, c_1, c_2 reported in Eq. (3.6) are functions of the supplied hot water temperature $T_{w,h}$ and their values fully define the characteristic curves of a single-stage heat pump.

For a multi-stage heat pump, the heat pump thermal capacity and *COP* depend also on the number of activated compressors *n*; this means that the six coefficients a_1, a_2, b_1, b_2, c_1, c_2 depend also on the number of compressors switched on:

$$\begin{cases} P_{HP,h,n/N}(i) = a_{1,n/N}\left(T_{w,h}\right){T_{ext}}^2(i) + b_{1,n/N}\left(T_{w,h}\right)T_{ext}(i) + c_{1,n/N}\left(T_{w,h}\right) \\ COP_{n/N}(i) = a_{2,n/N}\left(T_{w,h}\right){T_{ext}}^2(i) + b_{2,n/N}\left(T_{w,h}\right)T_{ext}(i) + c_{2,n/N}\left(T_{w,h}\right) \end{cases} \quad \text{for } n = 1,...,\text{N} \tag{3.7}$$

The notation n/N means that the corresponding value is calculated by considering *n* compressors switched on among the N total compressors of the multi-stage heat pump. In this way, the performance of a MSHP characterized by N compressors can be completely defined by means of 6xN coefficients.

The situation is similar if one considers an inverter-driven heat pump; in this case the heat pump thermal capacity and *COP* vary with the inverter frequency, as well as with the hot water temperature and the outdoor air temperature. By fixing M values of frequency from the minimum (Φ_{min}) to the maximum (Φ_{max}), the values of the heat pump thermal capacity and *COP* can be evaluated by knowing 6xM coefficients, as evidenced by the following Equation:

$$\begin{cases} P_{HP,h,\phi_j}(i) = a_{1,\phi_j}\left(T_{w,h}\right) T_{ext}{}^2(i) + b_{1,\phi_j}\left(T_{w,h}\right) T_{ext}(i) + c_{1,\phi_j}\left(T_{w,h}\right) \\ COP_{\phi_j}(i) = a_{2,\phi_j}\left(T_{w,h}\right) T_{ext}{}^2(i) + b_{2,\phi_j}\left(T_{w,h}\right) T_{ext}(i) + c_{2,\phi_j}\left(T_{w,h}\right) \end{cases} \quad \text{for } j = 1,...,\text{M} \quad (3.8)$$

The values of the coefficients a, b, c reported in Eqs. (3.6)- (3.8) can be obtained by interpolating the technical data given by the manufacturer, reported in agreement with the standard EN 14825.

3.3.4. Calculation of the heat pump system seasonal efficiency

Once defined the building through the BES and developed the characteristic curves of the heat pump, the model calculates the thermal energy delivered and the electrical energy absorbed by the heat pump in each bin.

If for a generic bin the heat pump thermal capacity at full load is equal to or lower than the required building load, the corresponding capacity and COP values at full load must be used and the thermal energy delivered by the heat pump for heating, $E_{HP,h}(i)$, is equal to the product between the maximum heat pump capacity and the bin duration ($t_{bin}(i)$). Otherwise, $E_{HP,h}(i)$ is equal to $E_{b,h}(i)$. Finally one can write:

$$\begin{cases} E_{HP,h}(i) = P_{HP,h,FL}(i)\ t_{bin}(i) & \text{if } P_{HP,h,FL}(i) \le P_{b,h}(i) \\ E_{HP,h}(i) = E_{b,h}(i) & \text{if } P_{HP,h,FL}(i) > P_{b,h}(i) \end{cases} \quad (3.9)$$

where $P_{HP,h,FL}(i)$ is the thermal capacity at full load of the heat pump in the i-th bin, evaluated in correspondence to N/N and Φ_{max} characteristic curves for a MSHP and an IDHP, respectively.

For values of the external temperature higher than $T_{biv,h}$, the heat pump thermal capacity exceeds the required load and the heat pump efficiency (i.e. COP) depends on the modulation capability of the unit. In particular, single-stage heat pumps can only perform on-off cycles to match the building energy demand. As reported by Ref. [81], on-off cycles introduce energy losses, since the electric energy consumption of the heat pump does not vanish during the off-period of the cycle and, for each start-up, the compressor must restore the pressure difference between condenser and evaporator.

The efficiency losses due to on-off cycles are taken into account by following the approach of the standard [56], which introduces for each bin the correction factor f_{corr}. The coefficient f_{corr} is evaluated as:

$$f_{corr}(i) = \frac{CR(i)}{C_c \ CR(i) + (1 - C_c)} \tag{3.10}$$

In the reported Equation, CR is the Capacity Ratio and C_c is the degradation coefficient. The capacity ratio CR is defined as the ratio between the building load and the heat pump thermal capacity at the same outdoor temperature conditions. If the heat pump capacity is equal to or lower than the building demand, CR is equal to 1 and the correction factor for on-off cycles turns out equal to 1. The degradation coefficient C_c indicates the heat pump efficiency decrease for on-off cycles and should be determined by the manufacturer by means of experimental tests. If C_c is not determined by tests, a default value of 0.9 reported by the standard [56] shall be used. However, as observed by Madonna et al. in [59], this value in general tends to underestimate the real energy losses due to on-off cycling

Since MSHPs and IDHPs are able to modulate the thermal capacity delivered in order to follow the building load and delay the use of on-off cycles, the COP correction factor f_{corr} is calculated considering the value of the capacity ratio corresponding to the heat pump capacity with only one compressor switched on or at the minimum inverter frequency. In fact, it is evident from Figure 3.8 and Figure 3.9 that the on-off cycling condition begins when no further capacity modulation is possible (i.e. when T_{ext} is larger than $T_{cyc,h}$).

The COP in correspondence of a number n of active compressors (for MCHPs) or in correspondence of a generic inverter frequency (for IDHPs) is evaluated for each bin by means of Eqs. (3.6)-(3.8). The effective COP value, COP_{eff}, which takes into account the on-off cycles losses, is obtained as follows:

$$COP_{eff}(i) = COP(i) \ f_{corr}(i) \tag{3.11}$$

For an On-off HP, the electric energy absorbed by the unit in the i-th bin $E_{HP,h,el}(i)$ is:

$$E_{HP,h,el}(i) = E_{HP,h}(i) / COP_{eff}(i) \tag{3.12}$$

For a MSHP, in order to evaluate $E_{HP,h,el}$ (i), it is mandatory to know how many compressors are activated for each bin and for how long time. In a generic bin, if the heating load required by the building is higher than the heat pump thermal capacity corresponding to n/N compressors switched on, but it is lower than the thermal capacity corresponding to $(n+1)$/N stages switched on, then $n+1$ compressors are activated for a fraction of the bin duration t_{bin} and n compressors are activated for the remaining period, so as the total energy delivered by the heat pump equals the building energy need.

For example, if in the i-th bin of duration t_{bin} (i) a MSHP with N compressors has to deliver to the building an amount of energy between the energy which would be supplied with n-1 stages and n stages working for the whole bin duration, then the period with n working stages ($t_{bin,n/N}$ (i)) can be estimated as:

$$t_{bin,n/N}(i) = \frac{E_{b,h}(i) - P_{HP,h,(n-1)/N}(i)\ t_{bin}(i)}{P_{HP,h,n/N}(i) - P_{HP,h,(n-1)/N}(i)} \tag{3.13}$$

Consequently, the time period in which the MSHP operates with n-1 compressors switched on ($t_{bin,(n-1)/N}$ (i)) is equal to:

$$t_{bin,(n-1)/N}(i) = t_{bin}(i) - t_{bin,n/N}(i) \tag{3.14}$$

In this way, the electric energy consumption of the MSHP in the i-th bin is evaluated as:

$$E_{HP,h,el}(i) = \begin{cases} \dfrac{E_{HP,h}(i)}{COP_{eff}(i)} & \text{if } P_{b,h}(i) < P_{HP,h,1/N}(i) \\ \dfrac{P_{HP,h,n/N}(i)\ t_{bin,n/N}(i)}{COP_{n/N}(i)} + \dfrac{P_{HP,h,(n-1)/N}(i)\ t_{bin,(n-1)/N}(i)}{COP_{(n-1)/N}(i)} & \text{if } P_{HP,h,(n-1)/N}(i) \le P_{b,h}(i) < P_{HP,h,n/N}(i) \\ \dfrac{E_{HP,h}(i)}{COP_{N/N}(i)} & \text{if } P_{b,h}(i) \ge P_{HP,h,N/N}(i) \end{cases} \tag{3.15}$$

where COP_{eff} is evaluated according to Eq. (3.11).

If one considers an IDHP, in order to evaluate the electric energy absorbed by the heat pump, for each bin it is mandatory to know the value of the inverter frequency (Φ_{eff}): as shown in Eq. (3.5) the performance of an IDHP depends on the rotating speed of the compressor (in addition to the external and supplied water temperatures). For values of the external temperature between $T_{biv,h}$ and $T_{cyc,h}$, Φ_{eff} is the value of the inverter frequency in correspondence of which the thermal capacity delivered by the heat pump ($P_{HP,h,\Phi eff}(i)$) equals the thermal load required by the building ($P_{b,h}(i)$). Once evaluated $P_{HP,h,\Phi eff}(i)$ as the ratio between $E_{HP,h}(i)$ (which is in this case equal to $E_{b,h}(i)$) and $t_{bin}(i)$, the effective frequency Φ_{eff} is evaluated through linear interpolations of the M values of $P_{HP,h,\Phi eff}$, obtained from Eq. (3.8), as a function of $P_{HP,h}$. To be noted that if $P_{HP,h,\Phi eff}(i)$ turns out lower than $P_{HP,\Phi min}(i)$, it is set equal to $P_{HP,h,\Phi min}(i)$). On the other hand, $COP_{\Phi eff}$ is obtained by interpolating the M values of COP derived from Eq. (3.8) as a function of $\Phi_{eff}(i)$.

Thus, the electric energy consumption of the IDHP in the i-th bin is:

$$E_{HP,h,el}(i) == \begin{cases} \dfrac{E_{HP,h}(i)}{COP_{eff}(i)} & \text{if } P_{b,h}(i) < P_{HP,h,\phi_{\min}}(i) \\ \dfrac{E_{HP,h}(i)}{COP_{\phi_{eff}}(i)} & \text{if } P_{HP,h,\phi_{\min}}(i) \le P_{b,h}(i) < P_{HP,h,\phi_{\max}}(i) \\ \dfrac{E_{HP,h}(i)}{COP_{\phi_{\max}}(i)} & \text{if } P_{b,h}(i) \ge P_{HP,h,\phi_{\max}}(i) \end{cases} \tag{3.16}$$

in which COP_{eff} is evaluated according to Eq. (3.11).

For each kind of heat pump considered in this Thesis, if the heat pump thermal capacity in the i-th bin is lower than the building thermal load (i.e. T_{ext} lower than $T_{biv,h}$), the missing energy $E_{BU,h}(i)$ is delivered by the back-up system, if present. Thus, for each bin one can write:

$$E_{BU,h}(i) = E_b(i) - E_{HP,h}(i) \tag{3.17}$$

The corresponding energy input of the back-up system, $E_{BU,h,abs}(i)$, is equal to the ratio between $E_{BU,h}(i)$ and the efficiency of the back-up system, $\eta_{BU}(i)$:

$$E_{BU,h,abs}(i) = E_{BU,h}(i) / \eta_{BU}(i) \tag{3.18}$$

In case of electric resistances, the thermal energy that the back-up electric heaters deliver is obviously equal to the electric energy that they absorb: the back-up efficiency is set equal to 1 for each bin of the heating season and the back-up system absorbs electrical energy; we refer to this kind of systems as bivalent mono-energetic heat pump systems. On the contrary, in case of boiler, it is possible to set the value of its generating efficiency for the *i*-th bin: we refer to bivalent bi-energetic systems since the back-up system utilizes a different energy source (i.e. natural gas) with respect to the electric heat pumps.

3.3.5. Seasonal performance factor evaluation in heating mode

The standard EN 14825 [56] reports the procedure to calculate different seasonal performance coefficients for an electric air-to-water heat pump system. The Seasonal Coefficient of Performance of the heat pump, $SCOP_{net}$, is defined as the ratio between the thermal energy delivered by the heat pump during the whole heating season and the corresponding electric energy absorbed. The energy supplied and absorbed by the back-up system does not apply for the evaluation of $SCOP_{net}$, which refers only to the heat pump unit.

The seasonal values of energy delivered and absorbed by the heat pump are obtained by summing the corresponding values of each bin:

$$SCOP_{net} = \frac{\sum_i E_{HP,h}(i)}{\sum_i E_{HP,h,el}(i)} \tag{3.19}$$

Another seasonal performance coefficient for winter is the Seasonal Coefficient Of Performance of the whole system (composed by the heat pump and the back-up system), $SCOP_{on}$, evaluated as the ratio between the total energy delivered by the system during the heating season (equal to the building required energy demand) and the total energy absorbed by the system. If one considers a mono-energetic system (i.e. the back-up system is composed by electric resistances) $SCOP_{on}$ is defined as:

$$SCOP_{on} = \frac{\sum_i E_{HP,h}(i) + \sum_i E_{BU,h}(i)}{\sum_i E_{HP,h,el}(i) + \sum_i E_{BU,h,abs}(i)} \tag{3.20}$$

The seasonal performance factors considered in this Section (namely $SCOP_{net}$ and $SCOP_{on}$) refer to the active mode of a heat pump, defined as the hours in which the building load is present and the heating or cooling function of the unit is activated. However, energy consumptions generally occur also when the heat pump is not effectively used to fulfil the building energy demand, such as the energy consumption due to the crankcase heater utilization or the electric panel absorption during the stand-by mode of the unit. These energy consumptions are considered by the standard EN 14825 [56] in the definition of another seasonal performance coefficient, namely $SCOP_{ref}$, which takes into account the global electric consumption of the heat pump unit during the heating season:

$$SCOP_{ref} = \frac{\sum_i E_{HP,h}(i) + \sum_i E_{BU,h}(i)}{\sum_i E_{HP,h,el}(i) + \sum_i E_{BU,h,abs}(i) + H_{to,h}P_{to,h} + H_{sb,h}P_{sb,h} + H_{ck,h}P_{ck,h} + H_{off,h}P_{off,h}} \tag{3.21}$$

where $H_{to,h}$, $H_{sb,h}$, $H_{ck,h}$ and $H_{off,h}$ are the number of hours during which the heat pump operates in thermostat-off mode, stand-by mode, crankcase heater mode and off mode during the heating season, respectively. $P_{to,h}$, $P_{sb,h}$, $P_{ck,h}$ and $P_{off,h}$ are the electrical power input of the unit which are linked to the thermostat-off mode, stand-by mode, crankcase heater mode and off mode, respectively. Typically, the values of $P_{to,h}$, $P_{sb,h}$, $P_{ck,h}$ and $P_{off,h}$ are not given by the manufacturer; in addition, the duration of the above-mentioned periods is not univocally defined but it depends on the control logic of the real heating system. For these reasons, the calculation of $SCOP_{ref}$ is not performed in this Thesis.

On the other hand, if the back-up system is represented by a gas boiler, the coefficient $SCOP_{on}$ can be evaluated according to:

$$SCOP_{on} = \frac{\sum_i E_{HP,h}(i) + \sum_i E_{BU,h}(i)}{\sum_i E_{HP,h,el}(i) + \sum_i \frac{E_{BU,h,abs}(i)}{f_p}} \tag{3.22}$$

In Eq. (3.22) f_p is the conversion coefficient between electrical and primary energy. The European Directive [5] indicates a value of f_p equal to 2.5, a value which reflects the estimated 40% average EU power generation efficiency. In Italy, the value of f_p is defined by the current legislation in [82] and its value is equal to 2.42.

3.4. The mathematical model for the cooling operating mode

In this Section the mathematical model for the evaluation of the seasonal performance factor during summer is presented. Similarly to the model presented in Section 3.3 for the heating operating mode, the developed mathematical model is based on the bin methodology reported by the standard EN 14825 [56]; again, the model allows to evaluate the seasonal performance of the different kinds of air-to-water reversible heat pumps (i.e. single-stage, multi-stage and inverter-driven units) previously considered.

3.4.1. Evaluation of bin distribution, building energy demand and heat pump characteristic curves

The developed mathematical model for the evaluation of seasonal coefficient of performance for cooling operating mode (*SEER*) of a reversible air-to-water heat pump is still based on the bin-method.

As mentioned in Section 3.2, the standard EN 14825 [56] considers a single reference climate and directly reports the bin profile for this reference cooling season, the developed method derives the bin distribution for a generic location by means of two alternative approaches: the first one is based on the methodology reported in Ref. [57] and is based on a normal distribution of the outdoor air temperature, while according to the second approach, it is possible to derive the seasonal bin distribution by using the hourly values of outdoor temperature reported by the TRY of the specific location.

The histogram of Figure 3.10 highlights the bin profiles obtained for the Italian city of Palermo (38.12 °N, 13.37 °E) according to the two approaches mentioned before, considering a cooling season from May 1st to September 30th and compares them to the bin trend of the reference climate provided by the standard EN 14825 and assumed as representative of the whole Europe.

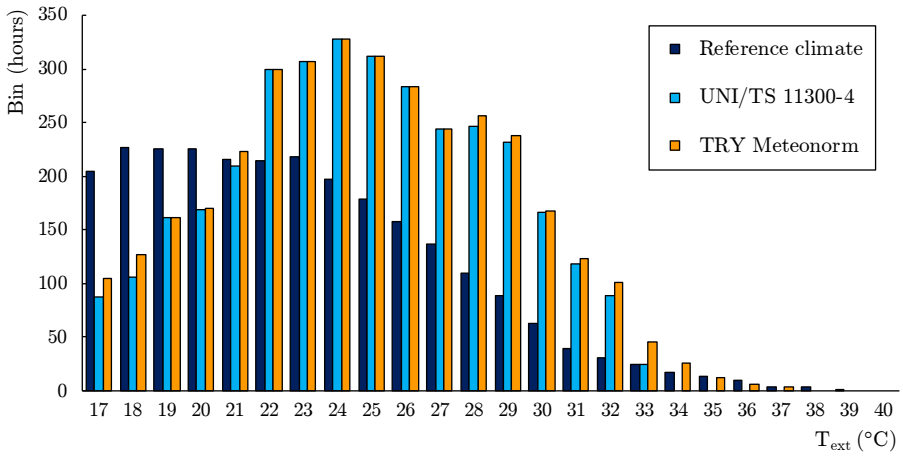

Figure 3.10. Bin distribution for the reference cooling season and for Palermo (Italy) derived from the standard UNI 11300-4 and the TRY of the location.

First, one can note that the bin distributions obtained through UNI/TS 11300-4 and TRY methods are very similar one another: as achieved for the heating season bin profile of Bologna (Section 3.3.2), the bin trend obtained by hourly values of external temperature can be effectively approximated with a normal distribution. Then, by comparing the bin distributions of Palermo and of the reference climate one another, it is evident that the season severity is very different between the considered locations: for example, the mode of the distribution is equal to 24°C for Palermo and equal to 18°C for the reference climate. Since the values of outdoor temperature has a strong influence on the heat pump energy performance, the method proposed by EN 14825 is not particularly accurate for the evaluation of the system seasonal efficiency, especially for Southern Europe sites.

For the calculation of the building cooling load, the summer building energy signature (BES) is used, according to Ref. [56]. In the case of a straight BES curve, the cooling load required by the building in the *i*-th bin, $P_{b,c}\,(i)$, can be obtained through Eq. (3.23), once the values of the zero-load external temperature (Cooling Limit External Temperature, CLET) and of the cooling peak load $P_{des,c}$ are known:

$$P_{b,c}(i) = P_{des,c}\left(\frac{CLET - T_{ext}(i)}{CLET - T_{des,c}}\right) \tag{3.23}$$

The corresponding cooling energy demand can be expressed as:

$$E_{b,c}(i) = P_{b,c}(i)\ t_{bin}(i) \tag{3.24}$$

in which $E_{b,c}(i)$ represents the building cooling energy demand evaluated for the i-th bin.

It is important to highlight that the BES methodology applied to the cooling season introduces a significant approximation; in fact, during the hot season the building cooling load can not be evaluated as a function of the external air temperature only: the incident solar irradiation is the most significative heat gain for the building. For this reason, the solar radiation should be taken into account in the evaluation of the building cooling load, for example by employing the sol-air temperature [11] in place of the external air temperature as independent variable of the BES method.

The cooling capacity $P_{HP,c}$ delivered by a reversible air-source single-stage heat pump depends only on the external temperature T_{ext}, for a fixed temperature $T_{w,c}$ of the cold water supplied to the building. As explained in Section 3.3.3, the heat pump characteristic curve can be obtained by interpolating the technical data of cooling capacity and *EER* given by the manufacturer as a function of the outdoor temperature, by using second-order polynomial functions. For multi-stage heat pumps (MSHPs) and inverter-driven heat pumps (IDHPs), the unit characteristic curve is actually a series of curves equal to the number N of compressors (MSHPs), or it is given by a family of curves obtained by varying the inverter frequency between the maximum and minimum value (IDHPs).

In a similar way, the characteristic curves of the heat pump Energy Efficiency Ratio, *EER*, are obtained through interpolations of the manufacturer technical data.

Similarly to Section 3.3.3, the cooling capacity and the *EER* of a reversible air-to-water heat pump may be expressed as a function of the i-th bin, depending on the unit typology, according to the following Equations:

$$\begin{cases} P_{HP,c}(i) = d_1\left(T_{w,c}\right){T_{ext}}^2(i) + e_1\left(T_{w,c}\right)T_{ext}(i) + f_1\left(T_{w,c}\right) \\ EER(i) = d_2\left(T_{w,c}\right){T_{ext}}^2(i) + e_2\left(T_{w,c}\right)T_{ext}(i) + f_2\left(T_{w,c}\right) \end{cases} \tag{3.25}$$

$$\begin{cases} P_{HP,c,n/N}(i) = d_{1,n/N}\left(T_{w,c}\right){T_{ext}}^2(i) + e_{1,n/N}\left(T_{w,c}\right)T_{ext}(i) + f_{1,n/N}\left(T_{w,c}\right) \\ EER_{n/N}(i) = d_{2,n/N}\left(T_{w,c}\right){T_{ext}}^2(i) + e_{2,n/N}\left(T_{w,c}\right)T_{ext}(i) + f_{2,n/N}\left(T_{w,c}\right) \end{cases} \text{ for } n = 1,...,\text{N} \tag{3.26}$$

$$\begin{cases} P_{HP,c,\phi_j}(i) = d_{1,\phi_j}\left(T_{w,c}\right){T_{ext}}^2(i) + e_{1,\phi_j}\left(T_{w,c}\right)T_{ext}(i) + f_{1,\phi_j}\left(T_{w,c}\right) \\ EER_{\phi_j}(i) = d_{2,\phi_j}\left(T_{w,c}\right){T_{ext}}^2(i) + e_{2,\phi_j}\left(T_{w,c}\right)T_{ext}(i) + f_{2,\phi_j}\left(T_{w,c}\right) \end{cases} \text{ for } j = 1,...,\text{M} \tag{3.27}$$

Eq. (3.25) refers to a single-stage On-off HP, while Eq. (3.26) and Eq. (3.27) refer to a MSHP composed by N compressors and an IDHP, respectively.

The values of the coefficients *d*, *e*, *f* reported in Eqs. (3.25)-(3.27) are functions of the supplied cold water temperature $T_{w,c}$ and their values can be obtained by interpolating the technical data reported in standard EN 14825 given by the manufacturer; the above-mentioned coefficients fully define the characteristics of an air-to-water reversible heat pump operating in cooling mode.

3.4.2. Energy calculation in cooling operating mode

Once defined the building through the BES and evaluated the characteristic curves of the heat pump, the mathematical model shown in this Thesis calculates the cooling energy delivered and the electrical energy absorbed by the heat pump in each bin.

If for the i-th bin the heat pump cooling capacity at full load is equal to or lower than the required cooling load, the corresponding capacity and *EER* values at full load must be used and the cooling energy delivered by the heat pump for cooling, $E_{HP,c}(i)$, is equal to the product between the maximum heat pump capacity and $t_{bin}(i)$. Otherwise, $E_{HP,c}(i)$ is equal to $E_{b,c}(i)$. In conclusion, it is possible to write:

$$\begin{cases} E_{HP,c}(i) = P_{HP,c,FL}(i)\ t_{bin}(i) & \text{if } P_{HP,c,FL}(i) \le P_{b,c}(i) \\ E_{HP,c}(i) = E_{b,c}(i) & \text{if } P_{HP,c,FL}(i) > P_{b,c}(i) \end{cases} \quad (3.28)$$

where $P_{HP,c,FL}(i)$ is the cooling capacity at full load of the heat pump in the i-th bin, evaluated in correspondence to N/N and Φ_{max} characteristic curves for a MSHP and an IDHP, respectively.

For values of the external temperature lower than $T_{biv,c}$, the heat pump cooling capacity exceeds the required load and it must be modulated in order to match the building energy demand. As pointed out in Section 3.3.4, single-stage On-off HPs can only perform on-off cycles, introducing cycling losses, while MSHPs and IDHPs are able to modulate their cooling capacity within a range of external temperature values, in order to delay the use of on-off cycles.

Similarly to Section 3.3.4, the effective EER value EER_{eff}, which takes into account the on-off cycles energy losses, is obtained as follows:

$$EER_{eff}(i) = EER(i)\ f_{corr}(i) \quad (3.29)$$

in which the correcting factor f_{corr} is evaluated according to Eq. (3.10), but in this case the capacity ratio CR is defined as the ratio between the building cooling load and the heat pump cooling capacity at the same outdoor temperature conditions.

According to the Equations reported in Section 3.3.4, the electric energy absorbed by an On-off HP heat pump in cooling operating mode during the i-th bin $E_{HP,c,el}(i)$ is evaluated by means of the following Equation:

$$E_{HP,c,el}(i) = E_{HP,c}(i) / EER_{eff}(i) \quad (3.30)$$

For a MSHP, in order to evaluate $E_{HP,c,el}(i)$, it is mandatory to know also in cooling operating mode the number n of compressors switched on for each bin and their activating time period ($t_{bin,n/N}(i)$). Similarly to Section 3.3.4, in the i-th bin the time period with n working compressors ($t_{bin,n/N}(i)$) can be estimated according to Eq. (3.31), while the time period in which the MSHP operates with n-1 compressors switched on ($t_{bin,(n-1)/N}(i)$) is expressed as:

$$t_{bin,n/N}(i) = \frac{E_{b,c}(i) - P_{HP,c,(n-1)/N}(i)\ t_{bin}(i)}{P_{HP,c,n/N}(i) - P_{HP,c,(n-1)/N}(i)} \tag{3.31}$$

Thus, the electric energy consumption of a reversible MSHP operating in cooling mode in the generic *i*-th bin is evaluated as:

$$E_{HP,c,el}(i) = \begin{cases} \dfrac{E_{HP,c}(i)}{EER_{eff}(i)} & \text{if } P_{b,c}(i) < P_{HP,c,1/N}(i) \\ \dfrac{P_{HP,c,n/N}(i)\ t_{bin,n/N}(i)}{EER_{n/N}(i)} + \dfrac{P_{HP,c,(n-1)/N}(i)\ t_{bin,(n-1)/N}(i)}{EER_{(n-1)/N}(i)} & \text{if } P_{HP,c,(n-1)/N}(i) \le P_{b,h}(i) < P_{HP,c,n/N}(i) \\ \dfrac{E_{HP,c}(i)}{EER_{N/N}(i)} & \text{if } P_{b,c}(i) \ge P_{HP,c,N/N}(i) \end{cases} \tag{3.32}$$

As reported in Section 3.3.4, if one considers an IDHP the developed model at first evaluates for each bin the effective inverter frequency $\Phi_{eff}(i)$ through linear interpolations of the M values of $P_{HP,c,\,\Phi eff}$, (obtained from Eq. (3.27)) and then the unit efficiency $EER_{\Phi eff}$ is obtained by interpolating the M values of *EER* derived from Eq. (3.27) as a function of $\Phi_{eff}(i)$. Finally, the electric energy consumption of the IDHP in the *i*-th bin is calculated:

$$E_{HP,c,el}(i) == \begin{cases} \dfrac{E_{HP,c}(i)}{EER_{eff}(i)} & \text{if } P_{b,c}(i) < P_{HP,c,\phi_{\min}}(i) \\ \dfrac{E_{HP,c}(i)}{EER_{\phi_{eff}}(i)} & \text{if } P_{HP,c,\phi_{\min}}(i) \le P_{b,c}(i) < P_{HP,c,\phi_{\max}}(i) \\ \dfrac{E_{HP,c}(i)}{EER_{\phi_{\max}}(i)} & \text{if } P_{b,c}(i) \ge P_{HP,c,\phi_{\max}}(i) \end{cases} \tag{3.33}$$

As highlighted before in Section 3.2, the standard EN 14825 [56] does not consider a back-up system for cooling operating mode. For this reason, if the heat pump cooling capacity in the *i*-th bin is lower than the building cooling load (i.e. when T_{ext} is higher than $T_{biv,c}$), a fraction of the building energy demand $E_{b,c}\ (i)$ is not satisfied by the heat pump system.

3.4.3. Seasonal performance factor evaluation in cooling mode

Finally, the seasonal energy performance of the system is obtained by summing the calculated values of each bin. Since no back-up systems are considered for the heat pump cooling operating mode, only one seasonal coefficient is defined: the Seasonal Energy Efficiency Ratio, $SEER_{on}$ (Eq. (3.34)), evaluated as the ratio between the total cooling energy provided by the heat pump and the corresponding electric energy absorbed:

$$SEER_{on} = \frac{\sum_i E_{HP,c}(i)}{\sum_i E_{HP,c,el}(i)} \tag{3.34}$$

One can note that the cooling energy delivered by the heat pump during the whole season may not be equal to the entire building energy demand: as highlighted in the previous Section, for bins characterized by values of T_{ext} higher than the bivalent temperature $T_{biv,c}$, the building load is not entirely covered by the heat pump. If the heat pump capacity is small (i.e. $T_{biv,c}$ is lower than $T_{des,c}$) the thermal comfort of building users is not assured without a back-up system..

Similarly the seasonal performance factor $SEER_{on}$ refers to the performance of the device in active mode during the cooling season; in addition, it is possible to define $SEER_{ref}$, a seasonal performance coefficient which takes into account the overall electric consumption of the heat pump during the cooling season:

$$SEER_{ref} = \frac{\sum_i E_{HP,c}(i)}{\sum_i E_{HP,c,el}(i) + H_{to,c}P_{to,c} + H_{sb,c}P_{sb,c} + H_{ck,c}P_{ck,c} + H_{off,c}P_{off,c}} \tag{3.35}$$

where $H_{to,c}$, $H_{sb,c}$, $H_{ck,c}$ and $H_{off,c}$ are the number of hours during which the heat pump operates in thermostat-off mode, stand-by mode, crankcase heater mode and off mode during the cooling season, respectively. $P_{to,c}$, $P_{sb,c}$, $P_{ck,c}$ and $P_{off,c}$ are the electrical power input of the unit associated to thermostat-off mode, stand-by mode, crankcase heater mode and off mode, respectively. For the same reasons explained in Section 3.3.5, the calculation of $SEER_{ref}$ is not performed in this Thesis.

3.5. Validation of the developed mathematical model

As reported in Sections 3.3 and 3.4, the mathematical model based on the bin method presented in this Thesis employs the performance data (i.e. thermal/cooling capacity and *COP*/*EER*) of an air-to-water heat pump, evaluated for different values of external temperature, supply water temperature, number of active compressors and inverter frequency, to calculate the seasonal performance of the system. It is evident that more the input data are detailed, more the seasonal performance calculation is accurate.

The mathematical method discussed in this work has been developed in collaboration with a heat pump manufacturer located near Bologna (Italy). All the data about the heat pump performance quoted in this Thesis have been given by the manufacturer.

In this Section, a validation of the calculation methodology proposed in the previous Sections for the prediction of the performance of an air-to-water heat pump has been made by using the experimental data given by the manufacturer. More in detail, three heat pump units characterized by the same size were selected by the catalogue of the manufacturer: an On-off HP, a MSHP composed by two compressor and an IDHP. Their performance data, for both heating and cooling operating mode, was obtained by the manufacturer through experimental results by considering the working conditions reported in EN 14825 [56] (see Section 3.2). These data are employed to develop the characteristic curves of the selected heat pumps by means of the procedure reported in Sections 3.3.3 and 3.4.1 (for heating and cooling mode, respectively).

Table 3.6. Polynomial coefficients of the On-off HP characteristic curves obtained by means of the developed model.

Heating mode						Cooling mode					
$P_{HP,h}$			*COP*			$P_{HP,c}$			*EER*		
a_1	b_1	c_1	a_2	b_2	c_2	d_1	e_1	f_1	d_2	e_2	f_2
0.026	0.72	18.49	0.0017	0.086	3.38	0.034	-2.27	56.86	0.0045	-0.376	10.49

First, the On-off HP is considered. The values of the polynomial coefficients obtained from Eqs. (3.6) and (3.25) are shown in Table 3.6: by means of these coefficients, the characteristic curves of the selected On-off HP can be defined.

In Figure 3.11 the experimental values of the heat pump thermal/cooling capacity and *COP*/*EER* are reported and compared with the characteristic curves derived from the developed model (heating and cooling modes are represented in Figure 3.11a and Figure 3.11b, respectively).

By observing these Figures, it is evident that the heat pump characteristic curves developed by means of the mathematical model shown in this Thesis properly fit the experimental data obtained by the manufacturer: the discrepancies between the experimental measures and the results of the proposed model are very low. If one considers the heating operating mode (see Figure 3.11a), the maximum difference between the experimental data and the predictions of the suggested method is lower than 10%, in correspondence of an external air temperature of -7°C; on the contrary, if one considers the cooling operating mode, the maximum discrepancy between experimental and numerical data is lower than 4%.

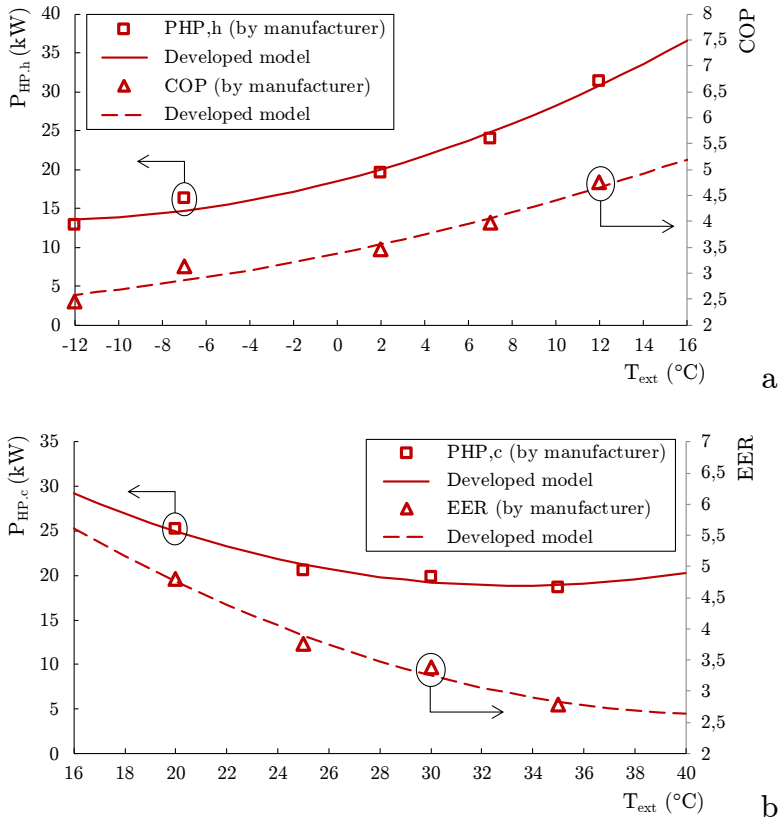

Figure 3.11. Characteristic curves of the selected On-off HP evaluated for heating (a) and cooling (b) mode, compared to performance data given by the manufacturer.

The same analysis is performed considering a MSHP model. The heat pump performance data obtained from experimental measures and the related characteristic curves developed by means of the described method are reported in Figure 3.12 and Figure 3.13 for heating and cooling mode, respectively.

The characteristic curves obtained through the developed model are in agreement with the experimental data also in this case: the maximum difference between the data series is under 15% for heating operating mode and under 5% for cooling operating mode.

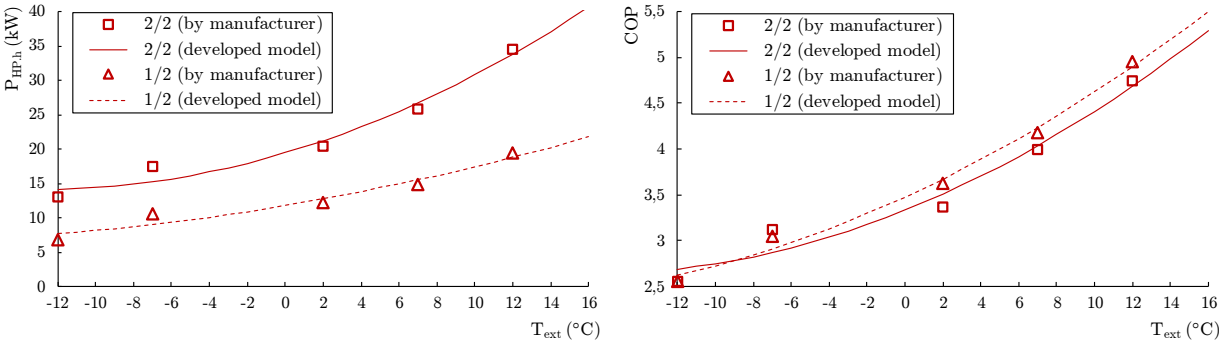

Figure 3.12. Characteristic curves of the selected MSHP evaluated for heating mode, compared to performance data given by the manufacturer (thermal capacity on the left, *COP* on the right).

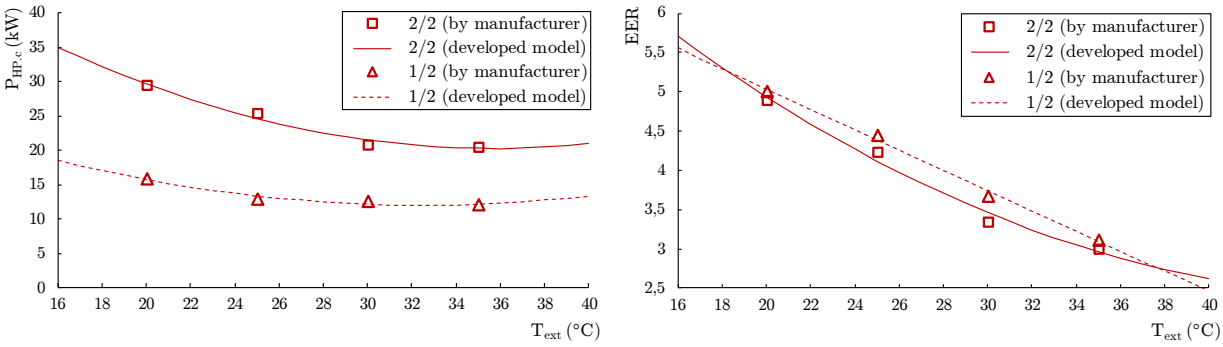

Figure 3.13. Characteristic curves of the selected MSHP evaluated for cooling mode, compared to performance data given by the manufacturer (thermal capacity on the left, *EER* on the right).

Finally, the same analysis is performed taking into account an IDHP model. The heat pump performance data obtained through experimental measures by the manufacturer in correspondence of the maximum and minimum inverter frequency are reported in Figure 3.14 and Figure 3.15 for heating and cooling

mode, respectively. In the same Figures, the characteristic curves of the selected inverter-driven unit are shown: the comparison between experimental values and the heat pump performance data obtained from the developed mathematical model confirms a good agreement among the two different approaches. The maximum discrepancy between the experimental measures and the results of the proposed model is below 8% for heating mode and below 5% for cooling mode.

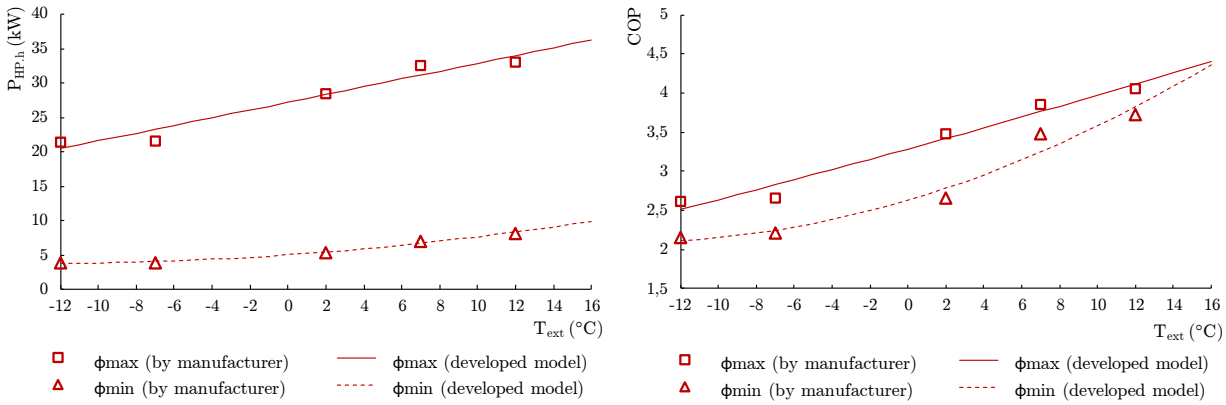

Figure 3.14. Characteristic curves of the selected IDHP evaluated for heating mode, compared to performance data given by the manufacturer (thermal capacity on the left, *COP* on the right).

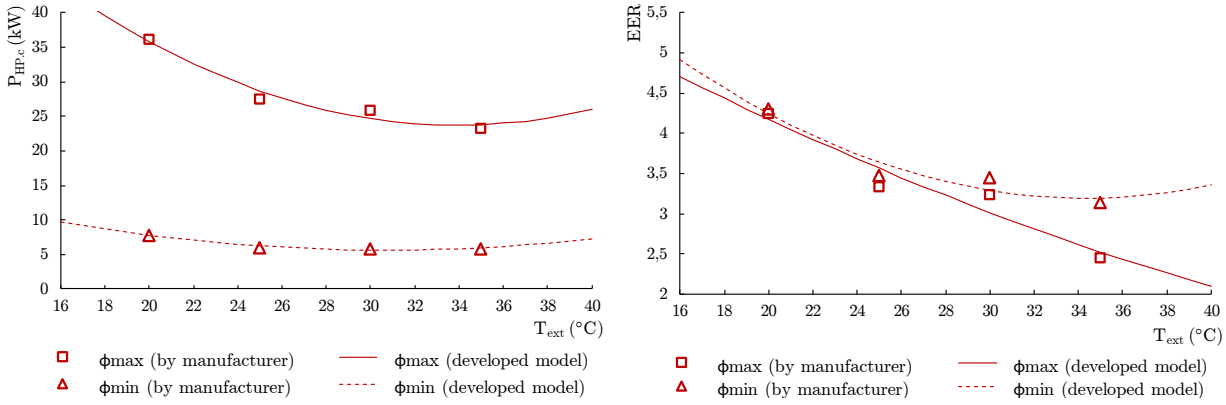

Figure 3.15. Characteristic curves of the selected IDHP evaluated for cooling mode, compared to performance data given by the manufacturer (thermal capacity on the left, *EER* on the right).

In conclusion, the reduced difference evidenced by the comparison between the experimental data and the predictions of the presented calculation procedure can be considered a good benchmark for this method.

3.6. Annual Performance Factor evaluation

In order to analyze the global energy performance of a heat pump system during the whole year, a further performance index is introduced. The Annual Performance Facor (*APF*) takes into account the energy efficiency of the system for both heating and cooling operating modes and it is defined as the ratio between the total thermal and cooling energy delivered by the heat pump system (heat pump and back-up) during the year and the overall energy absorbed.

If the heating back-up system is composed by electric resistances, the *APF* is defined as:

$$APF = \frac{\sum_i E_{HP,h}(i) + \sum_i E_{BU,h}(i) \sum_i E_{HP,c}(i)}{\sum_i E_{HP,h,el}(i) + \sum_i E_{BU,abs}(i) \sum_i E_{HP,c,el}(i)} \tag{3.36}$$

while in case of a bi-valent bi-energetic heat pump system (i.e. gas boiler as back-up) the *APF* is given by:

$$APF = \frac{\sum_i E_{HP,h}(i) + \sum_i E_{BU,h}(i) + \sum_i E_{HP,c}(i)}{\sum_i E_{HP,h,el}(i) + \sum_i \frac{E_{BU,h,abs}(i)}{f_p} + \sum_i E_{HP,c,el}(i)} \tag{3.37}$$

If one performs an assessment of the annual performance of a heat pump system, the comparison between heating and cooling performance of the system is needed. Thus, it is useful to introduce an indicator of the existence of seasonal unbalanced building loads (Unbalance Indicator, *UI*), defined by means of the following Equation:

$$UI = \frac{P_{des,c}}{P_{des,h}} \tag{3.38}$$

when *UI*=1 the absolute value of the design building load is the same both for heating and cooling; when *UI* is larger than 1 the building thermal load during

summer is larger than the winter load and the opposite occurs for UI lower than 1.

It is possible to assess the heat pump oversizing/downsizing with respect to the design load required by the building by introducing the heating and cooling oversizing parameters (OP_h and OP_c) defined as:

$$OP_h = \frac{P_{HP,h,FL} - P_{des,h}}{P_{des,h}} \tag{3.39}$$

$$OP_c = \frac{P_{HP,c,FL} - P_{des,c}}{P_{des,c}} \tag{3.40}$$

where $P_{HP,h,FL}$ and $P_{HP,c,FL}$ are the heat pump thermal and cooling capacity delivered by the heat pump at full load, in correspondence of the outdoor design temperature $T_{des,h}$ and $T_{des,c}$, respectively.

A value of OP equal to 0 means that the selected heat pump is able to deliver exactly the building design peak load; for OP values lower than 0 the heat pump is downsized with respect to the building load, while OP values larger than 0 indicates an oversized heat pump.

In order to analyze the annual energy performance of the HVAC system, an overall indicator of the downsizing/oversizing degree of the system (OP_{tot}) is introduced:

$$OP_{tot} = \frac{DD_h OP_h + DD_c OP_c}{DD_h + DD_c} \tag{3.41}$$

where OP_h and OP_c are weighted on the degree days linked to the heating (DD_h) and cooling (DD_c) seasons.

Degree days are a simple indicator to assess the climate severity of a specific location [83]. They are defined with respect to a base temperature, namely the outside temperature above which the building needs no heating/cooling. The most appropriate base temperature for a particular building depends on the set-point temperature imposed to the HVAC system. During winter, the base temperature is usually setted to 18 °C or 20 °C, which is adequate for indoor comfort, while

during summer an appropriate base temperature may be imposed equal to 26 °C. Heating and cooling degree days are defined through the following Equations:

$$DD_h = \sum_i (T_{base,h} - T_{ext}(i))^+ \tag{3.42}$$

$$DD_c = \sum_i (T_{ext}(i) - T_{base,c})^+ \tag{3.43}$$

where $T_{base,h}$ and $T_{base,c}$ are the indoor base temperature for heating and cooling season, respectively and the superscript + means that only positive terms are taken into account in the sum.

There are several ways calculate heating and cooling degree days: the more detailed temperature data are recorded, the more accurate degree days calculation can be performed. $DD_{h/c}$ are often calculated using simple methods that employ daily average temperature readings instead of more detailed temperature records such as hourly or sub-hourly records. In this Thesis, heating and cooling degree days are calculated by means of hourly values of the external temperature.

3.7. Case studies

In order to highlight the influence of the heat pump control logic on the seasonal performance of the system, two case studies are reported in this Thesis. The developed mathematical models described in previous Sections 3.3-3.4 have been applied to evaluate the seasonal efficiency of a heat pump system coupled to a residential building; furthermore, in the first case study presented in this Section the influence of the heat pump modulation capability (i.e. its control logic) on the energy performance of the system during the heating season has been assessed by considering different heat pump typologies and different residential buildings. Therefore, in the second reported case study the annual performance of HVAC systems based on a reversible air-to-water heat pump has been evaluated as a function of the heat pump typology, the location in which the system is placed and the unit sizing: in this case study, the influence of unbalanced seasonal heating/cooling loads has been pointed out.

The topics of this section are discussed in Refs. [84] and [85].

3.7.1. Assessment of the influence of the heat pump modulation capacity on the seasonal performance of a heating system

The mathematical model for winter operating mode presented in Section 3.3 is applied in this Section to evaluate the seasonal performance factor of single-stage on-off, multi-stage and inverter-driven heat pumps, integrated by electric resistances as back-up system, and employed to provide heating to several buildings, located in Bologna (44.27°N, 11.20°E). The influence of the choice of the bivalent temperature ($T_{biv,h}$), in order to maximize the seasonal efficiency of different models of air-to-water heat pumps (On-off HP, MSHP, IDHP) coupled to a radiant floor heating system, is here investigated.

Three models of heat pump are considered in this analysis; these models have been selected with similar rated performances at full load, in order to evaluate their seasonal performance under similar conditions.

Table 3.7. Selected heat pumps rated performance (7°C dry bulb, 6°C wet bulb for outdoor air temperature; 40-45°C inlet/outlet water temperature) and their main technical characteristics.

Heat pump typology	On-off HP	MSHP	IDHP
Heating Capacity (kW)	35.6	34.2	34.9
COP	3.42	3.17	3.06
Electrical power input (kW)	10.4	10.8	11.4
Frequency (Hz)	50	50	30-120
TOL (°C)	-10	-10	-18
Compressors number	1	2	1
Compressor model	Maneurop SH-140-4	SANYO 1: CSBN453H8H 2: CSBN453H8H	Siam ANB52FTTMT
Refrigerant fluid	R410A	R410A	R410A
Refrigerant circuits	1	1	1

In Table 3.7 the main technical characteristics declared by the manufacturer at rated conditions for the selected heat pumps are quoted. As indicated in Table 3.7, all the considered heat pumps are reversible and use R410A as refrigerant. The On-off HP has one fixed speed scroll compressor, while the MSHP is characterized by two identical fixed speed scroll compressors, connected in

parallel, each one with a size which is about the half of the On-off HP compressor. On the contrary, the IDHP has a variable-speed scroll compressor driven by an inverter which allows modulating its rotating speed. In order to highlight the performance of the three selected heat pumps, in Table 3.7 the thermal capacity and the *COP* at full load conditions of the selected heat pumps are reported as a function of the outdoor air temperature, respectively. The technical data of the selected heat pumps are given by the manufacturer and they are collected for a value of the hot water temperature ($T_{w,h}$) produced by the heat pump equal to 35 °C, typical value of the supplied water temperature in the hydronic loop of a radiant floor heating system.

As shown clearly by the data of Figure 3.16 and Figure 3.17, for a fixed value of the supplied hot water temperature ($T_{w,h}$=35 °C) the three selected heat pumps have the same thermal capacity (Figure 3.16) but their energy performance (i.e. *COP*) is quite different at the same outdoor temperature (Figure 3.17): the On-off HP is characterized by the best *COP* at full load within the whole range of outdoor temperature considered; on the contrary, the selected MSHP and IDHP have similar performance at full load.

However, during the whole heating season, heat pumps are called to work at full load only for a limited period of time. As shown later, the duration of this period in which the unit is able to work at full load depends on the kind of the heat pump considered and, of course, by the choice of the bivalent temperature. As a consequence, for a correct evaluation of the seasonal performance factor it is important to take into account the behavior of the unit at partial load. In fact, when the heat pump works at partial loads the differences among On-off HP, MSHP and IDHP become more and more evident because these devices are characterized by different modulation capacity and react in a different way to the reduction of the required thermal load.

More in detail, if the On-off HP is considered, at large outdoor temperature, when the building load is lower, the heat pump thermal capacity can be reduced only by starting a series of on-off cycles of the compressor. During these unsteady working conditions the unit loses efficiency: for each start-up there are a series of energy losses which are accounted for by means of the C_c coefficient of Eq. (3.10).

On the contrary, the MSHP presents a smarter control system to reduce the delivered thermal capacity at larger outdoor temperatures. In this case the selected MSHP has 2 compressors of the same size connected in parallel, each one smaller than the single compressor of the On-off HP, connected to a single refrigeration loop. When the building thermal load decreases, the controller of the

unit can switch off one compressor and consequently decreases also the refrigerant mass flow rate within the refrigeration loop.

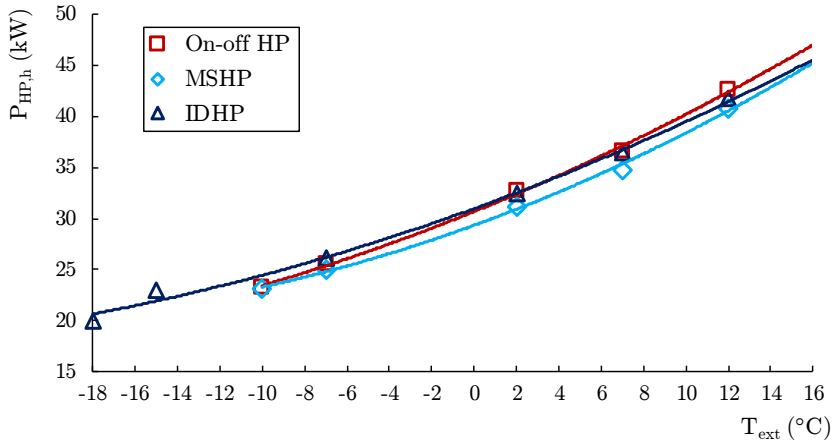

Figure 3.16. Thermal capacity of the selected heat pumps as a function of the outdoor temperature (data obtained at full load for $T_{w,h}$=35°C).

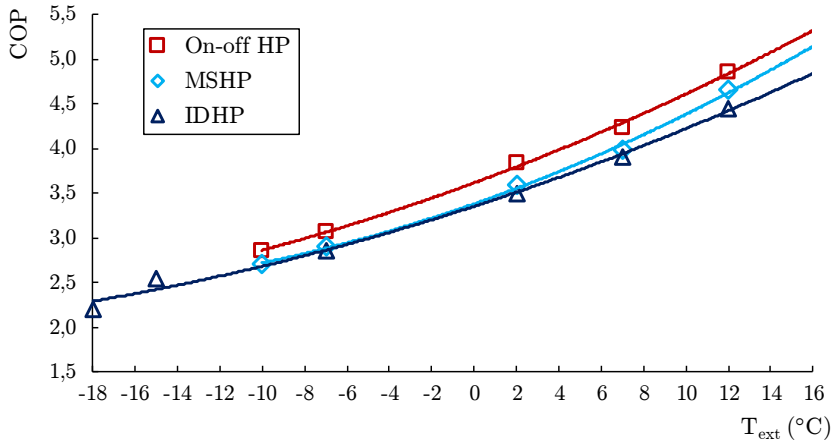

Figure 3.17. *COP* of the selected heat pumps as a function of the outdoor temperature (data obtained at full load for $T_{w,h}$=35°C).

In Table 3.8 the energy performance (i.e. thermal capacity and *COP*) of the selected MSHP is shown as a function of the outdoor air temperature and of the number of activated compressors (reported data are given by the manufacturer for $T_{w,h}$=35°C). Data reported in Table 3.8 demonstrate that MSHP performance improves when the number of activated compressors is reduced; in fact, when one compressor is turned off, the refrigerant mass flow rate in the refrigeration loop is reduced but the total heat transfer area of evaporator and condenser is still the

same. In these conditions the thermal efficiency of the evaporator and of the condenser slightly increases: one can note a *COP* increase that ranges between 2% and 7%, depending on the value of external temperature. It is possible to conclude that the MSHP is able to work at partial load with larger *COP* values with respect to the On-off HP for two reasons: the enhancement of *COP* highlighted above and, as will be shown later, the delay of the on-off cycles adoption to match the required building load.

Table 3.8. Performance of the selected MSHP at full load (2/2 data) and at partial load (1/2 data) for a fixed value of the hot water temperature ($T_{w,h}$=35 °C).

External temperature (°C)	MSHP performance at full load		MSHP performance at partial load		Efficiency increase at partial load
	$P_{HP,h,2/2}$ (kW)	$COP_{2/2}$	$P_{HP,h,1/2}$ (kW)	$COP_{1/2}$	
-10	23.1	2.7	12.3	2.76	+2.2%
-7	25	2.9	13.2	2.95	+1.7%
2	31.2	3.59	16.7	3.71	+3.3%
7	34.8	3.98	19.3	4.26	+7.0%
12	40.8	4.65	22.3	4.89	+5.2%

If one considers the IDHP, the thermal capacity delivered to the building by the heat pump can be adapted to the required energy demand in a continuous way by changing the compressor rotating speed. In this case, the inverter frequency can be varied from a minimum of 30 Hz (minimum compressor rotating speed) to a maximum of 120 Hz, corresponding to the full load working condition (maximum compressor rotating speed). When the building thermal load decreases the inverter reduces the compressor rotating speed: in this way the refrigerant mass flow rate within the refrigeration loop and consequently the heat pump thermal capacity decrease. Also in this case, until the outdoor temperature is lower than the value in correspondence of which the on-off cycling starts ($T_{cyc,h}$, see Section 3.3.3), the heat pump avoids On-off cycles by matching exactly the building thermal load and in this way cycling energy losses are strongly reduced. In addition, when the IDHP compressor operates with a reduced rotating speed its efficiency initially increases. This behavior is illustrated by Figure 3.18, in which the trend of the *COP* of the selected IDHP is shown as a function of the inverter frequency for different values of the external air temperature.

Each *COP* curve is obtained for a fixed value of the outdoor temperature between -18°C and 12°C. Figure 3.18 shows that, once fixed a value of T_{ext}, at full load the heat pump works at the lowest *COP* value and this value reaches a maximum when the inverter frequency is halved with respect to the maximum frequency (120 Hz). Also in this case, when the outdoor temperature is larger than $T_{cyc,h}$, the IDHP compressor rotates at its minimum rotating speed and the unit starts to perform on-off cycles.

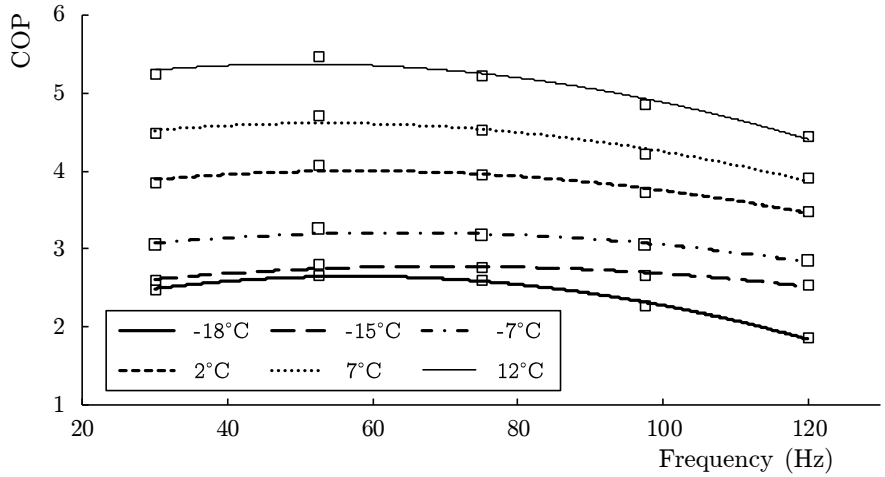

Figure 3.18. *COP* of the selected IDHP as a function of inverter frequency for different values of the outdoor temperature (data obtained for $T_{w,h}$=35°C).

It is possible to summarize the above considerations by observing that the MSHP and the IDHP are able to work with a larger *COP* with respect to the on-off unit because for this kind of heat pumps it becomes possible to delay the starting of the on-off compressor cycles, thus reducing the energy losses at partial loads. More $T_{cyc,h}$, is larger with respect to the bivalent temperature, more the *COP* at partial load can be improved by adopting a MSHP or an IDHP with respect to a single-stage On-off HP.

The values assumed by $T_{biv,h}$ and $T_{cyc,h}$ depend not only by the heat pump but also by the thermal load required by the building; for this reason, in order to highlight the role played by the thermal energy demand of the building, for a fixed size of the heat pump, the selected units have been coupled to 11 different buildings located in Bologna, each one characterized by a different thermal load. In this way, for each case different values of $T_{biv,h}$ and $T_{cyc,h}$ are obtained. BES is used to univocally identify the building thermal needs (see Section 3.3.2). All the BES have been obtained by considering a Heating Limit External Temperature

(HLET) equal to 16°C. As evidenced in Table 3.9 the bivalent temperature ranges between about -5°C (building # 1) and about 6.5°C (building #11); this means that the selected units are able to cover completely the thermal needs of the building #1 in Bologna where the design outside temperature ($T_{des,h}$) is equal to -5°C (Figure 3.6); on the contrary, the other buildings (#2-#11) are characterized by larger thermal loads, which the selected heat pumps are able to cover only partially. In these cases, an electrical heater is considered as back-up system. As described before, each simulation has been performed by considering the heat pump coupled to a radiant floor heating system working with hot water having a fixed temperature equal to 35°C ($T_{w,h}$), value independent from the outside temperature. In Table 3.9, the values of $T_{cyc,h}$ are also summarized for the 11 buildings considered.

Table 3.9. Building design loads and values of $T_{biv,h}$ and $T_{cyc,h}$ obtained through simulations.

Case	Design load (kW)	On-off HP	MSHP		IDHP	
		$T_{biv,h}$ (°C)	$T_{biv,h}$ (°C)	$T_{cyc,h}$ (°C)	$T_{biv,h}$ (°C)	$T_{cyc,h}$ (°C)
1	28	-4.5	-4.0	3.1	-4.6	8.2
2	31	-3.1	-2.6	4.0	-3.3	8.8
3	34	-2.0	-1.5	4.8	-2.1	9.4
4	37	-1.0	-0.5	5.5	-1.0	9.8
5	40	-0.1	0.5	6.1	-0.1	10.2
6	45	1.2	1.7	7.0	1.2	10.8
7	50	2.3	2.8	7.7	2.3	11.2
8	55	3.2	3.6	8.3	3.3	11.6
9	60	4.0	4.5	8.9	4.1	12.0
10	67	5.0	5.4	9.5	5.1	12.3
11	75	5.9	6.3	10.1	6.0	12.7

By means of the model described in this Thesis, it is possible to analyze the influence of $T_{biv,h}$ and $T_{cyc,h}$ (in the case of MSHP and IDHP) on the seasonal energy performance of the system ($SCOP_{net}$ and $SCOP_{on}$), as well as the energy delivered by the units during the season and the energy delivered by the electric back-up system when the heat pump thermal capacity is lower than the thermal

load needed by the building. As an example, in the following Figures the results obtained for the building #7 are reported.

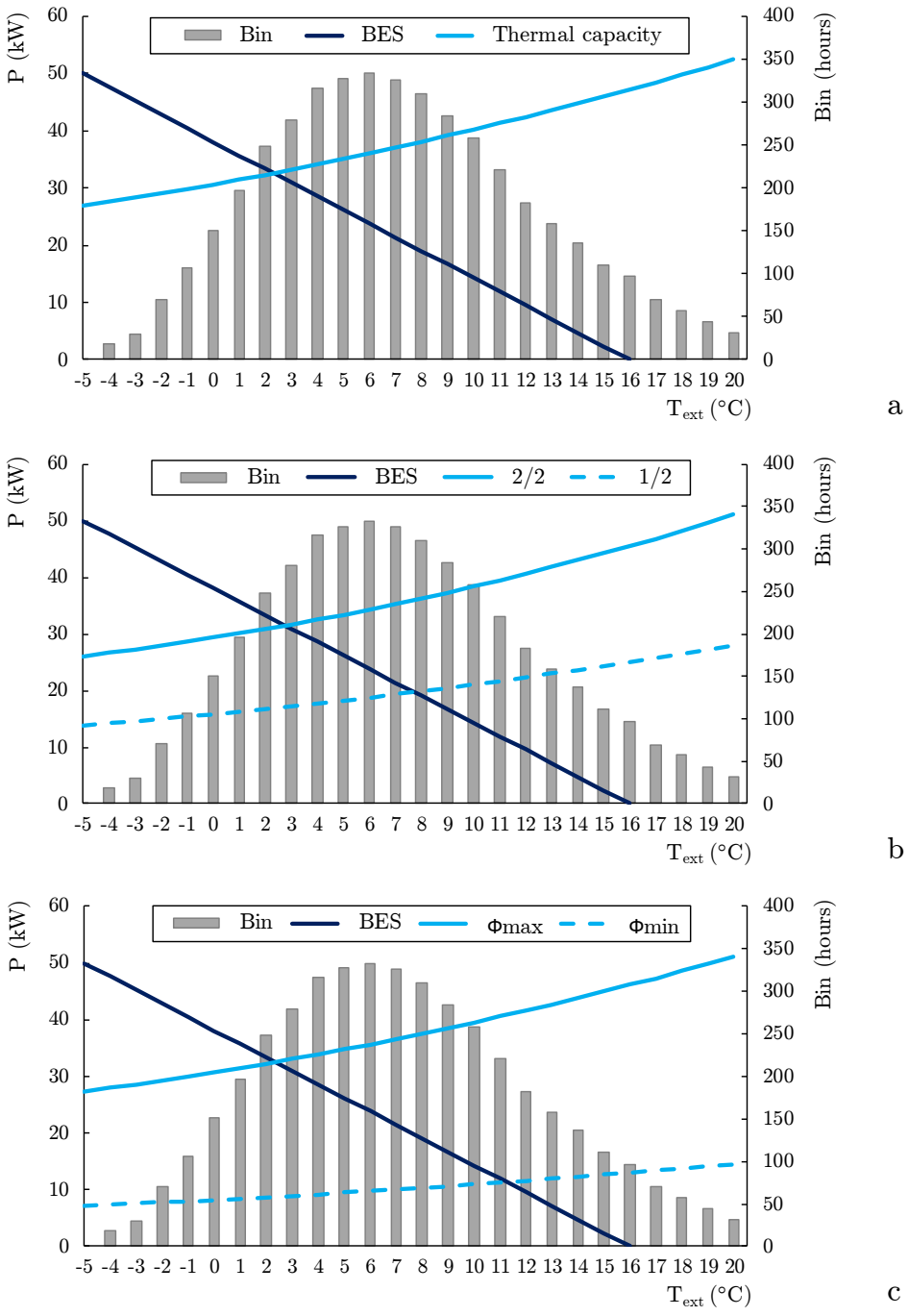

Figure 3.19. Bin trend, BES (case #7), heat pump thermal capacity at full load and at partial load: On-off HP (a), MSHP (b) and IDHP (c).

The typical bin distribution of Bologna is reported in Figure 3.19a, Figure 3.19b and Figure 3.19c together with the BES of building #7 (blue line) and the thermal capacity at full load and at partial load of the considered On-off HP (Figure 3.19a), MSHP (Figure 3.19b) and IDHP (Figure 3.19c), respectively.By comparing Figure 3.19a, Figure 3.19b and Figure 3.19c it is possible to observe that the three considered units are characterized by the same bivalent temperature ($T_{biv,h} \approx 2.5\,°C$ in this case); this is a consequence of the similar thermal capacity at full load demonstrated by the three selected heat pumps (see Figure 3.16). Figure 3.19b and Figure 3.19c show also the different capacity modulation of the MSHP and IDHP, respectively: more in detail, the MSHP can modulate its delivered thermal capacity avoiding the on-off cycles when the outside temperature is between $T_{biv,h}$ (2.78 °C) and $T_{cyc,h}$ (7.73 °C). Furthermore, Figure 3.19c shows that the selected IDHP is able to match the required building thermal load when the outside temperature ranges between 2.34 °C and 11.24 °C (i.e. $T_{biv,h}$ and $T_{cyc,h}$, respectively).

In Figure 3.20a, Figure 3.20b and Figure 3.20c a comparison between the energy delivered for each bin by the three selected heat pumps ($E_{HP,h}$) and the building thermal energy demand ($E_{b,h}$) is shown for the case #7. In the same Figures, the thermal energy delivered by the back-up system ($E_{BU,h}$) is reported. The trend of the building energy demand as a function of the outdoor temperature follows the profile of the bin distribution of Bologna, with a maximum in correspondence of an outdoor temperature equal to 5 °C. The heat delivered by the heat pump follows a similar trend; in addition, the energy supplied by the heat pump matches perfectly the profile of the building energy demand for values of outdoor temperature larger than the bivalent temperature.

When T_{ext} is lower than $T_{biv,h}$, the energy delivered by the heat pump becomes lower than the building energy demand. In Table 3.10 the value of seasonal building energy demand ($E_{b,h}$) is quoted and compared with the seasonal value of the thermal energy delivered by the heat pumps ($E_{HP,h}$); the difference between these two values highlights the downsizing of the units with respect to the building thermal request. Since these three heat pumps are characterized by a similar size, this difference is similar for the three cases; in Table 3.10 this difference is indicated as $E_{BU,h}$ because it is the energy delivered by the back-up system during the whole winter.

It is noticeable that the electric heaters are activated below the bivalent temperature and then work in parallel with the heat pump. The energy delivered by the back-up system ranges between 5.6% and 7% of the seasonal building

thermal needs and it becomes maximum (7%) for the MSHP, which is characterized by the highest bivalent temperature with respect to the selected On-off HP and IDHP.

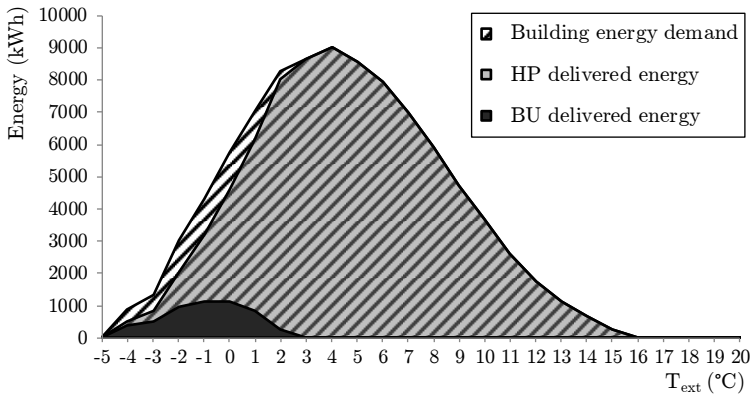

a

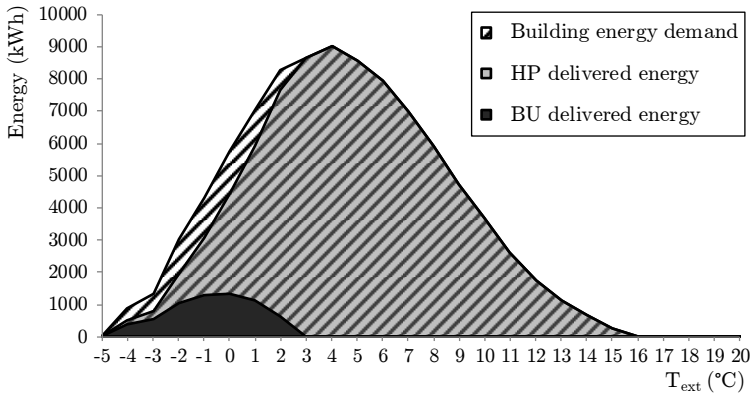

b

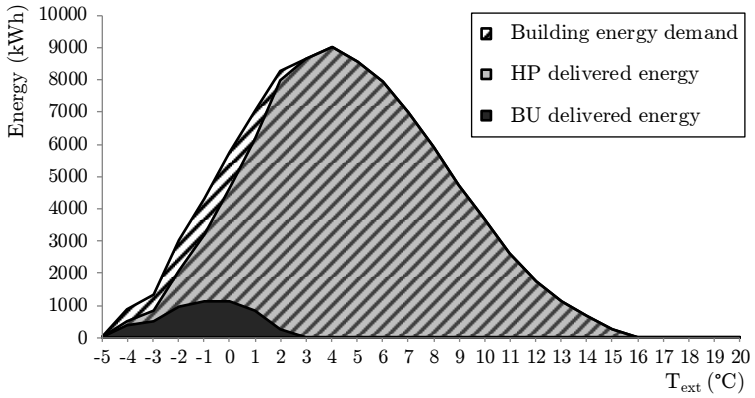

c

Figure 3.20. Building energy demand, thermal energy delivered by the heat pump and by the back-up system as a function of the outdoor temperature (case #7): On-off HP (a); MSHP (b); IDHP (c).

In Table 3.10 the electric energy consumption of the three selected heat pumps ($E_{HP,h,el}$), calculated by applying the model described in this Thesis, are reported. It is evident that the selected IDHP is characterized by the minimum electric energy consumption with respect to the On-off HP and the MSHP. The best performance of the IDHP is also highlighted by the obtained values of $SCOP_{on}$ and $SCOP_{net}$; the IDHP is characterized by a value of $SCOP_{net}$ which is larger than 9% with respect to the value obtained adopting the On-off HP and 8.5% with respect to the MSHP. In terms of $SCOP_{on}$ this difference becomes equal to 7% with respect to the On-off HP and 10% with respect to MSHP.

Table 3.10. Values of seasonal performance of the whole heat pump system for case #7.

Heat pump	$SCOP_{net}$	$SCOP_{on}$	$T_{biv,h}$ (°C)	$T_{cyc,h}$ (°C)	$E_{b,h}$ (kWh)	$E_{HP,h}$ (kWh)	$E_{HP,h,el}$ (kWh)	$E_{BU,h}$ (kWh)
On-off HP	3.80	3.29	2.3	/	92 509	87 337	22 972	5 173
MSHP	3.82	3.21	2.8	7.7	92 509	86 209	22 543	6 300
IDHP	4.15	3.53	2.3	11.2	92 509	87 353	21 033	5 156

The evaluation of the seasonal performance of the heat pumps coupled to the 11 buildings considered in this analysis enables to analyze the influence of a different sizing of the unit on the seasonal efficiency of the system; in fact, by considering all the 11 buildings, for each system it is possible to assess the system seasonal performance factor over a large range of values of the bivalent temperature, from -4.64°C to 6.31°C. In Figure 3.21 the trend of $SCOP_{net}$ as a function of the bivalent temperature is represented; the reported values take into account the behavior of the heat pumps at partial loads during the whole season.

If one considers Figure 3.21, it is evident that the influence of $T_{biv,h}$ on the seasonal performance of the selected heat pumps is very different one another. Both the MSHP and the On-off HP present increasing $SCOP_{net}$ when the bivalent temperature grows; however, it is evident that the $SCOP_{net}$ of an On-off HP is more sensible to the choice of a different $T_{biv,h}$ with respect to a MSHP. On the contrary, the IDHP is characterized by a value of $SCOP_{net}$ more stable when $T_{biv,h}$ is changed; however, the data reported in Figure 3.21 put in evidence that $SCOP_{net}$ for the IDHP decreases when the bivalent temperature increases, which is an opposite trend with respect to On-off HP and MSHP. In order to explain these trends, it is important to keep in mind that both MSHP and IDHP are less influenced by the increase of the bivalent temperature for their improved

capacity, if compared with an On-off HP, to modulate the delivered thermal capacity, hence adapting their delivered energy to the building request. For this reason, the modulating units may delay the use of on-off cycles, which start only when the outdoor temperature exceeds $T_{cyc,h}$.

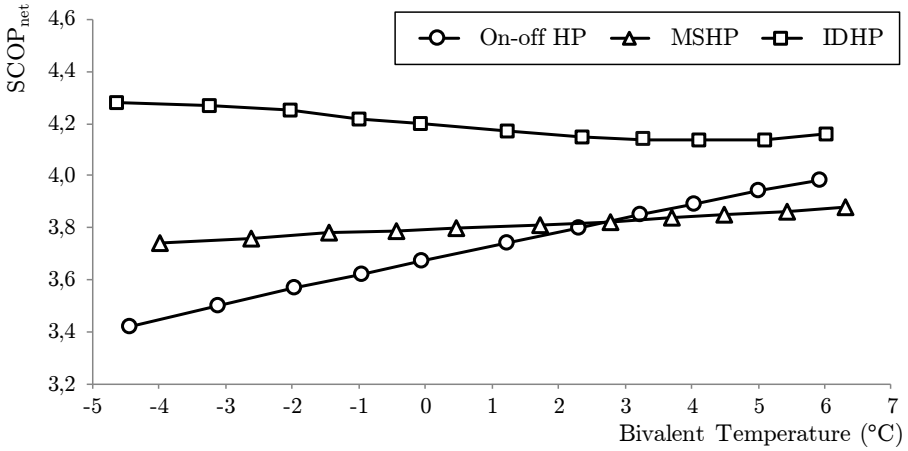

Figure 3.21. $SCOP_{net}$ as a function of the bivalent temperature.

Moreover, the MSHP works with the best efficiency when only one compressor is active, precisely when the thermal load is equal to one compressor thermal capacity. For the IDHP it is important to highlight that its $T_{cyc,h}$ is generally higher than the $T_{cyc,h}$ of a MSHP; in this way, the decrease of the $SCOP_{net}$ due to the increase of the on-off cycles becomes less important at low values of the outdoor temperature.

In Figure 3.22 the trend of $SCOP_{on}$ with respect to the bivalent temperature is shown. When the bivalent temperature is increased, the values of $SCOP_{on}$ evaluated for MSHP and IDHP present the same decreasing trend. On the contrary, the single-stage On-off HP is initially characterized by an increasing $SCOP_{on}$ when $T_{biv,h}$ increases up to 0 °C; after that, the value of $SCOP_{on}$ decreases when $T_{biv,\mathrm{h}}$ is increased in agreement with the other heat pump models. The decreasing trend of $SCOP_{on}$ when the bivalent temperature is increased is linked to the use of the electric back-up: in fact, higher bivalent temperature means higher energy consumptions of the back-up system, which works with lower COP values (theoretically COP=1 for an electric heater).

In the case of a single-stage On-off HP with a low bivalent temperature the total energy delivered by the electric back-up becomes negligible and the increase of $SCOP_{net}$ when the bivalent temperature increases is more significant than the

utilization of the back-up system: this evidence explains the maximum of the $SCOP_{on}$ trend. Furthermore, this fact means that, adopting a mono-compressor On-off HP, there is a specific value of the bivalent temperature (larger than the design temperature) which maximizes the value of $SCOP_{on}$. On the contrary, when a IDHP is selected, the maximum value of $SCOP_{on}$ is obtained by adopting a bivalent temperature equal to the design temperature ($T_{biv,h}=T_{des,h}$). The MSHP has an optimal bivalent temperature which is in between the design temperature and the optimal bivalent temperature for an On-off HP.

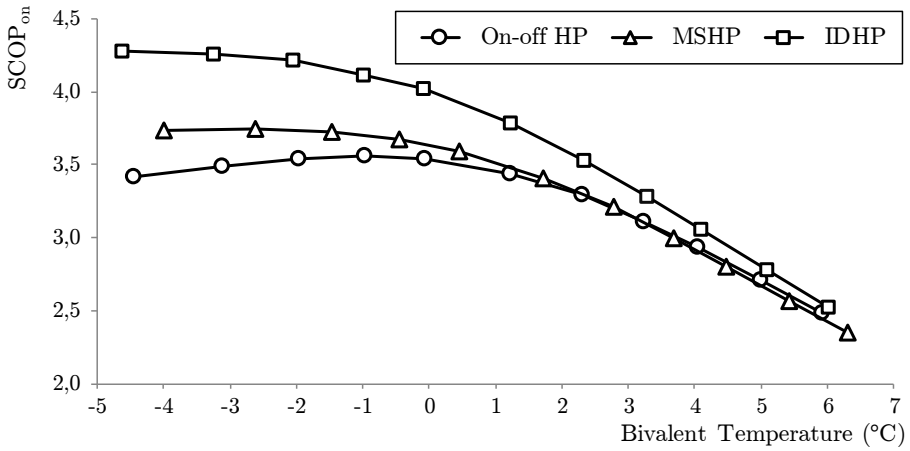

Figure 3.22. $SCOP_{on}$ as a function of the bivalent temperature.

These results highlight that the optimal sizing of a heat pump system is strongly influenced by the modulation characteristics of the adopted heat pump. With a fixed building thermal load, mono-compressor on-off heat pumps present an optimal bivalent temperature higher than multi-compressor and inverter-driven units. Thus, down-sizing a mono-compressor heat pump and over-sizing multi-compressor and inverter-driven units lead to an optimization of the system seasonal efficiency.

3.7.2. Annual performances of reversible air-to-water heat pumps

In this case study, the estimation of the seasonal performance, both in heating and cooling mode, of different typologies of electric reversible air-to-water heat pumps, located in different European climates, is shown. The aim of this study is to highlight in which way the energy consumption of these systems is influenced by the heat pump capacity modulation, the unit sizing and the climate. The

relationship between outdoor conditions, heating and cooling loads, heat pump typology and the system efficiency is presented in order to provide a complete set of information to assess the optimal sizing rules.

A typical three-story office building having the characteristics summarized in Table 3.11 has been considered. The schedule of the heat pump system coupled to the office building reflects its occupancy profile: during workdays (from Monday to Friday) the heating/cooling plant is switched on from 6.00 to 20.00, on Saturday the heat pump system is activated from 6.00 to 14.00 while on Sunday the system is turned off.

Table 3.11. Geometrical and thermal characteristics of the office building.

Net floor area (m^2)	Dispersing surface area (m^2)	Windows area (m^2)	Net volume (m^3)	S/V ratio (m^{-1})	External wall U-value (W/m^2 K)	Floor U-value (W/m^2 K)	Windows U-value (W/m^2 K)
787	1 416	139	2 125	0.52	0.37	0.46	1.70

In order to take into account the influence of different climates on the annual performance of the air conditioning system, the office building has been placed in three different locations: Frankfurt (50.6° N, 8.4° E), Istanbul (41.0° N, 41.6° E) and Lisbon (38.4° N, -9.7° E), which can be considered representative, according to the goal of this work, of Colder, Average and Warmer heating reference climates indicated by the standard EN 14825 [56] (even if different from Helsinki, Strasburg and Athens, cited by the standard).

Table 3.12. Main climatic data of the selected locations.

	Frankfurt	Istanbul	Lisbon
Heating season			
Length of the season	1st October - 30th April	1st November - 15th April	1st December - 31st March
DD_h ($T_{base,h}$=20°C)	3 233	1 973	863
Cooling season			
Length of the season	1st June - 31st August	1st June - 30th September	1st May - 30th September
DD_c ($T_{base,c}$=26°C)	405	1 079	1 251

In Table 3.12 the duration of the heating and cooling season is reported together with the value of the Heating Degree Days (DD_h) and Cooling Degree Days (DD_c) of each location (see Eqs. (3.42) and (3.43)). The base temperatures for heating and cooling season, $T_{base.h}$ and $T_{base.c}$, have been considered equal to 20 °C and 26 °C, respectively.

The local profile of external temperature bins of both heating and cooling season have been calculated by means of the hourly outside temperature distribution of the Typical Reference Year (TRY) obtained by the Meteonorm database [80].

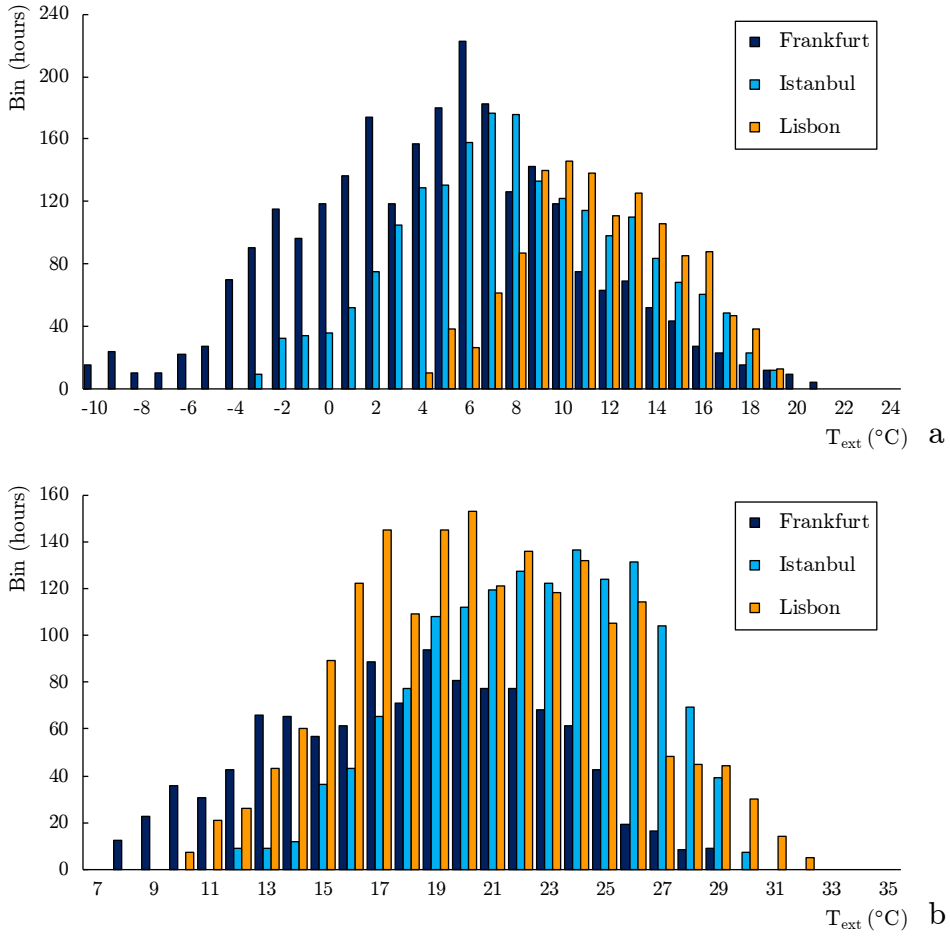

Figure 3.23. Bin profiles of external temperature values during heating (a) and cooling season (b).

The bin distributions of the selected climates present different trends, as evidenced in Figure 3.23. Figure 3.23a highlights that the heating season in

Frankfurt is the coldest among the selected locations: it presents a design temperature $T_{des,h}$ of -10°C with an average value $T_{avg,h}$ of 4.9°C. Istanbul and Lisbon are characterized by a milder heating season, with $T_{des,h}$ equal to -3°C and 4°C, respectively, and $T_{avg,h}$ equal to 8.3°C and 11.6°C, respectively.

The hot seasons of the considered climates are more similar one to another, as evidenced by Figure 3.23b. The most severe condition for the heat pump is set in Lisbon, with a value of the design temperature $T_{des,c}$ of 32°C and with an average outdoor temperature $T_{avg,c}$ equal to 20.7°C. Istanbul cooling season is characterized by similar values ($T_{des,c}$ equal to 30°C and $T_{avg,c}$ equal to 22.4°C) but the length of the season is one month shorter than in Lisbon (see Table 3.12). Finally, Frankfurt presents a cooling design temperature of 29°C and an average air temperature equal to 18.1°C; in this location bins are shifted towards lower outdoor temperature values.

The calculation of building net thermal energy demand for space heating and cooling has been performed on a monthly basis according to the standard EN ISO 13790 [86]. As a result, the monthly net thermal energy required by the building for heating and cooling have been obtained.

Considering an operating time for the heat pump system that follows the scheduling profiles described previously, both during the heating and cooling season, it is possible to calculate the monthly average thermal/cooling capacity that the heat pump has to supply to the building by dividing the thermal energy demand for the number of operating hours of each month. The monthly values of thermal/cooling capacity have been correlated to the monthly average values of the outdoor air temperature via the BES procedure (see Section 3.3.2).

By observing Figure 3.24, it is evident that in Frankfurt the heating peak load ($P_{des,h}$=31.3 kW) is larger than the cooling peak load ($P_{des,c}$=13.6 kW); on the other hand, in Istanbul seasonal peak loads are more balanced ($P_{des,h}$=20.1 kW, $P_{des,c}$=15.8 kW) like in Lisbon, where the maximum peak load is associated to the cooling season ($P_{des,h}$=14.1 kW, $P_{des,c}$=16.3 kW). Frankfurt is representative of typical situations in which the maximum thermal load is reached during winter and strongly unbalanced loads are present moving from the heating to the cooling season. Istanbul is representative of sites in which maximum thermal loads are always reached during winter, but loads moving from the cold to the hot season are only slightly unbalanced. Finally, Lisbon is representative of locations in which the cooling season is more severe than the heating one, but loads are balanced from one season to the other.

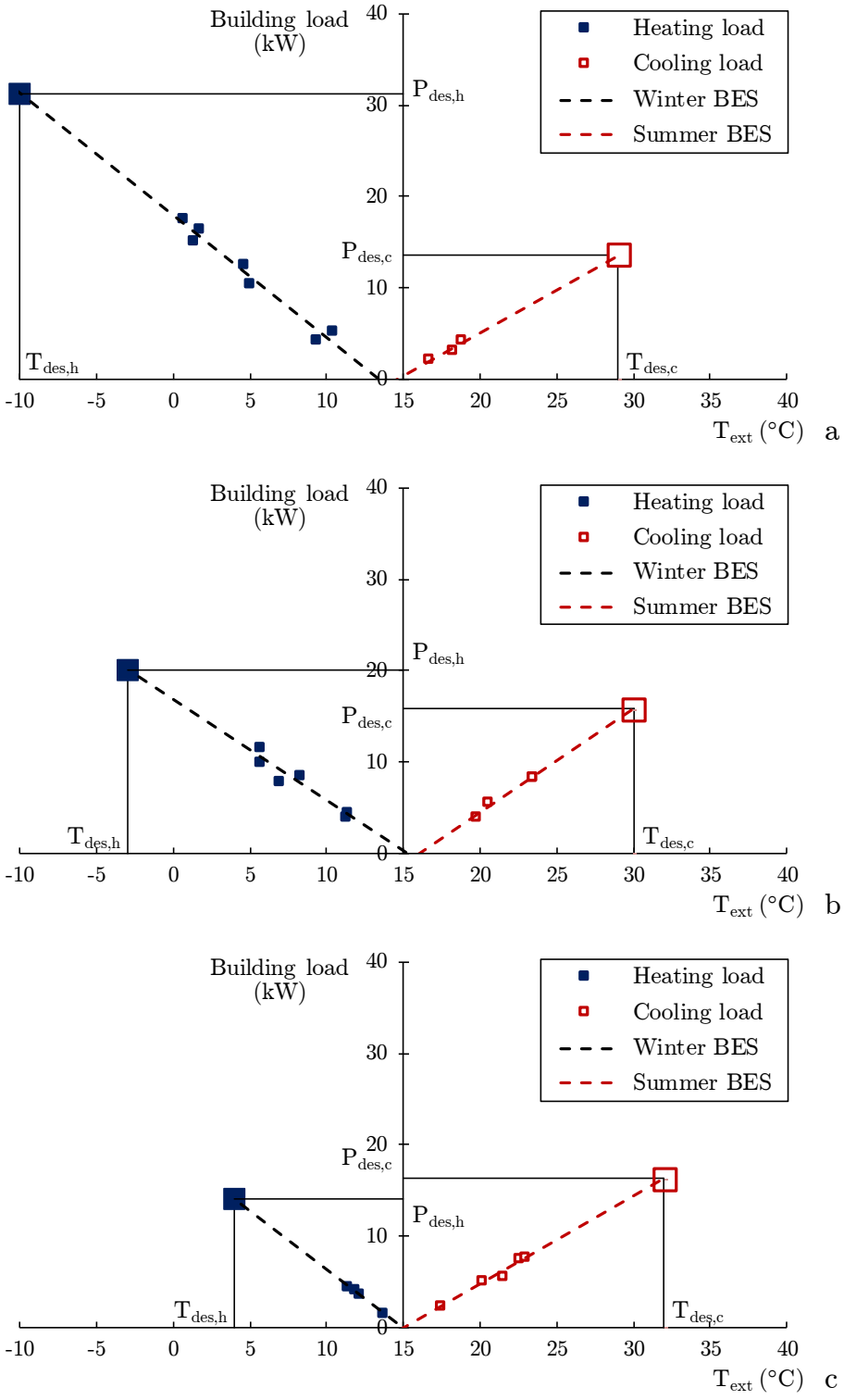

Figure 3.24. BES for heating and cooling season: Frankfurt (a), Istanbul (b) and Lisbon (c).

The three climates considered in this case study are characterized by different values of the unbalance indicator UI (see Section 3.6): in Frankfurt, characterized by higher heating load, it is equal to 0.43, while in Istanbul and Lisbon, characterized by more balanced loads, it is equal to 0.79 and 1.16, respectively.

The HVAC system coupled to the office building is based on a reversible air-to-water heat pump, which satisfies both heating and cooling loads; electric heaters have been considered as back-up system during the cold season, whereas no back-up systems are considered for the hot season. The building terminal units consist of two-pipe fan-coils, sized with a supply water temperature of 45 °C during winter and 7 °C in summer; in this analysis, $T_{w,h}$ and $T_{w,c}$ have been fixed to the above-mentioned temperatures during the entire heating and cooling seasons.

The heat pump typologies described in this Thesis have been considered: single-stage On-off HPs, MSHPs and IDHPs. For each heat pump typology, different units, which differ for their nominal thermal capacity, have been selected: the most powerful heat pump model for each typology has been chosen in order to match the peak load during the most severe season. Then, other smaller units have been considered, to evaluate the influence of heat pump sizing on the seasonal and annual performance of the system.

For Frankfurt and Istanbul climates (prevalent heating load), the choice of the smallest nominal thermal power is based on the cooling peak load. For Lisbon (dominant cooling load), the heating and cooling loads are almost balanced but the hot season is slightly more severe; therefore, the heat pump sizing is based on the cooling peak load. In fact, even if smaller heat pumps would be more suitable during the cold season, then the cooling demand would not be satisfied during the entire summer, since no back-up system for cooling is present in the HVAC system.

Eleven different units have been considered; the technical datasheet at full capacity given by the manufacturer of the heat pumps are reported in Table 3.13, Table 3.14 and Table 3.15 for On-off HPs, MSHPs and IDHPs, respectively. Each unit is identified by a progressive number (# HP unit).

Table 3.13. Thermal/cooling capacity and *COP*/*EER* at full load of the simulated On-off HPs.

# HP unit	1		2		3		4	
HP typology	On-off HP		On-off HP		On-off HP		On-off HP	
Heating mode ($T_{w,h}$=45°C)								
T_{ext} (°C)	$P_{HP,h}$ (kW)	*COP*	$P_{HP,h}$ (kW)	*COP*	$P_{HP,h}$ (kW)	*COP*	$P_{HP,h}$ (kW)	*COP*
-7	17.8	2.55	20.0	2.56	21.9	2.58	26.4	2.59
2	20.6	2.94	23.6	2.96	25.9	2.97	31.6	2.95
7	22.9	3.31	27.0	3.33	29.8	3.36	36.3	3.37
12	25.7	3.74	31.0	3.76	34.3	3.81	41.1	3.78
Cooling mode ($T_{y,c}$=7°C)								
T_{ext} (°C)	$P_{HP,c}$ (kW)	*EER*	$P_{HP,c}$ (kW)	*EER*	$P_{HP,c}$ (kW)	*EER*	$P_{HP,c}$ (kW)	*EER*
20	22.3	4.28	27.2	4.30	31.0	4.31	35.9	4.33
25	21.2	3.73	26.1	3.80	29.5	3.76	34.3	3.82
30	20.2	3.30	24.7	3.32	27.8	3.26	32.7	3.35
35	19.2	2.82	23.3	2.88	26.1	2.79	30.9	2.86

The seasonal energy performance of a HVAC system characterized by a single reversible unit, as the one simulated in this case study, is heavily affected by the device sizing. In fact, heat pumps work at full load only for a limited period of the whole heating/cooling season and their capacity to modulate the delivered thermal/cooling capacity is crucial for a correct analysis of the seasonal performance of the system. In the case of strongly unbalanced seasonal peak loads, as obtained for Frankfurt, the heat pump can fit exactly only one of the two peak loads (the heating one, in this case): during the other season the unit results oversized with respect to the building load and it needs to strongly modulate the delivered capacity.

Table 3.14. Thermal/cooling capacity and *COP*/*EER* at full load of the simulated MSHPs.

# HP unit	5		6		7		8	
HP typology	MSHP		MSHP		MSHP		MSHP	
Compressors	2		2		2		2	
Heating mode ($T_{w,h}$=45°C)								
T_{ext} (°C)	$P_{HP,h}$ (kW)	*COP*	$P_{HP,h}$ (kW)	*COP*	$P_{HP,h}$ (kW)	*COP*	$P_{HP,h}$ (kW)	*COP*
-7	14.6	2.47	16.7	2.42	20.0	2.48	24.6	2.44
2	19.1	3.04	21.8	2.97	26.0	3.00	32.1	2.99
7	22.2	3.36	25.1	3.31	30.1	3.35	37.3	3.33
12	25.6	3.67	29.1	3.71	34.8	3.75	43.0	3.72
Cooling mode ($T_{w,c}$=7°C)								
T_{ext} (°C)	$P_{HP,c}$ (kW)	*EER*	$P_{HP,c}$ (kW)	*EER*	$P_{HP,c}$ (kW)	*EER*	$P_{HP,c}$ (kW)	*EER*
20	21.8	4.62	25.3	4.68	30.7	4.64	37.1	4.67
25	20.8	4.13	24.2	4.18	29.3	4.08	35.6	4.15
30	19.9	3.59	22.8	3.62	27.9	3.57	34.0	3.66
35	18.8	3.15	21.6	3.18	26.4	3.11	32.4	3.20

In Table 3.16 the heating and cooling capacity at full load ($P_{HP,h,FL}$ and $P_{HP,c,FL}$) of the selected heat pumps, evaluated in correspondence of the design heating/cooling outdoor temperature, are shown and compared with the heating and cooling peak loads of the office building, by considering the selected locations.

Table 3.15. Thermal/cooling capacity and *COP*/*EER* at full load of the simulated IDHPs.

# HP unit	9		10		11	
HP typology	IDHP		IDHP		IDHP	
Frequency range (Hz)	20-120		20-120		20-120	
Heating mode ($T_{w,h}$=45 °C)						
T_{ext} (°C)	$P_{HP,h}$ (kW)	*COP*	$P_{HP,h}$ (kW)	*COP*	$P_{HP,h}$ (kW)	*COP*
-7	15.1	2.11	21.3	2.10	24.4	2.14
2	18.6	2.52	26.1	2.54	30.1	2.55
7	21.2	2.82	29.6	2.76	33.2	2.78
12	24.6	3.22	33.8	3.18	38.6	3.19
Cooling mode ($T_{w,c}$=7 °C)						
T_{ext} (°C)	$P_{HP,c}$ (kW)	*EER*	$P_{HP,c}$ (kW)	*EER*	$P_{HP,c}$ (kW)	*EER*
20	21.9	3.89	30.7	3.85	34.4	3.81
25	20.9	3.37	29.4	3.33	32.9	3.31
30	19.7	2.89	28.0	2.85	31.3	2.86
35	18.5	2.46	26.6	2.42	29.6	2.45

It is possible to check the heat pump oversizing/downsizing with respect to the design peak loads by means of the oversizing parameters OP_h and OP_c, introduced in Section 3.6 by Eqs. (3.39)-(3.40). If one considers a generic heat pump unit, its downsizing/oversizing depends on the location in which the building is placed. For example, the MSHP number 6 is strongly oversized during the cooling season, with respect to the cooling peak loads of the office building situated in Frankfurt and Istanbul (OP_c=70% and OP_c=45%, respectively). On the other hand, the heat pump number 6 is downsized with respect to the heating loads in Frankfurt (OP_h=-51%) but in Istanbul it is only slightly downsized (OP_h=-6%). The values of OP_h and OP_c are reported in Table 3.16 for the simulated cases.

For each case, the thermal/cooling energy delivered by the heat pump and by the electric back-up (if needed), as well as the electrical energy overall consumptions of the system have been calculated, both for heating and cooling operating modes.

Table 3.16. Heating and cooling capacity at full load at the design temperature of the considered heat pumps and oversizing (or downsizing) with respect to building design loads.

Location	Frankfurt				Istanbul				Lisbon			
HP unit	$P_{HP,h,FL}$ (kW)	$P_{HP,c,FL}$ (kW)	OP_h	OP_c	$P_{HP,h,FL}$ (kW)	$P_{HP,c,FL}$ (kW)	OP_h	OP_c	$P_{HP,h,FL}$ (kW)	$P_{HP,c,FL}$ (kW)	OP_h	OP_c
1 (On-off)	16,3	20,4	-48%	+50%	18,5	20,2	-8%	+28%	21,5	19,8	+53%	+22%
2 (On-off)	18,2	25,0	-42%	+84%	20,9	24,7	+4%	+57%	-	-	-	-
3 (On-off)	19,9	28,2	-36%	+107%	22,9	27,8	+14%	+76%	-	-	-	-
4 (On-off)	23,2	33,0	-26%	+143%	-	-	-	-	-	-	-	-
5 (MSHP)	13,4	20,1	-57%	+48%	16,5	19,9	-18%	+26%	20,3	19,4	+44%	+19%
6 (MSHP)	15,4	23,1	-51%	+70%	18,8	22,9	-6%	+45%	-	-	-	-
7 (MSHP)	18,4	28,2	-41%	+107%	22,4	27,9	+12%	+77%	-	-	-	-
8 (MSHP)	22,6	34,3	-28%	+153%	-	-	-	-	-	-	-	-
9 (IDHP)	14,4	20,0	-54%	+47%	16,4	19,7	-18%	+25%	19,6	19,2	+39%	+18%
10 (IDHP)	20,2	28,3	-35%	+108%	23,2	28,0	+16%	+77%	-	-	-	-
11 (IDHP)	23,3	31,6	-26%	+133%	-	-	-	-	-	-	-	-

In Table 3.17 the values assumed by seasonal and annual performance factors (i.e. $SCOP_{on}$, $SEER_{on}$ and APF) introduced in Sections 3.3, 3.4 and 3.6 are shown. These indexes can be useful to put in evidence the influence of the heat pump typology, climate and unit sizing on the energy efficiency of the system.

In a site like Frankfurt characterized by a heating season more severe than the cooling season (UI=0.43), the heat pump size is generally chosen accordingly to the heating peak load. In this case, units number 4, 8 and 11 are the closest to the heating peak load, with downsized full capacity at design outdoor temperature (number 4: OP_h=-26%, number 8: OP_h=-28%, number 11: OP_h=-26%). Since in Frankfurt the cooling peak load is lower than the heating one, units number 4, 8 and 11 result largely oversized with respect to the cooling peak load, up to 153%

for unit number 8 (see Table 3.16). Therefore, during the cooling season the considered heat pumps have to deliver only a small fraction of their full cooling capacity by using their modulation capability.

Table 3.17. Seasonal and annual performance factors obtained for the considered heat pump units.

Location	Frankfurt			Istanbul			Lisbon		
HP unit	$SCOP_{on}$	$SEER_{on}$	APF	$SCOP_{on}$	$SEER_{on}$	APF	$SCOP_{on}$	$SEER_{on}$	APF
1 (On-off HP)	2.49	3.09	2.54	2.77	3.27	2.95	2.72	3.13	2.94
2 (On-off HP)	2.57	2.91	2.60	2.69	3.14	2.85	-	-	-
3 (On-off HP)	2.62	2.76	2.63	2.65	3.01	2.78	-	-	-
4 (On-off HP)	2.59	2.63	2.60	-	-	-	-	-	-
5 (MSHP)	2.53	4.29	2.64	3.15	4.34	3.52	3.31	4.22	3.79
6 (MSHP)	2.71	4.08	2.80	3.19	4.17	3.51	-	-	-
7 (MSHP)	2.89	3.85	2.96	3.16	4.05	3.45	-	-	-
8 (MSHP)	2.93	3.61	2.99	-	-	-	-	-	-
9 (IDHP)	2.29	4.35	2.40	2.93	4.33	3.35	3.23	4.25	3.75
10 (IDHP)	2.59	4.07	2.69	2.89	4.13	3.27	-	-	-
11 (IDHP)	2.66	4.02	2.75	-	-	-	-	-	-

In Istanbul heating and cooling peak loads are similar (UI=0.73), but the cold season is still more severe than the hot season; consequently, heat pump sizing is usually based on the heating design load. Owing to a lower value of heating peak load, units number 4, 8 and 11 have not been considered for Istanbul simulations due to their large cooling and heating capacity. The results point out that the best annual performance is achievable by considering the smallest units, i.e. models number 1 (OP_h=-8%), number 5 (OP_h=-18%) and number 9 (OP_h=-18%) for On-off HPs, MSHPs and IDHPs, respectively.

In Lisbon, the cooling season is more severe than the hot season and the heat pump selection is based on the cooling peak load. Hence, only the smallest units (number 1: OP_c=22%, number 5: OP_c=19%, number 9: OP_c=18%) have been considered in simulations. The HVAC system in Lisbon gives the best annual performance among the considered locations.

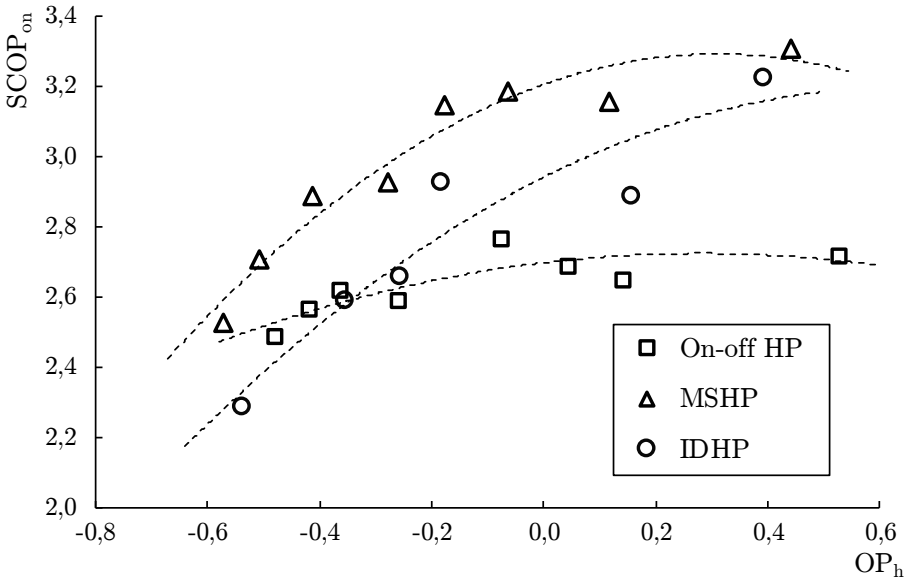

Figure 3.25. $SCOP_{on}$ as a function of the heating oversizing parameter OP_h.

In order to outline general rules for the optimal sizing of HVAC systems based on a reversible heat pump, in Figure 3.25 the values of $SCOP_{on}$ obtained through simulations are represented as a function of the heating oversizing parameter OP_h.

For downsized heat pumps (negative OP_h), the $SCOP_{on}$ decreases rapidly because it is negatively influenced by the electric heaters used as back-up system. When the heat pump capacity is tuned on the building thermal needs (OP_h between -20% and 20%), the $SCOP_{on}$ reaches its maximum value for On-off HPs; this value is generally lower than those obtained with MSHPs and IDHPs, due to their enhanced capability to reduce the number of on-off cycles by modulating the thermal capacity delivered. By adopting MSHPs and IDHPs it is possible to obtain higher $SCOP_{on}$ values even for OP_h larger than 20% with respect to On-off HPs.

In Figure 3.26 the $SEER_{on}$ trend is represented as a function of OP_c; results point out that, by scaling from larger to smaller units, the $SEER_{on}$ increases because the heat pumps reduce their need of on-off cycles. The maximum $SEER_{on}$ is obtained for values of OP_c close to zero; the values of $SEER_{on}$ for On-off HPs are lower than those obtained for IDHPs and MSHPs; in addition, Figure 3.26 highlights that the influence of OP_c on the value of $SEER_{on}$ is larger for On-off HPs with respect to IDHPs and MSHPs due to the enhanced modulating capability of the latter two heat pump typologies.

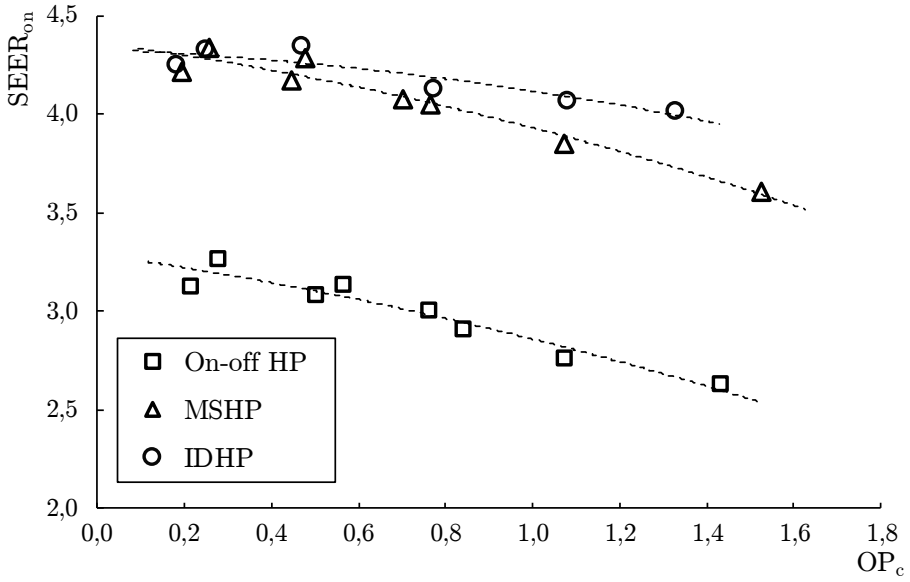

Figure 3.26. $SEER_{on}$ as a function of the cooling oversizing parameter OP_c.

In Figure 3.27 *APF* is shown as a function of OP_{tot}. Values of the unbalance indicator *UI* are also reported for each case. It is evident that the best annual performance is obtained by adopting MSHPs or IDHPs slightly oversized (OP_{tot} between 0% and 40%) with respect to building design energy needs.

On-off HPs are less influenced by the overall oversizing percentage than the other heat pump typologies: from OP_{tot}=-30% to OP_{tot}=20-40%, *APF* increases of about 10% for on-off units and of about 20% for modulating typologies. This result highlights the influence of heat pump sizing on the annual energy performance of the HVAC system.

Figure 3.27 confirms that On-off HPs are able to reach lower *APF* values (-16%) with respect to MSHPs and IDHPs. Reported data highlights also that the more accurate control of the thermal power delivered by multi-compressor and inverter-driven heat pumps can guarantee larger enhancements on *APF*, especially with unbalanced loads (*UI* larger or lower than 1) and a strong heat pump oversizing. In fact, the enhanced modulating capability of these devices strongly cuts down the difference between heat pump capacity and building thermal loads, avoiding on-off cycles penalization.

Furthermore, Figure 3.27 highlights the influence of unbalanced building loads on the annual system performance: *APF* is lower in correspondence of lower values of *UI*. In fact, a thermal load strongly unbalanced during winter (i.e. a low value of *UI*) leads to a higher use of electric back-up heaters.

These results suggest, for an optimal exploitation of the energy saving potential of heat pumps, a building design able to obtain balanced heating and cooling loads ($UI \cong 1$), so the heat pump can cover both heating and cooling loads by reducing the use of back-up systems. MSHPs and IDHPs must be preferred to On-off HPs due to their enhanced modulating capability, which reduces the use of on-off cycles during the year; nevertheless, their use in buildings with low UI markedly reduces the energy savings.

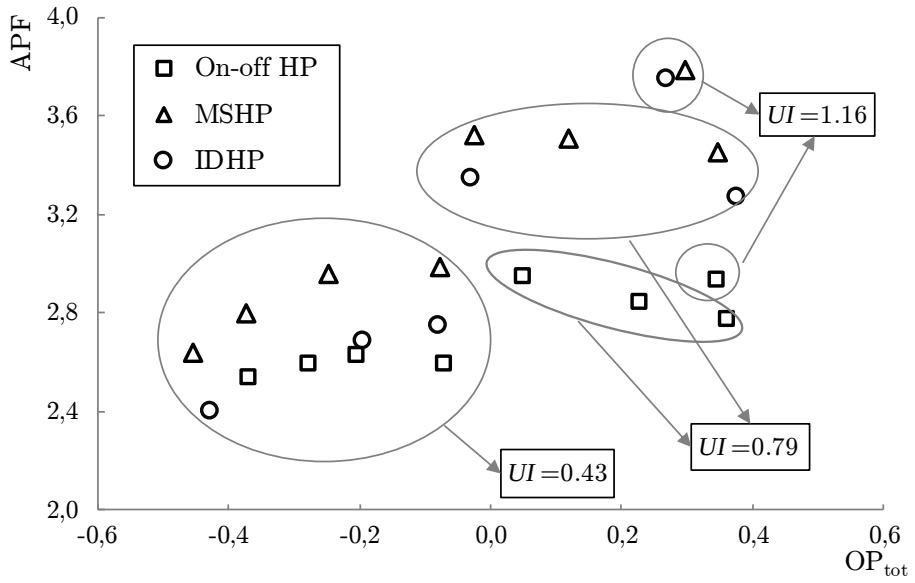

Figure 3.27. *APF* as a function of the overall oversizing parameter OP_{tot}.

As a rule for HVAC designers, the best energy performance of HVAC systems based on a single reversible electric heat pump is achieved if a multi-compressor or an inverter-driven heat pump is selected with a slight oversizing with respect to the annual building thermal loads, according to the overall parameter OP_{tot}.

Chapter 4

Dynamic modeling of air-to-water heat pump systems

In this chapter, the dynamic modeling of electric reversible air-to-water heat pumps through the dynamic software TRNSYS [87] is introduced. The dynamic simulation is used for the hourly or sub-hourly simulation of reversible air-to-water heat pumps employed for both building heating and cooling. A series of specific TRNSYS models will be presented: by means of them it is possibile to simulate the whole system building-HVAC plant when three heat pump typologies (i.e. single-stage heat pumps (On-off HPs), multi-stage heat pumps (MSHPs) and inverter-driven heat pumps (IDHPs) are used.

Unlike the mathematical model based on the bin-method described in the previous Section 3, dynamic simulations take into account the unsteady state behavior of the thermal plants based on heat pumps and for this reason these models are appropriate to study the behavior of this kind of systems during significant loads time variations or in order to optimize the control strategy of the same devices, following the hourly or sub-hourly evolution of the significant status parameters.

4.1. Heat pump dynamic simulation models in literature

A more detailed method to evaluate the mean seasonal performance of a whole heat pump system is the dynamic simulation, which is able to take into account the dynamic variation of the building load, of the heat pump source temperature and, consequently, of the heat pump performance. It can also consider the presence of a thermal storage tank coupled to a heat pump.

If one considers a dynamic simulation model, the calculations about a generic system are carried out at quasi-steady-state conditions, by considering the system in steady-state conditions within each time interval, which corresponds to the

time step assumed for the calculation method of the building thermal load (typically ranging from 1 minute to 1 hour).

For the modeling of heat pumps by means of dynamic softwares two approaches are usually followed:

i. the performance map based models;
ii. the thermodynamic models.

For the dynamic modeling of heat pumps a series of performance map based models have been proposed by different dynamic simulation softwares (e.g. TRNSYS [87], Modelica [88], EnergyPlus [89], ESP-r [90]); these models ignore the thermodynamic cycle linked to the heat pump. In these models the behavior of the heat pump is modeled by interpolating a series of characteristic working points of the unit, introduced by the user.

On the contrary, a thermodynamic model of a heat pump is obtained by introducing in the software the characteristics of the main components of the cooling cycle (namely evaporator, compressor, condenser and expansion valve) by studying the dynamic interaction among these elements and the thermal reservoirs connected to the heat pump (i.e. the hydronic loop or the external source).

Following these approaches, in recent years, several researchers have employed dynamic simulation softwares to develop mathematical models of heat pump systems and to compare their energy performance.

As an example, Rasoul Asaee et al. [91] used the dynamic software ESP-r to evaluate the energy performance of a solar assisted heat pump within the retrofit of an existing Canadian house: the simulated system employs two storage tanks to store the solar energy collected during the day and utilize it later. The behavior of the heat pump is evaluated by means of a performance-map approach: the single components of the unit are not modelled and the calculation of the system performance is based on data provided by the user. The Authors used a second order polynomial function to calculate the *COP* values: the equation reported in their work considers the hot and cold side temperatures as independent variables, while the interpolating coefficients (a_0-a_2) are derived from a commercial water-to-water heat pump. Then, the thermal capacity supplied by the heat pump is calculated based on the instantaneous values of *COP*, return water temperature and water flow rate; finally, the electrical power absorbed by the compressor is evaluated. The control logic of the system was optimized to maximize the use of

solar energy for space heating and domestic hot water production. The Authors focused their work on the simulation of the whole heating system and few details were given to the heat pump modelization: on the contrary, the models developed in this Thesis are able to simulate the behavior of different kinds of heat pump systems.

On the other hand, Chamoun et al. [92] developed the dynamic model of a new high temperature heat pump which uses water as refrigerant fluid. Authors employed the thermodynamic approach to simulate the behavior of the individual elements of the unit: more in detail, they used a new combined finite volume and moving boundary approach to model the plate heat exchangers of the heat pump and a moving boundary method to implement purging and flash evaporation systems. The dynamic model was developed using Modelica as modeling environment and it was employed to study the evolution the heat pump performance as a function of external sources temperature variations, in order to improve the management control strategy of the whole system.

Hu et al. [93] and Dong et al. [94] followed the same thermodynamic approach to simulate a hybrid ground source heat pump system, which combines geothermal source and a cooling tower to reject thermal energy for dominant cooling load applications, and an air-to-air heat pump used for both heating and cooling modes, respectively. Both the dynamic models of the mentioned systems were developed within Modelica environment. Hu et al. [93] proposed a self-optimizing control logic based on extremum seeking control to maximize the system energy performance. The Authors modelled the heat transfer between borehole heat exchangers and the ground by means of a finite volume method, while the main components of the system (namely cooling tower, compressor, condenser, expansion valve and evaporator) were simulated according to the components included within Modelica libraries. The described dynamic model was applied under different scenarios, such as fixed cooling load, sinusoidal trend of external dry-bulb and wet-bulb temperature and realistic conditions. On the other hand, Dong et al. [94] employed a multi-input control scheme to regulate both heating and cooling operation of an air-to-air heat pump: the internal temperature and the suction superheating degree are controlled by the compressor capacity and the expansion valve opening, respectively. The dynamic behavior of condenser and evaporator was evaluated according to a fin-and-tube parallel flow approach based on the standard Modelica library, while the model of a variable-speed fan, a screw compressor and an electronic expansion valve was developed bu the Authors. Several simulations were performed considering both constant,

stair-case and dynamic profiles of external temperature and thermal/cooling loads. Unlike the above-mentioned works, the dynamic models presented in this Thesis simulate the behavior of the whole building/HVAC plant system, by taking into account the variability of heat pump sources and building load during the year.

Maccarini et al. [95] simulated the performance of a novel two-pipe HVAC system which employs a water-to-water heat pump coupled to a water loop to provide space heating and cooling simultaneously. The innovative system was modelled by the Authors using the equation-based Modelica language and several simulations were performed considering different construction sets of the envelope of a typical office building. The performance map based approach was used to evaluate the behavior of the heat pump: at each simulation time-step, the unit efficiency is calculated as a function of the condenser and evaporator temperatures by means of second order polynomial function. The interpolating coefficients were calculated by fitting a set of performance data obtained from the technical datasheets of a commercial heat pump. In this analysis, the heat pump was assumed to deliver the thermal/cooling load required by the building during the whole year; no additional data on the control strategy of the system were reported by the Authors: on the contrary, the main aim of this Thesis is the assessment of the influence of different control logics on the system energy performance.

Likely the most used dynamic simulation software is EnergyPlus: several researchers developed dynamic models to analyze and optimize the energy performance of heat pump systems. As an example, Yongug et al. [96] performed several simulations of a hybrid cooling system composed by a screw water chiller and a ground source heat pump by using EnergyPlus. The calculation of the system seasonal performance was carried out taking into account partial load operating conditions and was performed by varying the operating schedule of the system and the set-point values of the main variables. The energy performance of both heat pumps (namely the screw water chiller and the ground source unit) was modelled by using performance data at reference conditions supplied by the user; furthermore, the cooling capacity and the *EER* of the water chiller is calculated through second order polynomial functions, while the performance of the ground source heat pump is evaluated by using a linear curve-fitting model. In both cases, the independent variables of the interpolating functions are the temperatures of the heat pump sources, while the interpolating coefficients are obtained from experimental measures. It can be noted that the developed model is based on specific fitting coefficients: for this reason, it is not applicable to any

heat pump system; on the contrary, the dynamic heat pump models that will be described in this thesis can be applied to a generic unit.

Hong et al. [97] introduced a new variable refrigerant flow air-to-air heat pump model within EnergyPlus simulation environment. Compared with the current models implemented in EnergyPlus libraries, the new component is more based on physics and introduces significant innovations, such as it enables advanced control logics (i.e. variable fan speeds based on the zone temperature), it adds a detailed calculation of refrigerant pipe heat loss, it takes into account partial load conditions and, last but not least, it reduces the number of user input performance curves. In conclusion, the model developed by the Authors is able to consider the dynamic behavior of the main heat pump components: first, the model determines the effective evaporating or condensing temperature of the indoor unit according the load requirements, then the pressure and heat losses through the pipes are calculated and the condensing or evaporating temperature of the outdoor unit is determined. Finally, the compressor electrical power absorption is evaluated and the energy performance of the heat pump can be calculated. Unlike the dynamic model presented in this work, the numerical codes described in this Thesis allow to simulate the behavior of different kinds of heat pumps (i.e. On-off HPs, MSHPs and IDHPs) and to consider different control strategies to improve the overall energy performance of the system.

TRNSYS is another dynamic software widespread in academic and professional fields: several works related to heat pump systems modelling can be found in literature. For example, Byrne at al. [98] developed within TRNSYS environment the dynamic model of an innovative heat pump able to provide simultaneously heating and cooling needs for a small office or a residential building. The heat pump described in this work is composed by two source side heat exchangers (namely a water and an air heat exchanger) and a load side plate heat exchanger: during the heating operating mode the unit can operate as a water-to-water heat pump, thus providing at the same time thermal and cooling capacity. The Authors implemented a numerical code for each component of the heat pump by means of FORTRAN programming language, utilizing the thermodynamic simulation approach, and employed the heat pump performance data obtained through the model as input data for TRNSYS. Anyhow, the heat pump modelled by the Authors is a single-stage unit controlled by means of on-off cycles: they did not consider other heat pump typologies and the influence of different control strategies was not investigated.

On the other hand, Hengel et al. [34] carried out several simulations of a desuperheater applied to a solar assisted air-source heat pump and analyzed the influence of five different control strategies on the overall energy performance of the system. The simulations were performed through the software TRNSYS: the Authors used a semi-physical heat pump model (i.e. Type 877), which is based on the refrigerant thermodynamic cycle. The mentioned Type calculates the compressor efficiency by using the values of isoentropic and volumetric efficiency, while the heat exchangers performance are evaluated through their UA-values. More in detail, the a single-speed compressor was assumed and its efficiency was assessed using a performance map based on manufacturer data. Moreover, UA-values of condenser and evaporator were calculated through polynomial functions, still based on manufacturer data.

Emmi et al. [99] carried out several numerical simulations using TRNSYS on a solar assisted ground source heat pump located in a cold climate; in this application, the heat pump extracts heat from the ground through borehole heat exchangers and solar collectors are used to inject excess solar energy into the ground to avoid the derive of the soil temperature. The Authors assessed the influence of climatic conditions, the borehole length and the control strategy to maximize the seasonal energy efficiency; in their work, the heat pump performance was calculated by means of lookup table, which was implemented in a Microsoft Excel spreadsheet and then integrated in the TRNSYS model. Furthermore, the performance data of the ground source heat pump were collected from the manufacturer technical datasheets: these values were evaluated as a function of the heat sources temperatures (i.e. evaporating and condensing temperature). In conclusion, the Authors utilized a performance map approach to calculate the seasonal performance of an innovative ground source heat pump located in different locations but they did not take into account the influence of the heat pump modulation capacity and of the hydraulic loop on the energy performance of the system

The same performance map approach has been followed by Gustafsson et al. [100] to compare the energy performance of four HVAC systems, the first one based on an air-to-air heat pump coupled to a mechanical ventilation system and the others based on an exhaust air-to-water heat pump. Simulations were carried out coupling all systems to a single-family house by varying the envelope components U-value, climate and ventilation rate within TRNSYS environment; in particular, the heat pump behavior was modelled by means of a performance map, which data of heating capacity and *COP* were assessed through

experimental measures. All heating systems considered in that study were controlled by on/off differential controllers with hysteresis cycle; the monitoring variable was the indoor air temperature.

Al-Zahrani et al [101] assessed, by means of the software TRNSYS, the energy performance of a HVAC system composed by a water-to-water heat pump integrated with a hot water and a cold water storage tank, which allows to simultaneous satisfy cooling needs and DHW production. The Authors evaluated the seasonal performance of the system at different operation modes (i.e. day-time operation only, night-time operation only and whole-day operation) and the effect of the storage tank size. Also in this case a performance map based approach was used to simulate the behavior of the heat pump; furthermore, only an on-off control strategy was taken into account by the Authors. On the contrary, in the dynamic models shown in this Thesis advanced control logics can be used to regulate the system and, therefore, the energy losses linked to on-off cycles are evaluated.

In conclusion, dynamic simulation models are more detailed than the methods described in Chapter 3 (bin method) and require, of course, greater effort to be developed; nevertheless, they allow to simulate the real behavior of heat pump systems and to evaluate the influence of various factors on the energy performance of the system, evalutions that are impossible to perform with the quasi steady-state approach based on the bin method.

More in detail, the utilization of dynamic codes allows the user to calculate, analyze and optimize several variables which have a strong influence on the overall efficiency of a heat pump system. As an example, the effect of the hydraulic loop configuration and its thermal inertia on the heat pump performance, as well as the influence of different control strategies on the system behavior, cannot be taken into account by the stationary approach. In fact, a calculation procedure performed through the bin method is unable to consider the real configuration of the system since it is not based on a physical modelization of the system. Further analysis can be carried out by means of dynamic simulation softwares: the assessment of indoor hygro-thermal comfort, the modelization of on-off cycling losses, the evaluation of innovative control logics, the calculation of heat pump penalization due to the frosting phenomena and so on. All the mentioned aspects will be presented in the following Sections of this Thesis.

4.2. Dynamic simulation of air-to-water heat pump systems by means of TRNSYS

TRNSYS, which is the acronym of TRaNsient Simulation SYstem Simulation tool, is a dynamic simulation software developed by the "Thermal Energy System Specialists, LLC", located in Madison (Wisconsin, USA) in collaboration with the Solar Energy Laboratory of the University of Wisconsin, (Madison, USA) [87].

The TRNSYS dynamic simulation software is a program available since 1975 and continues to grow thanks to universities and other research institutions and nowadays is, together with Energy Plus [89], the most widespread dynamic simulation tool. TRNSYS is a modular software, which allows to the users to use existing tools by means of which the main HVAC and building envelope components can be modelled or to program and develop new components: it is possible to modify existing templates or create new ones, improving the potentiality of the software, according to the specific user needs, by means of the most common programming languages (C, C ++, FORTRAN, ...). Furthermore, TRNSYS can also be easily connected to other softwares for the management of data pre/post-processing (Microsoft Excel, Matlab, EES, etc.).

The field of TRNSYS applications include and is not limited to:

- solar systems (thermal and photovoltaic);
- low-energy buildings and HVAC systems;
- renewable energy systems as heat pumps or wind turbines;
- cogeneration and fuel cells;
- biological processes.

TRNSYS is composed by two major parts. The first one is an engine (the kernel), which reads, processes the input file and iteratively solves the equation system that describes the behavior of the simulated system. The kernel provides utilities for the calculation of the thermophysical properties, for the matrices inversion, for linear regressions or for data interpolations from an external file. The second part of TRNSYS is a wide library of components, each one modeling a single component of a generic system. The standard library includes about 150 models ranging from hydraulic pumps to multi-zone buildings, from wind turbines to control systems.

From an operative point of view TRNSYS works by using a suite of integrated programs:

- TRNSYS Simulation Studio: it is a graphical interface that easily allows the user to define the system to be simulated, the links between the several components considered in the system and the relevant boundary conditions;
- the simulation engine TRNDll.dll and the executable TRNExe.exe, which are subroutines of the software that deal with the numerical solution of the equation system that identifies the physical simulated system;
- the graphical interface that lets the user to set the input data of a generic building, namely TRNBuild.exe;
- the editor TRNEdit.exe, employed to develop new custom programs and subroutines.

The models selected from the TRNSYS library can be dragged and placed into the TRNSYS environment (within Simulation Studio) and linked one another: the outputs of one component may be simply connected to the inputs of another one, while the parameters of a model are defined by the user and kept constant along the simulation. When a simulation is running, for each time step the software engine iteratively solves the system of equations of all the components and provides the results in an output file readable and editable by the user.

The available library components, identified as "Types", are compiled in FORTRAN and are user-editable. On the other hand, the user can write his own models by means of a FORTRAN code and introduce them within TRNSYS environment.

For the modeling of heat pumps, TRNSYS proposes several Types (i.e. Types 917 and 941) that are based on a user supplied table which contains the main heat pump performance data derived from manufacturer datasheets or experimental data. Therefore, these heat pump Types are not a physical model of the unit itself and they avoid to consider a series of important aspects like the impact of the unit capacity control or the influence of defrosting cycles on its energy performance. Furthermore, TRNSYS does not perform a direct evaluation of the heat pump efficiency at partial loads.

If these features are important for a simulation, the designer may elaborate a modified Type which takes into account the above-mentioned aspects. In this Thesis, several models of air-to-water heat pump systems have been developed and they will be described in the next Sections of the Thesis, in order to fully exploit the potential of TRNSYS for the analysis of the influence of various

parameters (as partial load performance, different control strategies and so on…) on the heat pump seasonal performance. In order to simulate the behavior of a whole heating (or cooling) system, in this Thesis the heat pump Type has been coupled with models of the other components of the system, like terminal units, storage tank and building.

In the following parts of the Chapter the main models employed by the dynamic simulations presented in this Thesis are described in detail and the main advantage of these models are fully highlighted.

4.2.1. The standard Types 917 and 941

Electric air-to-water heat pumps can be simulated within TRNSYS environemnt by means of two different Types, namely Type 917 and Type 941, which are available from the TESS component library [102]. The logic of both Types is very similar: the heat pump is modelled as a "black box" without any link to the physical model of the unit. Type 917 takes into account the influence of the outdoor air humidity on the heat pump performance and evaluates the humidity change in the outdoor air flow across the external heat exchanger of the unit; on the contrary, in Type 917 the humidity effect is neglected.

Both these Types are based on look-up tables in which the heat pump performance (i.e. thermal/cooling capacity and electrical power input) are reported as functions of the Type input data. For Type 941 the independent variables are the temperature of outdoor air (T_{ext}) and water flow entering the unit ($T_{w,in}$), while for Type 917 the heat pump performance depend also on the outdoor air humidity ratio (RH_{ext}). Two look-up tables are needed to fully identify heat pump performance: the first one contains the heating performance data and the second one the unit cooling performance data. Typically, the input data may be obtained from the technical datasheets given by the heat pump manufacturers.

In both look-up tables, the values of thermal/cooling capacity delivered and electric power absorbed by the heat pump are normalized to the rated conditions, which are set by the user as parameters. An extract of heating and cooling performance data required by Types 941 is reported in Figure 4.1 and Figure 4.2, respectively.

It is evident that according to the normalization of heat pump performance, the provided values of heat pump capacity and electrical power input are dimensionless, because they are divided by the same quantity evaluated in

corresponence of the rated conditions. The rated electrical power absorbed by the unit and the corresponding normalized values in the look-up table must take into account the compressor and the outdoor blower fan power inputs but they avoid to consider the auxiliary heater power.

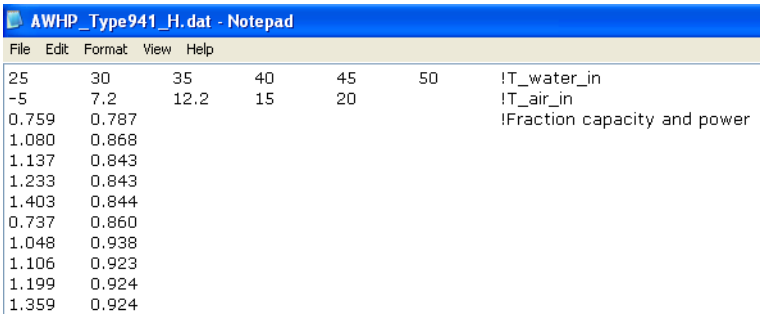
AWHP_Type941_H.dat - Notepad

File Edit Format View Help

25	30	35	40	45	50	!T_water_in
-5	7.2	12.2	15	20		!T_air_in
0.759	0.787					!Fraction capacity and power
1.080	0.868					
1.137	0.843					
1.233	0.843					
1.403	0.844					
0.737	0.860					
1.048	0.938					
1.106	0.923					
1.199	0.924					
1.359	0.924					

Figure 4.1. Extract of heating performance data required by Type 941.

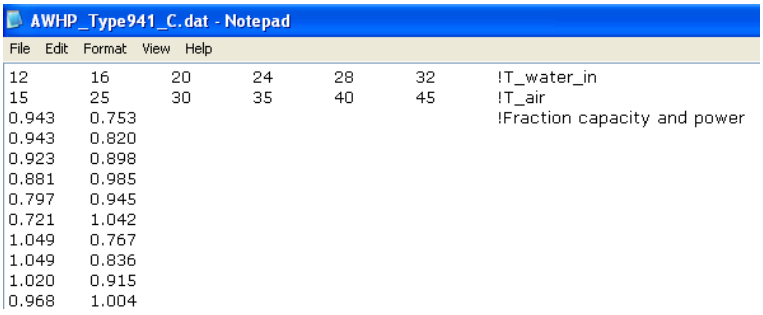
AWHP_Type941_C.dat - Notepad

File Edit Format View Help

12	16	20	24	28	32	!T_water_in
15	25	30	35	40	45	!T_air
0.943	0.753					!Fraction capacity and power
0.943	0.820					
0.923	0.898					
0.881	0.985					
0.797	0.945					
0.721	1.042					
1.049	0.767					
1.049	0.836					
1.020	0.915					
0.968	1.004					

Figure 4.2. Extract of cooling performance data required by Type 941.

The considered Types linearly interpolate among the performance data reported in the look-up tables as functions of the input values of external air and inlet water temperature. The models avoid to extrapolate beyond the provided data range, so, if values outside the data range are got to the component the maximum or minimum heat pump performance values are returned to the user as outputs. In conclusion, both Types return as outputs the values of the thermal (cooling) capacity $P_{HP,h}$ ($P_{HP,c}$) and of the absorbed electrical power $P_{HP,el,h}$ ($P_{HP,el,c}$), obtained by means of a linear interpolation between the data provided by the look-up tables.

The heat pumps modelled in TRNSYS can be equipped with an optional desuperheater, which can be employed to heat a secondary water stream, usually coupled to the domestic hot water (DHW) service. To disable this option, the user must set to zero the inlet flow rate of the secondary water stream (this is an

input of the Types). On the contrary, to use it, the conditions of the water stream entering the desuperheater have to be set and the user must specify the heat transfer coefficient of the desuperheater heat exchanger, both for heating ($U_{dspr,h}$) and cooling modes ($U_{dspr,c}$).

In cooling mode, the desuperheater recovers a part of the energy that would be rejected to the external air. In heating mode, it causes the heat pump to absorb at the same time the electric energy required both for space heating and for DHW production.

The electric power absorbed by the single compressor, P_{compr}, is computed by the above-mentioned Types as the value of electric power interpolated from the data file, $P_{HP,el,h}$, minus the blower power (which is entered as a model parameter). The thermal power rejected to the condenser, P_{cond}, and the thermal power absorbed by the evaporator, P_{eva}, are then evaluated through Eqs. (4.1) and (4.2):

$$P_{cond} = P_{HP,h} - P_{HP,DHW} \tag{4.1}$$

$$P_{eva} = P_{HP,h} - P_{compr} \tag{4.2}$$

If the heating capacity of the heat pump is insufficient to match the required building load in a generic time interval during the simulation, it is possible to set in the component an additional heating capacity, which is considered by the Type as an electric resistance. The back-up heating capacity, P_{BU}, is a parameter of the selected Types and its control signal is an input.

If the auxiliary system control signal is on (i.e. its input is equal to or greater than 0.5), the whole capacity of the back-up heater is applied to the primary water stream. The outlet temperature of the primary water stream, $T_{w,out}$, is then:

$$T_{w,out} = T_{w,in} + \frac{(P_{cond} + P_{BU})}{\dot{m}_w c_{p,w}} \tag{4.3}$$

where $T_{w,in}$ and m_w are the inlet temperature and mass flow rate of the primary water stream, respectively and $c_{p,w}$ is the specific heat capacity of water at constant pressure.

Finally, the *COP* of the unit, composed by heat pump and auxiliary heater, is evaluated by TRNSYS as:

$$COP = \frac{(P_{cond} + P_{BU})}{(P_{HP,el,h} + P_{BU})} \tag{4.4}$$

Starting from the thermal capacity extracted from the outdoor air stream entering the evaporator, it is possible to calculate the outlet temperature of the air stream ($T_{ext,out}$) as:

$$T_{ext,out} = T_{ext,in} - \frac{P_{eva}}{\dot{m}_{air} c_{p,air}} \tag{4.5}$$

where $T_{ext,in}$ and m_{air} are the external air stream inlet temperature and mass flow rate, respectively, and $c_{p,air}$ is the specific heat capacity of air at constant pressure.

If the cooling control signal of the heat pump model is on, the procedure to evaluate the heat pump performance in cooling operating mode is the same as the heating operating mode. Also in this case the heat pump is able to use a desuperheater to heat a secondary water stream while cooling the primary water stream. The value of the heat transfer coefficient which occurs in the desuperheater for cooling mode ($U_{dspr,h}$) can be different from the value used in heating mode.

The energy rejected by the condenser on the outdoor air and the energy extracted by the evaporator from the primary water flow in cooling mode are:

$$P_{cond} = P_{HP,c} + P_{compr} - P_{HP,DHW,c} \tag{4.6}$$

$$P_{eva} = P_{HP,c} \tag{4.7}$$

where $P_{HP,DHW,c}$ is the fraction of the thermal capacity which would be rejected to the condenser that is used to heat the secondary DHW stream. It can be expressed by means of the following Equation:

$$P_{HP,DHW,c} = U_{dspr,c}\left(T_{dspr} - T_{w,in,DHW}\right) \tag{4.8}$$

The outlet temperature of the primary water stream, the *EER* of the heat pump and the outlet temperature of the air stream are evaluated in cooling operating mode as:

$$T_{w,out} = T_{w,in} - \frac{P_{eva}}{\dot{m}_w c_{p,w}} \tag{4.9}$$

$$EER = \frac{P_{eva}}{P_{el,c}} \tag{4.10}$$

$$T_{ext,out} = T_{ext,in} + \frac{P_{cond}}{\dot{m}_{air} c_{p,air}} \tag{4.11}$$

In conclusion, the TRNSYS Types 941 and 917 can be efficiently employed to simulate the dynamic behavior of an air-to-water heat pump, but they have some limitations.

First of all, the above-mentioned TRNSYS models are able to simulate only a single-stage on-off unit: multi-stage and inverter-driven heat pumps are not directly considered within the standard Types. The models presented in this Thesis, on the contrary, are able evaluate the behavior of each heat pump typology available in the market today.

Moreover, if the auxiliary heating control signal of the considered Types is on, then the whole thermal capacity of the back-up system is indiscriminately delivered to the primary water stream, yielding an undesired variation of the primary water stream outlet temperature. For this reason, the possibility to modulate the back-up system thermal capacity has been introduced in the developed models. Furthermore, in real applications the auxiliary device can be either electric heaters or a gas boiler.

Finally, no *COP* (or *EER*) corrections for the energy loss caused by the heat pump on-off cycles are considered by standard TRNSYS Types. In the models developed in this Thesis a simple procedure which takes into account the degradation of the unit energy performance due to on-off cyclings has been introduced: the employed correction factors are based on a series of experimental tests performed by an Italian heat pump manufacturer.

4.2.2. The standard Type 996

Within TRNSYS environment, the behavior of a two-pipe fan coil is modelled by means of the Type 996, available from the TESS component library. The logic of this model is similar to the heat pump one: also in this case the Type does not represent the physical model of the unit but it is based on external files supplied by the user, which contain the fan coil performance data. Type 996 simulates a two-pipe fan coil unit for both heating and cooling operating modes: its main inputs are represented by the values of temperature and flow rate of the entering water stream (hot/cold water provided by the HVAC system) and by the values of temperature and flow rate of the entering air stream (the air of the thermal zone in which the fan coil is coupled). This type also considers the option to mix the air stream coming from the coupled thermal zone with outdoor air, but this option has not been explored in the models developed in this Thesis.

The user has to manage three different external files: the first one contains the heating performance data, in the second one the cooling performance data are reported and finally the third one contains the data on the electric power absorbed by the fan. As for the heat pump Types, the required performance data may be obtained from the technical datasheets given by the fan coil manufacturers. Again, similarly to heat pump models, the values of thermal/cooling capacity delivered and electric power absorbed by the fan motor are normalized with respect to the relative values obtained for rated conditions, which are set as parameters. An extract of heating, cooling and fan motor performance data required by Type 996 are reported in Figure 4.3, Figure 4.4 and Figure 4.5, respectively.

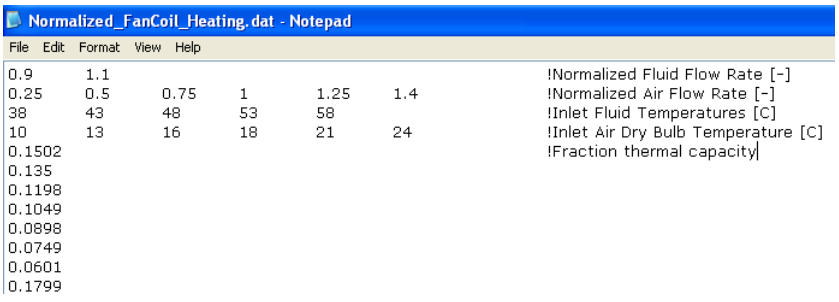

Figure 4.3. Extract of heating performance data supplied for Type 996.

If one considers the heating operating mode, the fan coil thermal capacity delivered to the air stream, $P_{FC,h}$, is evaluated by a linear interpolation of the data

reported in the heating performance external file. In this case, the independent variables are the temperature and flow rate of the entering water stream and the dry bulb temperature and the flow rate of the entering air stream. On the other hand, if one considers the cooling operating mode, the cooling capacity of the unit, $P_{FC,c}$, is calculated as a function of the above-mentioned variables and it furthermore depends on the wet bulb temperature of the entering air stream; in this case, in fact, the latent heat exchange between the fan coil unit and the air stream is not negligible. Finally, the data on the electric power absorbed by the fan are supplied as a function of the ratio between the air stream flow rate (an input for the Type) and the rated air flow rate (a parameter for the Type).

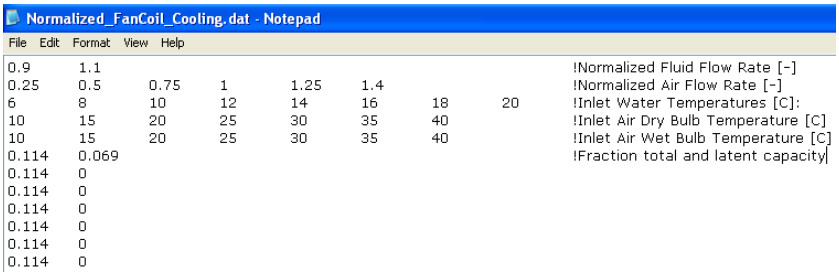

Figure 4.4. Extract of cooling performance data supplied for Type 996.

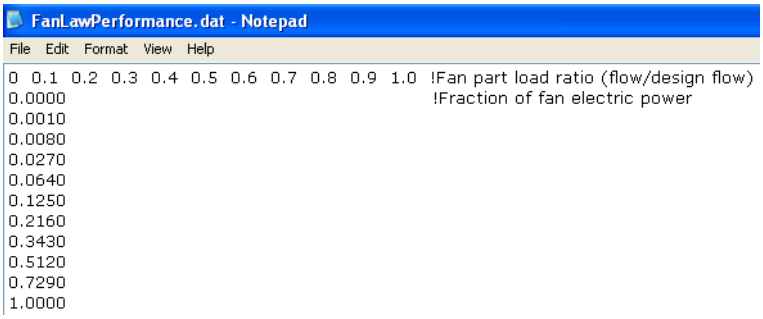

Figure 4.5. Extract of fan motor performance data supplied for Type 996.

The two-pipe fan coil model considered in this Section presents three different control signals. The heating control signal and the cooling control signal enable or disable the heating and cooling operating modes: as an example, if the heating control signal is equal to or greater than 0.5, then the model calls the subroutine for the calculation of heating operating mode. Furthermore, the fan speed control signal adjust the flow rate of the air stream: the value of this signal sets the fraction of the air stream effective flow rate entering the fan coil with respect to the rated value.

If one considers the heating operating mode, the model calculates in the first step the thermal capacity delivered by the unit, $P_{FC,h}$, by a linear interpolation of the data reported in the heating performance external file. Then, the model solves the energy balance equation between the air and water streams by means of the following Equations:

$$T_{w,out,FC} = T_{w,in,FC} - \frac{P_{FC,h}}{\dot{m}_{w,FC} c_{p,w}} \tag{4.12}$$

$$T_{air,out,FC} = T_{air,in,FC} + \frac{P_{FC,h}}{\dot{m}_{air,FC} c_{p,air}} \tag{4.13}$$

where $T_{w,out,FC}$ and $T_{w,in,FC}$ are the outlet and inlet temperature of the water stream coupled to the fan coil respectively, $m_{w,FC}$ is the flow rate of the water stream, $T_{air,out,FC}$ and $T_{air,in,FC}$ are the outlet and inlet temperature of the air stream coupled to the unit respectively, and $m_{w,FC}$ is the flow rate of the air stream.

Then, if one considers the cooling operating mode, the model calculates the cooling capacity delivered by the unit, $P_{FC,c}$, by interpolating the performance data reported in the corresponding external file and taking into account both sensible and latent heat transfer. The values of the outlet temperatures of water and air streams are then evaluated according to Eqs. (4.14) and (4.15):

$$T_{w,out,FC} = T_{w,in,FC} + \frac{P_{FC,c}}{\dot{m}_{w,FC} c_{p,w}} \tag{4.14}$$

$$T_{air,out,FC} = T_{air,in,FC} - \frac{P_{FC,sens,c}}{\dot{m}_{air,FC} c_{p,air}} \tag{4.15}$$

where $P_{FC,sens,c}$ is the sensible cooling capacity of the fan coil unit.

Finally, the electric power absorbed by the fan motor is calculated by interpolating the fan performance data as a function of the effective flow rate of the air stream.

4.2.3. The standard Type 534

In order to couple the heat pump to terminal units a thermal storage tank is generally used. There are several reasons that justify the adoption of an inertial storage in the hydronic loop and different types of tanks are used, according to the specific needs that the HVAC system has to manage.

As an example, in case of heating systems used for the production of domestic hot water (DHW), storage tank is mandatory to dampen the unavoidable peaks of the DHW request. Figure 4.6 shows the storage tank typically employed for the production of DHW in a traditional system, where a boiler is coupled to the tank by means of a coiled heat exchanger. The heating loop is in this case directly coupled to the boiler. If one considers a heating system that employs a heat pump as single heat generator, the same tank configuration is used but with an increased heat exchange surface. In both cases, the inertial tank directly stores domestic hot water.

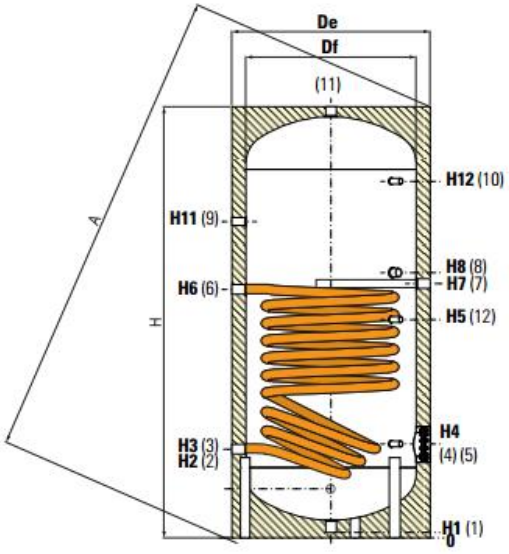

Figure 4.6. Storage tank for domestic hot water production, (from [103]).

In case of heating system, the adoption of a storage tank is also recommended because the installation of a buffer tank results one of the most effective and economical ways to optimize the performance of the system. In fact, the water tank is able to store the energy in excess when the unit is active and to deliver heat when the unit is turned off. In this way a thermal inertia is added to the system, allowing to decrease the total number of on-off cycles of the unit, with

the result of significantly decrease the energy cycling losses and increase the overall efficiency of the system. Furthermore, the water tank performs another important function to guarantee a correct operation of the HVAC system: it works as a sink for the disposal of heating or cooling energy during the shutdown of the unit. As an example, we can imagine the case of a chiller whose secondary loop is switched off because the building cooling load is met: in the following step the unit will be turned off by the control system, but the remaining unit cooling capacity needs to be disposed. This result will be achieved only if a minimum volume of water, able to receive this cooling capacity without freezing, is placed on the primary loop. Similarly, during heating operating mode a low thermal inertia may cause an improper overheating of the circulating water, causing the stop of the compressors by the safety thermostat.

From a mathematical point of view, the detailed modeling of the behavior of a storage tank is a very complex task in presence of thermal stratification. In this case, it is mandatory to model the tank with a level of detail which enables the calculation of the vertical gradient of the water stored within the tank. The stratification phenomenon directly affects the heat exchange within the tank and the performance of the appliances connected to the storage.

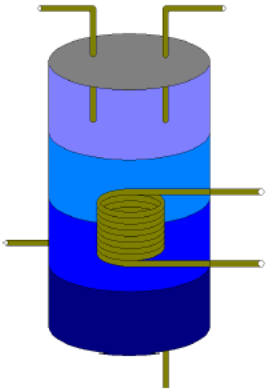

Figure 4.7. Logical layput of the thermal storage tank modelled by means of Type 534, (from [102]).

In TRNSYS, there are several models that simulate the behavior of different kinds of storage tanks. In this Thesis, we the Type 534 has been used. This component simulates the behavior of a cylindrical tank with a vertical configuration as reported in Figure 4.7: the subroutine of Type 534 models a constant volume fluid-filled storage tank, with the option to consider immersed

heat exchangers. The model also takes into account temperature-dependent fluid properties and allows to consider different fluids, such as pure water or glycol and water solution. The tank is subdivided into isothermal temperature nodes (in order to simulate the vertical fluid thermal stratification). The number of nodes can be imposed by the user: a greater number of nodes leads to more detailed results, but obviously involves a strong increase of calculation time. Each node is assumed to be constant-volume and isothermal; it interacts with the nodes above and below through several mechanisms: thermal conduction between consecutive nodes and fluid convection, due to the inlet flow streams or to natural convection.

The user can specify one of four different types of immersed heat exchangers (if present): horizontal or vertical tube banks, coiled or serpentine tube. Furthermore, auxiliary thermal capacity can be provided to each node by means of an auxiliary heating device. The fluid stored in the tank can interact with the fluid that flows within immersed heat exchangers, directly with up to five flow streams which pass into and out of the tank and with the environment in which the storage is placed (through heat losses from the tank blanket). In this way, by means of Type 534 it is possible to evaluate the following heat transfer phenomena:

- thermal losses through the tank blanket;
- direct heat exchange with fluid streams enetering and exiting the tank. In this case the height of streams attacks must be defined and the incoming water mixes with the fluid present in the surrounding nodes;
- heat exchange with other flow streams by means of immersed heat exchangers;
- inverted mixing flow rate, when a cold node is superimposed on a hot node.

The tank is divided into K horizontal nodes of the same volume. To be noted that the node 1 is assumed to be in correspondence of the top of the thermal storage while the node K is placed in correspondence of the botton of the tank.

In order to calculate for each timestep the temperature of tank nodes, the subroutine of Type 534 solves for the generic i-th node the following differential equation:

$$\frac{dT_{tank,i}}{d\tau} = \frac{P_{in,tank,i} - P_{out,tank,i}}{\rho_w c_{p,w} V_i} \qquad \text{for } i = 1,\ldots, \text{K} \tag{4.16}$$

where $P_{in,tank}$ and $P_{out,tank}$ are the heat flux incoming and outgoing from the i-th node of the tank, respectively, ρ_w is the water density and V_i is the volume of the i-th tank node. As will be shown later, the considered heat fluxes depend on the environment temperature and the inlet flow streams conditions (i.e. temperature and flow rate).

While there are several available methods to solve differential equations, the TRNSYS subroutine of Type 534 solves the problem by means of an approximate analytical solution. In this case, the analytical solution has several advantages over numerical solutions. For example, a numerical method can be strongly dependent on the simulation timestep and its convergence under particular conditions commonly encountered in DHW systems can be problematic. On the contrary, the analytical approach used by the Type 534 is independent from the timestep imposed in the simulation model but it requires an iterative procedure to solve the differential equation.

If one expands the terms reported in Eq. (4.16) it is possible to obtain:

$$\frac{dT_{tank,i}}{d\tau} = \frac{-P_{loss,top,i} - P_{loss,bottom,i} - P_{loss,edge,i} - P_{cnd,i} - P_{flow,i,j} - P_{mix,i} + P_{aux,i}}{\rho_w c_{p,w} V_i} \tag{4.17}$$

where $P_{loss,top,I}$, $P_{loss,bottom,I}$ and $P_{loss,edge,i}$ are the heat losses (or gains) through the tank blanket from the top, bottom or edge area of the storage, respectively, $P_{cnd,i}$ is conductive heat transfer that occurs between two adjacent nodes, $P_{flow,i}$ is a term that takes into account the heat directly exchanged with entering or outgoing flow streams, $P_{mix,i}$ represents the mixing heat transfer between adjacent nodes and $P_{aux,i}$ is the thermal capacity transferred to the fluid by an auxiliary heater immersed in the i-th node.

The first three terms of Eq. (4.17) can be evaluated by means of the following Equations:

$$P_{loss,top,i} = A_{top,i} U_{top,i} (T_{tank,i} - T_{env,top}) \tag{4.18}$$

$$P_{loss,bottom,i} = A_{bottom,i} U_{bottom,i} (T_{tank,i} - T_{env,bottom}) \tag{4.19}$$

$$P_{loss,edge,i} = A_{edge,i} U_{edge,i} (T_{tank,i} - T_{env,edge}) \tag{4.20}$$

where $A_{top,i}$, $A_{bottom,i}$ and $A_{edge,i}$ are the tank top, bottom and edge surface area, respectively, $U_{top,i}$, $U_{bottom,i}$ and $U_{edge,i}$ are the tank top, bottom and edge heat loss coefficient, respectively, and $T_{env,top}$, $T_{env,bottom}$ and $T_{env,edge}$ are the environment temperature for losses through the top, bottom and edge part of the storage, respectively.

To be noted that the heat losses through the top part of the tank are entirely attributed to the tank node 1 (i.e. $A_{top,i}=0$ for $i \neq 1$), while the heat losses through the bottom part of the tank are all attributed to the tank node K (i.e. $A_{bottom,i}=0$ for $i \neq$ K) and the heat losses through the edge part of the tank are equally distributed among all tank nodes. Furthermore, the model employed by this subroutine allows the user to specify different environment temperatures for the top, bottom and edge surfaces of the tank, in order to increase the flexibility of the simulation.

The nodes of the storage tank model can interact one another via thermal conduction; anyway, the conduction between nodes can be turned off by the user. The formulation of the conductive heat transfer from the i-th tank node is:

$$P_{cnd,i} = \frac{k_{i+1} A_{i+1} (T_{tank,i} - T_{tank,i+1})}{L_{cnd,i+1}} + \frac{k_{i-1} A_{i-1} (T_{tank,i-1} - T_{tank,i-1})}{L_{cnd,i-1}} \tag{4.21}$$

where k_{i+1} and k_{i-1} are the thermal conductivity of the fluid stored in the i-th node and evaluated for the average temperature between this node and the node below or above it, respectively, A_{i+1} and A_{i-1} are the interface area between the i-th node and the one below or above it, respectively, and $L_{cnd,i+1}$ and $L_{cnd,i-1}$ are the vertical distance between the centre of the i-th node and the centre of the node below or above, respectively.

The model of storage tank implemented within Type 534 allows to have several flow streams which pass into and out of the tank. The user has to define the nodes in correspondence of which inlet and outlet ports of each stream are placed. Moreover, these inlet and outlet locations are fixed throughout the whole simulation. The temperature at the outlet of a flow stream is simply the average

temperature of the node containing the outlet port along the considered timestep. On the other hand, the user provides the values of inlet temperature and flow rate for each entering streeam.

The heat transfer due to flow streams into a generic tank node is then expressed as:

$$P_{flow,i} = \sum_j \dot{m}_{in,i,j} c_{p,w} T_{in,j} + \sum_j \dot{m}_{in,i+1,j} c_{p,w} T_{tank,i+1} + \sum_j \dot{m}_{in,i-1,j} c_{p,w} T_{tank,i-1} \qquad (4.22)$$

where $m_{in,i,j}$ is the mass flow rate of the j-th stream which enters in the i-th tank node from an external hydraulic loop, $m_{in,i+1,j}$ and $m_{in,i-1,j}$ are the mass flow rate of the j-th stream which enters in the i-th tank node from the node below and above, respectively, and $T_{in,j}$ is the temperature of the j-th stream which enters in the i-th tank node from the outside.

In this model, the inlet fluid that enters into a node is completely mixed with the fluid stored in that node before this stream moves on to the adjacent node (the fluid flow moves from the inlet node to the outlet node). For sake of clarity, we consider a water stream that enters in the tank from node 4 and exits from node 1 (the top node). The inlet temperature and flow rate of this stream are equal to 10°C and 200 kg/hr, respectively, and the tank has an initial temperature of 30°C. The cold inlet flow stream mixes with the hot water stored in the node 4, causing a decrease of the tank node temperature to 25°C (for example). Then, a water stream of 200 kg/hr and temperature of 25°C crosses the boundary towards node 3, where it mixes with the fluid stored in this node. Again, the fluid stream moves on towards node 2 and eventually exits through the port outlet placed in node 1.

During the simulation, the fluid stored in the tank may become thermally unstable (i.e. a node is characterized by a higher temperature than the one of the node above). If this occurs, the model takes into account the fluid mixing between the unstable nodes. This tank model calculates the mixing effect using a simplified procedure that speeds up the simulation but introduces some inaccuracies in the energy balance of the system. In the first step. the subroutine of Type 534 evaluates the temperatures of the nodes, then completely mixes the nodes which are unstable at the end of the timestep. While this "averaging" of the tank node temperatures (thus an infinite flow mix between the unstable nodes) is not a bad assumption, the energy balance of the whole tank is not entirely correct, if one

considers that the tank losses and other heat flows have been taking into account the tank temperatures before mixing.

The mixing heat transfer between nodes is formulated as:

$$P_{mix,i} = \dot{m}_{mix,i+1} c_{p,w} (T_{tank,i} - T_{tank,i+1}) + \dot{m}_{mix,i-1} c_{p,w} (T_{tank,i} - T_{tank,i-1}) \qquad (4.23)$$

where $m_{mix,i+1}$ and $m_{mix,i-1}$ are the mixing flow rate between the i-th node and the node below and above, respectively.

Finally, the considered tank model relies on external sources to eventually add heat to the storage tank. This feature can be used to simulate auxiliary heating devices such as electrical resistances or combustion heating elements. In order to consider the effect of auxiliary heating the user has to define the thermal input rate $P_{aux,i}$ for each node of the tank in correspondence of which the heating element is placed.

In this Thesis, only storage tanks with no immersed heat exchangers are considered. Despite the use of heat exchangers is a typical solution to couple the heat pump to the hydraulic distribution loop, their simulation has not been carried for several reasons. The heat transfer occurring between a heat exchanger immersed in a thermal storage and the stored water is a very complex physical phenomenon, which strongly depends on the geometric configuration of the system; for this reason, the evaluation of heat transfer coefficients is a difficult task and a general formulation cannot be expressed. Consequently, no heat exchangers are considered in this Thesis, in order to avoid excessive uncertainty within simulation input data.

4.2.4. The plugin TRNBuild

In order to deeply investigate the dynamic behavior of a heat pump system, it is mandatory to simulate also the building coupled to the thermal plant: only by means of an integrated building-HVAC system approach it is possible to completely analyze the energy performance of the system. The modeling of building envelope and the evaluation of building energy demand is performed by means of the plugin TRNBuild [104], a subroutine of TRNSYS that guides the user towards the implementation of the building model, through a series of simple operations and data definitions.

The first step of any building modeling is the definition of the thermal zones which will be simulated in TRNBuild. The definition of zones depends on the complexity of the developed model: a thermal zone can be a single room, if one simulates a single apartment, a single apartment, if one simulates a multi-family building or a whole building if one simulates an entire district. For each thermal zone, the user must specify its volume, the initial values of indoor temperature and relative humidity and the data needed to assess the general characteristics of the zone, such as the infiltration rate, the internal gains and the comfort parameters of the building inhabitants. In Figure 4.8 the interface of the plugin TRNBuild is shown.

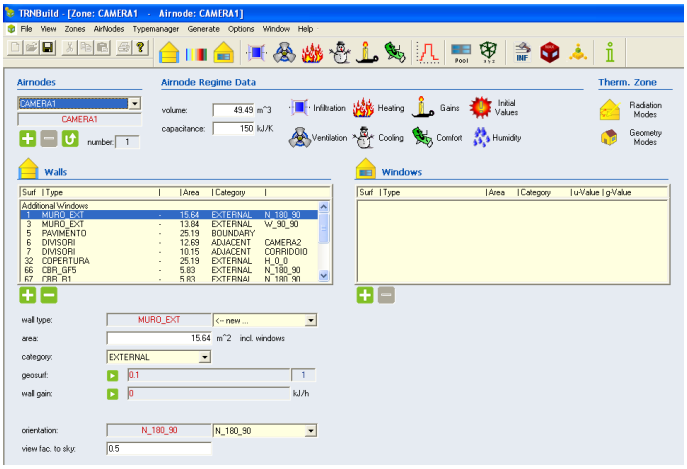

Figure 4.8. TRNBuild main features.

Once the thermal zones have been defined, the user has to define the thermophysical properties of walls and windows that delimit the considered zone. The subsection "Wall Type Manager" allows to model the walls of the building through the description of the layers which compose it: thickness, thermal transmittance, capacitance and density values of each layer must be imposed by the user and the thermal characteristics of the wall are evaluated by TRNBuild as a combination of those values. In this phase, it is possible to employ the standard material library included in the software or the user can develop his own layer, on the basis of the real characteristics of masonry. Then, all surfaces defined in the previous step must be properly allocated in space: for each surface, the relative boundary condition must be imposed. For surfaces that separate the thermal zone from the external environment, the "external" boundary condition must be selected and their orientation with respect to cardinal axes must be

specified. An "adjacent" surface, instead, is a component that separates different thermal zones of the building while a "boundary" surface is in contact with an environment whose characteristics are imposed by the user, (for example the basement, which is strictly in contact with ground). Finally, the transparent components of the building envelope are characterized by the subsection "Window Type Manager", by means of which the gross area of the window, the frame area, the structure of the glazing and its thermal characteristics are defined. Again, the user can choose between the standard libraries provided by TRNSYS or create his own components.

Once the definition of the building envelope is completed, the user should impose the initial conditions in order to start the simulation: the initial values of relative humidity and air temperature for each simulated thermal zone and the boundary conditions must be entered.

TRNBuild can provide to the user about 100 different outputs, such as the free-running temperature in the zone, the amount of solar radiation absorbed by the external walls, the sensible or latent heating and cooling power demand required by the thermal zone and so on.

4.3. Dynamic simulation models of a heating system based on air-to-water heat pumps

In this Section, the dynamic models of different kinds of heating ststems based on an air-to-water heat pump introduced. These models, implemented by means of the software TRNSYS, allow to simulate the dynamic behavior of the whole building-HVAC plant system. In fact, all the components of the heating system have been considered in this Thesis: the generating subsystem, which is based on an air-to-water heat pump, the hydraulic distribution loop which connect the heat pump to the building and the building itself. A logical scheme of the developed models is reported in Figure 4.9: in the following Sections of this Thesis the numerical codes implemented with TRNSYS to simulate the performance of different kinds of heat pump and the considered hydraulic configurations will be deeply analyzed. The dynamic simulation of the building and the calculation of the required thermal/cooling loads is performed through the plugin TRNBuild (Section 4.2.4).

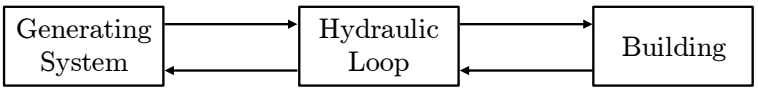

Figure 4.9. Logic scheme of the developed dynamic models of the system building-HVAC plant.

4.3.1. The considered hydraulic distribution loops

The aim of this Thesis is the evaluation and the optimization of monovalent systems (i.e. with the heat pump as the unique generator). In order to limit the hourly number of the heat pump on-off cycles a thermal storage is generally inserted in the hydronic loop. In fact, in order to avoid an excessive number of heat pump on-off cycles, linked to energy losses and compressor mechanical stress, a proper value of thermal inertia is needed. The influence of the volume of water tank on the seasonal performance of the system will be discussed in Section 4.5.3.

Type 534 has been used to simulate the behavior either of a thermal storage (TS) directly placed in the hydraulic loop to increase the the thermal inertia of the system (puffer application) or of a hydraulic separator (Sep), used to decouple the primary hydraulic loop from the secondary hydraulic loop. In this Thesis, we refer to the first case as Direct Hydraulic Loop (DHL) configuration and to the second case as Indirect Hydraulic Loop (IHL) configuration.

The layout of a typical heating system based on an air-to-water heat pump and characterized by a DHL is reported in Figure 4.10. The three main parts of the system are highlighted by dashed lines: one can note the building, equipped with fan-coils as terminal units, the hydraulic loop, composed by a thermal storage, a fixed speed circulating pump and pipes for the water distribution, and the generating subsystem, based on a heat pump as unique generator. As mentioned before, the function of the thermal storage tank (puffer) is to increase the total thermal inertia of the system. In this case, only one pair of flow streams (the first one entering and the second one outgoing from the tank) has to be defined by the user.

In Figure 4.10 the controllers of the main elements of the system are also represented and their logical behavior is highlighted by dash-dot lines. As pointed out by Figure 4.10, the physical variables used as control parameter for the heat pump and the emitters are the return water temperature and the indoor air temperature, respectively.

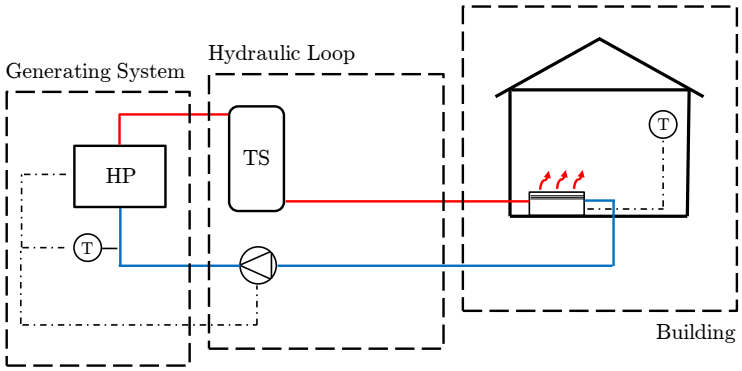

Figure 4.10. Logic layout of a DHL heating system with the thermal storage placed in the supply line.

More in detail, the choice to adopt the return water temperature as monitored variable for the control of the thermal/cooling capacity delivered by the heat pump is due to the need to avoid the instability of the control signal; in fact, the thermal inertia of the heat pump is much lower than the inertia of the hydraulic loop and the building: for this reason, the use of the supply water temperature ($T_{w,out}$) as monitored variable would cause unacceptable oscillations of the control signal.

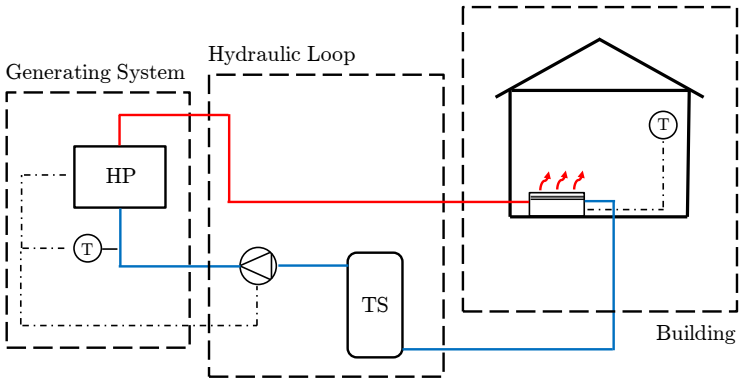

Figure 4.11. Logic layout of a DHL heating system with the thermal storage placed in the return line.

The heating system represented in Figure 4.10 is characterized by a storage tank placed in the supply line; as pointed out by Figure 4.11, the thermal storage tank can be placed also in the return line of the hydronic loop. The storage tank can be placed in the supply line in order to guarantee thermal comfort to the building users also during the defrosting cycles performed by the heat pump. In fact, during a defrosting cycle the unit heating capacity decreases and a large

thermal inertia placed between the heat pump and the building can mitigate the decrease of the supply water temperature send to the emitters.

On the contrary, the adoption of a thermal storage tank along the return line is conservative for the heat pump, since it protects the unit from sudden variations of the return water temperature which can be caused by variable building loads. In the following Sections of this Thesis, the optimal size of the storage tank and the influence of its position on the seasonal performance of the system will be deeply analyzed.

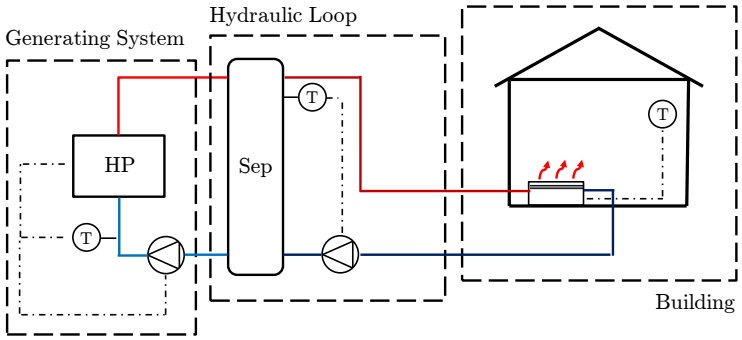

Figure 4.12. Logic layout of an IHL heating system characterized by constant flow rate in the secondary loop.

The use of an IHL is another typical solution followed by the designers in order to couple the heat pump to the building: in Figure 4.12 the layout of a heating system composed by a primary and a secondary loop coupled by a hydraulic separator is represented. In this case, two pairs of flow streams, which represent respectively the flows of primary and secondary loop, have to be defined as input data for the separator.

An IHL system is characterized by a major complexity with respect to a DHL system and it is used to decouple the heat pump flow rate (primary flow rate) from the emitters flow rate (secondary flow rate) in presence of a large number of terminal units. The emitters and the heat pump are controlled with the same logic described previously for a DHL system (i.e. indoor air temperature and return water temperature are used as monitored variables); on the other hand, the control of the secondary loop circulating pump is typically performed monitoring the temperature of the water stored in the separator.

The heating system depicted in Figure 4.12 can be characterized by the use of fixed-speed circulating pumps in both primary and secondary loop. In this Thesis, in order to complete this analysis, the case in which the secondary loop is manged

with a variable flow rate has been also carried out. In fact, the use of variable flow rate terminal units (e.g. fan-coils equipped with thermostatic valves) and the adoption of a variable-speed circulating pump in the secondary loop (see Figure 4.13) allow to reduce the pumping energy consumption and influence the stability and the seasonal energy performance of the heat pump.

In this Thesis, the different hydraulic configurations reported in this Section have been implemented within TRNSYS environment and the seasonal performance of the corresponding systems has been compared one another in Section 4.5.3.

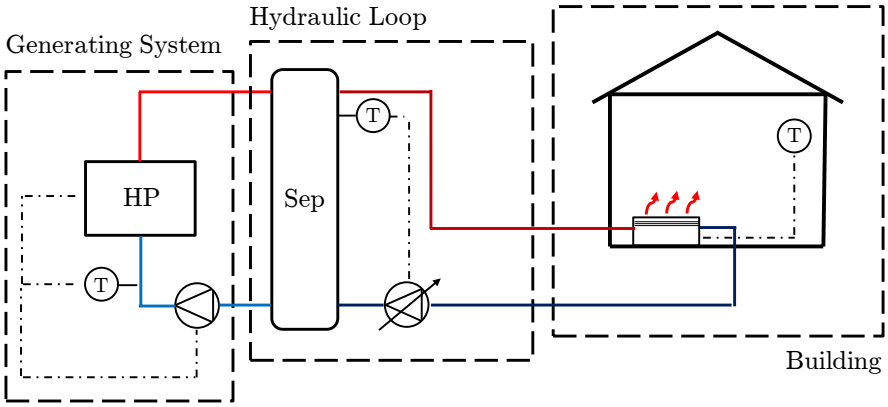

Figure 4.13. Logic layout of an IHL heating system characterized by variable flow rate in the secondary loop.

4.4. Dynamic modeling of an air-to-water heat pump

In this Section, the models developed for the dynamic simulation of air-to-water heat pump systems are described. These models, developed within TRNSYS environment, are able to simulate the behavior of the heat pump typologies considered in this Thesis (i.e. single-stage mono-compressor heat pumps (On-off HPs), multi-stage heat pumps (MSHPs) and inverter-driven heat pumps (IDHPs)), while the standard TRNSYS library considers On-off HPs only (see Section 4.2.1).

4.4.1. TRNSYS model for a single-stage heat pump

As explained in Section 4.2.1, the standard TRNSYS library includes two different models which can be used to simulate the behavior of air-to-water heat pumps (i.e. Types 917 and 941).

Typically, the control system of a single-stage heat pump is based on an on-off controller (see Section 2.3.1 for further details) because this kind of unit does not have the possibility to modulate its delivered capacity: in fact, an On-off HP operates at full load for each operating condition and the only way to match the required load is to perform a series of on-off cycles. Therefore, the compressor has only two operating states, namely "compressor on" or " compressor off", and the on-off controller is the most suitable and simple solution to control the system.

The control logic of a single-stage heat pump is based on the water return temperature ($T_{w,in}$), which means that the value of this variable is constantly monitored by the controller: the temperature sensor is located on the indoor heat exchanger inlet (i.e. condenser inlet for the heating operating mode and evaporator inlet for the cooling operating mode). The set-point imposed by the controller is the desired value that the return water temperature must reach; therefore, the internal module of the controller evaluates the temperature difference between the set-point temperature and the actual value of the monitored return water temperature: on the basis of this difference, the on-off controller will activate or deactivate the compressor of the heat pump. In many cases, the temperature of hot or cold water supplied to the building is not directly monitored by the control system but it is indirectly controlled by means of the set-point value imposed for the water return temperature.

In order to define the behavior of the on-off controller coupled to a single-stage heat pump, the user has to define the values of control parameters. Typically, an on-off control system is based on a hysteresis logic to avoid an excessive switching frequency of the control signal (see Section 2.3.1). For this reason, the control algorithm is fully expressed by specifying the values of the set-point temperature and the Dead Band for both heating ($T_{SP,h}$ and DB_h, respectively) and cooling mode ($T_{SP,c}$ and DB_c, respectively). It is important to highlight that in the developed controller the Dead Bands are considered centered around the set-point temperature. The behavior of the implemented control systems is represented in Figure 4.14 and Figure 4.15 for heating and cooling operating modes, respectively.

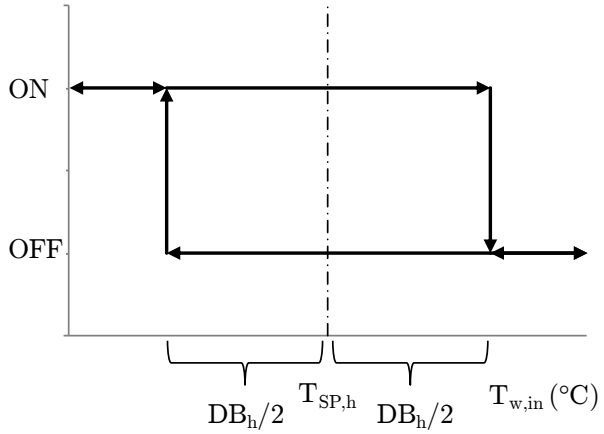

Figure 4.14. Hysteresis cycle of the on-off control system (heating mode).

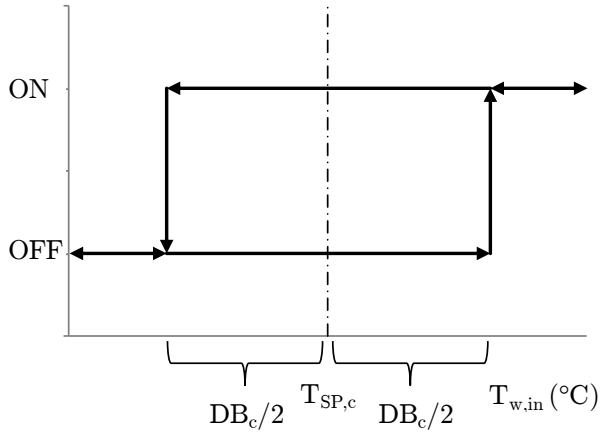

Figure 4.15. Hysteresis cycle of the on-off control system (cooling mode).

Finally, the control algorithm imposed by the on-off controller for the heating operating mode is evaluated by means of the following Equations:

$$\text{if } HS(t-\Delta\tau)=\text{on} \begin{cases} HS(t)=\text{on} & \text{if } DT_h(t) < DB_h/2 \\ HS(t)=\text{off} & \text{if } DT_h(t) > DB_h/2 \end{cases} \tag{4.24}$$

$$\text{if } HS(t-\Delta\tau)=\text{off} \begin{cases} HS(t)=\text{on} & \text{if } DT_h(t) < -DB_h/2 \\ HS(t)=\text{off} & \text{if } DT_h(t) > -DB_h/2 \end{cases} \tag{4.25}$$

where HS is the heating control signal of the heat pump (see Section 4.2.1), evaluated at the current timestep t or at the previous timestep (t - $\Delta\tau$) and DT_h is the temperature difference between the value of the return water temperature ($T_{w,in}$) evaluated at the current timestep t and the set-point temperature for heating operating mode ($T_{SP,h}$).

On the contrary, the algorithm imposed by the on-off controller for the cooling operating mode can be expressed as:

$$\text{if } CS(t-\Delta\tau)=\text{on } \begin{cases} CS(t)=\text{on} & \text{if } DT_c(t) > -DB_c/2 \\ CS(t)=\text{off} & \text{if } DT_c(t) < DB_c/2 \end{cases} \tag{4.26}$$

$$\text{if } CS(t-\Delta\tau)=\text{off } \begin{cases} CS(t)=\text{on} & \text{if } DT_c(t) > DB_c/2 \\ CS(t)=\text{off} & \text{if } DT_c(t) < DB_c/2 \end{cases} \tag{4.27}$$

where CS is the cooling control signal of the heat pump (see Section 4.2.1) and DT_c is the temperature difference between $T_{w,in}$ and the set-point temperature for cooling operating mode ($T_{SP,c}$), evaluated for the current timestep t.

In real systems, single-stage heat pumps typically operate according to a 5 K Dead Band around the selected set-point temperature. As an example, if one considers the heating mode for a set-point temperature equal to 40 °C, the compressor will be activated when the water return temperature $T_{w,in}$ is lower than 37.5 °C (i.e. $T_{SP,h}$ - $DB_h/2$); on the contrary, the compressor will be switched off when $T_{w,in}$ is larger than 42.5 °C (i.e. $T_{SP,h}$ + $DB_h/2$).

4.4.2. TRNSYS model for a multi-stage heat pumps

Multi-stage heat pumps are able to modulate their delivered thermal capacity simply by varying the number of active compressor stages (i.e. the number of compressors switched on). As reported in the previous Section, the standard TRNSYS library does not include the model of a multi-stage air-to-water heat pump; for this reason, a new component has been implemented during this PhD. The developed model calculates the heat pump performance at partial load (i.e. thermal/cooling capacity and COP/EER) and, furthermore, it is able to evaluate the number of active compressors which are needed to match the required load.

In detail, if one considers a MSHP characterized by N compressors, the model of the unit developed in TRNSYS accounts for N standard Types 941 (or 917 if the humidity effect has to be taken into account). Each standard Type included in the MSHP model represents a specific working condition of the multi-stage unit; for example, in order to simulate the behavior of a MSHP composed by three compressors (N = 3), three different Types 941 (or 917) has to be inserted in the model: the first one reports the heat pump performance data evaluated for one active compressor (i.e. 1/3 working condition), the second one reports the same data evaluated with two active compressors (i.e. 2/3 operating condition) and finally the third one represents the full load working condition (i.e. 3/3 active compressors). For each Type included in the MSHP model, the user has to supply the performance data of the heat pump in the corresponding working condition, according to the procedure reported in Section 4.2.1 (see Figure 4.1 and Figure 4.2 for further details). The heat pump performance data (i.e. thermal/cooling capacity and *COP*/*EER*) can be obtained by the manufacturer technical datasheets and are the same data employed for the mathematical model of a MSHP used with the bin method and described in Section 3.3.3.

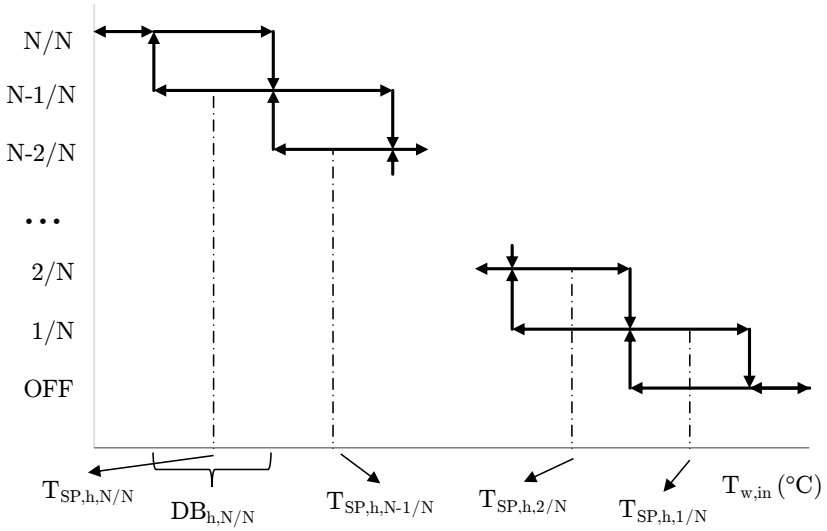

Figure 4.16. Hysteresis cycle of the control system of MSHP composed by N compressors (heating mode).

Since a multi-stage heat pump is characterized by N on-off compressors, the control logic of the unit is similar to the one proposed in the Section 4.4.1 for an On-off HP; in fact, each compressor has only two operating states, namely compressor switched on or switched off. Furthermore, the monitored variable is

the return water temperature also for this kind of heat pump. Nevertheless, in this case an improved control logic is needed, because the system controller has to evaluate the working condition that is needed to match the load required the building, thus the number of active compressors.

For this purpose, the standard Type 970 (N-stage differential controller) is employed. By means of this Type, N on-off control functions can be generated and used to regulate a N-stage heat pump. The user has to specify the values of the controller parameters, equal in this case to 2 * N: in fact, a set-point temperature and a deadband must be defined for each stage of the controller (namely $T_{SP,h,n/N}$ and $DB_{h,n/N}$).

In Figure 4.16 the behavior of the control system implemented for a N-stage heat pump is represented for heating operating mode.

Finally, the control algorithm imposed by the controller of the MSHP operating in heating mode is evaluated by means of the following Equations:

$$\text{if } HS_{n/N}(t - \Delta\tau)=\text{on } \begin{cases} HS_{n/N}(t) = \text{on} & \text{if } DT_{h,n/N}(t) < DB_{h.n/N} / 2 \\ HS_{n/N}(t) = \text{off} & \text{if } DT_{h,n/N}(t) > DB_{h,n/N} / 2 \end{cases} \text{ for } n = 1,\ldots,\text{N} \tag{4.28}$$

$$\text{if } HS_{n/N}(t - \Delta\tau)=\text{off } \begin{cases} HS_{n/N}(t) = \text{on} & \text{if } DT_{h,n/N}(t) < -DB_{h,n/N} / 2 \\ HS_{n/N}(t) = \text{off} & \text{if } DT_{h,n/N}(t) > -DB_{h,n/N} / 2 \end{cases} \text{ for } n = 1,\ldots,\text{N} \tag{4.29}$$

where $HS_{n/N}$ is the heating control signal of the n-th stage of the MSHP and $DT_{h,n/N}$ is the temperature difference between $T_{w,in}$ and $T_{SP,h,n/N}$ evaluated at the current timestep t for the n-th stage of the unit.

On the contrary, the algorithm imposed by the on-off controller for the cooling operating mode is described by means of the reported Equations:

$$\text{if } CS_{n/N}(t - \Delta\tau)=\text{on } \begin{cases} CS_{n/N}(t) = \text{on} & \text{if } DT_{c,n/N}(t) < DB_{c.n/N} / 2 \\ CS_{n/N}(t) = \text{off} & \text{if } DT_{c,n/N}(t) > DB_{c,n/N} / 2 \end{cases} \text{ for } n = 1,\ldots,\text{N} \tag{4.30}$$

$$\text{if } CS_{n/N}(t - \Delta\tau)=\text{off } \begin{cases} CS_{n/N}(t) = \text{on} & \text{if } DT_{c,n/N}(t) < -DB_{c,n/N} / 2 \\ CS_{n/N}(t) = \text{off} & \text{if } DT_{c,n/N}(t) > -DB_{c,n/N} / 2 \end{cases} \text{ for } n = 1,\ldots,\text{N} \tag{4.31}$$

where $CS_{n/N}$ is the cooling control signal of the n-th stage of the MSHP and $DT_{c,n/N}$ is the temperature difference between $T_{w,in}$ and $T_{SP,c,n/N}$ evaluated at the current timestep t for the n-th stage of the unit.

However, the control functions HS and CS, evaluated for each stage of the heat pump by means of Eqs. (4.28)-(4.29) and (4.30)-(4.31), can not be directly connected to the input control signal of the corresponding Type 941 (or 917). In fact, different control signals could be in the "on" condition during the same timestep and a non-physical operating condition may occur (for example, one and two active compressors at the same time). As an example, we can consider Figure 4.16: if in a certain timestep the value of the return water temperature $T_{w,in}$ is below ($T_{SP,h,2/N}$ - $DB_{h,2/N/2}$), then according to Eqs. (4.28) and (4.29) both control functions $HS_{2/N}$ and $HS_{1/N}$ are related to the "on" condition. For this reason, the effective control signals of the n-th stage of a MSHP, evaluated for heating and cooling modes ($HS_{n/N,eff}$ and $CS_{n/N,eff}$, respectively), can be expressed as:

$$\begin{cases} HS_{n/N,eff}=\text{off} & \text{if } HS_{n/N} = HS_{n+1/N} \\ HS_{n/N,eff}=\text{on} & \text{if } HS_{n/N} = HS_{n+1/N} \end{cases} \quad \text{for } n=1,\ldots,\text{N} - 1$$
$$HS_{n/N,eff}=HS_{N/N} \quad \text{for } n=\text{N} \tag{4.32}$$

$$\begin{cases} CS_{n/N,eff}=\text{off} & \text{if } CS_{n/N} = CS_{n+1/N} \\ CS_{n/N,eff}=\text{on} & \text{if } CS_{n/N} = CS_{n+1/N} \end{cases} \quad \text{for } n=1,\ldots,\text{N} - 1$$
$$CS_{n/N,eff}=CS_{N/N} \quad \text{for } n=\text{N} \tag{4.33}$$

If one considers a real controller of a MSHP, the Dead Band of the control systems is usually defined as the ratio between the nominal temperature difference among supply and return water (typically 5 K) and the number of compressors. For example, in multi-stage heat pump characterized by two compressors (N = 2), both Dead Bands are 2.5 K broad. However, this choice can be optimized in

order to maximize the seasonal performance of the system as described in the following Sections.

4.4.3. TRNSYS model for an inverter-driven heat pump

Heat pumps provided with an inverter-driven motor may operate at different rotating speeds, depending on the inverter frequency. For this reason, an IDHP is characterized by an enhanced modulation capacity, with respect to On-off HPs and MSHPs: for this kind of device, the delivered thermal/cooling capacity can be modulated continously, within the inverter modulation range.

It is important to highlight that the modulation capability of a variable-speed heat pump should not be overrated; in fact, when the compressor rotating speed is lower than the minimum allowed value, a strong reduction of its volumetric efficiency occurs. Furthermore, at low compressor frequencies the lubrificating oil does not prevent the refrigerant return to the suction side: for a compressor with a nominal frequency of 120 Hz, the rotating speed can be reduced only down to 20-30 Hz if safety operating conditions have to be ensured. This problem affects all the compressors used in commercial heat pumps but the use of scroll compressors allows a further modulation compared to rotary devices and nowadays some compressor manufacturers assure lower minimum allowed frequencies (20 Hz instead of 30 Hz) [105]. Furthermore, the efficiency of the electric motor coupled to the compressor usually decreases for lower inverter frequencies.

For this kind of systems, a PID control system (see Section 2.3.2) is typically employed to modulate the delivered thermal/cooling capacity. In this case, the monitored variable can be the return water temperature ($T_{w,in}$), as for On-off HPs and MSHPs, or, according to the enhanced modulation capability of the unit, the supply water temperature ($T_{w,out}$).

In addition to the minimum allowed compressor rotating speed, the value of PID parameters (i.e. K_p, T_i and T_d, see Section 2.3.2 for further details) affects the heat pump modulation capability. As pointed out by Figure 4.17, the higher the reactivity of the control system, the higher the overshoot of the compressor rotating speed (i.e. the difference between the minimum and the minimum allowed value of the compressor frequency); therefore, more the controller reacts faster to a variation of the monitored variable, which is in this case the water temperature at the heat pump inlet or at the heat pump outlet, the larger the minimum thermal load deliverable by the heat pump avoiding the compressor

frequency to fall below its minimum allowed value (given by the manufacturer). A higher reactivity of the controller occurs when the proportional gain K_p is increased and the integral time T_i is reduced.

On the contrary, the higher the stability of the control system, the longer the time to assure that the heat pump delivered capacity matches the required load (i.e. the longer the water temperature reaches its set-point value).

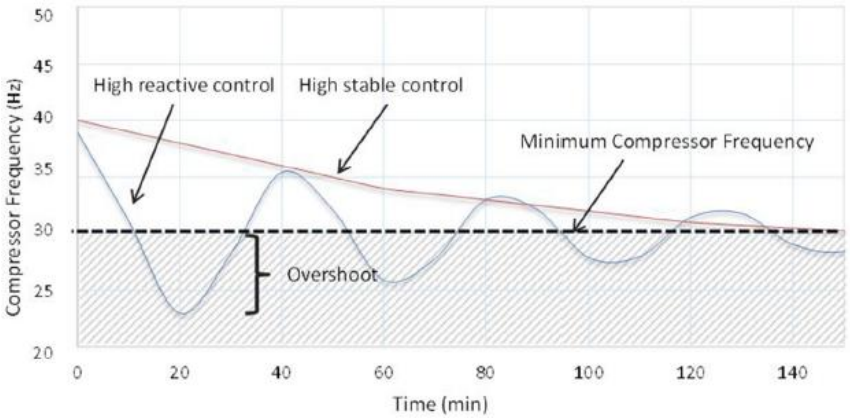

Figure 4.17. High reactive and high stable behavior of a PID controller (from [51]).

In order to simulate the behavior of an inverter-driven heat pump within TRNSYS environment, it is necessary to implement a new model, which is able to calculate the heat pump performance (i.e. its thermal/cooling capacity and *COP*/*EER*) as a function of three independent variables: the external temperature T_{ext}, the return water temperature $T_{w,in}$ and the inverter frequency Φ. For this reason, Type 581 (Multi Dimensional Data Interpolation) is employed to define the heat pump performance; this component performs a multi-dimensional data interpolation within the data supplied by the user, with the limitation that there are a maximum number of independent and dependent variables (4 and 5, respectively) which can be set. It is important to highlight that Type 581 does not extrapolate data beyond the range given by the user: if the given conditions fall outside the supplied range, therefore the value of the given last point is returned.

In Figure 4.18 and Figure 4.19 the thermal capacity and *COP* data of an IDHP, given by the manufacturer, are reported, respectively.

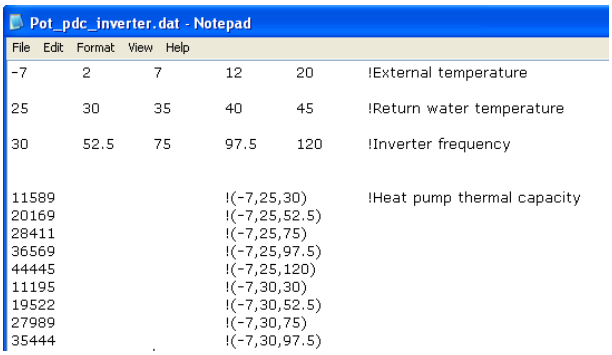

Figure 4.18. Use of Type 581 to supply thermal capacity data of as a function of external temperature, return water temperature and inverter frequency.

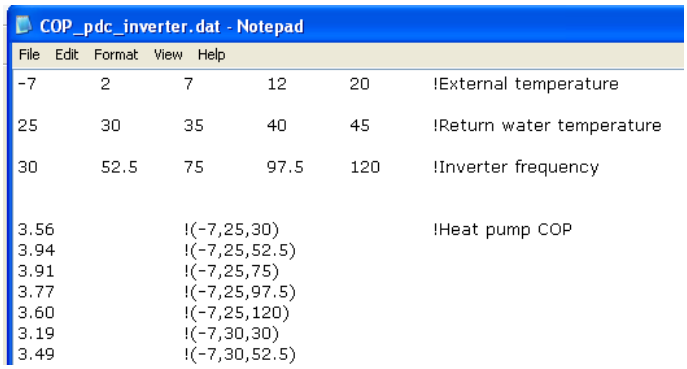

Figure 4.19. Use of Type 581 to supply *COP* data of as a function of external temperature, return water temperature and inverter frequency.

Once defined the input data for the heat pump performance evaluation (i.e. T_{ext}, $T_{w,in}$ and Φ), the Types 581 return the values of thermal/cooling capacity ($P_{HP,h}$ and $P_{HP,c}$, respectively) and *COP*/*EER* by means of a multi-dimensional interpolation.

Then, the value of the supply water temperature can be evaluated by means of the following Equations for heating and cooling operating modes:

$$T_{w,out} = T_{w,in} + \frac{P_{HP,h}}{\dot{m}_w c_{p,w}} \tag{4.34}$$

$$T_{w,out} = T_{w,in} - \frac{P_{HP,c}}{\dot{m}_w c_{p,w}} \tag{4.35}$$

The PID controller is modelled by using the Type 23. The main characteristics of this Type are reported in Figure 4.20. The user has to define the values of the PID parameters (i.e. Φ_{max}, Φ_{min}, K_p, T_i and T_d) and the value of the set-point temperature (i.e. $T_{w,out,SP}$), then the supply water temperature, evaluated by means of Eq. (4.34) or Eq. (4.35), has to be used as the monitoring value. Type 23 returns the value of the effective inverter frequency Φ_{eff}, which can be used as the input of Types 581.

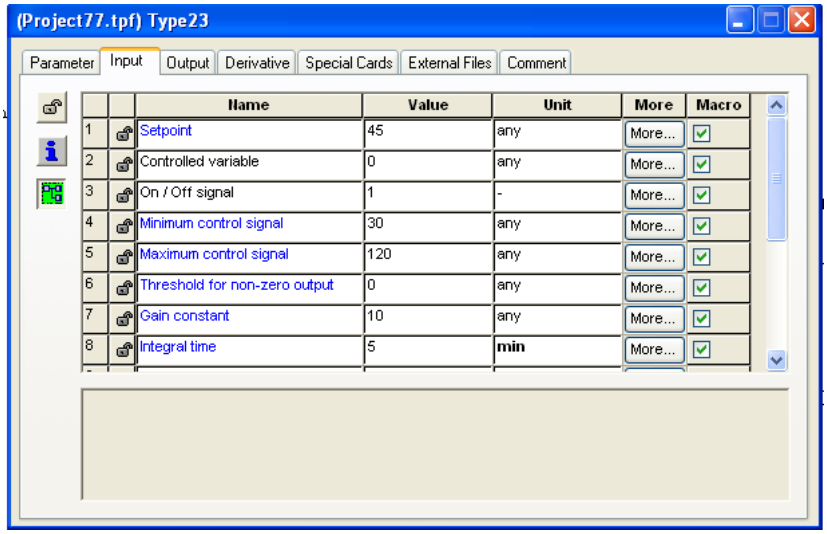

Figure 4.20. TRNSYS Type 23 (PID controller) characteristics.

When the minimum inverter frequency (Φ_{min}) is reached no further capacity modulation is possible; in this case on-off cycles must be performed by the heat pump to match the building required load. For this reason, an on-off controller is introduced in the control logic of the IDHP. The behavior of this controller is based on a hysteresis cycle and is the same of the one reported in Section 4.4.1; therefore, the user has to define the set-point temperature ($T_{w,out,SP}$) and the dead band (DB) of the hysteresis cycle. In this case, the on-off controller is active only when the effective inverter frequency (i.e. the output value of Type 23) is set to the minimum frequency.

The layout of the developed model of an IDHP is reported in Figure 4.21. In the same Figure, the controllers of the unit (i.e. PID and on-off Types) are highlighted.

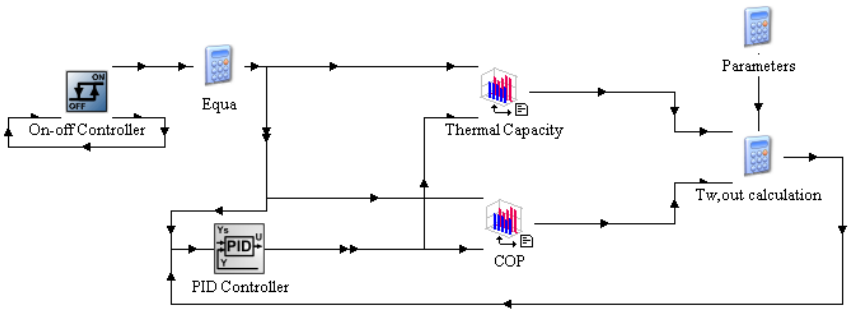

Figure 4.21. Layout of the dynamic model of an inverter-driven heat pump and its control system.

4.4.4. TRNSYS model for the evaluation of heat pump cycling losses

As pointed out in Section 2.4 and in Section 3.2, heat pump systems perform a certain number of on-off cycles during the heating/cooling season in order to modulate the delivered thermal/cooling capacity; furthermore, according to the modulation capability of the unit (i.e. its control system), the amount of the above-mentioned on-off cycles varies: the higher the modulation capacity of the unit, the higher the reduction of on-off cycles performed by the heat pump.

When an on-off cycle is carried out by the unit, energy losses are introduced in the system. In fact, when the heat pump is completely switched off, the refrigerant fluid migrates from the high-pressure side to the low-pressure side of the compressor and during the following start-up the compressor has to restore this pressure difference, dissipating energy.

The standard Types which represent an air-to-water heat pump included whitin TRNSYS library does not take into account cycling losses: when the unit is switched on (i.e. when its control signal goes from 0 to 1), the heat pump performance is not penalized and the steady-state values of thermal/cooling capacity and *COP*/*EER* are calculated by means of a linear interpolation of user supplied data.

For this reason, in order to take into account the energy losses due to on-off cycles, a cycling penalization is included in the developed dynamic models. More in detail, two corrective factor are introduced, the first one which evaluates the reduction of the delivered thermal capacity during a start-up (CF_h and CF_c for heating and cooling operating modes, respectively) and the second one which takes into account the reduction of the absorbed electric power ($CF_{el,h}$ and $CF_{el,c}$

for heating and cooling modes, respectively). Furthermore, the definition of above-mentioned corrective factors is not sufficient to characterize the energy losses linked to on-off cycles: the duration of the transient period, for both the delivered capacity and the electric input has to be defined as well. In fact, for each start-up of the heat pump, a time counter evaluates the increasing duration of the transient (t_{SU}), by comparing its value with the duration of transient periods (i.e. $t_{pen,h}$ and $t_{pen,c}$, the characteristic times for delivered capacity transient during heating and cooling mode, and $t_{pen,el,h}$ and $t_{pen,el,c}$, the characteristic times for electric power input transient during heating and cooling mode). Finally, one can calculate for the heating operating mode the values of the effective delivered thermal capacity $P_{HP,h,eff}$ and of the effective electric absorbed power $P_{el,h,eff}$ by means of the following Equations:

$$\begin{cases} P_{HP,h,eff} = P_{HP,h} CF_h & \text{if } t_{SU} < t_{pen,h} \\ P_{HP,h,eff} = P_{HP} & \text{if } t_{SU} > t_{pen,h} \end{cases} \tag{4.36}$$

$$\begin{cases} P_{el,h,eff} = P_{el,h} CF_{el,h} & \text{if } t_{SU} < t_{pen,el,h} \\ P_{el,h,eff} = P_{el,h} & \text{if } t_{SU} > t_{pen,el,h} \end{cases} \tag{4.37}$$

on the other hand, the same values (namely $P_{HP,c,eff}$ and $P_{el,c,eff}$) can be calculated for the cooling operating mode as follows:

$$\begin{cases} P_{HP,c,eff} = P_{HP,c} CF_c & \text{if } t_{SU} < t_{pen,c} \\ P_{HP,c,eff} = P_{HP,c} & \text{if } t_{SU} > t_{pen,c} \end{cases} \tag{4.38}$$

$$\begin{cases} P_{el,c,eff} = P_{el,c} CF_{el,c} & \text{if } t_{SU} < t_{pen,el,c} \\ P_{el,c,eff} = P_{el,c} & \text{if } t_{SU} > t_{pen,el,c} \end{cases} \tag{4.39}$$

One can conclude that, according to the above observations, the developed dynamic models take into account the energy losses linked to on-off cycles, forcing the units to operate with a reduced electrical input power and a reduced heating/cooling capacity during each start-up. It is important to stress that the values of CF_h, CF_c, $CF_{el,h}$, $CF_{el,c}$, $t_{pen,h}$, $t_{pen,c}$, $t_{pen,el,h}$ and $t_{pen,el,c}$ are referred to the specific heat pump unit simulated and depend on the technology level of the

adopted on-board control system; the above-mentioned values have to be evaluated by means of experimental measures and are generally declared by the heat pump manufacturer. Unfortunately, it is not common to see these values indicated in the manufacturer datasheets and the companies offer a resistance to communicate this kind of information to the designers.

Furthermore, the parameters introduced in this Section strongly depends on the typology of the expansion valve installed on the heat pump. The lamination valve is one of the main components of the unit: it introduces the pressure drop between condenser and evaporator, allowing to maintain the proper pressure gradient between the two components. The expansion valve control system monitors the superheating degree of the refrigerant vapor in the suction side of the compressor: the function of the valve is to maintain the superheating degree to its set-point value (typically 5 K).

An expansion valve is composed by a metallic body in which a variable geometry opening is placed, allowing the modulation of the refrigerant cross-sectional area. The extension of this area depends on the position of a needle, which is controlled by the feedback control signal on the superheating degree. If the needle position and the cross-sectional area are coupled by a linear relationship, one can refer to a linear expansion valve; on the contrary, if this function is exponential one can refer to an equal percentage valve. Typically, the expansion valves employed by heat pumps belong to the second category: equal percentage valves are characterized by a fine pressure drop modulation even for low refrigerant flowrates.

Nowadays, heat pumps can be equipped with Thermostatic Expansion Valves (TEVs) or Electronic Expansion Valves (EEVs). In a TEV the actuator that moves the neddle is a diaphragm. As pointed out by Figure 4.22, the diaphragm is subject to three different pressures: the spring pressure (p_0), the pressure of the refrigerant in the capillary tube coupled to the bulb sensor (p_1) and in the internal port coupled to the evaporator (p_2). The latter pressure coincides, unless the pressure losses, with the evaporation pressure.

As shown in Figure 4.22, the thermostatic expansion valve can be divided into three chambers:

- A first chamber, communicating with the remote bulb through a capillary tube, is positioned on the top of the diaphragm. The bulb is a temperature sensor, coupled to the evaporator outlet via a high conductive thermal material; furthermore, the capillary tube is filled with the refrigerant fluid which flows in

the heat pump. The bulb-capillary system measures the temperature of the refrigerant leaving the evaporator, converts the temperature signal into a pressure signal and transduces this pressure to the upper wall of the diaphragm. According to the small size of the bulb-capillary system, a variation of the temperature coming from the bulb sensor corresponds to an instantaneous change of pressure on the upper surface of the diaphragm.

- A second chamber, communicating with the entrance of the evaporator by a capillary equalization tube. Also in this case, a variation of the evaporation pressure is reflected almost instantaneously in a variation of the pressure acting on the lower surface of the diaphragm.

- A third chamber contains the needle and the opening port; this port allows the refrigerant to flow from the lower inlet to the upper outlet of the chamber and realizes the lamination process.

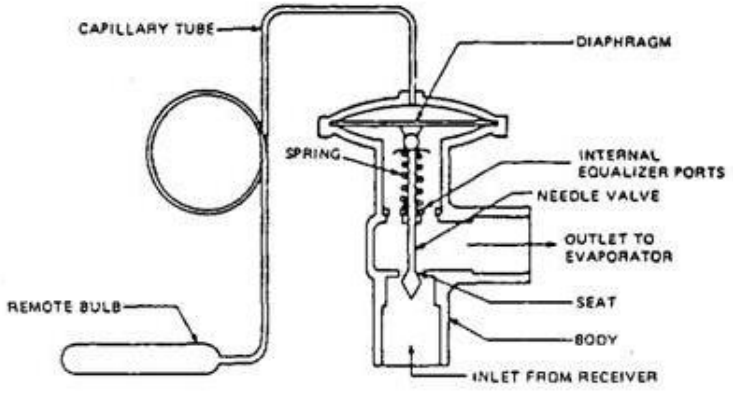

Figure 4.22. Schematic representation of a TEV (from [106]).

If the refrigerant leaving the evaporator is in saturation condition (i.e. dry saturated vapor), the pressure p_1 exerted on the upper surface of the diaphragm coincides with the pressure p_2 and the resultant pressure on the diaphragm is the pressure p_0 given by the spring. The expansion valve is sized in order to ensure a null pressure difference between the diaphragm sides when the refrigerant leaving the evaporator reaches the desired superheating value. In conclusion, the membrane is in equilibrium only when the refrigerant superheat degree at the evaporator outlet coincides with the desired set-point.

The control logic of the TEV is relatively simple:

- If the superheat degree of the refrigerant at the evaporator outlet increases, the valve opens the orifice and the refrigerant flowrate through the evaporator increases; in this case, the position of the two-phase front advances toward the evaporator outlet, thus allowing a decrease in the superheat degree;

- On the contrary, if the superheat degree of the refrigerant leaving the evaporator decreases, the valve further closes the orifice and the flow rate delivered by the valve decreases, causing an increase of the superheating degree.

An electronic expansion valve (EEV) can be considered the electronically controlled version of a thermostatic expansion valve. The actuator, which in the case of a TEV is a diaphragm subject to three pressures, in an EEV is a stepping motor controlled by an electronic device. The capillary tube and the bulb sensor are replaced respectively by a pressure transducer and a temperature probe. These pressure and temperature signals are processed by a microprocessor unit which evaluates the superheat value (monitored output) and, by implementing a PID algorithm (see Section 2.3.2), processes a control signal and imposes it to the stepping motor.

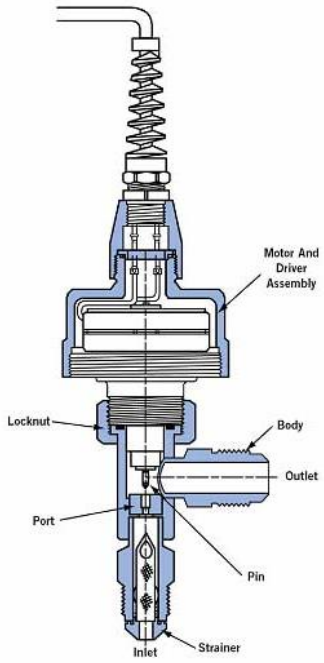

Figure 4.23. Schematic representation of an EEV (from [106]).

The most important characteristic of an EEV is its accuracy in the calculation of the desired refrigerant flowrate. In fact, the microprocessor dedicated to the expansion valve, by means of the PID control logic based on the overheating degree, allows to manage a series of additional functions that are very useful to optimize the performance of the heat pump under steady-state and transient conditions. Among these additional features, one function can be very useful to increase the energy performance of the heat pump during a start-up, if compared to the case of a TEV: the possibility to completely close the orifice of the valve when the compressor is switched off. This function allows to avoid an undesirable migration of refrigerant from the condenser to the evaporator during the off period, which involves the equalization of the evaporation and condensation pressure. To be noted that the restoration of the pressure difference between the high and low pressure sides of the heat pump is the main cause of energy losses during the unit start-up.

The values of the parameters introduced in this Section to evaluate the on-off cycles energy losses depends on the expansion valve typology (i.e. thermostatic or electronic). A series of experimental measures performed in cooperation with a heat pump manufacturer has been allowed to obtain the typical values of these parameters (i.e. the length of the transient periods and the average reduction of the absorbed electric power and the thermal capacity) for both a TEV and an EEV. The ranges of the penalization parameters of an on-off cycle are reported in Table 4.1. It is important to highlight that the differences obtained between heating and cooling operating modes are negligible and a single value for each parameter has been taken into account in this work.

Table 4.1. Typical values of on-off cycles penalization parameters with respect to the expansion valve typology.

Expansion valve typology	$t_{pen,el,h/c}$ (s)	$CF_{el,h/c}$	$t_{pen,h/c}$ (s)	$CF_{h/c}$
TEV	60 - 90	0.95 - 1.00	240 - 300	0.55 - 0.65
EEV	60 - 90	0.95 - 1.00	100 - 130	0.75 - 0.85

4.4.5. TRNSYS model for the simulation of defrosting cycles

Finally, the energy losses due to the defrosting cycles performed by an air-source heat pump during the heating season have been modelled. As pointed out in Section 2.2.3, when the relative humidity of the external air is larger than 50%

and the external temperature falls below 6°C the formation of a frost layer occurs on the surface of the outdoor heat exchanger (i.e. the evaporator) and its thickness increases with time. As a consequence, the heat transfer coefficient decreases due to the additional thermal resistance given by the frost layer; in addition, the refrigerant evaporating pressure tends to decrease and this phenomena further accelerates the frost layer growth due to the decrease of the outdoor coil surface temperature.

For all these reasons a defrost cycle is needed to remove ice. The main techniques carried out by the heat pump to melt ice have been reported in Section 2.2.3: inversion of the refrigerant cycle, hot gas by-pass, compressor stop or use of electric resistances; nevertheless, reversible heat pumps generally carry out the inversion of the cycle to perform a defrost cycle. Due to the defrosting cycles, the heat pump performance is strongly reduced. In fact, when the frost layer is removed by inverting the cycle, the effect is twofold: the thermal energy delivered to the building decreases and, furthermore, the building heating demand increases due to the thermal energy carried off by the heat pump operating in cooling mode (the indoor heat exchanger works as the evaporator in this operating mode).

The behavior of the heat pump during a typical defrosting cycle is reported in Figure 4.24: before activating the inversion cycle, the heat pump is switched off for a period imposed by the system controller (t_{off}) equal for example to 1 minute. After this first period the compressor is turned on, the reversing valve of the heat pump is switched, the fans at the outdoor heat exchanger are stopped and finally the heat pump operates in cooling mode. Typically, the device works by following the cooling cycle until the temperature at the bottom part of the external coil rises above the desired set-point value (typically 10-12°C): once this temperature is reached, the outdoor coil should be free of ice and the compressor is switched off again.

The duration of a defrost cycle (t_{DC}) is generally fixed by the heat pump manufacturer and it typically ranges from 1 to 10 minutes. When the defrost cycle is finished, another stand-by period (t'_{off}) is carried out by the heat pump (i.e. the unit is switched off); after this period, the 4-way valve reverses and the heat pump returns to the heating cycle.

When the outdoor climatic conditions (i.e. relative humidity and temperature of external air) fall within the frosting region, the heat pump performs the whole defrosting cycle described previously at regular timed periods: typically, one or two defrost cycles for hour can be sufficient to remove the frost layer.

The duration of the whole defrosting cycle $t_{DC,tot}$ can be finally expressed as follows:

$$t_{DC,tot} = t_{off} + t_{DC} + t'_{off} \tag{4.40}$$

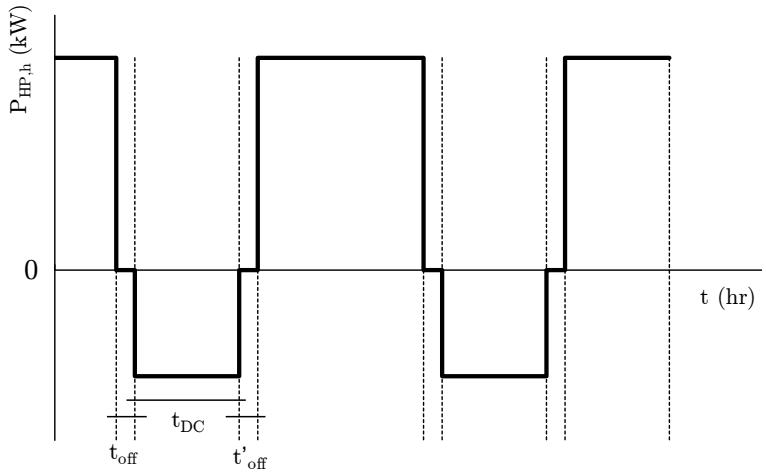

Figure 4.24. Typical defrosting cycle for an air-source heat pump based on the inversion of the refrigerant thermodynamic cycle.

The frost formation is a very complex physical phenomena and is strongly influenced by the geometry of the outdoor heat exchanger: for this reason, a simplified dynamic model, which does not take into account the evaporator geometry, able to estimate the reduction of the heat pump performance is developed on the basis of the inversion of the refrigerant thermodynamic cycle, by following the approach reported in [107].

Experimental results [41] showed that no frost is practically accumulated on the surface of the outdoor heat exchanger when the external air temperature is outside the range of 0 to 6°C: in fact when the ambient temperature is above 6°C the coil surface temperature is warm enough to avoid ice formation while below 0°C the moisture content of the external air is too low for the frost layer formation. In addition, the moisture air content is the parameter which mostly influences the frost formation: a series of experimental results reported in literature ([39]-[42]) show that ice accumulates on the outdoor heat exchanger of a heat pump only for values of the relative humidity above 50%.

Defrosting cycles have been simulated in this Thesis by means of a simplified logic based on the inversion of the refrigerant cycle. The defrost control system

evaluates the external air temperature and relative humidity as control variables: when the outdoor climatic conditions fall within the "frosting region" (i.e. relative humidity above 50% and air temperature within 0-6°C range) a series of defrosting cycle is performed according to the logic described previously. More in detail, one cycle per hour is carried out by the heat pump if the climatic conditions are critical for a long period. The duration of the characteristic periods of a defrost cycle (i.e. t_{off}, t_{DC} and t'_{off}) is defined by the user and depends on the used control logic. Furthermore, a penalization factor is applied for each defrost cycle (i.e. an increase of the electrical consumptions).

4.5. Case studies

The numerical models developed within TRNSYS and described in Sections 4.3 and 4.4 have been applied to optimize the control strategy of a heat pump system coupled to building. In the first reported case study the influence of the heat pump control logic on the indoor thermal comfort guaranteed by the heating system within a school building is evaluated. Therefore, in the second and in the third reported case study several simulations have been carried out to show how the optimization of the system control strategy allows to obtain a reduction of the on-off cycles performed by the heat pump during the year and the enhancement of the system energy performance.

The topics discussed in this Section are treated in Refs. [55] and [108].

4.5.1. Influence of the control system of a heating plant based on a heat pump on the Indoor Thermal Comfort

In order to assess the indoor thermal comfort guaranteed by a heating system based on an air-to-water heat pump coupled to low-temperature emitters, the dynamic model of a school building and the relative HVAC plant has been developed. Actually, the school heating system is composed by condensing boilers coupled to high-temperature radiators; in this case study the refurbishment of this plant by introducing a multi-stage heat pump and the enhancement of its control strategy is discussed to evaluate the potential energy saving linked to the retrofit measure and especially to improve the indoor thermal comfort conditions.

The educational building considered in this case study is the primary and secondary school Istituto Comprensivo G. Marconi, located in Castelfranco Emilia

in province of Modena (north of Italy, 44.55°N; 11.02°E). According to Italian law [109], Castelfranco Emilia is characterized by 2 269 Heating Degree Days and it is collocated collocated in climatic zone E: for this reason the standard heating season ranges from October 15th to April 15th, corresponding to 183 days.

The school was built in 1950 and is located near the center of Castelfranco Emilia (see Figure 4.25). From Figure 4.25 it is evident that the building is characterized by an irregular hollow shape.

Figure 4.25. Position of Istituto G. Marconi within Castelfranco Emilia.

The investigated school building consists of a four-storey structure and is characterized by an elevation of 15.4 m above ground level (global height of 16.9 m due to basement level). The structure is articulated in classrooms, corridors, toilets, a zone with staff offices and a gym. Above the second floor, an unconditioned attic zone is present. Figure 4.26 reports a view of the building.

Figure 4.26. Streetview of the South side of Istituto G. Marconi.

The building net conditioned volume is equal to about 18 392 m^3, while the ratio between dispersing surface and gross heated volume is 0.32 m^{-1}. The geometrical data of each storey, as net floor area, windows area and surface area, are reported in Table 4.2.

Table 4.2. Geometrical data of Istituto G. Marconi.

Building zone	Net floor area (m^2)	Surface area (m^2)	Windows area (m^2)	Net volume (m^3)
Basement	820	1 629	51	2 296
Ground Floor	773	986	192	3 447
First Floor	1 209	1 266	278	4 956
Second Floor	1 209	2 658	303	4 942
Gym	436	905	46	2 752
Total	4 446	7 443	869.4	18 392

According to the construction period of the school (1950), the energy performance of the building envelope is very low. In Italy, the first law concerning on building energy efficiency was published in 1976 (law n. 373/1976, [110]): for this reason, the school is not compliant with actual Italian law requirements in terms of U-value of envelope components and heating system performance. In the reported case study, four different opaque envelope components were considered, which main thermophysical data are reported in Table 4.3.

As pointed out by the comparison with actual U-values limits ($U\text{-value}_{lim}$) reported in Table 4.3, the elements of the building envelope are characterized by a very poor quality. On the other hand, school windows have been replaced during 1980 but they are still characterized by low energy performance. The main data about the school windows are shown in Table 4.3: with no low-emissive treatment and air as spacing gas. Finally, windows g-value is assumed equal to 0.75.

The HVAC system which provides the school space heating energy demand is composed by two condensing gas boilers. The rated heating capacity of each boiler is 150 kW and they are characterized by a rated efficiency at full load of 99.2%. The system control strategy is based on climatic compensation, which varies the temperature of the supply hot water as a linear function of external air temperature; on the contrary, the air temperature within the school classrooms is not monitored by the control system because no room or zone thermostats are

present. The heating system is characterized by a vertical distribution loop and the non-insulated pipes are placed within the external walls or directly inside the school corridors. The emitters consist of high-temperature cast-iron radiators, placed under the windows of the school rooms.

Table 4.3. Thermophysical data of the school envelope components.

Envelope component	Thickness (m)	U-value (W/m^2K)	U-value$_{lim}$ (W/m^2K)	Material
External wall	0.50	1.35	0.30	Brick
Internal wall	0.40	1.32	/	Brick
Windows	/	3.71	1.90	Double glass
Floor	0.36	1.76	0.31	Concrete
Roof	0.31	1.53	0.26	Concrete

The DHW is not produced by the heating system: electric boilers are placed in each bathroom and provide the thermal energy required for DHW production. A preliminary analysis of the DHW energy consumption pointed out that this energy demand can be considered negligible with respect to space heating energy requirement and for this reason such analysis has not been performed. Furthermore, the space cooling of the building zones and the ventilation of classrooms is not provided by the HVAC system: air changes are ensured by infiltrations through the envelope and by natural ventilation (i.e. manual windows opening). Rooms lighting is provided by means of fluorescent lamps when the natural light is not sufficient.

The total number of students is 577, subdivided in 25 classrooms; on the other hand, teacher and school staff is composed by 51 units. The occupancy of school rooms, which influences the internal heat gains, is reported in Table 4.4: students are present within classrooms from Monday to Friday, in the range 8:00-16:00, while teahcers and school staff occupancy schedule ranges from 7:00 to 17:00 from Monday to Friday and from 8:00 to 14:00 during Saturday. Furthermore, the operating schedule of the heating system is reported in Table 4.4: since the indoor temperature is not monitorated, the heating system is controlled by means of a programmable thermostat, which time schedule is based on the school occupancy, regardless of the required thermal load and internal conditions.

Table 4.4. Ooccupancy schedule of the building and heating system operating schedule.

	Monday-Friday	Saturday	Sunday
Students occupancy	8.00 - 16.00	/	/
School staff occupancy	7.00 - 17.00	8.00 - 14.00	/
Heating system schedule	6.00 - 19.00	6.00 - 14.00	/

As mentioned before, the dynamic model of the building was developed by means of TRNSYS 17 [87]. In the first step, the three-dimensional model of the school was carried out by means of the software Google Sketch-Up and then it was imported into TRNSYS environment with the dedicated plugin Trnsys3d. In Figure 4.27 a view of the developed 3D model is shown.

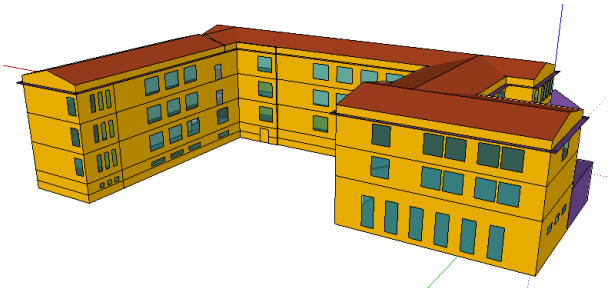

Figure 4.27. 3D model of Istituto G. Marconi developed by means of Google Sketch-Up.

According to the geometrical data reported in Table 4.2 and Table 4.3, the characteristics of the building envelope were defined within TRNBuild by considering five different kinds of thermal zones, in order to take into account the differences between equipment, occupancy profile and thermal gains: classrooms (CR), offices (O), corridors (C), toilets (WC) and the gym (G). A total of ninety-one thermal zones was created in the model; as an example, layout, orientation and zoning of the first floor of Istituto G. Marconi are reported in Figure 4.28.

The simulation of the school energy performance was performed by using a simulation time step equal to 1 minute and by considering the standard heating season as simulation time interval (i.e. from October 15th to April 15th, 183 days). The Typical Reference Year (TRY) of Bologna, included within TRNSYS weather data file, was employed as climatic input data of the developed model.

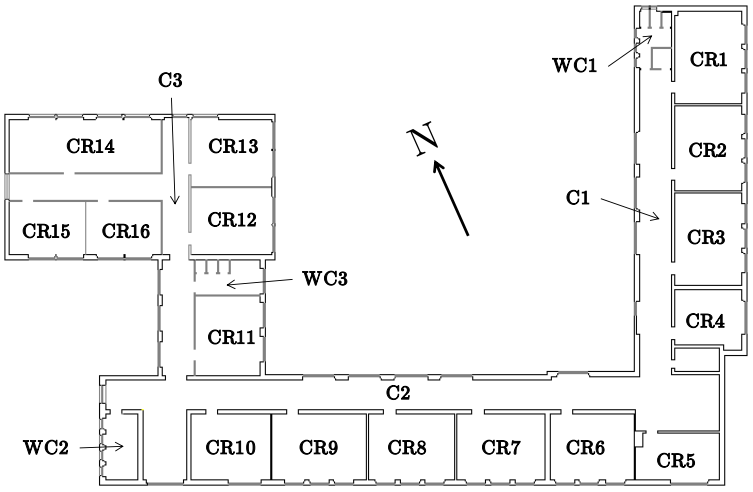

Figure 4.28. Layout, orientation and zoning of the first floor of Istituto G. Marconi.

The following step of the school energy performance assessment was the modelization of the building heating system, which was performed within Simulation Studio environment. Then, the energy requirement for space heating during the standard heating season was calculated. More in detail, the index used to assess the energy performance of Istituto G. Marconi was the Energy Performance Index for heating (EP_h), reported by the Italian Standard UNI TS 11300-2 [111]: this parameter is defined as the ratio between the total primary energy for heating required by the building and the total net floor area of the school.

Obtained results point out a total energy need of 359 146 kWh of primary energy during the heating season, corresponding to an EP_h value of 80.8 kWh/m^2. This value reflects the real operating schedule of the heating system (i.e. the intermittent schedule reported in Table 4.4. On the other hand, a calculation performed under steady-state conditions, as the one imposed by law for building energy labeling, was then performed to compare the results: according to the last-mentioned methodology, the building energy needs were calculated again by considering a constant internal temperature of 20 °C and the heating system operating 24/7. Results obtained under steady-state conditions show an overall primary energy consumption for space heating equal to 749 366 kWh, corresponding to a value of EP_H equal to 168.6 kWh/m^2. It is evident that the energy demand of the school evaluated in standard conditions is strongly overestimated with respect to the one calculated taking into account the effective operating conditions. This result is typical for applications, such as schools,

characterized by discontinuous operating regimes ([112], [113]) and in these cases the use of standard stationary models can be misleading for the evaluation of the economic feasibility of an energy saving measure.

Furthermore, the analysis of school users thermal comfort during heating season was performed by means of the developed dynamic model. The Predicted Mean Vote (PMV) and the Operative Temperature (T_{op}) were selected to assess the thermal comfort of students. According to EN ISO 7730 [114], the values of PMV T_{op} were calculated as a function of air temperature, humidity and mean radiant temperature of the school classrooms. In order to assess the thermal comfort, the values of other influencing parameters were defined: the air velocity was fixed equal to 0.2 m/s, while school occupants metabolic rate was estimated in 1.2 met (sedentary activity); finally, a typical light clothing (1 clo) for users was assumed.

The assessment of students thermal comfort was performed by considering the first floor of the school as a sample (see Figure 4.28): the bin distribution of T_{op} calculated for three classrooms located at the first floor is reported in the following Figure 4.29. In order to evaluate the influence of orientation (i.e. the climate) on the hygro-thermal conditions which occur within the school, three different classrooms, characterized by similar thermal loads and different orientations were considered: classroom 8, facing South (red columns), classroom 2 facing East (yellow columns) and classroom 16 facing West (blue columns).

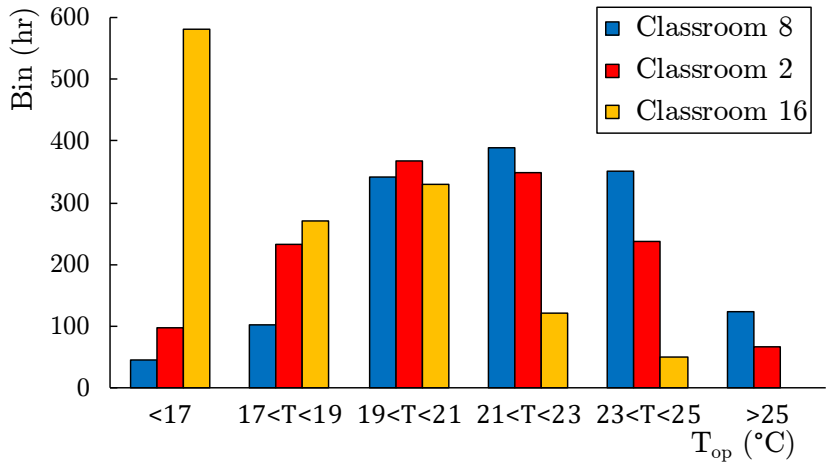

Figure 4.29. Bin distribution of T_{op} for the selected classrooms of Istituto G. Marconi.

It is evident from Figure 4.29 that the distribution of T_{op} has different trends among the considered classrooms. The values of T_{op} calculated for South and East

classrooms (i.e. classrooms 8 and 2, respectively) falls more frequently within the range 19-25 °C; on the other hand, classroom 16 (facing west) is characterized by a larger thermal discomfort: result points out that the operative temperature falls below 17 °C for about 40% of the room occupancy period during the heating season. This result can be explained by the lower value of solar gains entering in classroom 16: the highest incident solar irradiation is reached in the afternoon, while lessons end at 16 and the free solar gains are not exploited.

Such a discomfort condition is mainly due to the heating system control strategy. In fact, the control system consists of a climatic compensation coupled to a programmable thermostat; therefore, the indoor conditions are not monitored and the heating system follows the operating schedule reported in Table 4.4. During idle night hours the air temperature within classrooms strongly decreases because of the poor quality of the building envelope; for this reason, a strong thermal discomfort, confirmed by an interview conducted with school users during the building inspection, is observed during the morning, due to low values of the operative temperature.

In order to enhance the energy performance of the building and to improve the indoor thermal comfort conditions, the refurbishment of the building heating system was evaluated by means of the developed dynamic model. In particular, the main goal of the proposed retrofit measure is to evaluate if the adoption of a low-temperature heating system would introduce significant benefits for the users in terms of indoor thermal comfort.

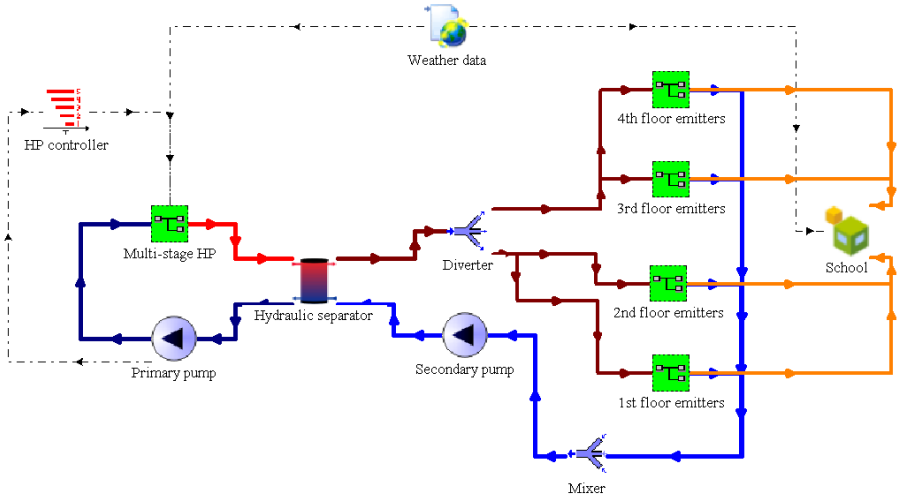

Figure 4.30. Dynamic model of Istituto G. Marconi after the heating system refurbishment.

Specifically, a multi-compressor air-to-water heat pump was considered in place of actual condensing boilers. Furthermore, according to the renovation of heat generators, the high-temperature radiators which actually represents the emitters of the system were replaced with low-temperature aluminum radiators. Finally, the heating system control strategy was improved by taking into account a new climatic compensation logic. The layout of the developed dynamic model is shown in Figure 4.30: the main components of the school model, as the multi-stage heat pump, the hydraulic separator, the circulating pumps and the emitters are reported.

The multi-stage heat pump selected for the heating system renovation is a four-compressors model (N = 4, see Section 2.2.2); the heat pump rated performance in heating mode at full load are the following: thermal capacity and *COP* equal to 311.1 kW and 3.57, respectively (rated conditions: outdoor air temperature = 7°C and supply water temperature = 45°C). In Table 4.5 the values of heat pump thermal capacity and *COP* given by the manufacturer for several values of outdoor air temperature (i.e. -7°C, 2°C, 7°C, 12°C), by scaling from four to one working compressors are shown; reported data are evaluated for a temperature of supplied hot water fixed to 45°C. It is evident from Table 4.5 that the heat pump operates with the best efficiency when only two compressors are switched on (i.e. 2/4 data series).

Table 4.5. $P_{HP,h}$ and *COP* of the heat pump selected for the heating system refurbishment of Istituto G. Marconi as a function of T_{ext} and the number of working compressors.

n/N	1/4		2/4		3/4		4/4	
T_{ext} (°C)	$P_{HP,h}$ (kW)	*COP*	$P_{HP,h}$ (kW)	*COP*	$P_{HP,h}$ (kW)	*COP*	$P_{HP,h}$ (kW)	*COP*
-7	56.4	2.52	112.8	2.72	166.8	2.70	218.1	2.64
2	73.7	3.19	147.3	3.44	209.7	3.28	270.6	3.17
7	84.0	3.59	168.0	3.85	241.2	3.71	311.1	3.57
12	97.5	4.09	195.0	4.39	275.7	4.17	354.6	3.99

The logic of the multi-stage heat pump control system is highlighted in Figure 4.31: the function that selects the number of operating compressors is shown as a function of incoming water temperature $T_{w,in}$. In order to define the number of compressors that the heat pump has to switch on to match the thermal load

required by the building, the control system considers the number of working compressors at the previous timestep and compares the current value of $T_{w,in}$ with four fixed set-points (36°C, 37°C, 38°C and 39°C in in Figure 4.31). Each set-point is characterized by a 1 K centered dead-band that induces a hysteresis logic on the control signal, avoiding continuous fluctuations (see Section 2.3.1 for further details).

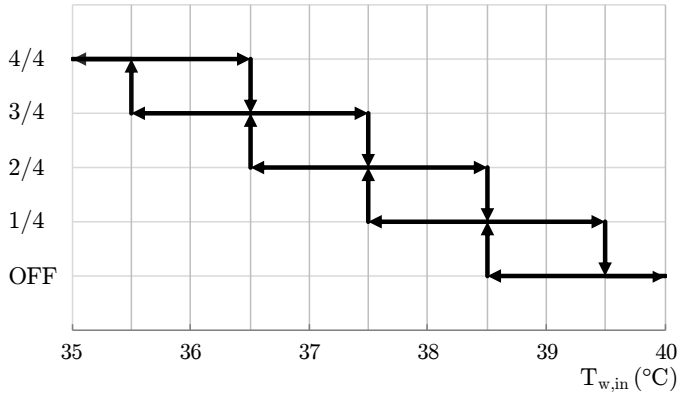

Figure 4.31. Behavior of the control system of the multi-stage heat pump selected for the heating system refurbishment.

An example of the behavior of the heat pump control system is shown in Figure 4.32: heat pump thermal capacity and inlet/outlet water temperatures are reported as a function of simulation time for a typical day of the heating season (5th January). One can note from Figure 4.32 the behavior of the heat pump control system: the average thermal load required by the building within the considered time interval is about 180 kW and the heat pump operates alternately with two and three compressors switched on (2/4 and 3/4 data series, respectively). By focusing within hours 110 and 112 (see Figure 4.32b), a detailed analysis of the controller behavior can be performed: in correspondence of hour 110, the heat pump operates with two active compressors, but the thermal capacity of the unit is lower than the building required load, since incoming water temperature decreases with time. When $T_{w,in}$ drops below 36.5°C in correspondence of hour 111.4, the control system activates a third compressor (see Figure 4.31) and the thermal capacity delivered by the heat pump increases over 200 kW. For this reason, the heating system capacity is now higher than the required thermal load and $T_{w,in}$ rapidly increases: after about 20 minutes it exceeds 37.5°C and the controller switches off the third compressor (see again Figure 4.31).

It is important to highlight that the heat pump operates at full load (i.e. with four active compressors) only at the beginning of the considered interval (i.e. the morning of the 5th January), for about one hour. During night in fact, the heat pump is switched off according to the heating system operating schedule and the temperature of the heating system loop strongly decreases: for this reason, in the morning heat pump maximum thermal capacity is required and the unit works at full load.

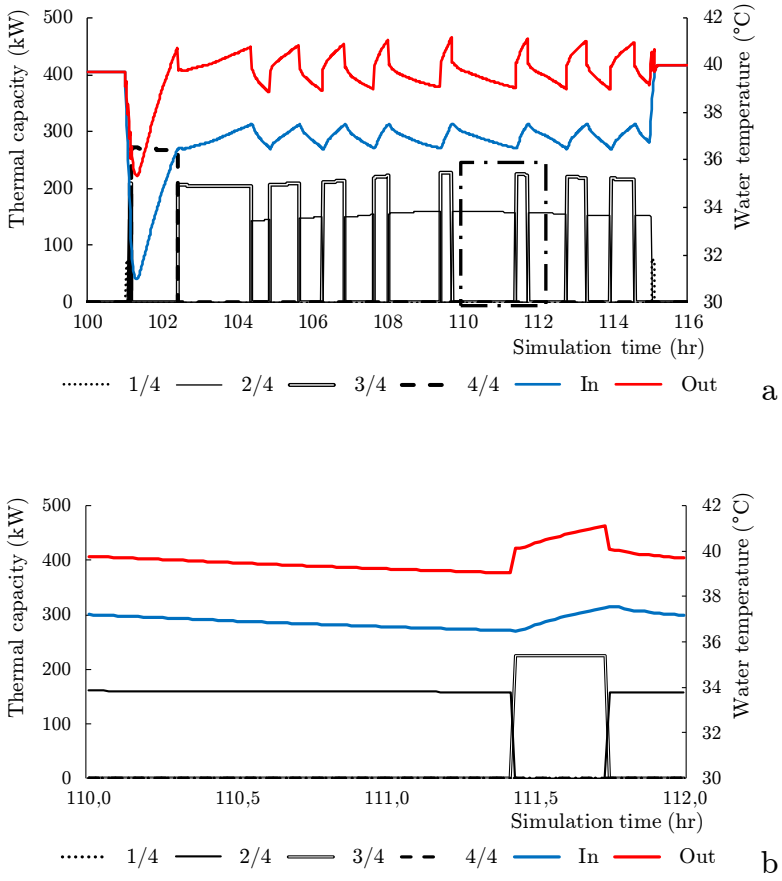

Figure 4.32. Heat pump thermal capacity and inlet/outlet water temperatures during a typical day of the heating season.

Once implemented in the dynamic model of Istituto G. Marconi the changes linked to the heating system refurbishment described previously, the energy performance of the renewed system has been evaluated. Results point out that the EP_h index decreases up to 43.6 kWh/m² after the retrofit of the heating system, a value which corresponds to a reduction of about 46% in the overall primary energy required by the school for space heating. This result highlights

the importance of heating system renovation in existing buildings. The selected multi-stage heat pump is characterized by a seasonal performance factor $SCOP_{on}$ (in this case equal to $SCOP_{net}$ due to the absence of any back-up system, see Section 3.3.5), equal to 3.94.

Finally, the influence of heating system renovation on thermal comfort conditions occurring during winter within school classrooms has been assessed. Main results are summarized in Figure 4.33 and Table 4.6.

Figure 4.33 reports the bin distribution of the values of T_{op} within the sample classrooms located at the first floor of the school (classrooms 8, 2 and 16), evaluated after the heating system refurbishment (i.e. HP data series), and compares this distribution to the T_{op} distribution before the retrofit (i.e. Boiler data series). This comparison highlights that the renovation of the heating system has no positive effects on indoor thermal comfort. Furthermore, classroom 16, characterized by West orientation, presents a slight improvement in indoor comfort conditions: the values of operative temperature are slightly shifted towards higher values. On the contrary, south and east oriented classrooms (i.e. classrooms 8 and 2, respectively), are characterized by worse comfort conditions: the values of T_{op} within these classrooms follow a flat trend and an acceptable level of thermal comfort is ensured for only 20% of the heating season. Moreover, the further discomfort condition caused by large values of operative temperature becomes relevant for classrooms 2 and 8.

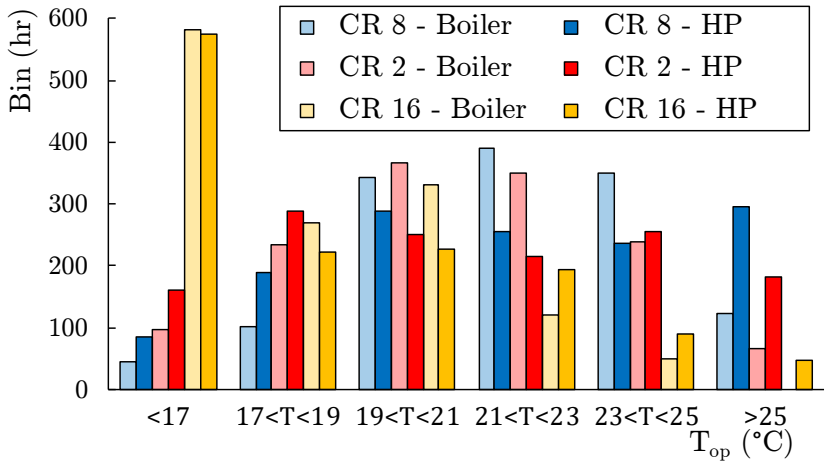

Figure 4.33. Comparison between the bin distributions of T_{op} before and after the heating system refurbishment.

The control strategy of the renovated heating system is the main cause for the worsening of indoor comfort conditions. The control logic of the existing heating system affects the supply water temperature according to a climatic compensation; for this reason, the impact of control strategy on energy consumption and thermal comfort is stronger during intermediate seasons, when external climate is milder and the required load is lower. In fact, when outdoor temperature increases, supply water temperature decreases by following a linear correlation. On the contrary, the multi-stage heat pump control system affects the number of active compressors: when the building thermal load decreases, the heat pump delivered thermal capacity becomes lower but the supply water temperature only slightly decreases; for this reason, in the milder part of heating season classrooms overheating occurs.

Values reported in Table 4.6 confirm the negative impact of heating system refurbishment on indoor thermal comfort. The bin distribution of PMV hourly values among the three considered classrooms highlight that before heating system retrofit, indoor thermal comfort is ensured (i.e. $-0.5 < PMV < 0.5$) for about 60%, 45% and 12% of the length of the heating season for classrooms 8, 2 and 16, respectively.

Table 4.6. Bin distribution of hourly PMV values before and after heating system refurbishment.

	Before heating system refurbishment			After heating system refurbishment		
Classroom	8 (S)	2 (E)	16 (W)	8 (S)	2 (E)	16 (W)
$PMV<-1$	118	254	800	231	191	764
$-1<PMV<-0.5$	346	447	386	329	510	261
$-0.5<PMV>0.5$	817	607	166	582	528	290
$0.5>PMV>1$	71	44	0	158	73	37
$PMV>1$	0	0	0	52	50	0
Total (hr)	1 352	1 352	1 352	1 352	1 352	1 352

The impact of heating system retrofit is relevant, since a strong reduction of thermal comfort can be pointed out: PMV values within (-0.5; 0.5) range were evaluated for 43%, 39% and 21% of the heating season duration. Furthermore, one can observe that overheating becomes significant for classrooms facing South and East (rooms number 8 and 2, respectively).

The performed simulations allow to conclude that a low-temperature heating system based on a multi-stage heat pump is not a suitable solution to improve the indoor thermal comfort, as highlighted by the worse distribution of T_{op} and PMV reported in Figure 4.33 and Table 4.6.

4.5.2. Optimization of the control strategy of a heat pump system coupled to a residential building

The models developed in this Thesis have been used in this case study to evaluate the influence of the heat pump modulation capacity on the seasonal performance of a heating system coupled to a residential building. In addition, the optimization of the heat pump control strategy has been carried out in order to reduce the number of on-off cycles performed by the unit during the heating season. More in detail, the dynamic models presented in Sections 4.4.1, 4.4.2 and 4.4.3 for a single-stage heat pump (On-off HP), a multi-stage heat pump (MSHP) and an inverter-driven heat pump (IDHP), respectively, have been used to assess the energy performance of three devices characterized by the same size coupled to the same building.

The residential building considered in this case study is a single-family house, built in the 1990s, located in Bolzano (46.16°N, 12.15°E, North of Italy), and composed by a single floor. The dynamic model of the building was implemented by means of the plugin TRNBuild (Section 4.2.4); as pointed by Figure 4.34, eight thermal zones have been considered in the model: the single-family house is composed by three bedrooms (R1, R2 and R3), two bathrooms (B1 and B2), a corridor (C), a kitchen (K) and a living room (LR).

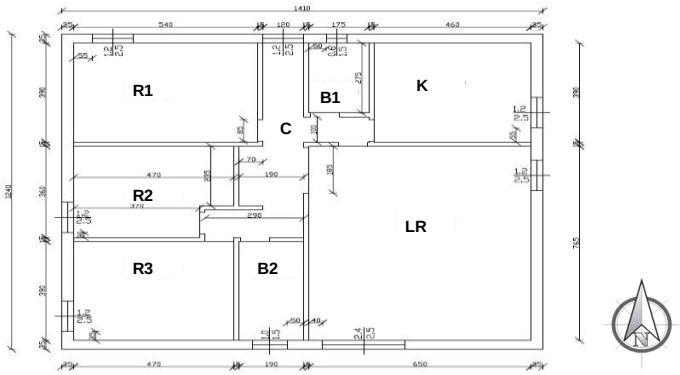

Figure 4.34. Layout of the residential building and indication of simulated thermal zones.

The main geometrical and thermo-physical data concerning the considered building are reported in Table 4.7: the house is characterized by a net floor area and a gross heated volume equal to 162 m^2 and 560 m^3, respectively. As highlighted in Table 4.7 by the U-values of the main components of the building envelope, the thermal insulation of the opaque and transparent structures is typical of its construction period.

Table 4.7. Geometrical and thermo-physical data of the residential building.

Net floor area (m^2)	Gross volume (m^3)	S/V (m^{-1})	External wall U-value (W/m^2K)	Floor U-value (W/m^2K)	Ceiling U-value (W/m^2K)	Windows U-value (W/m^2K)	Ventilation rate (hr^{-1})
162	560	0.93	0.45	0.93	0.56	2.83	0.3

In the following step of the analysis, the thermal load required by the building during the heating season and the total energy demand for space heating have been evaluated by means of TRNSYS, according to a standard procedure: the internal temperature set-point was fixed equal to 20°C and the heating system was considered active 24/7. Furthermore, this calculation was performed by using the hourly climatic data included in the Typical Reference Year (TRY) of Bolzano, included in TRNSYS weather data file and obtained from the Meteonorm datafile [80]. In Figure 4.35a, the hourly building thermal load evaluated by means of TRNSYS is reported as a function of the hourly external air temperature T_{ext}; furthermore, the Building Energy Signature (BES) is highlighted.

According to the climatic data, the external design air temperature $T_{des,h}$ is equal to -9°C, corresponding to a building design peak load $P_{des,h}$ equal to 11.1 kW. Since Bolzano is characterized by 2 791 heating Degree Days (DD_h), current Italian Law [109] includes this location in the climatic zone E and its standard heating season ranges from 15th October to 15th April (183 days): the annual thermal energy demand of the building, evaluated for the above-mentioned heating period and taking into account standard input data (i.e. constant internal air temperature and heating system always active), is equal to 26 312 kWh. In Figure 4.35b the bin distribution of Bolzano and the building energy demand within the heating season are reported.

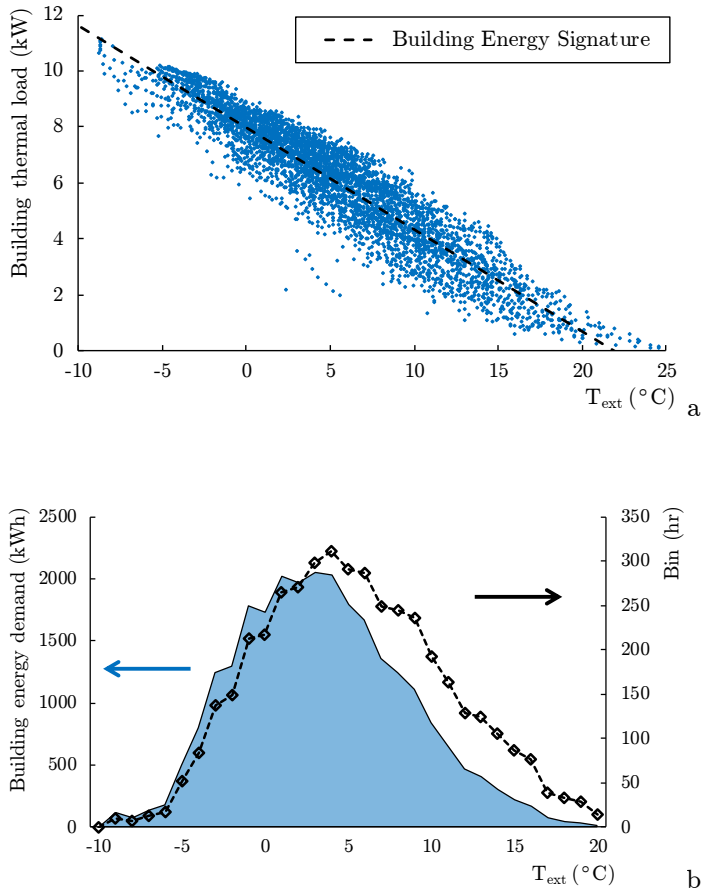

Figure 4.35. Hourly building thermal load with the highlighting of the BES (a), building energy demand and bin distribution as a function of T_{ext} (b).

The HVAC system coupled to the residential building considered in this case study is based on electric air-to-water heat pumps, sized on the building design load; for this reason, no back-up systems have been considered. In order to evaluate the influence of thermal capacity modulation on the seasonal performance of the system, three different units characterized by the same size have been selected (namely an On-off HP, a MSHP and a IDHP). The complete performance data of the simulated units, given by the manufacturer at full load and at partial load, are reported in Figure 4.36, Figure 4.37 and Figure 4.38 for On-off HP, MSHP and IDHP, respectively.

The selected IDHP uses a brushless DC scroll compressor and the inverter can vary the compressor rotating frequency between the range 30-120 Hz. Thermal capacity and *COP* of the variable-speed unit are reported in Figure 4.38a and Figure 4.38b, respectively.

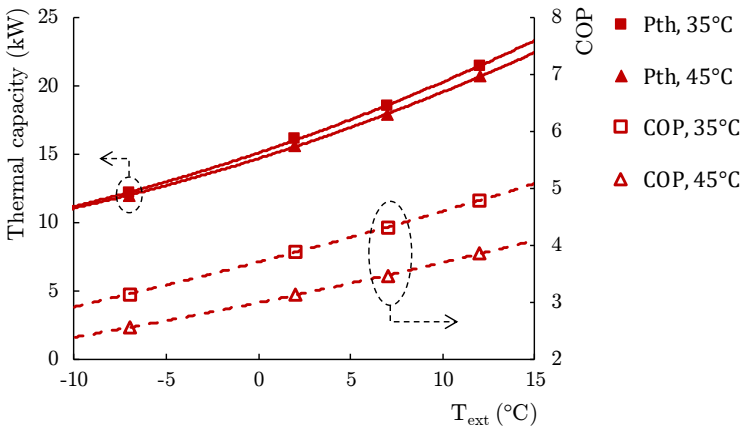

Figure 4.36. On-off heat pump thermal capacity and *COP* as a function of T_{ext} and $T_{w,out}$.

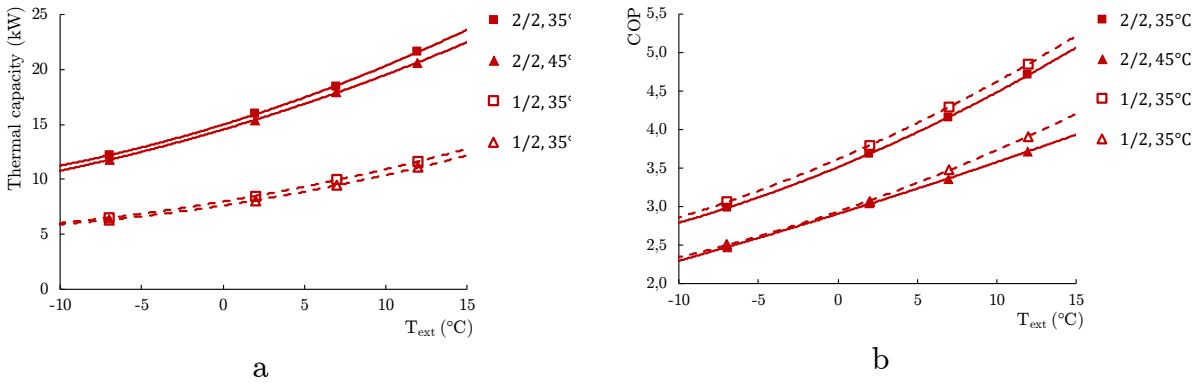

Figure 4.37. MSHP thermal capacity (a) and *COP* (b) as a function of T_{ext}, $T_{w,out}$ and number of compressors switched on.

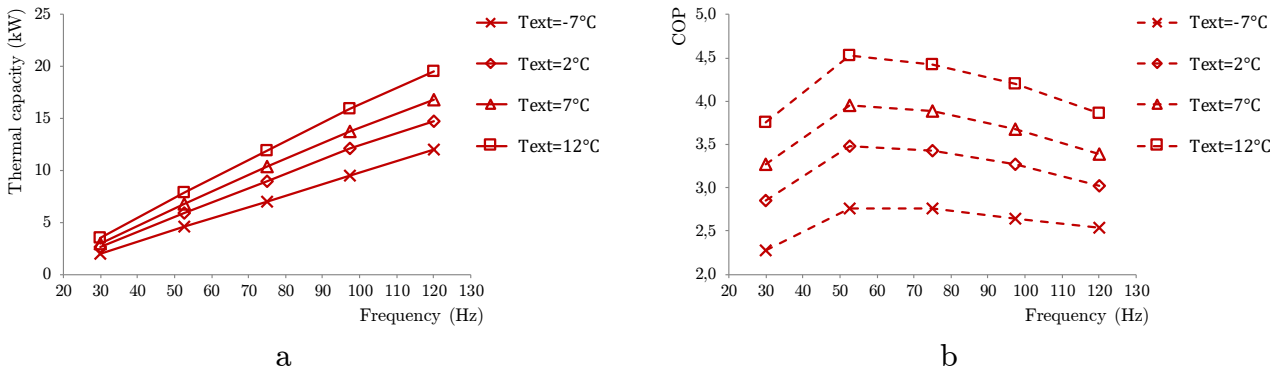

Figure 4.38. IDHP thermal capacity (a) and *COP* (b) as a function of T_{ext}, $T_{w,out}$ and inverter frequency.

Figure 4.38a shows that the heat pump thermal capacity is proportional to the inverter frequency in the whole range of external air temperature values. On the other hand, the maximum efficiency of the heat pump is obtained for a frequency which ranges from 40 Hz to 60 Hz: therefore, the *COP* increases up to 20% by scaling from the nominal frequency (120 Hz) to an intermediate frequency (50 Hz).

Figure 4.39 depicts both the BES representing the building thermal load (blue dashed line) and the thermal capacity of the considered heat pumps at full and at partial load.

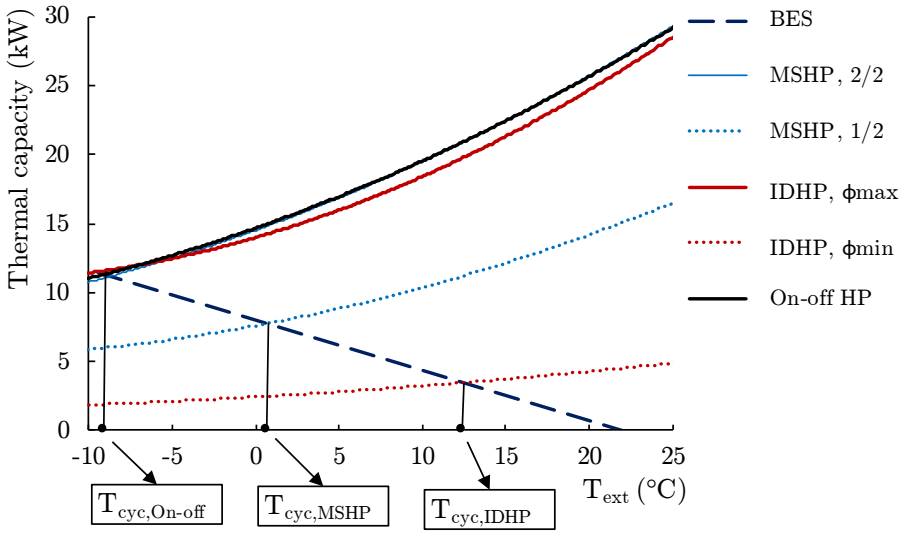

Figure 4.39. BES, thermal capacity at full load and at partial load of the considered heat pumps as a function of T_{ext}.

It is evident from Figure 4.39 that the selected units are characterized by the same size and are able to overrate the thermal load required by the building for the whole heating season: the bivalent temperature ($T_{biv,h}$) is close to -9°C (i.e. the design external temperature of Bolzano) for all the simulated devices. As highlighted in the previous part of this Thesis, for values of the external air temperature higher than the bivalent temperature, the heat pump thermal capacity exceeds the building required load and a modulating or an on-off control strategy is needed. One can see from Figure 4.39 that the single-stage unit performs on-off cycles during the whole heating season to match the building energy demand: due to the lack of any form of thermal capacity modulation, the external temperature in correspondence of which the on-off cycling starts for this kind of heat pump ($T_{cyc,h}$) is equal to the bivalent temperature (i.e. -9°C). On the

other hand, the multi-stage heat pump selected for this analysis is composed by two compressors (N = 2); for this reason, this unit is able to switch off one compressor when the thermal load is reduced. In Figure 4.39 the blue dotted line reports the MSHP thermal capacity with one working compressor; the intersection between this line and the BES fixes $T_{cyc,h}$, which is equal to 1°C. One can conclude that the multi-stage unit avoids on-off cycles, thus the energy cycling losses, for values of the external temperatures ranging between -9°C and 1°C.

Finally, the thermal capacity delivered by the IDHP at the minimum inverter frequency is shown in Figure 4.39 (red dotted line). The variable-speed unit is able to reduce its delivered thermal capacity up to 75% of the full load thermal capacity; for this reason, due to its enhanced modulation capability with respect to the other heat pumps, the inverter-driven unit performs on-off cycles only for values of T_{ext} larger than 12.5°C ($T_{cyc,h}$).

Figure 4.40a shows the logic of the control system adopted by the On-off HP. In order to avoid large variations of the supply water temperature $T_{w.out}$ to the terminal units, the heat pump works according to a 5 K dead band around the selected set-point for the return water temperature, $T_{SP,h}$ defined in this case equal to 40°C.

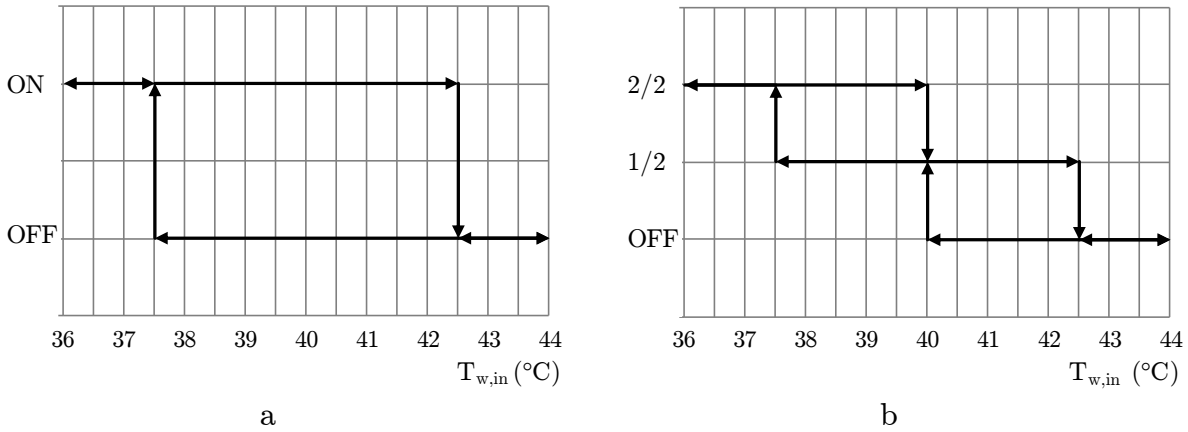

Figure 4.40. Behavior of the control system of single-stage (a) and multi-stage (b) heat pumps.

The MSHP control system works following the logic shown in Figure 4.40b. More in detail, the set-point temperature of the return water for the activation of the first compressor ($T_{SP,h,1/2}$) is 41.25°C, while the set-point value for the

activation of the second compressor ($T_{SP,h,2/2}$) is 38.75 °C; both dead bands are wide 2.5 K.

For the selected IDHP, a PID algorithm has been used in order to set the inverter frequency in agreement with the procedure reported in Section 4.4.3. As pointed out in that Section, the variable monitored by the PID controller is the supply water temperature $T_{w.out}$; furthermore, the set-point value of this variable is fixed to 45 °C. When the minimum inverter frequency (30 Hz) is reached and no further thermal capacity modulation is possible, on-off cycles are performed to match the building energy demand. The setting of the PID parameters has been assessed according to the manufacturer data: the values of the proportional gain K_p, the integral time T_i and the derivative time T_d have been set equal to 10, 300 s and 0 s, respectively (pure PI logic).

Then, the values of parameters needed by the developed model to take into account the cycling losses (see Section 4.4.4) have been defined. All the considered heat pumps are characterized by a thermostatic expansion valve (TEV): according to the experimental data given by the heat pump manufacturer, the length of the transient periods for the absorbed electric power ($t_{pen,el,h}$) and the delivered thermal capacity ($t_{pen,h}$) are equal to 75 s and 150 s, respectively, while the average reduction of these variables ($CF_{el,h}$ and CF_h) is equal to 4% and 42%, respectively. These data are summarized in Table 4.8.

Table 4.8. Cycling losses parameters for the simulated heat pumps.

$t_{pen,el,h}$ (s)	$CF_{el,h}$	$t_{pen,h}$ (s)	CF_h
75	0.96	250	0.58

The building emitters are made up by two-pipe fan-coils, sized according to a design supply temperature equal to 45 °C while the heating plant is characterized by a direct hydraulic loop (DHL) operating with a fixed speed circulating pump: the logical layout of the system is reported in Figure 4.10 (DHL). In order to increase the thermal inertia of the system a 200 l thermal storage tank is placed in the supply line; the tank has been introduced to limit the frequency of the heat pump on-off cycles under 6 switches per hour, which is the maximum number of hourly on-off startups suggested by the heat pumps manufacturer.

Dynamic simulations of the heating system described previously have been performed by adopting a simulation time step equal to 1 minute. The seasonal

energy performance of the three selected heat pumps have been evaluated by comparing the values of $SCOP_{net}$ and $SCOP_{on}$ (see Section 3.3.5 for their formulation).

In Figure 4.41 the daily on-off cycles performed by On-off HP, MSHP and IDHP are represented as a function of the daily average outdoor air temperature (grey, blue and red data series, respectively).

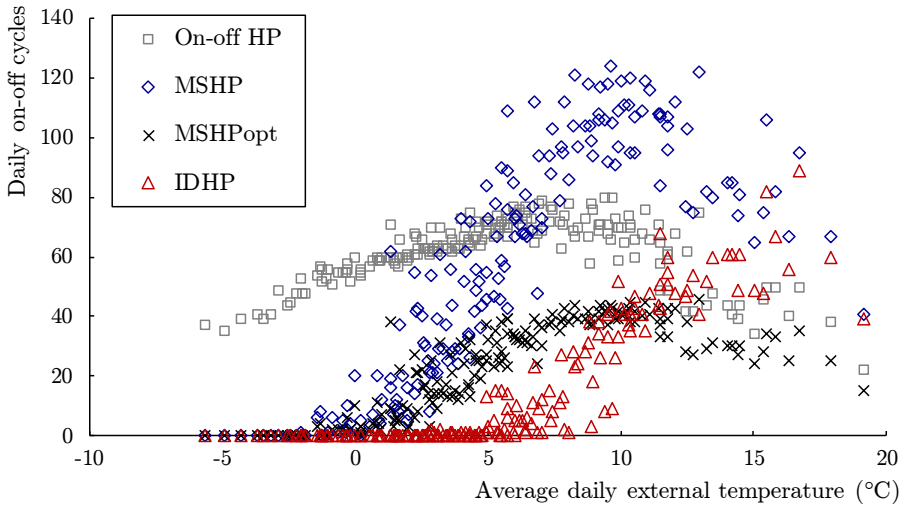

Figure 4.41. Daily on-off cycles of the simulated systems as a function of the daily average external air temperature.

By considering the trend of daily on-off cycles performed by the single-stage unit (grey data series) it is evident that, as expected, this kind of heat pump performs on-off cycles during the whole heating season. The on-off cycles trend presents a maximum of about 80 cycles/day for values of the daily average external temperature ranging from 0°C to 10°C; in correspondence of values of T_{ext} out of this range the daily on-off cycles drop to 40 cycles/day. When the external air temperature is lower, the building thermal load is higher and the average duration of the single on-off cycle increases because the on periods of the cycle increase. On the other hand, when the building thermal load decreases (i.e. for higher external air temperature), the average duration of the single on-off cycle decreases again due to the increased duration of the off period.

The trend of the daily start-ups evaluated for the MSHP presents several differences, if compared to the On-off HP trend. First, for seventeen days during the cold season (9% of the heating period), the MSHP avoids the use of on-off cycles: when the daily average external air temperature drops below -2°C, no on-

off cycles are needed to match the building thermal load. In fact, when the outdoor air temperature ranges between -9°C and -2°C, the MSHP works alternatively with one and two active compressors, preventing any cycling losses. On the contrary. when the external air temperature rises and exceeds $T_{cyc,h}$ (in this case equal to 1°C, see Figure 4.39) the multi-stage unit has to activate the on-off control logic; in this case, the number of daily start-ups increases and it reaches a maximum value of about 120 cycles/day in correspondence of a daily average air temperature equal to 10°C: above this value, the number of daily on-off cycles decreases due to the same reason of the On-off HP (i.e. the increase of the off duration within a cycle).

Results point out that when the MSHP operates outside its modulation range performs a higher number of on-off cycles with respect to the On-off HP: this is linked to the control system logic described in Figure 4.40b; comparing Figure 4.40a with Figure 4.40b it is evident that the multi-stage unit employs dead bands that are the half of the dead band employed by the On-off HP and this is the main reason for which MSHP tends to operate with a higher number of start-ups with respect to the on-off unit.

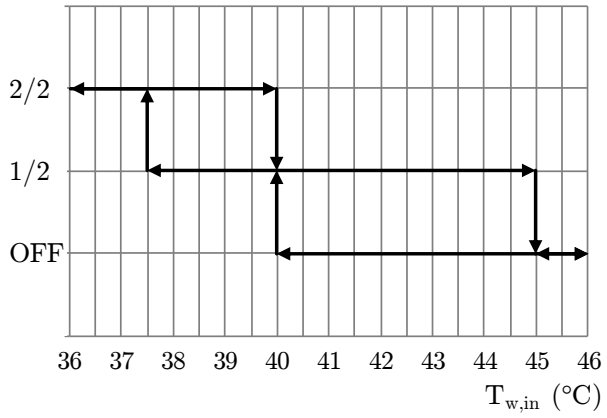

Figure 4.42. Optimized control logic for the multi-stage unit ($MSHP_{opt}$).

This result suggests to adopt a different amplitude of the dead band for MSHP when the outside temperature is higher than $T_{cyc,h}$ in order to reduce the on-off cycles performed by this unit. Figure 4.41 shows that the adoption of the optimized control strategy ($MSHP_{opt}$) reported in Figure 4.42 reduces the number of on-off cycles performed by the MSHP. When the outdoor temperature is lower than $T_{cyc,h}$ the control logic of the unit does not change: the set-points for the activation of the two compressors are the same (i.e. 38.75°C and 41.25°C, see

Figure 4.40b) and the dead bands are both wide 2.5 K. On the contrary, when the external air temperature is higher than $T_{cyc,h}$, the return water temperature set-point for the activation of the first compressor ($T_{SP,h,1/2}$) rises to 42.5 °C, while the relative dead band doubles to 5 K. By observing Figure 4.41 it is possible to conclude that the daily on-off cycles performed by the optimized MSHP are strongly reduced, especially for large values of the outdoor air temperature.

By considering the trend of daily on-off cycles for the IDHP, it is evident by Figure 4.41 that this unit allows to avoid cycling losses for a significant part of the heating season: when the daily average external temperature is lower than 5 °C, no on-off cycles are performed by the heat pump because the unit thermal capacity is reduced by varying the inverter frequency. Thus, on-off cycles do not occur for 82 over 183 days (corresponding to the 45% of the heating season). Moreover, results point out that the maximum number of daily start-ups of the variable-speed heat pump is close to 90 cycles/day; this value is obtained in correspondence to an average daily external temperature of 16 °C.

Table 4.9 reports the seasonal performance of the simulated systems. The different values of $SCOP_{on}$ are essentially due to the control logic of the units: the results shown in Table 4.9 point out that the On-off HP is characterized by the lowest value of $SCOP_{on}$ and by the highest number of on-off cycles during the heating season. The energy saving of the modulating units (MSHP and IDHP) with respect to the single-stage device goes from 6% for MSHP (8% for $MSHP_{opt}$) up to 18% for IDHP.

Table 4.9. Seasonal performance of the simulated systems as a function of the HP typology.

Heat pump typology	$E_{HP,h}$ (kWh)	$E_{HP,h,el}$ (kWh)	$SCOP_{on}$	Cycles
On-off HP	26 159	9 189	2.76	11 393
MSHP	26 420	8 733	2.93	10 335
$MSHP_{opt}$	26 530	8 595	2.99	4 272
IDHP	26 503	7 864	3.25	2 697

More in detail, the number of the heat pump start-ups decreases of about 9% and 76% for MSHP and IDHP respectively if compared with On-off HP: as pointed out by Figure 4.39, the main difference between MSHP and IDHP is due to the larger modulation range in terms of external air temperature which

drastically reduces the need of on-off cycles for IDHP. The obtained results put in evidence that the higher the modulation capability of the heat pump, the higher the seasonal performance factor of the system.

Finally, in Table 4.9 it is possible to compare the performance of the different systems and to verify the impact of different control algorithms applied to the MSHP system. The adoption of the optimized logic ($MSHP_{opt}$) strongly influences the total number of start-ups: during the whole season the amount of on-off cycles decreases up to 60% if compared to the typical MSHP control logic, limiting the compressor mechanical stress and the cycling losses. On the other hand, results point out only a slight increase of the $SCOP_{on}$ (+2%) with respect to the usual MSHP control logic: despite the strong reduction of cycling losses, the use of a wider dead band increases the average return water temperature (42.5 °C versus 41.25 °C) and the heat pump performance is lowered.

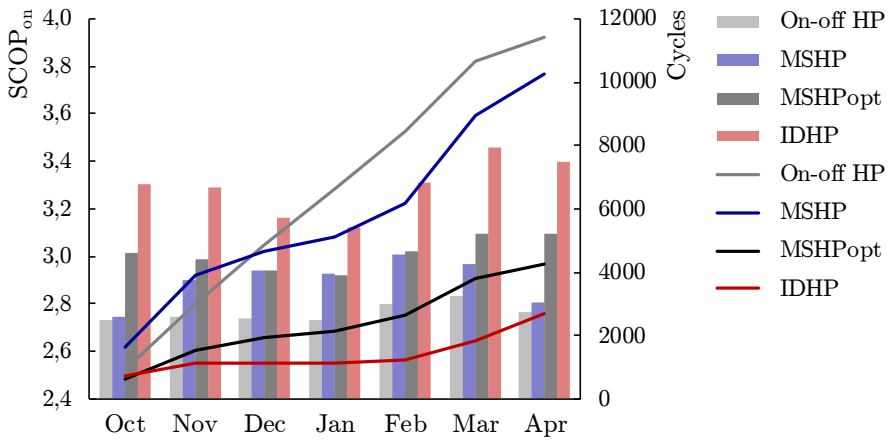

Figure 4.43. Monthly values of $SCOP_{on}$ and cumulative on-off cycles.

Figure 4.43 reports the seasonal profiles of the monthly $SCOP_{on}$ of the simulated systems. It is interesting to observe that the modulating units are characterized by a variable slope of the cumulative on-off profiles. Moreover, Figure 4.43 puts in evidence how the IDHP is able to avoid the on-off cycles during the central months of the heating season (from November to February) while the MCHP only reduces the number of on-off cycles in the colder part of the season. Since the efficiency of the IDHP is only slightly affected by the number of heat pump start-ups, the energy performance of the system mainly depends on the outdoor conditions: the monthly values of $SCOP_{on}$ are lower during the colder period of the season and higher in correspondence of the milder months. Finally,

it is interesting to observe in Figure 4.43 that the slope of the cumulative number of on-off cycle for the On-off HP is constant along the heating season: this is due to the fact that the single-stage unit operates at full capacity throughout the cold season, performing on-off cycles with a similar frequency, as confirmed by Figure 4.41.

One can conclude that the number of on-off cycles performed by a heat pump during the heating season is a significant value (linked also to the operative life of the heat pump) which is strictly correlated to the seasonal performance factor of the system, especially for heat pumps sized on the maximum building thermal load. Results point out that the optimization of the heat pump control logic would achieve a significant decrease of the seasonal on-off cycles carried out by the unit: as an example, the variation of the set-point and the dead band values setted by the heat pump controller as a function of the external climatic conditions allows to reduce the number of cycles up to 60%.

4.5.3. Assessment of the optimal thermal storage size of a heating system based on an air-to-water heat pump

The main aim of this last case study is to put in evidence the influence of the hydraulic distribution subsystem and of the thermal storage volume on the seasonal performance of a heating system based on an air-to-water heat pump. Several simulations are carried out taking into account different heat pump typologies (namely single-stage and multi-stage units) and different hydraulic loops: primary loop only (direct configuration) and primary/secondary loop (indirect configuration). Finally, the energy losses due to heat pump on-off cycling are evaluated.

More in detail, the dynamic behavior of a heating system composed by an air-to-water heat pump coupled to a residential building located in Bologna (Italy) is simulated. The building investigated in this last case study is a detached single-family house composed by four rooms: kitchen (K), living room (LR), bedroom (B) and bathroom (BR); furthermore, above the mentioned thermal zones an unheated attic, covered by a pitched roof, is present. The plan of the building and a view of the corresponding 3D model developed within Google SketchUp environment are reported in Figure 4.44.

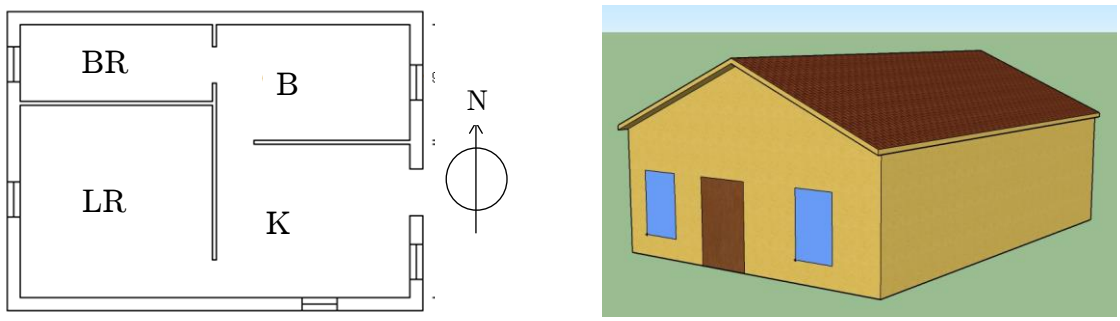

Figure 4.44. Plan of the building (left) and 3D model developed by means of Google SketchUp (right).

The residential building considered in this analysis is characterized by a net floor area of 70 m² and a gross heated volume of sbout 304 m³. The U-values of the main elements of the building envelope are reported in the following Table 4.10: it is evident from the reported data that the simulated single-family house has a poor-quality envelope, since no thermal insulation is present within its components.

Table 4.10. U-values of the building envelope components.

External wall U-value (W/m²K)	Floor U-value (W/m²K)	Ceiling U-value (W/m²K)	Internal wall U-value (W/m²K)	Windows U-value (W/m²K)
1.38	1.51	1.08	2.55	2.82

The dynamic model of the described building is developed by means of the software TRNSYS. Furthermore, the plugin TRNBuild (see Section 4.2.4) is employed to simulate the building thermal zones and define the thermal characteristics of the envelope: in this study five zones are considered, the first four for the building rooms and the last one for the attic. According to the standard methodology applied for the previous case study (i.e. internal air temperature equal to 20 °C, heating system active 24/7, standard heating season), the thermal load required by the building and the net energy demand for space heating are calculated. Similarly to Castelfranco Emilia and Bolzano (i.e. the locations of the cases studied in Sections 4.5.1 and 4.5.2, respectively), the city of Bologna is included in climatic zone E by current Italian Law [109] since it is characterized by 2 259 DD_h and, again, the standard heating season ranges from 15th October to 15th April. Results obtained from the plugin TRNBuild point out

that the building design peak load $P_{des,h}$ is equal to 7.9 kW, in correspondence of the external design temperature $T_{des,h}$ (which is equal to -7°C in this case). Finally, the seasonal thermal energy need of the building is calculated by TRNBuild and is equal to 20 435 kWh/year.

The terminal units used in the building are composed by four 2-pipe fan coils, one for each room, sized on the design peak load according to a design supply temperature equal to 45°C.

Several simulations are carried out by varying the generating system (i.e. the heat pump typology) and the configuration of the hydraulic loop: the considered cases are reported in Table 4.11. More in detail, the dynamic model of four different typologies of heating system are implemented with TRNSYS: cases A and B refer to a direct hydraulic loop (DHL) system, coupled with a single-stage heat pump (On-off HP) and a multi-stage heat pump (MSHP), respectively, while cases C and D refer to a MSHP coupled with an indirect hydraulic loop (IHL) distribution system characterized by fixed and variable flow rate in the secondary loop, respectively.

Table 4.11. Description of the heating systems developed within TRNSYS.

Case	HP typology	Hydraulic loop configuration	Thermal storage position	Variable/Fixed flow rate
A0	On-off HP	DHL	No storage	Fixed
A1	On-off HP	DHL	Supply line	Fixed
A2	On-off HP	DHL	Return line	Fixed
B0	MSHP	DHL	No storage	Fixed
B1	MSHP	DHL	Supply line	Fixed
B2	MSHP	DHL	Return line	Fixed
C	MSHP	IHL	/	Fixed
D	MSHP	IHL	/	Variable

In order to evaluate the influence of the heat pump modulation capacity two different units characterized by the same size have been selected. In particular, the dynamic models of an On-off HP and a MSHP composed by three compressors (N = 3) have been implemented: their performance data (i.e. thermal capacity and *COP*) given by the manufacturer for several values of the external air temperature are shown in Table 4.12. As pointed out by the reported data, the

considered heat pumps are characterized by the same performance at full load (i.e. 1/1 data series for the single-stage unit and 3/3 data series for the multi-stage unit) and are able to completely match the heating load required by the building: in fact, their delivered thermal capacity in correspondence of the external design temperature (i.e. -7°C) is larger than the building peak load and no back-up system is needed.

Table 4.12. $P_{HP,h}$ and COP of the selected heat pumps as a function of T_{ext} and of the working compressors (data evaluated for $T_{w,in}/T_{w,out} = 40/45$°C).

HP typology	On-off HP		MSHP					
n/N	1/1		3/3		2/3		1/3	
T_{ext} (°C)	$P_{HP,h}$ (kW)	COP	$P_{HP,h}$ (kW)	COP	$P_{HP,h}$ (kW)	COP	$P_{HP,h}$ (kW)	COP
-7	8.2	2.48	8.2	2.48	5.6	2.43	2.9	2.23
2	10.2	3.04	10.2	3.04	7.1	3.07	3.7	2.79
7	11.5	3.41	11.5	3.41	8.0	3.39	4.2	3.16
12	13.2	3.86	13.2	3.86	9.1	3.82	4.8	3.60

As highlighted in Section 4.3.1, the heat pump control system uses the return water temperature ($T_{w,in}$) as monitoring variable: more in detail, the controllers of both units are based on an on-off control logic, characterized by a hysteresis cycle (see Section 2.3.1 for further details).

The return water temperature set-point ($T_{SP,h}$) for the single-stage heat pump is equal to 40°C and the corresponding dead band DB_h is equal to 3 K. On the other hand, three set-point values and three dead bands are needed for the multi-stage unit control system (Section 4.4.2): the set-point temperatures for the activation of the first ($T_{SP,h,1/3}$), the second ($T_{SP,h,2/3}$) and the third ($T_{SP,h,3/3}$) compressor are equal to 41°C, 40°C and 39°C, respectively. Finally, the dead band related to each stage activation is the same and is 1 K broad.

The energy losses linked to on-off cycles are taken into account in the evaluation of the seasonal performance factor of the system (see Section 4.4.4 for details). The experimental data obtained by the heat pump manufacturer point out that the transient periods for the absorbed electric power ($t_{pen,el,h}$) and the delivered thermal capacity ($t_{pen,h}$) are equal to 75 s and 250 s, respectively, while

the average reduction of the absorbed electric energy and the supplied thermal energy during each start-up ($CF_{el,h}$ and CF_h) is equal to 4% and 31%, respectively.

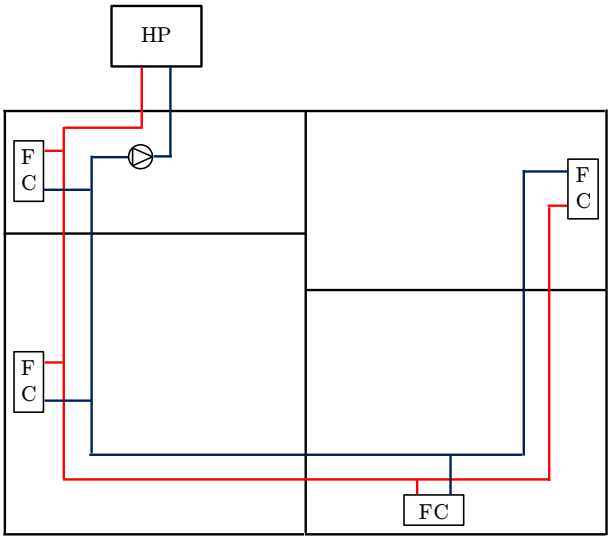

Figure 4.45. Layout of the heating system configuration A0.

A first series of simulations were run by considering a DHL configuration and by varying the heat pump typology, the position and the volume of the thermal storage (cases A and B). In Figure 4.45 the logical layout of the heating system configuration A0 (i.e. On-off HP, DHL configuration, no thermal storage) is reported. It is important to highlight that in cases A0 and B0, characterized by the absence of an additional storage tank, the thermal inertia of the system is only given by the water stored in the distribution pipes, which is equal to 47 liters. Finally, the rated electric power of the circulating pump is 63 W.

Table 4.13. Thermal storage volumes considered in the simulations.

Thermal storage volume (l)	0	10	20	30	60	120	480
Water volume / rated capacity ratio (l/kW)	4.1	5.0	5.8	6.7	9.3	14.5	45.8

As previously reported in this Section, different sizes of the thermal storage tank have been considered in this first series of simulations, in order to evaluate the influence of the thermal inertia on the seasonal performance of the system. In Table 4.13 the values of the considered tank volumes and of the ratio between

the total water volume and the rated thermal capacity of the heat pump (i.e. evaluated for T_{ext} and $T_{w,out}$ of 7°C and 45°C, respectively) are reported.

In Figure 4.46 the number of on-off cycles performed by the On-off HP during the year is represented as a function of the volume and the position of the thermal storage.

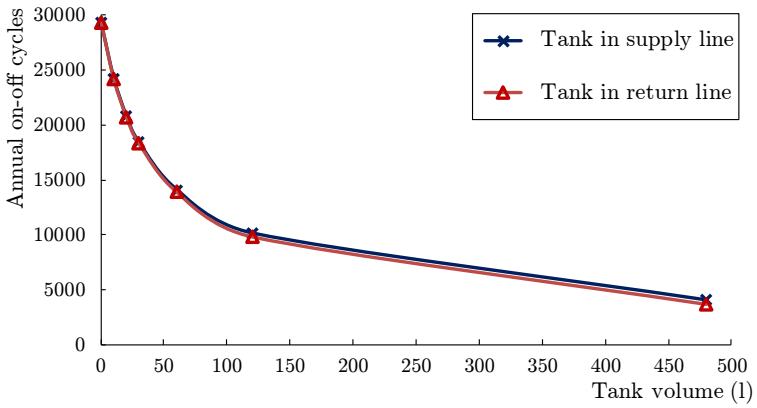

Figure 4.46. Annual on-off cycles as a function of volume and position of the thermal storage (heating system A).

By observing Figure 4.46 it is evident that more the thermal storage volume increases, more the total number of on-off cycles decreases. In fact, in a heating system characterized by a larger thermal inertia the frequency of temperature oscillations is slower and the number of heat pump on-off cycles is lower. The amplitude of the temperature variations are also reduced. The position of the thermal storage only slightly influences the heat pump on-off cycles: the placement of the tank in the return line allows to reduce the number of cycles, with respect to a placement in the supply line, but the difference is negligible (about 7% for the 480 liters tank). Results point out that the optimal value of the thermal storage volume for cases A ranges from 30 to 60 l, which correspond to 6.7 - 9.3 l/kW. In fact, according to the obtained results, the number of hourly on-off cycles does not exceed 6 cycles/hr, which is the maximum value allowed by the compressor to avoid an excessive mechanical stress.

Then, the same simulations are carried out by considering the heating system configuration B, characterized by the same hydraulic loop of the configuration A (i.e. direct hydraulic loop) but with a multi-stage heat pump. Due to the enhanced modulation capability of the MSHP the number of on-off cycles performed by the unit strongly decreases up to 60%, if compared to heating configuration A for all

considered storage volumes. For this reason, the optimal value of stored water - rated heating capacity ratio ranges in this case from 4 to 7 l/kW (i.e. tank volume ranging from 0 to 30 l).

Further simulations are performed taking into account an indirect hydraulic loop configuration (cases C and D), by introducing an hydraulic separator between the primary and the secondary loop. The layout of case C is reported in Figure 4.12: in this case, the circulating pumps of primary and secondary loop operate at fixed-speed and they are characterized by a rated electric power absorption of 34 W and 30 W, respectively. In case D (layout reported in Figure 4.13) a thermostatic valve is inserted for each fan-coil and for this reason the secondary loop and the relative circulating pump are characterized by a variable flow rate. The adoption of two separate loops, the first one (primary loop) characterized by constant flow rate and the second one (secondary loop) characterized by variable flow rate, introduces a double benefit: the stability of the heat pump operation is guaranteed and a decrease of pumping energy consumption up to 35% with respect to the baseline case A0 can be observed.

In Figure 4.47 the on-off cycles performed by the heat pump coupled to heating system configurations C and D are shown as a function of the thermal storage volume: in these simulations, the tank size ranges from 30 to 500 l.

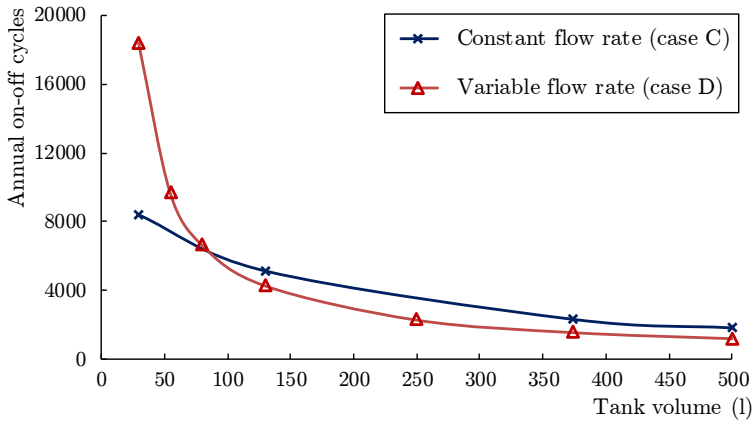

Figure 4.47. Annual on-off cycles as a function of the thermal storage volume (heating system configurations C and D).

Results reported in Figure 4.47 show that the configurations C and D present different trends. More in detail, the profile of on-off cycles performed by the heating system characterized by constant flow rate in the secondary loop (case C) is similar to cases A and B reported in Figure 4.46: the total number of cycles

decreases when the volume of the tank increases. Furthermore, the heating system configurations B and C are characterized by the same behavior: also in this case the number of on-off cycles performed by the MSHP reduces up to 60% with respect to the On-off HP. According to these results, one can conclude that the adoption of an IHL has no effects on the control stability.

On the contrary, it is evident from Figure 4.47 that the trend of on-off cycles evaluated for case D (IHL with variable flow rate in the secondary loop) presents several differences with respect to other configurations. For volumes of the storage lower than 80 -100 l the number of annual start-ups of the heat pump is larger than the corresponding value evaluated for the cases B and C. On the other hand, when the tank volume increases, the number of cycles strongly decreases and a reduction of about 30% with respect to the configuration C can be observed.

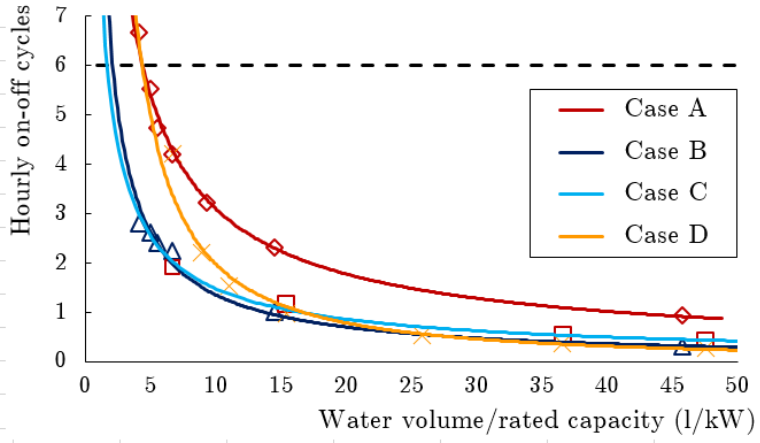

Figure 4.48. Hourly on-off cycles performed by the heat pump as a function of the ratio between water volume and the unit rated capacity.

These results are confirmed by the data reported in Figure 4.48. In this Figure, the number of hourly on-off cycles performed by the heat pump is shown as a function of the ratio between the water volume and the unit rated capacity for each considered heating system configuration. The obtained data point out that the hydronic loop configuration influences the minimum value of the storage tank volume needed to guarantee a hourly number of on-off cycles lower than 6. More in detail, for cases B and C the tank is not necessary, since the thermal inertia given by the distribution pipes is sufficient to limit the compressor start-ups. On the other hand, for cases A and D an additional tank should be placed within the hydronic loop to obtain maximum 6 on-off cycles per hour.

The seasonal energy performance of the simulated heating systems is evaluated as well. In Figure 4.49 the trend of *SCOP* evaluated for the heating system configuration A2 (On-off HP, DHL and thermal storage in the return line) is reported as a function of the tank volume.

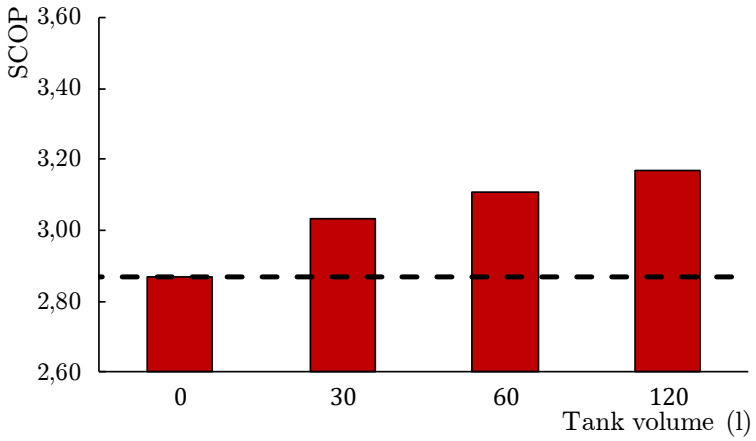

Figure 4.49. *SCOP* values for the heating system A2 as a function of the tank volume.

It is evident that the thermal inertia of the distribution loop strongly influences the seasonal performance factor of the simulated heating systems: more the thermal storage volume increases, more the seasonal efficiency of the heating system increases. As an example, the *SCOP* of the heating system A2 coupled to a 120 liters tank is larger of about 11% with respect to the *SCOP* of the configuration A0. The *SCOP* trend reported by Figure 4.49 is the opposite of the annual on-off cycles reported in Figure 4.46: as pointed out in Section 4.4.4, the heat pump cycling is linked to energy losses and the reduction of the unit start-ups increases the energy performance of the system.

Furthermore, in Figure 4.50 the *SCOP* values obtained for the heating system configurations A2, B2, C and D are reported as a function of the thermal storage volume and are compared to the *SCOP* of the case A0, considered as baseline (dashed line).

Figure 4.50 highlights that the adoption of a modulating heat pump guarantees a significant increase of the *SCOP*: according to the enhanced modulation capacity of the MSHP, the seasonal performance of the system increases up to 22% for configurations B, C and D with respect to the baseline case (configuration A0).

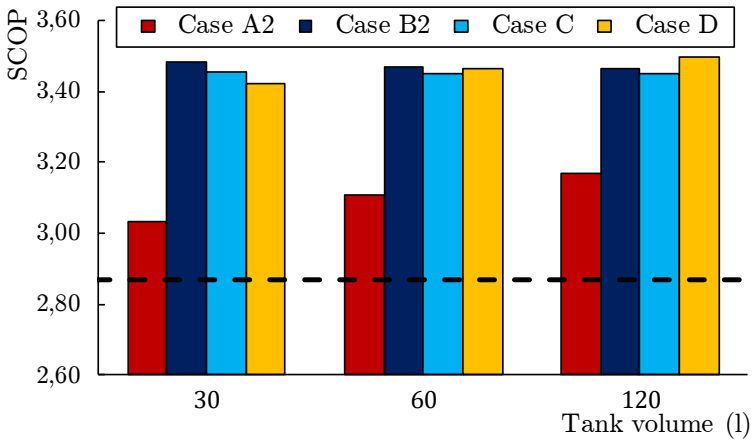

Figure 4.50. *SCOP* values for the considered heating systems as a function of the tank volume.

As pointed out by the on-off cycles trends reported by Figure 4.46 and Figure 4.47, the seasonal efficiency of configurations B and C are similar one another: the values of *SCOP* are slightly influenced by the thermal storage volume. On the contrary, in order to maximize the energy performance of the case D, characterized by variable flow rate in the secondary loop, a larger thermal inertia is needed: the *SCOP* of this heating system configuration is higher than the ones of other configurations for tank volumes larger than 120 l. Furthermore, the control stability (i.e. the hourly number of on-off cycles) is guaranteed for smaller values of the storage tank but in order to obtain an enhanced seasonal energy performance (with respect to case C) the optimal size of the hydraulic separator ranges from 100 to 150 l, corresponding to 13 to 17 l/kW.

One can conclude that the hydraulic configuration of a heat pump system strongly influence its seasonal performance. In fact, the hydronic loop typology, the position and the volume of the storage tank affects the number of on-off cycles performed by the heat pump and consequently its energy performance. More in detail, if the thermal inertia of the system increases a lower number of on-off cycles is carried out by the heat pump for all the considered configurations, according to an enhanced control stability. Furthermore, the placement of the thermal storage in the return line allow to minimize the number of cycles.

In Table 4.14 the optimal values of the ratio between the water volume stored in the system and the heat pump rated thermal capacity are represented as a function of the simulated systems. These values depend on the heat pump typology and the hydraulic configurations; as an example, the use of a modulating heat pump allows to decrease the size of the tank: the optimal ratio for the heating

system B is about 30% lower than the optimal ratio for the configuration A, based on a single-stage heat pump.

Table 4.14. Optimal values of the water volume - rated thermal capacity ratio for the considered configurations.

Heating system configuration	A	B	C	D
Optimal water volume - rated thermal capacity ratio (l/kW)	7 - 9	4 - 7	4 - 7	> 15

The adoption of the indirect hydraulic loop configuration may introduce a slight energy saving but only under particular conditions: first, a reduction of the overall energy consumption can be obtained for a heating system configuration characterized by variable flow rate in the secondary loop but a higher thermal inertia is needed. The stored water - rated thermal capacity ratio has to be higher than 15 l/kW to increase the energy performance of the system.

Finally, an indirect hydraulic configuration based on constant flow rate in the secondary loop does not introduce particular energy savings with respect to a direct hydronic configuration.

Chapter 5

Conclusions and recommendations for future work

5.1. Conclusions

In this Thesis a series of numerical models addressed to evaluate the seasonal performance of reversible air-to-water heat pumps have been developed by using two different approaches:

i. temperature class models (bin method);
ii. dynamic simulation.

The proposed models have been applied to the analysis of the behavior of different kinds of heat pump, coupled to residential and non-residential buildings to provide space heating and cooling with the aim to optimize their seasonal energy performance.

In the first part of this Thesis a series of mathematical models based on the bin method have been described. Unlike the calculation procedure reported by the standard EN 14825, which takes into account only single-stage heat pumps (On-off HPs), the developed codes represent an extension of the standard methodology and can be used to evaluate the performance at partial load and the seasonal performance factors of multi-stage heat pumps (MSHPs) and inverter-driven heat pumps (IDHPs). The mathematical model developed for heating and cooling modes has been used in order to calculate the Annual Performance Factor (*APF*) of reversible air-to-water heat pumps.

A detailed analysis on the influence of the heat pump modulation capacity on the seasonal performance of a heat pump system has been presented. In a first series of simulations, different kinds of heat pumps have been coupled to several buildings located in Bologna (Italy) by showing that the value of *SCOP* is strongly influenced by the heat pump typology and by the size of the unit. Results point out that modulating heat pumps (i.e. MSHPs and IDHPs) allow to achieve

the best seasonal performance factor and, furthermore, that the optimal sizing of the heat pump depends on its modulation capacity. The analysis shows that the highest value of *SCOP* for an IDHP can be obtained by sizing the unit on the basis of the building design load, whereas for On-off HPs the optimal value of the bivalent temperature is larger than the design temperature of the selected location. In addition, if one considers the annual performance of a HVAC system based on a reversible heat pump, the maximum exploitation of the energy saving potential of the heat pump can be achieved only with buildings characterized by balanced heating and cooling design loads. In fact, the adoption of a downsized heat pump for heating operating mode leads to a strongly decrease of the *SCOP*, due to the significant use of the back-up system while, on the contrary, an oversized heat pump is characterized by worse seasonal performance, both on heating and cooling season, because of the increase of on-off cycles.

In the second part of this work a series of dynamic models for the simulation of air-to-water heat pump systems have been developed by means of TRNSYS. The influence of several parameters, such as the heat pump control logic, the thermal inertia of the heating/cooling system and the energy losses linked to on-off cycles, has been deeply investigated.

Since in the standard component library included within TRNSYS only a single-stage heat pump is present, in this Thesis the dynamic models of multi-stage and inverter-driven heat pumps have been implemented starting from the Type 917. In particular, the main aim of this work has been the assessment of innovative control strategies, in order to maximize the heat pump energy performance and its operative life (linked to the number of on-off cycles). The energy losses linked to the heat pump on-off cycles have been introduced in the models in order to evaluate in a detailed way the influence of heat pump modulation capacity on the seasonal performance of the system.

Several simulations have been carried out to analyze the seasonal efficiency of different kinds of heat pump systems and the results show that the number of on-off cycles performed by a heat pump is a significant value strictly correlated to the seasonal performance factor of the system, especially for heat pumps sized on the design building load, and the operative life of the compressor. More in detail, the results point out that the heat pump modulation capacity is a parameter which significantly influences the unit start-ups: the adoption of a variable-speed heat pump allows to reduce the annual amount of on-off cycles up to 76% with respect to a single-stage heat unit. Furthermore, also a multi-stage heat pump would represent a suitable solution to enhance the system performance

factor but in this case an optimized control strategy is needed to fully exploit the heat pump energy saving potential.

In order to maximize the seasonal energy performance of the whole system, the optimization of the only heat pump control logic would get a partial result: for this reason, the influence of several factors as the hydronic loop configuration, the volume and the position of the storage tank on the seasonal performance of the HVAC plant has been assessed. The obtained results point out that the position of the thermal storage tank in the return line of a direct hydraulic loop system is the best solution to reduce the number of on-off cycles; in addition, more the tank volume increases, more the on-off cycles decreases. Nevertheless, an optimal value of the system thermal inertia, depending on the heating system configuration, can be defined: the maximum seasonal performance factor is obtained for a HVAC plant characterized by an indirect hydraulic loop configuration with variable flow rate in the secondary loop and a specific volume of stored water larger than 15 l/kW.

5.2. Recommendations for future work

The work presented in this Thesis has evidenced a series of promising directions for future applied researches in this domain. First, it is important to improve the analysis linked to the behavior of the heat pump during defrost cycles. The effect of defrost on the energy performance of heat pumps operating in heating mode must be better understood and translated in a more accurate numerical model. To do this, a series of experimental campaigns are currently in progress with the collaboration of the heat pump manufacturer. More in general, an experimental validation of the developed models is planned by installing a Hardware-in-the-Loop (HiL) setup in the laboratory of our Department for dynamic tests on heat pumps: the comparison of the results obtained by means of the models with the experimental results derived from a measuring campaign using the HiL system will be important in order to have a definitive benchmark of the models presented in this Thesis.

Regarding the TRNSYS models for the simulation of air-to-water heat pump systems, further improvements are planned to take into account the building energy demand for domestic hot water (DHW) production: a hydronic loop dedicated to the DHW production will be introduced and further investigations will be performed on the optimal control of this combi system. Moreover, it is

also important to study bivalent hybrid systems, namely heating plants in which the heat pump is not sized on the building design load and a back-up system is present: it should be interesting to evaluate the optimal configuration of this kind of systems by taking into account the thermal energy delivered by the back-up heater and the strategies to follow in order to obtain a significant reduction of heat pump on-off cycles.

Another important research line is the optimization of the heat pump control logic: the definition of the optimal control strategy of the system is not finished and it would be interesting to study other control logics, besides the adoption of the water return or supply temperature as the monitoring variable, such as climatic compensation based on the value assumed by the external temperature. This could allow a smarter modulation of heat pump capacity, according to the thermal needs, which could improve the seasonal performance factor of the system. Furthermore, to optimize the energy efficiency of the heat pump system, it would be necessary to develop other control logics, such as an auto-adaptive control to define the optimum temperature set-points and control dead bands, taking into account the external and internal temperatures and the instantaneous electricity price in presence of hybrid systems (i.e. boiler and heat pump). A final recommendation for future research activities is the simulation of heat pump systems characterized by variable flow rate within the heat pump side (primary loop): this solution could introduce significant energy savings (i.e. the reduction of pumping energy and the increase of heat pump efficiency) but the development of a proper control strategy becomes mandatory in this case because an erroneous management of the water flow rate in the primary loop can induce the blockage of the heat pump.

Chapter 6

Publications

6.1. International journals

- M. Dongellini, C. Marinosci, G.L. Morini, Energy audit of an industrial site: a case study, Energy Procedia 45 (2014), pp. 424-433. http://dx.doi.org/10.1016/j.egypro.2014.01.046.

- M. Dongellini, S. Falcioni, A. Martelli, G.L. Morini, Dynamic simulation of outdoor swimming pool solar heating, Energy Procedia 81 (2015), pp. 1-10. http://dx.doi.org/10.1016/j.egypro.2015.12.053.

- M. Dongellini, C. Naldi, G.L. Morini, Seasonal performance evaluation of electric air-to-water heat pump systems, Applied Thermal Engineering 90 (2015), pp. 1072-1081. http://dx.doi.org/10.1016/j.applthermaleng.2015.03.026.

- M. Dongellini, C. Naldi, G.L. Morini, Annual performances of reversible air source heat pumps for space conditioning, Energy Procedia 78 (2015), pp. 1123-1128. http://dx.doi.org/10.1016/j.egypro.2015.11.070.

- C. Naldi, M. Dongellini, G.L. Morini, Summer performances of reversible air-to-water heat pumps with heat recovery for domestic hot water production, Energy Procedia 78 (2015), pp. 1117-1122. http://dx.doi.org/10.1016/j.egypro.2015.11.068.

- M. Dongellini, S. Falcioni, G.L. Morini, Dynamic simulation of solar thermal collectors for domestic hot water production, Energy Procedia 82 (2015), pp. 630-636.
  http://dx.doi.org/10.1016/j.egypro.2015.12.012.

- C. Naldi, M. Dongellini, G.L. Morini, Climate influence on seasonal performances of air-to-water heat pumps for heating, Energy Procedia 81 (2015), pp. 100-107.
  http://dx.doi.org/10.1016/j.egypro.2015.12.064.

- M. Dongellini, M. Abbenante, G.L. Morini. Energy performance assessment of the heating system refurbishment on a school building in Modena, Italy, Energy Procedia 101 (2016), pp. 948-955.
  http://dx.doi.org/10.1016/j.egypro.2016.11.120.

- M. Dongellini, C. Naldi, G.L. Morini, Sizing effects on the energy performance of reversible air-source heat pumps for office buildings, Applied Thermal Engineering 114 (2017), pp. 1073-1081.
  http://dx.doi.org/10.1016/j.applthermaleng.2016.12.010

6.2. National journals

- C. Naldi, M. Dongellini, G.L. Morini, Effetto del clima sull'efficienza stagionale di sistemi di riscaldamento basati su pompe di calore aria-acqua, La Termotecnica LXIX, vol. 6 (2015), pp. 61-64.

- M. Dongellini, S. Falcioni, G.L. Morini, Modellazione dinamica di un impianto solare termico per il riscaldamento di una piscina scoperta, La Termotecnica LXIX, vol. 7 (2015), pp. 61-64.

6.3. International and national Conferences

- C. Naldi, M. Dongellini, G.L. Morini, E. Zanchini, Comparison between hourly simulation and bin-method for the seasonal performance

evaluation of electric air-source heat pumps for heating, 2nd IBPSA-Italy Conference, Bolzano, Italy, 4-6 February 2015.
Bolzano University Press, pp. 255-262, ISBN 978-88-6046-074-5.

- M. Dongellini, C. Marinosci, S. Melini, G.L. Morini, Effetto della presenza di appartamenti non riscaldati sui consumi energetici di palazzine ERP, 33rd AICARR National Conference, Bologna, Italy, 15th October 2015.
  pp. 273-284, ISBN 978-88-95620-64-0.

- C. Marinosci, M. Dongellini, S. Melini, G.L. Morini, Verifica dell' efficienza di un intervento di riqualificazione su una palazzina ERP con la firma energetica, 33rd AICARR National Conference, Bologna, Italy, 15th October 2015.
  pp. 423-434, ISBN 978-88-95620-64-0.

- M. Dongellini, M. Abbenante, G.L. Morini. Influenza della compensazione climatica e del sistema di generazione sulle condizioni invernali di comfort in aule scolastiche, 34th AICARR National Conference, Bologna, Italy, 20th October 2016.
  pp. 151-165, ISBN 978-88-95620-70-1.

- J.P. Campana, M. Magni, M. Dongellini, G.L. Morini. The benchmark of a new SIMULINK library for thermal dynamic simulation of buildings, 3rd IBPSA-Italy Conference, Bolzano, Italy, 8-10 February 2017.

- M. Dongellini, M. Abbenante, G.L. Morini, A strategy for the optimal control logic of heat pump systems: impact on the energy consumptions of a residential building, 12th Heat Pump Conference (HPC 2017), Rotterdam, Netherlands, 15-18 May 2017.

Bibliography

[1] Eurostat, Eurostat Database. [Online]. Available from: http://ec.europa.eu/eurostat/web/energy/data/database [Accessed January 2017], 2017.

[2] EU, Directive 2009/29/EC of the European Parliament and of the Council of 23 April 2009 amending Directive 2003/87/EC so as to improve and extend the greenhouse gas emission allowance trading scheme of the Community, Brussels, 2009.

[3] European Council, 2030 Climate and Energy Policy Framework, Brussels, 2014.

[4] EU, Directive 2010/31/EU of the European Parliament and of the Council of 19 May 2010 on the Energy Performance of Buildings, Brussels, 2010.

[5] EU, Directive 2012/27/EU of the European Parliament and of the Council of 25 October 2012 on Energy Efficiency, amending Directives 2009/125/EC, Brussels, 2012.

[6] EU, Directive 2009/28/EC of the European Parliament and of the Council of 23 April 2009 on the Promotion of the use of energy from renewable sources, Brussels, 2009.

[7] EurObserv' ER, Heat pumps barometer, [Online], available from: https://www.eurobserv-er.org/heat-pump-barometer-2016, 2016.

[8] EHPA – European Heat Pump Association, European Heat Pump Market and Statistics Report 2015, [Online], available from: http://www.ehpa.org/media/studies-and-reports, 2016.

[9] R. Chargui and H. Sammouda, Modeling of a residential house coupled with a dual source heat pump using TRNSYS software, Energy Conversion and Management, vol. 81, pp. 384-399, 2014.

[10] P. Bayer, D. Saner, S. Bolay, L. Rybach and P. Blum, Greenhouse gas emission savings of ground source heat pump systems in Europe: A review, Renewable and Sustainable Energy Reviews, vol. 16, pp. 1256-1267, 2012.

[11] Y. A. Çengel and M. A. Boles, Thermodynamics: An Engineering Approach. 5th edition, New York, McGraw- Hill, 2004.

[12] Haldane, T.G.N. The heat pump - an economical method of producing low grade heat from electricity, I.E.E. Journal, vol. 68, pp. 666-675, 1930.

[13] C. Arpagaus, F. Bless, J. Schiffmann and S. S. Bertsch, Multi-temperature heat pumps: A literature review, International Journal of Refrigeration, vol. 69, pp. 437-465, 2016.

[14] Geothermal energy, in ASHRAE Handbook - HVAC Applications, Atlanta (GA): American Society of Heating, Refrigerating and Air-Conditioning Engineers (ASHRAE). 2011, pp. 34.1-34.4.

[15] I. Sarbu and C. Sebarchievici, General review of ground-source heat pump systems for heating and cooling of buildings, Energy and Buildings, vol. 70, pp- 441-454, 2014.

[16] N. Lu, Q. Zhang, Z. Chen and D. Wu, Simulation and analysis on thermodynamic performance of surface water source heat pump system, Building Simulation, vol. 10, pp. 65-73, 2017.

[17] S. Zou and X. Xie, Simplified model for coefficient of performance calculation of surface water source heat pump, Applied Thermal Engineering, vol. 112, pp. 201-207, 2017.

[18] L. Schibuola and M. Scarpa, Experimental analysis of the performances of a surface water heat pump, Energy and Buildings, vol. 113, pp. 182-188, 2016.

[19] X. Bai, T. Luo, K. Cheng and F. Chai, Experimental study on fouling in the heat exchangers of surface water heat pumps, Applied Thermal Engineering, vol. 70, pp. 892-895, 2014.

[20] J. Zhen, J. Lu, G. Huang and H. Zhang, Groundwater source heat pump application in the heating system of Tibet Plateau airport, Energy and Buildings, vol. 136, pp. 33-42, 2017.

[21] H. Ma, C. Li, W. Lu, Z. Zhang, S. Yu and N. Du, Experimental study of a multi-energy complementary heating system based on a solar-groundwater heat pump unit, Applied Thermal Engineering, vol. 109, pp. 718-726, 2016.

[22] Z. Yu, Y. Zhang, S. Hao, J. Zhang, X. Li, B. Cai and T. Xu, Numerical study based on one-year monitoring data of groundwater-source heat pumps primarily for heating: a case in Tangshan, China, Environmental Earth Sciences, vol. 75, article number 1070, 2016.

[23] J. Kim and Y. Nam, A numerical study on system performance of groundwater heat pumps, Energies, vol. 9, article number 4, 2016.

[24] D. Wang, L. Lu and P. Cui, A new analytical solution for horizontal geothermal heat exchangers with vertical spiral coils, International Journal of Heat and Mass Transfer, vol. 100, pp. 111-120, 2016.

[25] G.-H. Go, S.-R. Lee, S. Yoon and M.-J. Kim, Optimum design of horizontal ground-coupled heat pump systems using spiral-coil-loop heat exchangers, Applied Energy, vol. 162, pp. 330-345, 2016.

[26] V. Verda, S. Cosentino, S. L. Russo and A. Sciacovelli, Second law analysis of horizontal geothermal heat pump systems, Energy and Buildings, vol. 124, pp. 236-240, 2016.

[27] G. Gan, Dynamic thermal simulation of horizontal ground heat exchangers for renewable heating and ventilation of buildings, Renewable Energy, vol. 103, pp. 361-371, 2017.

[28] S. K. Soni, M. Pandey and V. N. Bartaria, Ground coupled heat exchangers: A review and applications, Renewable and Sustainable Energy Reviews, vol. 47, pp. 83-92, 2015.

[29] F. Robert and L. Gosselin, New methodology to design ground coupled heat pump systems based on total cost minimization, Applied Thermal Engineering, vol. 62, pp. 481-491, 2014.

[30] C. Han and X. Yu, Sensitivity analysis of a vertical geothermal heat pump system, Applied Energy, vol. 170, pp. 148-160, 2016.

[31] K. Huchtemann and D. Muller, Evaluation of a field test with retrofit heat pumps, Building and Environment, vol. 53, pp. 100-106, 2012.

[32] A. Nguyen, Y. Kim and Y. Shin, Experimental study of sensible heat recovery of heat pump during heating and ventilation, International Journal of Refrigeration, vol. 28, pp. 242-252, 2005.

[33] A. Michopoulos, G. Martinopoulos, K. Papakostas and N. Kyriakis, Energy consumption of a residential building: Comparison of conventional and RES-based systems, International Journal of Sustainable Energy, vol. 28, pp. 19-27, 2009.

[34] F. Hengel, A. Heinz and R. Rieberer, Performance analysis of a heat pump with desuperheater for residential buildings using different control and

implementation strategies, Applied Thermal Engineering, vol. 105, pp. 256-265, 2016.

[35] Y. Bi, X. Wang, Y. Liu, H. Zhang and L. Chen, Comprehensive exergy analysis of a ground-source heat pump system for both building heating and cooling modes. Applied Energy, vol. 86, pp.2560– 2565, 2009.

[36] K. J. Chua, S. K. Chou, and W. M. Yang, Advances in heat pump systems: A review. Applied Energy, vol. 87, pp.3611– 3624, 2010.

[37] P. L. T. Brian, R. C. Reid and Y. T. Shah. Frost deposition on cold surfaces. Industrial and Engineering Chemistry Fundamentals, vol. 9, pp. 375-380, 1970.

[38] C. T. Sanders, Testing of air coolers operating under frosting conditions, in heat and mass transfer in refrigeration systems and in air-conditioning, International Institute of Refrigeration, pp. 383-396, 1972.

[39] W. Wang, J. Xiao, Q. C. Guo, W. P. Lu and Y. C. Feng, Field test investigation of the characteristics for the air source heat pump under two typical mal-defrost phenomena. Applied Energy, vol.12, pp. 4470-4480, 2011.

[40] W. Wang, Y. C. Feng, J. H. Zhu, L. T. Li, Q. C. Guo and W. P. Lu, Performances of air source heat pump system fo a kind of mal-defrost phenomenon appearing in moderate climate conditions, Applied Energy, vol. 112, pp. 1138-1145, 2013.

[41] J. H. Zhu, Y. Y. Sun, W. Wang, S. M. Deng, Y. J. Ge, L. T. Li, Developing a new frosting map to guide defrosting control for air-source heat pump units, Applied Thermal Engineering, vol. 90, pp. 782-791, 2015.

[42] J. Zhu, Y. Sun, W. Wang, Y, Ge, L. Li, J. Liu, A novel Temperature-Humidity-Time defrosting control method based on a frosting map for air-source heat pumps, International Journal of Refrigeration, vol. 54, pp. 45-54, 2015.

[43] J.G. Ziegler and N. B. Nichols, Optimum settings for automatic controllers, Transactions of the ASME, vol. 64, pp. 759-768, 1942.

[44] J. Gao, G. Huang and X. Xu, An optimization strategy for the control of small capacity heat pump integrated air-conditioning system, Energy Conversion and Management, vol. 119, pp. 1-13, 2016.

[45] G. Mader and H. Madani, Capacity control in air-water heat pumps: Total cost of ownership analysis, Energy and Buildings, vol. 81, pp- 296-304, 2014.

[46] ChynTec, Semi-hermetic Scroll Refrigerant Compressor Technical Manual, ChynTec International Co., Ltd., 2008.

[47] M. J. P. Janssen, J. A. de Wit and L. J. M. Kuijpers, Cycling losses in domestic appliances: an experimental and theoretical analysis, International Refrigeration and Air Conditioning Conference, Paper 91, 1990.

[48] W. Wu, W. Shi, B. Wang and X. Li, Annual performance investigation and economic analysis of heating systems with a compression-assisted air source absorption heat pump, Energy Conversion and Management vol. 98, pp. 290-302, 2015.

[49] G. Bagarella, R. Lazzarin and M. Noro, Annual simulation, energy and economic analysis of hybrid heat pump systems for residential buildings, Applied Thermal Engineering, vol. 99, pp. 485-494, 2016.

[50] H. Cheung and J. Braun, Performance comparison for variable speed ductless and single-speed ducted residential heat pumps, International Journal of Refrigeration, vol. 47, pp. 15– 25, 2014.

[51] G. Bagarella, R. Lazzarin and M. Noro, Sizing strategy of on-off and modulating heat pump systems based on annual energy analysis, International Journal of Refrigeration, vol. 65, pp.183-193, 2016.

[52] P. Fahlen and F. Karlsson, Optimizing and controlling media flows in heat pump systems, 8th IEA Heat pump conference, Las Vegas, USA, 2005.

[53] C. Cuevas and J. Lebrun, testing and modeling of a variable speed scroll compressor, Applied Thermal Engineering, vol. 29, pp. 469-478, 2009.

[54] H. Madani, N. Ahmadi, J. Claesson and P. Lundqvist, Experimental analysis of a variable capacity heat pump system focusing on the compressor and inverter loss behavior, International Refrigeration and Air Conditioning Conference at Purdue, 2010.

[55] M. Dongellini, M. Abbenante and G. L. Morini, A strategy for the optimal control logic of heat pump systems: impact on the energy consumptions of a residential building, 12th heat Pump Conference, Rotterdam, Netherlands, 2017.

[56] CEN, EN 14825:2016, Air conditioners, liquid chilling packages and heat pumps, with electrically driven compressors, for space heating and cooling – Testing and rating at part load conditions and calculation of seasonal performance, Brussels, 2016.

[57] UNI, UNI/TS 11300-4, Energy performance of buildings – Part 4: Renewable energy and other generation systems for space heating and domestic hot water production, Milan, 2012.

[58] E. Kinab, D. Marchio, P. Riviè re and A. Zoughaib, Reversible heat pump model for seasonal performance optimization, Energy and Buildings, vol. 42, pp. 2269-2280, 2010.

[59] F. Madonna and F. Bazzocchi, Annual performances of reversible air-to-water heat pumps in small residential buildings, Energy and Buildings, vol. 65, pp. 299-309, 2013.

[60] S. Tangwe, M. Simon and E. Meyer, Mathematical modeling and simulation application to visualize the performance of retrofit heat pump water heater under first hour heating rating, Renewable Energy, vol. 72, pp. 203-211, 2014.

[61] O. Ibrahim, F. Fardoun, R. Younes and H. Louahlia-Gualous, Air source heat pump water heater: Dynamic modeling, optimal energy management and mini-tubes condensers, Energy, vol. 64, pp. 1102-1116, 2014.

[62] M. Aprile, R. Scoccia, T. Toppi, M. Guerra and M. Motta, Modelling and experimental analysis of a GAX NH_3 - H_20 gas-driven absorption heat pump, International Journal of Refrigeration, vol. 66, pp. 145-155, 2016.

[63] H. Huisseune, C. T'Joen, P.D. Jaeger, B. Ameel, S.D. Schampheleire and M.D. Paepe, Performance enhancement of a louvered fin heat exchanger by using delta winglet vortex generators, International Journal of Heat and Mass Transfer, vol. 56, pp. 475-487, 2013.

[64] P.M. Congedo, C. Lorusso, M.G. De Giorgi, R. Marti and D. D'Agostino, Horizontal air-ground heat exchanger performance and humidity simulation by computational fluid dynamic analysis, Energies, vol. 9, article number 930, 2016.

[65] X.R. Kong, Y. Deng, L. Li, W.S. Gong and S.J. Cao, Experimental and numerical study on the thermal performance of ground source heat pump with a set of designed buried pipes, vol. 114, pp. 110-117, 2017.

[66] T. Afjei and R. Dott, Heat pump modelling for annual performance, design and new technologies, Proceedings of 12th Conference of International Building Performance Simulation Association, Sydney, pp. 2431-2438, 2011.

[67] I. Sarbu, D. Dan and C. Sebarchievici, Performances of heat pump systems as users of renewable energy for building heating/cooling, WSEAS Transactions on Heat and Mass Transfer, vol. 9, pp. 51-62, 2014.

[68] K. Huchtemann and D. Muller, Simulation study on supply temperature optimization in domestic heat pump systems, Building and Environment, vol. 59, pp. 327-335, 2013.

[69] K. Klein, K. Huchtemann and D. Muller, Numerical study on hybrid heat pump systems in existing buildings, Energy and Buildings, vol. 69, pp. 193-201, 2014.

[70] C. Shen and X. Li, Energy saving potential of pipe-embedded building envelope utilizing low-temperature hot water in the heating season, Energy and Buildings, vol. 138, pp. 318-331, 2017.

[71] F. Busato, R.M. Lazzarin and M. Noro, Energy and economic analysis of different heat pump systems for space heating, International Journal of Low-Carbon Technologies, vol. 7, pp. 104-112, 2012.

[72] C. Naldi, G.L. Morini and E. Zanchini, A method for the choice of the optimal balance-point temperature of air-to-water heat pumps for heating, Sustainable Cities and Society, vol. 12, pp. 85-91, 2014.

[73] CEN, EN 14511-2, Air conditioners, liquid chilling packages and heat pumps with electrically driven compressors for space heating and cooling – Part 2: Test conditions, Brussels, 2013.

[74] CEN, EN 14511-3, Air conditioners, liquid chilling packages and heat pumps with electrically driven compressors for space heating and cooling – Part 3: Test methods, Brussels, 2013.

[75] H. Park, J.S. Lee, W. Kim and Y. Kim, The cooling seasonal performance factor of a hybrid ground-source heat pump with parallel and serial configurations, Applied Energy, vol. 102, pp. 877-884, 2013.

[76] M. F. Fels, PRISM: An introduction, Energy and Buildings, vol. 9, pp. 5-18, 1986.

[77] CEN, UNI EN 15603, Energy performance of buildings - Overall energy use and definition of energy ratings. Brussels, 2008.

[78] UNI, UNI 10349-1: 2016, Heating and cooling of buildings - Climatic data - Part 1: Monthly averages for the evaluation of thermal energy performance of buildings, Milan, 2016.

[79] UNI, UNI EN 12831: 2006, Heating systems in buildings - Method for the calculation of the design heat load, Milan, 2006.

[80] Meteotest: Meteonorm Version 7.1, www.meteonorm.com, 2017.

[81] G. Bagarella, M. Lazzarin and B. Lamanna, Cycling losses in refrigeration equipment: An experimental evaluation, International Journal of Refrigeration, vol. 36, pp. 2111-2118, 2013.

[82] Ministero dello Sviluppo Economico, Ministero dell'Ambiente e della Tutela del Territorio e del Mare, Decreto interministeriale 26 giugno 2015: Applicazione delle metodologie di calcolo delle prestazioni energetiche e definizione delle prescrizioni e dei requisiti minimi degli edifici. Gazzetta Ufficiale n. 162 del 15 luglio 2015, Rome, 2015.

[83] R. De Coninck and L. Helsen, Practical implementation and evaluation of model predictive control for an office building in Brussels, Energy and Buildings, vol. 111, pp. 290-298, 2016.

[84] M. Dongellini, C. Naldi, and G.L. Morini, Seasonal performance evaluation of electric air-to-water heat pump systems, Applied Thermal Engineering, vol. 90, pp. 1072-1081, 2015.

[85] M. Dongellini, C. Naldi and G.L. Morini, Sizing effects on the energy performance of reversible air-source heat pumps for office buildings, Applied Thermal Engineering, vol. 114, pp. 1073-1081, 2017.

[86] CEN, EN ISO 13790:2008, Energy performance of buildings - Calculation of energy use for space heating and cooling, Brussels, 2008.

[87] S.A. Klein et al., TRNSYS 17: A Transient System Simulation Program, Solar Energy Laboratory, University of Wisconsin, Madison, USA, 2010.

[88] Modelica Association, Modelica. ⟨https://www.modelica.org⟩; 2016.

[89] US Department of Energy, EnergyPlus, ⟨http://apps1.eere.energy.gov /buildings/energyplus); 2015.

[90] ESP-r, ⟨http://www.esru.strath.ac.uk/Programs/ESP-r˙overview.htm⟩; 2016.

[91] S. Rasoul Asaee, V. Ismet Ugursal and I. Beausoleil-Morrison, Techno-economic assessment of solar assisted heat pump system retrofit in the Canadian housing stock, Applied Energy, vol. 190; pp. 439-452, 2017.

[92] M. Chamoun, R. Rulliere, P. Haberschill and J.L. Peureux, Experimental and numerical investigations of a new high temperature heat pump for industrial heat recovery using water as refrigerant, International Journal of Refrigeration, vol. 44, pp. 177-188, 2014.

[93] B. Hu, Y. Li, B. Mu, S. Wang, J.E. Seem and F. Cao, Extremum seeking control for efficient operation of hybrid ground source heat pump system, Renewable Energy, vol. 86, pp. 332-346, 2016.

[94] L. Dong, Y. Li, B. Mu and Y. Xiao, Self-optimizing control of air-source heat pump with multivariable extremum seeking, Applied Thermal Engineering, vol. 84, pp. 180-165, 2015.

[95] A. Maccarini, M. wetter, A. Afshari, G. Hultmark, N.C. Bergsoe and A. Vorre, Energy saving potential of a two-pipe system for simultaneous heating and cooling of office buildings, Energy and Buildings, vol. 134, pp. 234-247, 2017.

[96] J. Jongug, L. Sunil, H. Daehie and K. Yongchan, Performance evaluation and modeling of a hybrid cooling system combining a screw water chiller with a ground source heat pump in a building, Energy, vol. 35, pp. 2006-2012, 2010.

[97] T. Hong, K. Sun, R. Zhang, R. Hinokuma, S. Kasahara and Y. Yura, Development and validation of a new variable refrigerant flow system model in EnergyPlus, Energy and Buildings, vol. 117, pp. 399-411, 2016.

[98] P. Byrne, J. Miriel and Y. Lenat, Modelling and simulation of a heat pump for simultaneous heating and cooling, Building Simulation, vol. 5, pp. 219-232, 2012.

[99] G. Emmi, A. Zarrella, M. De Carli and A. Galgaro, An analysis of solar assisted ground source heat pumps in cold climates, Energy Conversion and Management, vol. 106, pp. 660-675, 2015.

[100] M. Gustafsson, G. Dermentzis, J.A. Myhren, C. Bales, F. Ochs, S. Holmberg and W. Feist, Energy performance comparison of three innovative HVAC systems for renovation through dynamic simulation, Energy and Buildings, vol. 82, pp. 512-519, 2014.

[101] S. M. Al-Zahrani, F. L. Tan and F. H. Choo, A TRNSYS simulation case study on utilization of heat pump for both heating and cooling, Energy Science and Technology, vol. 3, pp. 84-92, 2012.

[102] TESSLibs 17 - Component Libraries for the TRNSYS Simulation Environment, HVAC Library Mathematical Reference, University of Wisconsin, Madison, USA, 2012.

[103] Cordivari, Bollitori solari, [Online], available from: http://www.cordivari.it/Bollitori˙Solari/Bollitori, Cordivari srl, Teramo (Italy), 2017.

[104] TRNSYS 17 documentation, Multizone building modeling with Type56 and TRNBuild, University of Wisconsin, Madison, USA, 2012.

[105] Emerson-Copeland, Selection software v.7.11, [Online], available from: http://www.emersonclimate.com/europe/en-eu/Resources/Software˙Tools, 2017.

[106] Danfoss, Thermostatic expansion valves, [Online], available from: http://products.danfoss.com/productrange/refrigeration/thermostatic-expansion-valves, 2017.

[107] P. Vocale, G.L. Morini and M. Spiga, Influence of outdoor air conditions on the air source heat pumps performance, Energy Procedia, vol. 45, pp. 653-662, 2014.

[108] M. Dongellini, M. Abbenante and G. L. Morini, Energy performance assessment of the heating system refurbishment on a school building in Modena, Italy, Energy Procedia, vol. 101, pp. 948-955, 2016.

[109] Decree of the President of the Italian Republic no. 412, 26/08/93 and subsequent modifications, Gazzetta Ufficiale Italiana, vol 242, Rome, Italy, 1993.

[110] Italian Parliament, Ordinary law of Parliament no. 373 del 30/04/1976, Gazzetta Ufficiale Italiana, vol. 148, Rome, Italy, 1976.

[111] UNI, UNI/TS 11300-2, Energy performance of buildings – Part 2: Evaluation of primary energy need and of system efficiencies for space heating, domestic hot water production, ventilation and lighting for non-residential buildings, Milan, 2014.

[112] O. Guerra-Santin and L. Itard, Occupants' behaviour: determinants and effects on residential heating consumption, Building Research and Information, vol. 38, pp. 318-338, 2010.

[113] J. Teres-Zubiaga, K. Martin, A. Erkoreka and J. M. Sala, Field assessment of thermal behaviour of social housing apartments in Bilbao, Northern Spain, Energy and Buildings, vol. 67, pp. 118-135, 2013.

[114] CEN, EN ISO 7730-2006, Ergonomics of the thermal environment. Analytical determination and interpretation of the thermal comfort using calculation of the PMV and PPD indexes and local thermal comfort criteria, Brussels, 2006.